THE EFFECT OF A ZSM-5 CONTAINING CATALYST ON THE FLUIDISED BED FAST PYROLYSIS OF PINE WOOD

LOUISE ALISON COOKE

Doctor of Philosophy

THE UNIVERSITY OF ASTON IN BIRMINGHAM

September 1999

THE UNIVERSITY OF ASTON IN BIRMINGHAM

The Effect of a ZSM-5 Containing Catalyst on the Fluidised Bed Fast Pyrolysis of Pine Wood

Louise Alison Cooke, Doctor of Philosophy, 1999

SUMMARY

This thesis is concerned with the catalytic modification of fast pyrolysis hot vapour products in a 150 g h^{-1} fluidised bed reactor using a commercial ZSM-5 containing catalyst. Catalytic modification of pyrolysis liquids and vapours has the potential for improving the resulting liquid with respect to fuel applications, as a chemical resource or both.

A discussion is included on the relative benefits of fast pyrolysis over other thermochemical processes for the production of useful liquids and the selection of a fluidised bed fast pyrolysis reactor for use in the experimental work with the incorporation of a catalyst is described. A commercial ZSM-5 containing catalyst was chosen for study based on an evaluation of the chemical components of fast pyrolysis liquids and vapours, a review of the catalytic pyrolysis literature to date and the practical aspects of fast pyrolysis reactor environmental conditions.

A 150 g h^{-1} fluidised bed fast pyrolysis reactor, it's accessory equipment and operation were adapted for the incorporation of the powdered commercial catalyst. Biomass and catalyst were co-fed into the 150 g h^{-1} reactor, via an entrained flow feeder, and suitable operating procedures were investigated. The effect of run stability on the reliability of product yields was investigated for the co-fed 150 g h^{-1} reactor system and improvements in operating procedure made.

The effect of reactor size and temperature on product yield distributions were studied by comparison of non-catalytic runs carried out on the 150 g h^{-1} reactor and a 1 kg h^{-1} reactor. Product yield trends with temperature, typical of those found in the previous literature, were observed for fast biomass pyrolysis over the range 450-550 °C. The effects of reactor size on the product distributions were ascribed to differences in particle size and residence time between the two reactor systems.

The effects of catalyst concentration in the feed (0 %, 25 % and 50 %, by weight) and temperature (450-550 °C) on product yield distributions were studied on the 150 g h^{-1} reactor. The presence of catalyst reduced the yields of total liquids produced from a maximum at 75 wt% at 520 °C with no catalyst to 69 wt% at 510 °C with 25 % catalyst in the feed to 68 wt% at 520 °C with 50 % catalyst in the feed. A more marked effect on the liquid product distribution was noted at a catalyst concentration of 25 % compared to non-catalytic operation than at catalyst concentration of 50 %. Further experimentation should investigate the effect of catalyst concentrations between 0 % and 50 % to confirm these results and determine an optimum catalyst concentration for the production of specific compounds.

Key words: biomass, catalysis, flash pyrolysis

DEDICATION

I would like to dedicate this thesis to my parents Wendy Olivia and Anthony John Cooke and to the memory of my grandparents Olive Cooke and Frank Deakin.

ACKNOWLEDGEMENTS

I would like to thank my boyfriend Mark Eccleston for his advice, intellectual and emotional support throughout the writing of this thesis.

I also wish to acknowledge the financial support of the EPSRC, COPE and the EU under Research Contract no. AIR2-CT93-0889.

LIST OF CONTENTS

LIST OF TABLES

LIST OF FIGURES

LIST OF EQUATIONS

CHAPTER ONE

INTRODUCTION

1 INTRODUCTION

1.1 Purpose of work

Fast pyrolysis is an established thermal process that gives high yields of a potentially useful liquid from biomass (1). The raw fast pyrolysis liquid, often referred to as bio-oil, is relatively unstable compared to conventional fossil fuels and cannot be directly used in many applications (2). Modification of the liquid may enhance the yields of particular valuable chemicals for extraction (3); produce additional chemicals (4) or upgrade the liquid to a high value transport fuel (5). This work focuses on the effects that a catalyst has in the pyrolysis process on the liquid product characteristics.

This chapter explains why modification of biomass-derived fast pyrolysis liquid products is necessary and sets out the objectives of the work.

1.2 Background

The potential offered by biomass and related materials for solving some of the world's energy problems is now widely recognised (6). Biomass is the only renewable form of fixed carbon (1). It is also CO_2 neutral, i.e. the production and usage as an energy form does not increase the level of atmospheric CO_2 (1). A significant obstacle to the use of biomass is it's low heating value around 16-18 MJ kg^{-1} compared to oil derived fuels with heating values around 42-44 MJ kg^{-1} (7). Although the energy in biomass can be used directly in combustion the heat released must be used immediately and locally (8). Thermal processing of biomass to a liquid product increases it's bulk energy density (i.e. volumetric energy in MJ L^{-1}) and enables it to be stored and transported relatively easily (9) compared to solid or gaseous products.

The liquid product is of particular interest due to this easy storage and portability and also because it contains many potentially valuable chemicals (10). Liquids produced by fast pyrolysis, although readily combustible, are not ideal as fuels in general and particularly not for transport fuels (7) due to their relatively low heating values and the predominantly low concentration of specific chemicals preclude economic extraction (5). Further processing is thus required in order to improve fuel properties and to enhance the yield of interesting chemicals for which catalytic processing is an effective way.

1.3 Biomass

Biomass means 'living' 'matter' and is a complex, natural and renewable carbonaceous material (1). Biomass is generally considered to encompass plant based materials, including newly grown material such as wood, grass, rape seed, sugar cane; and residues and wastes such as straw, bagasse, pine kernels and almond shells. The majority of research in biomass pyrolysis has been carried out on wood such as poplar, pine, fir, eucalyptus, beech and aspen (11). Wastes including Municipal Solid Waste (MSW), Refuse Derived Fuel (RDF) and sewage sludge are also considered to be biomass (12, 13) as they are also complex carbon containing compounds or mixtures of compounds which can be thermally processed to an energy rich product. Biomass has attracted considerable interest as it's value can be increased with respect to fuel requirements and chemicals by the pyrolysis process.

1.4 Pyrolysis

The pyrolysis process, which the biomass is subjected to, has been defined as the thermal decomposition of a carbonaceous material in the complete absence of oxygen (14) or thermal processing in an oxygen deficient environment (15). Pyrolysis always produces gaseous, liquid and solid phases and the overall elemental balance of the liquid product is practically the same as the initial feed material (9). The liquid can be preferentially produced at the expense of the gaseous and solid phases by using a pyrolysis method called fast pyrolysis which, under specific operating conditions (16), maximises liquid yields at up to 75 wt% from dry wood and is discussed later.

1.5 Bio-oil

Bio-oil possesses some undesirable properties which can be a significant disadvantage in application. It has a low pH around 2-3 which can cause corrosion problems in storage, a high oxygen content of about 35 wt% due to the oxygenated compounds in the initial wood feed that results in a heating value about half that of petroleum fuels, viscosities of 100-2500 cP, which cannot be reduced by heating for use in conventional applications as the oil degrades on heating, and finally, although numerous chemicals are present in the oil, concentrations of specific compounds are generally too small for economic extraction.

1.6 Catalytic modification

It has been reported that catalytic modification of biomass derived fast pyrolysis products has the potential to improve some of the undesirable liquid properties by reducing the high oxygen content (9). It is the conversion of either the fresh vapour or condensed liquid products from biomass pyrolysis over a catalyst to yield a more valuable end product with respect to possible applications as a fuel or as a chemical resource. To date objectives of catalytic modification of biomass pyrolysis products have included:

- increasing the product energy density (6);
- reducing the number of compounds present in the liquid in order to improve the feasibility of extracting specific groups of compounds (5);
- enhancing the yield of certain speciality chemicals which are of particular value (9);
- improving the oil quality for compatibility with combustion applications in boilers, engines and turbines (17); and
- improving the oil properties sufficiently to allow use as a conventional transport fuel (18).

Catalytic modification of biomass derived fast pyrolysis products is of value due to the potential to expand the applications of the liquid product. The two main processes available for catalytic modification are hydrotreating of pyrolysis liquids at high pressures and zeolite processing of pyrolysis vapours at atmospheric pressure. Hydrotreating has disadvantages of the cost of high pressure equipment, the cost or need to generate hydrogen (via by-product CO/H_2O reformulation) and the questionable performance of available catalysts (19).

Zeolite processing is carried out at atmospheric pressure and does not require hydrogen or other expensive materials resulting in no significant additional costs to the pyrolysis process. Zeolites have given interesting and promising results in reducing oxygen, lowering viscosity and improving general oil qualities (9).

1.7 Objectives

This work aims to explore how zeolites can be used in pyrolysis and what effects they have on the liquid product composition. Specific objectives of the experimental work were:

- to explore the use of a commercial zeolite catalyst for the vapour phase catalytic modification of biomass derived pyrolysis products;
- to characterise the products; and
- to characterise the catalytic process including establishment of preferred operating conditions.

The basic concepts of fast pyrolysis and catalytic modification are explained and the reasons for studying the atmospheric catalytic modification of fast biomass pyrolysis vapours and liquids over alternate routes are justified in Chapter 2. A comprehensive literature review of previous catalytic research on fresh pyrolysis vapours, including the effect of equipment used, with corresponding results and yields achieved and the discussion of the most important discoveries is provided in Chapter 3. Chapter 4 describes the adaptation of the fast pyrolysis equipment operation in order to incorporate a catalyst into the process. The equipment used, it's configuration and operation for this study of atmospheric catalytic modification of biomass fast pyrolysis derived vapours is described in Chapter 5. Finally the experimental results are presented and discussed in Chapter 6 with conclusions and recommendations for further work in Chapters 7 and 8, respectively.

CHAPTER TWO

THERMAL CONVERSION PROCESSES

2 THERMAL CONVERSION PROCESSES

2.1 Thermal conversion processes for producing liquids

Thermal conversion processes can produce liquid fuels and chemicals from biomass in conjunction with gas and solid production. The proportions of gas, liquid and solids produced varies with the particular process type employed (14). The types of thermal conversion processes available which produce appreciable yields of liquids fall into two categories:

- pyrolysis (12); and
- liquefaction (20).

Fast pyrolysis at moderate temperatures and liquefaction maximise liquid production (20) whereas fast pyrolysis at high temperatures produces mainly gas (21), slow pyrolysis maximises solid charcoal production (14) and conventional pyrolysis produces approximately equal quantities of gas, liquid and solid (22). The product range from each thermal process is determined by the main reaction parameters of temperature, heating rate and vapour residence time which are different in each process (14). Both general processing types mentioned above (pyrolysis and liquefaction) can be divided into a number of more specific processes characterised by key operating parameters which in turn determine the specific yields of gas, liquid and solid produced. Process selection thus enables a specific product phase to be maximised (9). A summary of the thermal conversion technologies and their reaction parameters is given in Table 2.1.

2.2 Process requirements

The thermal conversion method chosen for study in this work should result in a relatively high yield of a reasonable quality liquid product, possess minimal technical uncertainties, entail minimal capital and operating costs and have a high feed to product energy efficiency. These factors are necessary so that the process studied will have the greatest chance of obtaining commercial development for producing a useful liquid from biomass. The thermal technologies are outlined and discussed in order to justify the equipment selected and overall process specified for use in this work.

Table 2.1 Thermal conversion technologies

Process	Reactor Temp.[a] (°C)	Pressure (MPa)	Heating Rate (°C s^{-1})	Vapour Residence Time (hours-days)	Catalyst Requirement	Atmosphere In Reactor	Yield (wt % dry feed)	Ref.[b]
Slow Pyrolysis	400-500	0.10	Very low	15 minutes-days	None	Pyrolysis product gases	Gas - 30 charcoal - 30 liquid - 15-20	2
Conventional Pyrolysis	Usually <500 occasionally up to 600	0.10	2-10	5 s-30 minutes	None	Pyrolysis product gases	Equal gas, liquid and solid	2
High Temperature Fast Pyrolysis	>700	0.10	> 1000	<1s	None	Pyrolysis product gases	Gas - 80	14
Moderate Temperature Fast Pyrolysis	450-600	0.10	> 1000	<2 s	None	Inert	Liquid - 75	7
Vacuum Pyrolysis	400-500	0.002 - 0.01	Medium	2-30 s	None	Inert	Liquid - 65	14
High Pressure Liquefaction	300-350	5-15	Very low	0.2-1.0 h	Alkali metals, transition metals	CO, H_2, CO and H_2	Liquid ~35	20
Solvolysis	200-280	0.1 - 10	Low	~20 minutes	None	Slurry in water or organic compound	Liquid - 35	23

Where:

Temp.[a]: Temperature; and

Ref.[b]: Reference.

2.3 Thermal conversion processes for maximising liquids production

Thermal processes which produce appreciable yields of liquid are evaluated in order to demonstrate that fast pyrolysis is the most suitable process available for the production of liquids from biomass. The individual processes of interest fall into one of two types of process: pyrolysis or liquefaction. The five process options available are: fast pyrolysis, vacuum pyrolysis, conventional pyrolysis, high pressure liquefaction and solvolysis based processes (a type of liquefaction). These processes are described thoroughly in Sections 2.3.1-2.3.5.

An evaluation and comparison of the processes with respect to product cost, liquid yield, degree of technical risks, liquid quality and energy efficiency is presented in Section 2.4.

2.3.1 Fast Pyrolysis

Fast pyrolysis is a relatively simple thermal conversion process that employs moderate conditions compared to the competing processes. In fast pyrolysis wood particles are rapidly converted to vaporised products which are immediately quenched in order to avoid secondary polymerisation reactions and thus the yield of liquids is maximised at the expense of char and gaseous products. Temperatures between 450-650 °C are employed with vapour residence times between 0.2-2 s. The rate of heating at the reaction layer is claimed to be greater than 1000 °C s^{-1} in an inert, atmospheric pressure, environment (9, 14). Many types of fast pyrolysis process have been investigated to date and various biomass heating methods have been used as described in Section 2.5.

High yields of liquids, between 76-80 wt% (on a dry feed basis) total liquid, are achievable with water making up between 15-18 wt% of the total liquid (14). Relatively low liquid viscosities between 40-1300 cP at 40 °C have been reported (9, 14). The liquid possesses a heating value between 16-18 MJ kg^{-1} (HHV), where HHV is high or gross heating value (24), and a relatively high oxygen content usually of around 30-40 wt% (9). The pH is around 2.4 (14). The main disadvantage of fast pyrolysis is the quality of the liquid produced which will be discussed in Section 2.4.1.

A fast pyrolysis process involves dry feeding of biomass, as either dried chips or particles, into a hot reactor where fast pyrolysis occurs. The vapour products pass out of the reactor continuously due to the upstream pressure provided by the constant inflow of wood particles. The vapours pass through a cyclone, where char is removed, and into a product collection system. The product collection system consists of a series of condensers and/or a quench unit. Pumping is frequently required either of a solvent in the case of a quench unit or of a working (heat exchanger) fluid in the case of condensers. An electrostatic precipitator or other aerosol collector, such as a demister, is a common addition to the last step of the product collection system at which stage the liquid (separated from the by-product gas) is ready for use. No further separation procedures are usually carried out although there is some fine char still present in the liquid which is considered to be part of the bio-oil product.

In principle, simple and inexpensive equipment can be used in fast pyrolysis processes. The main operating cost is the heating which can be provided in a commercial process by combustion of the by-product gas or char.

2.3.2 Vacuum pyrolysis

Vacuum pyrolysis is a thermal conversion process analogous to fast pyrolysis in that vapours and aerosols produced by biomass pyrolysis are rapidly quenched but the process is carried out at sub-atmospheric pressure and at a lower heating rate which has not been specified in the literature (25). Pyrolysis occurs at a moderate temperature and the application of a vacuum ensures very rapid removal of products from the reaction zone where they are immediately quenched. Secondary reactions involving polymerisation are thus avoided maximising liquid yields and producing less char than in other slow pyrolysis processes (25, 26). Reactor temperatures of 400-500 °C are used, pressures in the range of 2-20 kPa (27) with vapour residence times of 2-30 s and moderate heating rates (14). Heat transfer coefficients from 10 to 60 W $m^{-2} K^{-1}$ are quoted depending on the type of feedstock (25).

Only one vacuum pyrolysis process has been reported to date which was developed at Laval University in Canada (28). A conventional pyrolysis multiple hearth furnace type reactor was initially employed (28) but a new moving bed reactor has been commissioned recently in order to effect better heat transfer (28). Information about the new reactor design was only published recently and there is no performance data or product characteristics available. Yield data presented for vacuum pyrolysis is based on experiments from the early work on the multiple hearth.

Vacuum pyrolysis of wood yields approximately 65 wt% pyrolysis liquids with a water content of 23 wt% (29) although water contents as low as 4.4 wt% (of bio-oil product) have been reported (30). The heating value of the product liquid is between 22.5 MJ kg^{-1} (28) and 25 MJ kg^{-1} (14) on a dry basis. Viscosities of between 878-415469 mPas have been reported at 21 °C (31).

The subsequent description of a vacuum pyrolysis process is confined to a general process whereas the system used at the University of Laval (28) exhibited specific characteristics which are not requirements for the concept of vacuum pyrolysis.

Dried biomass is fed into a heated reactor at reduced pressure. The reduced pressure, created by a vacuum pump at the exit of the reactor, effects rapid removal of the product vapours at a constant rate. As with fast pyrolysis, moderate temperatures are used (Section 2.3.1). The vapours exiting the reactor pass into a product collection system and although the products were originally fractionated into different liquids at Laval University this is not a requirement of the vacuum concept which could utilise any suitably modified fast pyrolysis product collection system.

The vacuum pump is a high energy consuming (32) additional piece of equipment of the vacuum pyrolysis process compared to fast pyrolysis processes and greater capital costs are incurred from the suitably sized and robust equipment necessary for vacuum operation (33).

2.3.3 Conventional pyrolysis

Conventional pyrolysis is a hybrid technology which produces oil, gas and charcoal. It is typically characterised by low heating rates less than 10 °C s^{-1}, temperatures below 600 °C, atmospheric pressure and relatively long gas and solids residence times, i.e. gas and vapour residence times greater than 10 s and solid residence times from minutes to days (22, 1).

Tar and char are the primary products from conventional pyrolysis due to the slow pyrolysis reactions followed by the secondary reactions occurring during the long residence times (22). The liquid product is a two phase mixture of organics and water. Dry liquid yields of 25-30 wt% (d.a.f. feed basis) (14, 1) have been reported. Specifically, the yield of oil produced by the Alten process was quoted to be up to 20 wt%, black in colour, fairly viscous and contained up to 15 wt% char. It has been reported that the raw liquid product has a HHV of 26.4 MJ kg^{-1}, a viscosity of 750 cP at 40 °C and a pH of around 4 (14). Analytical studies of 'slow' pyrolysis oils have shown them to be very variable in quality (34).

A fluidised bed has been used at Alten (1) with air injected into the reactor to provide heat from partial combustion. Dry wood is fed into the reactor and the products pass out of the top of the reactor through a cyclone to remove char. The remaining vaporised liquids and gases pass into a quenching unit which uses recycled product water as a quench medium. The oil and water phases are then separated in a settlement tank.

The excess water produced which is not required for recycling creates a disposal problem due to the high chemical oxygen demand (COD) of typically 150 000 g L^{-1}. Theoretically, the product collection system could be the same as previously described for fast pyrolysis.

2.3.4 High pressure liquefaction

High pressure liquefaction encompasses a variety of processes all of which share common characteristics of high pressure and slurry processing in solvents in order to produce liquids with low oxygen contents. Moderate temperatures are employed and sometimes a reducing gas and usually a catalyst (20).

The feed is supported as a slurry in a solvent which can be either oil based (35, 36) or aqueous (37, 38, 39). Reaction has been carried out at temperatures in the range of 250-400 °C (40) and sometimes as high as 450 °C (41), but more typically between 300-350 °C, with pressures up to 35 MPa (42, 43). Residence times vary between 5 minutes (44, 45) to 4 hours (36). At the University of Toronto, steam liquefaction was completed in less than one minute (46). The reducing gas employed is usually hydrogen (42, 47) but carbon monoxide has also been investigated (48, 49, 50). Occasionally, high pressure liquefaction has been carried out in the absence of a reducing gas using nitrogen as a carrier (50, 51). Catalysts employed fall into two groups, firstly alkali catalysts present in the alkaline ash component of the wood, often supplemented with sodium or potassium carbonate (42, 50, 52), and secondly conventional catalysts such as nickel (53, 54, 55) or ruthenium (56).

The products are a slurry consisting of char, some unconverted solids, an organic phase and an aqueous phase and gases. The organic phase has been recovered from this mixture by various methods: centrifugation, distillation or solvent fractionation (57). One method involves a two stage extraction process, firstly by solid-liquid extraction and secondly by liquid-liquid extraction (58). The organic liquid recovery is complicated compared to the recovery of organic liquid from fast pyrolysis and as such presents a significant disadvantage.

Yields of liquids between 35-40 wt% of black liquor, water free liquid from dry wood (1, 40, 59) have been reported which possessed relatively high heating values of 30-35 MJ kg^{-1} (1, 40, 60), low oxygen contents between 10-25 wt% (40), although high viscosities of 2900 cP at 40 °C or 55 000 cP at 60 °C (40) indicate that the so-called 'liquid' is actually semi-solid at room temperature and is not pourable.

The main operations involved in high pressure liquefaction are: feedstock preparation (grinding), slurrying feedstock in a solvent, slurry pumping through preheater, addition of reducing gas, reaction in high pressure reactor, product separation of liquids and gases, solid-liquid separation and finally solvent recycling (58).

The high pressures involved in high pressure liquefaction necessitate robust equipment and involve additional safety requirements. Technical problems have been encountered with high pressure liquefaction related to the pumping of slurry into the reactor (61). In one case, the high pressure pump was found to plug with slurry concentrations above 8 % (61). Separation processes are required at the end of the process in order to separate product liquids from product solids using liquid-solid techniques or product liquids from working solvents using distillation.

2.3.5 Solvolysis

Solvolysis is a more recent alternative to high pressure liquefaction and is essentially used as a pretreatment step before either catalytic hydrotreating (23) or low pressure liquefaction (62). It evolved as the first step of a second generation, two-step process due to technical problems associated with the severe conditions involved in high pressure liquefaction (23). Wood is dissolved in a solvent and partially converted under mild conditions which achieves structural disintegration of the wood fibre and defibrillation (or separation) of individual polymer chains from the wood matrix by either mechanical methods or catalytic methods. Depolymerisation and dissolution takes place in the solvent providing a partially converted biomass-derived product which can be deoxygenated in a second step of either low pressure liquefaction or hydrotreating (45).

The actual solvolysis process produces a 'partially converted' liquid which is mixed with unconverted wood, char and solvent. It is necessary to further treat the resulting slurry of product oil, unreacted solvent and unreacted wood by either low pressure liquefaction or hydrotreating. By hydrotreating the solvolysis product mixture, which consists of liquid product and solvent, the solvent is recovered for recycling whilst the proportion of light products in the oil is increased. It is economically desirable to repeat the solvolysis-hydrotreatment cycle a number of times in order to recycle the solvent. The solvent prevents the condensation of intermediate components which lead to char formation (23).

There have been a number of solvolysis processes to date (23, 44, 63). The yields of liquids produced by solvolysis alone are not quoted in the literature as it is always combined with either hydrotreating or low pressure liquefaction as secondary steps. Combined solvolysis and hydrotreating typically produce liquid yields of 25 wt% light fraction oil and 30 wt% heavy fraction oil whilst combined solvolysis and low pressure liquefaction typically produce liquid yields of 40-55 wt%. Solvents such as phenols (63), alcohols (63) or water (23) are used at temperatures of 200-330 °C (23, 48, 64) with low pressures typically around atmospheric (63), although pressures of 8.3 MPa (64) and 14-28 MPa (65) have been reported to have been used and some untypical work has been carried out at pressures of 34.5 MPa (66). In a typical example of solvolysis, the final liquid product from 7 successive cycles of wood solvolysis in phenol (initial wood: phenol weight ratio 1:4) followed by hydrotreating (23) consisted of a 25 wt% (initial dry wood in) light fraction and a 30 wt% heavy fraction. By liquefying the solvolysis product mixture under relatively low pressures, wood conversions of up to 97 % have been achieved using creosote oil as a solvent although the yield of oil was not reported. Oil yields of 40-55 wt% have been achieved whilst using ethylene glycol as a solvent and the wood conversion was reported to be between 63-66 % (45).

The solvolysis step pretreats the wood/solvent slurry so that the wood is partially degraded and pumping of higher wood containing slurries are possible compared to un-solvolysed wood slurries pumped in high pressure liquefaction processes which cause more plugging problems. Higher wood content slurries are necessary for improved reactor economics as smaller systems can be used. The major operational steps in solvolysis are: feed preparation, dissolution in solvent which may include catalytic action via acids, mechanical action via a homogenising valve and mild thermal treatment (67).

2.3.6 Summary of thermal conversion processes for maximising liquids production

The five thermal conversion processes; fast pyrolysis, conventional pyrolysis, vacuum pyrolysis high pressure liquefaction and solvolysis; identified in this Section (2.3) for maximising liquids production from biomass are evaluated in the following Section (2.4).

2.4 Evaluation of liquid producing thermal conversion processes

The most important criteria of a thermal conversion process for producing a liquid for fuel or chemical applications (as highlighted in Section 2.2) are: low cost, high liquid yield, minimal technical risks and uncertainties, optimum liquid quality in terms of chemical characteristics and physical properties and a high feed to product energy efficiency. These criteria are reviewed in Section 2.4.1. The thermal conversion processes are compared and evaluated with respect to these criteria in Sections 2.4.2-2.4.5. Finally the critical assessment and appraisal of the processes is concluded in Section 2.4.6, and the choice of fast pyrolysis for catalytic modification in this work over the alternatives is justified.

2.4.1 Criteria

The overall objective of thermal biomass conversion for liquids production is to produce a liquid with the potential for fuel or chemical applications. The most successful process for achieving this objective may involve employment of catalysts at some point but the thermal conversion processes, pyrolysis and liquefaction, are compared directly with the absence of catalyst (Sections 2.4 to 2.4.6) before catalytic modification is addressed (Sections 2.7 to 2.8).

The ultimate aim of researching the process options available is commercial development of a process. The process has to be financially viable in order to be used commercially and the cost, therefore, is the ultimate criterion. Cost concerns all aspects of the process and involves all the other process criteria. The product cost will depend directly on the capital cost of initial equipment, operating costs and the cost of biomass feed. The other process criteria, which influence cost indirectly, are: liquid yield, technical risks and uncertainties, product quality and the feed to product energy efficiency. A desirable process will involve a low product cost, high liquid yield with minimal technical risks and uncertainties, a reasonable quality liquid product and high energy efficiency.

It should be noted that cost analysis in the literature has been based on technoeconomic assessments of total processes (20, 68, 69, 70) from receipt of biomass at the plant to sale of the final product. These technoeconomic assessments often incorporate catalytic upgrading as part of the process and are inconsistent between one another. The five thermal conversion options: fast pyrolysis, vacuum pyrolysis, conventional pyrolysis, high pressure liquefaction and solvolysis processes are, therefore, difficult to satisfactorily appraise using these feasibility studies (20, 69, 70). The main costs for each process are discussed and compared according to the capital cost and operating costs which include heat required, consumable materials used, manpower costs and any technical equipment power costs. A preliminary feasibility study of the Laval vacuum pyrolysis process (69) indicated that process feasibility depends strongly on the cost of the raw material, although this is true of all biomass conversion processes (70). The feedstock cost has not been considered in this comparison, however, as it is independent of process type as most processes can handle a range of feeds. Mandatory feed preparation costs, e.g. feedstock drying, screening and grinding, are included. The operator or technician cost is not considered as it is insignificant in commercial plants with capacities in excess of 5 t h^{-1} compared to the other costs discussed.

The technical risks and uncertainties are:

- the degree of potential problems arising from process equipment failure and process line trouble spots which require specific attention and may cause operation to stop; and
- unknown problems which may appear during scaling-up to commercial plant size from pilot plant equipment; respectively.

These criteria are discussed subjectively in this work as an extended discussion is out of the scope. These risks must be minimised to avoid processing disruptions. This criterion is important as a general measure of reliability and robustness of the process during operation.

The liquid yield criterion is measured as wt% liquid (on a dry basis) produced from dried biomass feed. It is an important parameter when selecting a process as it represents how efficiently the process converts biomass to liquid product. The liquid yield is particularly important when considered with liquid quality. Liquid quality can be measured in terms of chemical characteristics and physical properties of liquids produced, their variability with time and behaviour under heating conditions. These qualities are difficult to define due to the limited available liquid knowledge and will depend strongly on their application. Valuable chemicals from pyrolysis liquids, either extractable chemicals or upgradable chemicals present in the pyrolysis liquid, represent a higher potential value than fuel products from pyrolysis liquids as they are more expensive.

The potential of chemical groups present in the oil for modification or upgrading to more useful chemicals or fuel products is very important.

Economic projections suggest that the most likely application of liquid producing thermochemical biomass processes will be extraction of chemicals combined with fuel production (20). It is therefore important to consider improving fuel properties of the liquid with the possibility of increasing the valuable chemicals content of the liquid for extraction.

The physical properties of the liquid will dictate how successfully it can be further processed, used in a fuel application or passed through an extraction process for chemicals. The liquid, or vaporised liquid, must be in a reasonable physical form, i.e. factors which can act as catalyst poisons, engine contaminants and potential technical process problem instigators must be limited. Important physical properties include: viscosity, pH, char content and ash content. The proportion of medium molecular weight compounds should also be minimised as they easily polymerise to high molecular weight compounds which form char.

Energy efficiency will be dependent upon liquid yield and liquid product heating values compared to the initial biomass heating value. Energy efficiency is, therefore, not an independent criterion, rather a useful expression of two other criteria combined.

2.4.2 Cost

Fast pyrolysis capital costs appear to be low compared to the alternative processes as an inexpensive feeding system is required and the reactor needs only to withstand atmospheric pressures (71).

Vacuum pyrolysis requires more expensive equipment than fast pyrolysis to cope with larger reactor and collection system volumes and more severe mechanical strains created by the vacuum for a comparable mass of product (33). There is also a waste disposal problem with by-product water having a COD between 190-255 g L^{-1} (72). Also, the additional vacuum pump increases the capital cost and the multiple hearth reactor or moving bed incurs additional cost compared to a fluidised bed (16).

Conventional pyrolysis equipment involves a rotary drier, settlement tank, liquid gas cyclone and filter for liquid removal from gas. This makes it more expensive than fast pyrolysis although, conceptually, some of these extra costs may not be necessary, no work has been undertaken to support this idea.

High pressure liquefaction requires a pump in order to feed the slurry into a reactor which is capable of withstanding high pressures. High pressure equipment is more expensive than atmospheric pressure equipment due to the higher level of material specification required in pressure vessel manufacture.

Solvolysis also requires a pump for slurry feeding and in some cases a homogenising valve has been incorporated which further increases capital costs. Also, as solvolysis is only a partial biomass conversion process, either moderate pressure liquefaction or hydrotreating is necessary as a secondary stage to the process entailing extra capital costs due to the amount of equipment needed.

As far as operating costs and materials are concerned fast pyrolysis appears to be the cheapest option again, the heating requirement being the major ongoing cost which is necessary for all processes and can be resolved on a commercial scale by combustion of by product char and gas. Vacuum pyrolysis is more expensive due to the high energy consuming vacuum pump and heat requirements are higher due to inefficient heat transfer in the multiple hearth although it is claimed to have been overcome with the aforementioned moving bed reactor (28). Vacuum and conventional pyrolysis incur additional costs to fast pyrolysis due to their waste water disposal requirements. High pressure liquefaction and solvolysis are much more expensive than pyrolysis due to the requirements for solvents, reducing gases, catalysts and the energy consuming pumps required for continuous slurry pumping although feed dryers are not required for slurry processing.

Some of these rough comparisons are supported by technoeconomic assessment literature. Economic assessment of the high pressure liquefaction Manoil process (48) concluded that there was little potential for further development of the process due to the high capital and process costs involved. A technoeconomic study comparing high pressure liquefaction to atmospheric fast pyrolysis carried out by Elliott et al. (20) showed that atmospheric pressure pyrolysis is more economical than high pressure liquefaction for the production of boiler fuel as a primary product and for the production of gasoline and diesel fuel products. In a rough economic analysis of the Compiegne group two-steps solvolysis and hydrotreating process, Bouvier et al. (23) found that it was less expensive than the high pressure liquefaction processes PERC and LBL of the same capacity. This was reported to be due mainly to the capital investment costs involved.

2.4.3 Liquid yield

The liquid yield is considered alone in this Section and the yields of liquids reported relate to varying qualities with respect to heating values, chemical characteristics and physical properties. Liquid yield is considered in conjunction with heating value in Section 2.4.6 to give a better overall perspective of the products from the competing processes.

The highest yield of liquid achieved by the processes examined is obtained by fast pyrolysis with a typical maximum yield of 75 wt% wet oil on a dry wood basis (which has a typical water content of ~20 wt%). No other thermal conversion process can produce yields of liquid as high.

Multiple hearth furnace vacuum pyrolysis has achieved 65 wt% wet liquid on a dry wood basis (with a water content of 15 wt%) (29). This is an adequate liquid yield being only slightly less than that achieved by fast pyrolysis. Liquid yields of 55 wt% have been reported from the moving bed vacuum reactor (25).

Conventional pyrolysis produces a liquid yield between 20-30 wt%.

The yield of liquids derived from high pressure liquefaction are typically between 40-45 wt% (73) which, although better than the yield of liquid from conventional pyrolysis, are too low to be competitive against fast pyrolysis or vacuum pyrolysis.

Solvolysis, as a stand-alone process, produces yields of liquid of up to 70 wt% (74) from the original wood but this contains approximately 20-30 wt% of solvent (combined with the partially converted biomass) which can only be removed by further processing, either moderate pressure liquefaction or hydrotreating. It is, therefore, unsuitable as a stand-alone conversion process as removal of the solvent and upgrading of the wood derived liquid is required.

Combined solvolysis and hydrotreating can achieve a 25 wt% light fraction liquid and a 30 wt% heavy fraction liquid whereas combined solvolysis and moderate pressure liquefaction using an ethylene glycol solvent has achieved between 40-55 wt% total liquid yields. Combined solvolysis processes, therefore, can produce yields of liquids comparable to those derived from high pressure liquefaction but lower than those derived from fast pyrolysis or vacuum pyrolysis.

2.4.4 Technical risk and uncertainty

In general, processes that involve a specific complex piece of equipment or a series of individual components tend to have a higher risk of technical problems although difficult product streams also represent increased technical problems as in the case of conventional pyrolysis and solvolysis and particularly in the case of high pressure liquefaction processes. Fast pyrolysis is potentially less technically problematic than the alternatives due to it's relative simplicity. The vacuum pyrolysis process poses a greater technical risk associated with poor heat transfer and the use of a vacuum. The Alten conventional pyrolysis process suffered particular problems with respect to char separation from the pyrolysis vapours and gas cleaning prior to flaring. These factors increase technical uncertainties with an associated increase in the cost of the final product. High pressure liquefaction and solvolysis processes are open to increased technical uncertainty because of the difficult nature of slurry feeding, especially in high pressure liquefaction, and product separation. Slurry feeding in the case of high pressure liquefaction is potentially more problematic than solvolysis due to the high operating pressures and higher proportions of solid wood in the slurry feed.

In the case of high pressure liquefaction there is a trade-off between operating costs and technical risk since the high pressure pumps are prone to plugging with slurry concentrations over 8 % (61) but economic analysis indicated that higher concentration slurries were essential for productivity. Safety demands are also important considerations with high pressure operating conditions and entail increased technical risks.

The liquefaction processes (high pressure and solvolysis) are potentially more problematic technically than the pyrolysis processes (fast and vacuum), high pressure liquefaction being potentially more problematic than solvolysis.

2.4.5 Product liquid analysis

The characteristics of liquid oils from different types of process are compared in this Section. Difficulty is experienced in comparing the chemical product distributions and physical property analysis between different bio-oils due to variation in the methods of collection, fractionation, analysis and interpretation from one research group to another. In 1988 a Centralised Biomass Liquefaction Analysis was carried out by McKinley et al. (31). Data for the discussion presented in this Section is taken from the results of this project as it is the most comprehensive analysis of different oils, carried out using the same methods of analysis and interpretation, to date. There were no analyses carried out on conventional pyrolysis liquids and comparable information on these liquids could not be found in the literature.

Table 2.2. shows the bio-oils analysed by McKinley et al. (31). Seven oils are presented: two vacuum pyrolysis liquids, three fast pyrolysis liquids, one high pressure liquefaction oil and one solvolytic/low pressure liquefaction oil. The yields of liquids achieved from each process, the reaction parameters under which they were produced, the feed used, the yields of groups of chemicals identified in the liquid product and physical properties of the liquid products are presented. The yields and composition of specific groups of chemicals presented are carboxylic acids, monosaccharides, phenols, ketones and lactones which represent a general assessment of the proportion of major chemical product groups obtained from the bio-oils.

It is apparent from the data presented in Table 2.2 that the chemical group yields vary within the thermal process type, e.g. the two different vacuum pyrolysis oils display a different product distribution from one another, and a 'typical' analysis does not appear to exist. The yields of different chemical groups depend on the process parameters and feedstock as well as the conversion method. Groups of chemicals are interesting because if certain types of chemicals are produced from a specific feedstock under specific reaction parameters:

- reaction mechanisms resulting in the group products can be postulated enabling a greater understanding of the process and ultimately the possibility to manipulate the product distribution; and
- chemicals which have potential applications as groups can be extracted as a group, e.g. phenolics for phenol-formaldehyde resins (75).

Table 2.2 Centralised Liquefaction Analysis carried out by McKinley (31) showing process run data, product yields achieved, chemicals identified and physical properties of liquids analysed

Process Type	Vacuum Pyrolysis		Fast Pyrolysis			High Press. Liquefaction[a]	Solvolysis and Liquefaction[b]
Process	Vacuum	Vacuum	Fast (WFP)	Fast (WFP)	Fast (NREL)	HPL[c] (PERC)	L[d] (UDES-S)
Sample Code	VP - 425	VP - 450	WL - 500	WL - 504	NREL	HPL	UDES-S
Feed	Populus Deltoides	Populus Deltoides	IEA poplar	IEA poplar	IEA poplar	Douglas fir	Populus Deltoides
Feed Moisture Content (wt%)	4.1	5.9	6.25	4.6	0	3	-
Feed Particle Size (mm)	6.35-12.7	6.35-12.7	0.59	1.0	3.175	0.420	-
Average Temperature (°C)	425	450	500	504	500	370 - 330 [e]	228
Pressure (MPa)	0.002	0.001	0.10	0.10	0.10	20.8	3.4
Vapour Residence Time (s or min)	30 s	30 s	r.t. 0.55 s	r.t. 0.48 s	r.t. 0.75 s, & 1 s[f]	35 s, 18 min[g]	8 min
Atmosphere	vacuum	vacuum	recirc. gas: CO, CO_2	recirc. gas: CO, CO_2	nitrogen	CO:H_2 60:40	-
Catalyst	-	-	-	-	-	Na_2CO_3 (aq)	-
Feed Rate (kg h^{-1})	0.8	3.4	-	-	-	-	-
Product Yields (wt% dry feed)							
Organic Liquid	50.1	50.9	75.0	77.0	64.3	53.3	n/a
Char	25.0	21.3	12.1	11.8	12.0	-	n/a
Aqueous Liquid	15.2	16.5	n/d	n/a	-	n/d	n/a
Gas	9.7	11.3	12.4	11.0	16.0	n/d	n/a
Closure	100	100	99.5	99.8	92.3	-	n/a
Chemical Groups Identified (wt% dry feed)							
Carboxylic Acids	8.27	2.23	4.23	5.66	6.9	3.31	0.83
Monosaccharides	1.36	5.48	1.04	1.08	1.99	0	-
Phenols, Ketones and Lactones	7.78	1.93	3.58	4.02	7.42	0.49	0.33
Total	17.41	9.64	8.85	10.76	16.31	3.80	1.16
Physical Properties							
Water (wt%)	10.5	1.93	20.0	19.2	17.0	5.07	0.95
Density (g L^{-1})	1.241	1.121	1.234	1.234	1.219	1.164	-
Viscosity @ 21 °C (mPas)	878	415469	1876	787	515	n/d[h] - solid	-
Viscosity @ 49 °C (mPas)	145	6785	209	123	98	n/a[i] - solid	-

Where:

[a]: refers to high pressure liquefaction;

[b]: refers to solvolysis in ethanol followed by moderate pressure liquefaction;

HPL[c]: high pressure liquefaction;

L[d]: liquefaction;

[e]: refers to 370 °C at fired heater exit and 330 °C at reactor exit;

[f]: refers to 0.75 s at 500 °C and 1 s at 400 °C;

[g]: refers to 35 s in fired heater and 18 minutes in reactor.;

n/d[h]: not determined; and

n/a[i]: not applicable.

The physical properties of the liquids are important for the reasons previously listed in Section 2.4.1. as they are a measure of the potential for direct fuel use; for extraction of valuable, marketable chemicals; or for economic further processing. It can be seen that the water content of bio-oil is lower with the liquefaction processing routes than with fast and vacuum pyrolysis. The densities of the liquids are relatively similar throughout and the viscosities (with the exception of the vacuum pyrolysis sample VP-450) are lower for vacuum and fast pyrolysis than for the liquefaction route, which could not be measured as the sample was solid at the temperatures used for testing, i.e. 21 °C and 49 °C. Heating value, pH levels and char contents of oils were not tested.

It was not possible to determine the viscosities of the liquids produced from solvolysis and low pressure liquefaction, solvolysis and hydrotreating and high pressure liquefaction since, according the McKinley et al. (31) data, they were too viscous. The high viscosity indicates a high proportion of high molecular weight compounds which make the liquid problematic for direct fuel use, economic chemical extraction or further processing.

It is important to note that since McKinley et al.'s (31) Centralised Analysis was carried out, many research organisations have continued with research into specific chemicals production from biomass pyrolysis. This research has involved optimisation of process parameters for particular chemicals which are not necessarily represented in the analysis presented above (78, 79, 80).

The properties of liquids derived from all five thermochemical conversion processes produced and analysed by various researchers (1, 2, 14, 45, 81), are summarised in Table 2.3. The data presented is more comprehensive than the McKinley et al. (31) data but disparities may exist between the liquid analyses.

The values reported for pH, char, ash and densities (where available) are comparable between the processes. At 20 °C the viscosity of the fast pyrolysis oil is lower than the viscosity of the high pressure liquefaction oil which will make storage and handling easier for the fast pyrolysis oil. The liquids produced by high pressure liquefaction have lower oxygen contents and consequently higher heating values than the liquids produced by pyrolysis processes. This is balanced by the higher yield of liquid obtained from fast pyrolysis compared to high pressure liquefaction. Liquid yield and heating value are considered together in the next Section.

Table 2.3 Liquid qualities with respect to fuel requirements

Liquid Property or Characteristic	Fast Pyrolysis	Vacuum Pyrolysis	Conventional Pyrolysis	High Pressure Liquefaction	Solvolysis
Oxygen Content (wt%)	35-44 (1, 2, 14)[a]	24-43 (1, 14)[b]	27-35 (1, 2)	10-25 (45)	22-42 (45)
Water Content (wt%)	16-26 (81, 2, 14)	18-38 (1, 14)	4.5-15 (1, 81, 14)	5.1 (57) – 25 (40)	0.1-1.9[c] (45)
HHV (MJ kg^{-1})	16-30 (1, 2, 14)[b]	21-25 (1, 14)[a]	22-26 (1, 14)[a]	30-40 (1)	40[e] (82)
Viscosity (cP) (temperature – see notes)	40-1300 (14)[h], ~107 (2)[i]	5 (14) – 292500[h]	750 (14)[h], ~240 (2)[i]	2900-55000[d] (40, 57), 200000 (45)[i]	20-1280[f] (45, 82); 1.2-20[g] (82)
Density (g cm^{-3}) @ 21 °C	1.22-1.23[j] (83), 1.2-1.23[l] (1), 1.19-1.26[m] (2, 14)	1.23[l] (1)	1.17[m] (2) - 1.22[l] (1)	0.82-0.93[j] (42), 1.11[k] (45) - 1.15[m] (57)	1.20-1.31[k] (45)
pH	~2.4-2.5 (14)	-	2-4 (1, 14)	-	-
Char (wt%)	2-9.2 (1, 2)	-	3-10 (1, 2)	-	-
Ash (wt%)	0.1-0.2 (1)	-	<0.05-1.50 (1)	-	-

Where:

[a]: is dry liquid product;

[b]: is raw liquid product;

[c]: includes solvent;

[d]: 2900 cP at 40 °C and 55000 cP at 60 °C;

[e]: LHV (MJ kg^{-1}) for hydrotreated solvolysis oil;

[f]: solvolysis oil without any secondary treatment, cP at 20 °C;

[g]: solvolysis oil followed by hydrotreating, cP at 20 °C;

[h]: cP – unspecified temperature;

[i]: cP at 20 °C;

[j]: g cm^{-3} at 15 °C;

[k]: g cm^{-3} at 21 °C;

[l]: g cm^{-3} at 55 °C; and

[m]: g cm^{-3} - unspecified temperature.

2.4.6 Energy efficiency

Liquid quality required will vary depending on the application. Liquid yield and quality should be examined together because financial success of a commercial process cannot be based on one independently of the other. It is very difficult to compare chemical components for individual or group extraction as was apparent in Section 2.4.5. It is more feasible to examine physical properties for fuel applications. This is possible by calculating the feed to product energy efficiency. The energy efficiency is described by Equation 2.1.

$$\text{Energy efficiency (\%)} = \frac{\text{Liquid product HHV (MJkg}^{-1}) \times \text{Liquid product yield (\%)}^{*}}{\text{Biomass feed HHV (MJkg}^{-1})}$$

Equation 2.1. Energy efficiency of thermochemical conversion from biomass to liquid product

Where:

*: Liquid product yield (wt%) from wood, dry basis.

Table 2.4 shows calculated energy efficiencies for the competing processes from typical liquid product HHV and liquid product yield values, assuming an initial biomass HHV of 20 MJ kg^{-1}.

It can be seen that in decreasing order, the energy efficiencies are: fast pyrolysis, vacuum pyrolysis, high pressure liquefaction, solvolysis with hydrotreating and finally conventional pyrolysis. This is an approximation as biomass type, which affects the liquid product heating value, is not specified.

Table 2.4 Calculated energy efficiencies for the competing processes

Process	Fast pyrolysis	Vacuum pyrolysis	Conventional pyrolysis	High pressure liquefaction	Solvolysis[a] and HT[b]
Liquid yield (wt% dry basis)	75	65	25-30	35-40	22
Liquid HHV (MJ kg^{-1} dry basis)	20-23	21-23	22-26	30	40
Energy efficiency (%)	75-86	68-75	27-39	52-60	48

Where:

Solvolysis[a]: Liquid heating value quoted is LHV and therefore biomass heating value used in calculation is also LHV; and

HT[b]: hydrotreating.

2.4.7 Evaluation

The process criteria discussed in the previous Sections 2.4.2 to 2.4.6 and the degree with which each of the five process options satisfies each criterion is represented in Table 2.5. Arbitrary numbers are allocated between 1 for very poor and 5 for very good to indicate how well the criterion is satisfied by the process.

Table 2.5 Process satisfaction of criteria

	Low Capital Cost	Low Operating Cost	High Product Liquid Yield	Low Technical Risk and Uncertainty	High Product Quality	High Energy Efficiency	Total
Fast Pyrolysis	4	5	5	5	4	5	28
Vacuum Pyrolysis	2	4	4	4	4	4	22
Conventional Pyrolysis	3	3	1	3	2	2	14
High Pressure Liquefaction	1	1	2	2	3	4	13
Solvolysis	1	2	2	2	5	3	15

Fast pyrolysis is superior to all of the other process options with respect to capital and operating costs and technical risks and uncertainties. Yields of chemical groups vary within the thermal process option depending on specific process parameters and feedstock although the proportion of potentially interesting chemicals present in fast and vacuum pyrolysis liquids appears greater from the data of McKinley et al. (31) to those from the solvolysis and high pressure liquefaction processes. This may be due, however, to the percentage of identifiable compounds being lower in the solvolysis and high pressure liquefaction liquids.

The physical properties of liquids derived from fast and vacuum pyrolysis liquids are more desirable than high pressure liquefaction liquids with respect to viscosity, according to the study of McKinley et al. (31). The extended compilation of bio-oil properties, Table 2.3, from various sources (1, 2, 14, 45, 81) indicated that fast pyrolysis liquid viscosities were lower than vacuum pyrolysis but comparable to conventional pyrolysis and solvolysis (without further treatment) product liquids.

The heating value of fast pyrolysis product liquids in Table 2.3 was shown to be lower than high pressure liquefaction product liquids and hydrotreated solvolysis liquids (heating values for solvolysis liquids alone were not available) but greater than vacuum and conventional pyrolysis liquids indicating a higher degree of deoxygenation achieved by high pressure liquefaction and hydrotreating processes compared to pyrolysis processes.

Vacuum pyrolysis is an effective process for liquids production as product quenching is rapid and conditions are moderate, however, the heat transfer rates are low and capital costs, operating costs and technical uncertainties are greater compared to fast pyrolysis due to the vacuum pump and more robust and larger volume equipment required for vacuum processing.

Conventional pyrolysis processes for producing liquid alone is inadequate due to the low liquid yields achieved and economic feasibility lies in utilisation of both char and liquid products.

High pressure liquefaction produces a higher quality liquid with respect to heating value than fast pyrolysis and vacuum pyrolysis but the liquid is also very viscous and generally problematic to use compared to fast and vacuum pyrolysis liquids. Also, high pressure liquefaction is not a desirable process economically or technically due to the high pressure required which creates greater capital costs, operating costs, additional safety requirements and technical risks compared to other processes.

The solvolysis process is inadequate as a stand-alone process, due to it's limited wood conversion and the fact that product usability usually relies on some form of liquid-liquid extraction. Evaluation of the solvolysis process is particularly difficult due to it being a partial process and the inconsistency in the bases of information published. Combined solvolysis and hydrotreating or solvolysis and low pressure processes introduce similar technical and economical disadvantages to high pressure liquefaction, although to a lesser extent as was discussed in Sections 2.4.2 and 2.4.4.

2.4.8 Conclusion

Compared to high pressure liquefaction oils, fast pyrolysis oils have been found to have a higher oxygen content but are less viscous and can be produced in greater yields at less cost (73). The lower viscosity of fast pyrolysis oils is a significant advantage in applications and when considering the suitability of the liquid for further processing.

The fast pyrolysis process also shows advantages over the other processes in:

- ease of operation;
- cost of operation; and
- potential for commercial development.

Fast pyrolysis is a superior process to liquefaction and vacuum pyrolysis technically and economically which is why it has been chosen for use in this work.

2.5 Fast pyrolysis liquid characteristics

Having chosen fast pyrolysis as the most suitable thermochemical process for producing liquid from biomass, it is necessary to examine the liquid itself. It has already been established that the raw liquid is not suitable for high grade fuel applications and that potentially valuable chemicals are not always present in sufficient proportions to make extraction economical. The liquid produced by fast pyrolysis possesses some unusual and special characteristics being both oleophobic and hydrophilic (1). The fast pyrolysis liquid product contains a complex mixture of oxygenated organic compounds including: aldehydes and ketones, carboxylic acids, sugars, short chain and long chain aliphatic hydrocarbons and single and multiple ring aromatic compounds. The fast pyrolysis liquid composition will depend on:

- feedstock; and
- reaction conditions.

Only about 40 wt% of fast pyrolysis liquids are identifiable at present (10). Table 2.6 presents the yields of specific chemical groups from quantitative gas chromatography (GC) analysis of three fast pyrolysis liquids at the Institute of Wood Chemistry (10).

The liquids presented in Table 2.6 were produced by: fluidised bed fast pyrolysis of pine wood, rotating cone pyrolysis of softwood and fluidised bed fast pyrolysis of beechwood, respectively. Reaction conditions were not specified for the three pyrolysis liquids. Approximately 30 wt% (water free liquid basis) of the fast pyrolysis liquids could be quantitated although a larger proportion of compounds were identified (10).

Table 2.6 Quantitative results from direct GC analysis of different fast pyrolysis liquids (10)

Compound (wt% water free liquid)	Pine Fluidised Bed Pyrolysis Liquid	Softwood Rotating Cone Pyrolysis Liquid	Beechwood Fluidised Bed Pyrolysis Liquid
Carboxylic Acids	3.22	3.04	4.65
Aldehydes	13.33	14.00	8.13
Ketones	1.23	0.75	0.91
Monossaccharides	5.42	5.29	3.52
Alcohols	7.02	4.25	3.90
Phenols	3.24	1.78	2.12
Ethers	0.14	0.00	0.52
Total	33.46	29.11	23.23

The fast pyrolysis liquid can contain 10-30 wt% water. If more water is added to the fast pyrolysis liquid a limited quantity can be absorbed before phase separation occurs into a viscous organic phase and an aqueous phase (6). Generally there is an upper limit of water addition of around 40 % but this depends on the feedstock. Fast pyrolysis liquid has an elemental composition similar to that of the original feed (1). The raw liquid is chemically very complex and is highly oxygenated, containing typically 40 wt% oxygen (8), which is mainly incorporated in organic acids, aldehydes, ketones and phenols (10).

Table 2.7 presents typical fuel properties of fast pyrolysis liquids compared to typical specifications for different grades of fuels (84).

The comparison of fast pyrolysis liquids to conventional fuels is difficult due to the scarcity of fast pyrolysis liquid physical property data available and it's inconsistency both between fast pyrolysis liquids and conventional fuels. Despite the disparities, however, it is apparent from Table 2.7 that pyrolysis liquids are significantly different to conventional fuels. Difficulties have been reported in the direct use of fast pyrolysis liquid as a fuel due to its thermal instability, char content, alkali metal content (85) and corrosivity (86) although recent experience suggests that these difficulties have been exaggerated (87).

Table 2.7 Typical fuel properties of fast pyrolysis liquids compared to required specifications for light, medium and heavy fuel oil

Physical Property	Fast Pyrolysis	Light Fuel Oil	Medium Fuel Oil	Heavy Fuel Oil
Water and Sediment, wt% max.	10-30	0.015-0.05	0.1-1.0	0.25-2.0, 1.0 (88)
HHV (MJ kg^{-1})	14-20	44.0	43.2	39.4-40.7
HHV (MJ L^{-1})	23 (88)	-	-	38 (88)
Viscosity (cP) @ 40 °C	40-1300[a]	1.5-5.5[b]	-	-
Viscosity (cSt) @ 50 °C	13-22 (88)	-	-	650-700 (88)
Viscosity (cSt) @ 100 °C	-	-	< 20	37-50
Density (g L^{-3}) @ 15 °C	1.15-1.25	0.82-0.876	0.9-1.0	0.85[a] (88), 0.99-1.02
Flash Point (°C)	66 (88)	-	-	30 (88)
Pour point (°C)	-27 (88)	-	-	30 (88)

Where:

[a]: unspecified temperature; and

[b]: at 40 °C.

These problems can be reduced or overcome by:

- improving the quality of the liquid through modification of the process parameters;
- adapting the engine or turbine to account for these difficult properties (88);
- upgrading the oil to crude hydrocarbons for refining to diesel or gasoline (5);
- thermal processing of primary vapours to produce char and gas fuel for applications (85);
- hot filtration of pyrolysis liquids to remove char (89);
- fractionation of liquid as it is condensed so that specific boiling point ranges of chemicals can be collected together in order to reduce or even avoid refining or later fractionation (27); or
- reaction of either freshly produced fast pyrolysis vapours or condensed liquids over either conventional hydrotreating (90) or atmospheric pressure catalysts (91, 92, 93).

The chemicals present in fast pyrolysis liquids are also potentially valuable as bulk or speciality chemicals but are generally in such small concentrations that extraction and recovery is both uneconomic and difficult.

This can be improved by:

- feedstock pretreatment (94) to enhance yields of particular chemicals, e.g. levoglucosan (95); or
- reacting over catalysts which create a converging effect on the product distribution which has been reported to enhance certain useful chemical groups (96, 97).

It can be seen that the opportunities for improvement of the fast pyrolysis oil are significantly increased if catalysts are used at some point in the process. They are particularly useful if high grade fuel properties are required and if it is necessary to alter chemical product distributions with a view to extraction. It has already been reported following economic projections (20) that the most likely application for bio-oils will be chemical extraction combined with fuel production. Catalytic modification of fast pyrolysis liquids, therefore, currently shows a high potential for utilisation of the oil and has been chosen in this work.

2.6 Catalysts for modifying pyrolysis liquids and vapours

Catalysts can be used for improving liquid fuel heating value, chemical characteristics and/or physical stability. Catalytic modification is, therefore, an important route for modifying pyrolysis vapours. The effects of catalytic modification of pyrolysis vapours or liquids are very difficult to predict due to the complex composition of chemicals present and the potential for the primary vapours to undergo numerous secondary reactions. It is not possible, therefore, to attempt to predefine the reactions that will occur with a particular feed in a specific reactor system under certain reaction conditions and a specified catalyst present. It is hoped and planned, however, that using catalysts will have a two fold effect of reducing the overall oxygen content, with a concomitant increase in heating value of the oil, and the narrowing of the product yield distribution.

The main two processes identified to date for catalytic modification of biomass pyrolysis products are hydrotreating and reaction over zeolites. It is out of the scope of the current work to discuss hydrotreating in detail but the main disadvantages of hydrotreating compared to atmospheric pressure catalytic processing are outlined.

Hydrotreating typically employs conventional catalysts to modify the pyrolysis products whilst in the liquid phase and requires hydrogen and high pressure operation (98). The amount of hydrogen required for hydrotreating makes the process expensive and inefficient and high pressure operation results in high capital costs for processing plants (99). Atmospheric pressure catalytic processing is an alternative to hydrotreating. The main advantage of atmospheric pressure catalytic processing over hydrotreating is that atmospheric pressure can be used, there is no hydrogen requirement (100) and pyrolysis products can be modified in the vapour phase. Many different catalysts have been used (91, 101, 102, 103) for modifying fast pyrolysis products at atmospheric pressure. A more detailed discussion can be found in Chapter 3, Section 3.4.1. Of these, zeolite processing is advantageous due to the acidic nature of the catalysts, which promotes dehydrogenation reactions, combined with shape-selective characteristics that influence the resulting products.

Zeolite upgrading of pyrolysis vapours using specific process conditions and particular zeolite catalysts have been demonstrated to favour the production of specific chemicals or groups of chemicals, for example: benzene, toluene, xylene (BTX) (104); C_5 - C_{10} hydrocarbons (97); olefins (4) and methyl aryl ethers (MAE) (96).

2.7 Point of catalyst incorporation into fast pyrolysis process

The point at which the catalyst is incorporated into the process is very important, not only from a practical point of view, but also in terms of the stage at which the pyrolysis reaction is at. Catalytic modification of pyrolysis products in the liquid phase is not considered here as the majority of liquid phase catalysis has concentrated on hydrotreating (105) which was discounted in the previous Section.

Catalytic modification of pyrolysis vapours can occur:

- during the pyrolysis process whilst the products are in the vapour phase and before they are condensed in the liquid collection system; or
- on revapourised pyrolysis liquid, after product quenching, in a separate catalytic reactor.

If the catalyst is used before condensation of the pyrolysis products, it will form an intricate part of the fast pyrolysis process but if the catalyst is used after condensation, the catalyst can be completely decoupled and the bio-oil processed in an entirely different process and location.

It is desirable, however, that the catalyst acts on the vapours before they are condensed in order to:

- minimise the extent of secondary polymerisation-type reactions occurring on and after condensation;
- improve the overall thermal efficiency; and
- reduce the equipment costs as much as possible.

The scope of this work will concentrate, therefore, on catalytic modification of freshly produced biomass vapours only. Catalytic modification of the pyrolysis product after condensation is not considered. There are three available arrangements of contacting a catalyst with freshly produced pyrolysis vapours:

- in-bed catalysis - where the catalyst is located directly inside the pyrolysis zone;
- in-reactor catalysis - where the catalyst is located post-pyrolysis zone but still within the pyrolysis reactor; and
- close-coupled secondary catalysis - where the catalyst is located in a separate catalytic reactor which is connected directly to the pyrolysis reactor at the point where primary pyrolysis vapours are leaving the pyrolysis reaction zone.

This is predominantly a practical issue, rather than one of reaction chemistry, and will be discussed in more detail in Section 2.8. Ideally, the catalyst should be placed directly into the pyrolysis zone in order to have the maximum effect on the resulting product distribution.

This is not always possible, however, and the following Sections describe the different types of fast pyrolysis methods available, evaluate their flexibility for catalyst incorporation and identify the best process for experimentation.

2.8 Evaluation of fast pyrolysis methods for inclusion of a catalyst

After selecting fast pyrolysis from a review of thermochemical processes that produce liquids (Sections 2.1-2.4) it is necessary to identify which method of fast pyrolysis has the most potential for commercial development with inclusion of a catalytic stage.

It has been stated previously that there are a number of fast pyrolysis methods developed to date characterised by reactor temperatures between 450-600 °C, with heating rates at the reaction layer in excess of 1000 °C s^{-1}, vapour residence times from 0.2-2 s and rapid quenching (9,14). The main differences between these methods arise in the mode of heating employed (22) and hence the maximum particle sizes that can be processed. The heating mode dictates important process characteristics which are of concern if catalysts are to be incorporated into the process. The current fast pyrolysis processes available are described and the suitability of each process for coupling with catalytic modification systems is discussed leading to specification of an arrangement to be used throughout this work.

Heterogeneous catalysis of pyrolysis products in the vapour phase was selected because:

- the catalysts of most interest are solid; and
- it is possible to separate solid catalyst from product vapours using an effective cyclone.

Close coupled secondary bed catalysis is feasible for the majority of fast pyrolysis processes. For this reason, the main emphasis for comparison between the fast pyrolysis processes is whether they can accept a catalyst into the pyrolysis reactor in an in-bed catalytic mode. In-bed catalysis has advantages over close coupled catalysis in a secondary reactor with respect to equipment costs.

2.8.1 Ablative heating methods

Ablative heating forces the biomass particles against a hot surface to provide the heat transfer to the biomass and there are several methods, and thus processes, for applying this heat. The hot surface may be in the form of a flat metal surface, such as a disc (106), a cyclone (107) or metal tube (108).

The biomass particles are pressed against the hot surface and moved rapidly at the same time either by rotating blades in the case of a heated plate (106) or centrifugal forces when the biomass particle stream is injected tangentially into a cyclone (107) or vortex tube (108). Ablative pyrolysis relies on the sliding contact of quickly moving biomass particles with a heated surface which makes pyrolysis zone catalysis impractical in all cases of ablative pyrolysis. In-reactor post pyrolysis catalysis is possible depending on the particular ablative reactor and close-coupled secondary catalysis is nearly always possible.

2.8.1.1 Vortex reactor

At the National Renewable Energy Laboratory in the U.S. a 'vortex' reactor is used for ablative fast pyrolysis (109). The reactor consists of a cylindrical barrel, which the researchers refer to as a 'vortex tube', through which the biomass particles are fed tangentially by a supersonic jet of either steam or nitrogen. The reactor wall is electrically heated and machined with a helical rib to force particles in to a very tight spiral pathway. Very high heat transfer rates are possible with this ablative-type of heating. As a result of the supersonic jet, the reactor is pressurised to between 7-15 kPa.

A tangential recycle loop is placed at the exit of the reactor to recycle partially pyrolysed feedstock and large char particles. The optimum wall temperature for liquids production is 625 °C which results in a vapour exit temperature of 525 °C. There is a high attrition risk for the catalyst inside the vortex reactor and it is doubtful whether a catalyst would survive. Catalysis in a secondary bed close coupled to the ablative reactor has been tested, however, and details can be found in Chapter 3.

2.8.1.2 Rotating cone reactor – University of Twente

At the University of Twente in the Netherlands a rotating cone reactor was developed initially as an ablative pyrolysis system with the intention of delivering heat to the biomass particles via a hot rotating cone (110). This initial design did not create sufficient heat transfer to ablate the particles.

A new improved design, described as a hybrid-type reactor (111), involves heat transfer from hot sand particles to the biomass and can no longer be considered an ablative reactor. The rotating cone is placed in a fluidised bed of sand so that the sand particles move upwards by the centrifugal forces induced by the rotating cone and fall back over the wall into the fluidised bed. Biomass particles are fed from the top of the cone into it's centre whereby they also travel upwards along the cone walls where pyrolysis occurs. Char and sand particles enter another fluidised bed surrounding the first fluidised bed, via a small orifice at the base of the cone, where the char is combusted and sand is fed to a riser which recycles it to the top of the cone. The catalyst attrition problems described with other ablative pyrolysis methods would also be expected to occur with the rotating cone reactor. It is not considered further in this work as there is not sufficient experimental data available at present.

2.8.1.3 Cyclone reactor – University of Nancy

A cyclone reactor was used to pyrolyse wood sawdust at relatively high fast pyrolysis temperatures between 600-1060 °C (112). This process produced an 80 wt% gas yield and 15 wt% liquid. In this operating mode (i.e. at high temperatures) the system was unsuitable for catalytic upgrading of liquids due to the low liquid yield produced and also would encounter similar attrition problems to the vortex reactor.

2.8.1.4 Aston University ablative reactor

The ablative reactor at Aston University consisted of a heated metal plate against which biomass particles were forced and moved by rotating blades. Very high heat transfer rates were achieved with yields of liquid of up to 68 wt% with a water content of 10 wt% at 600 °C and 1.44 s apparent vapour residence time (113).

In-bed catalyst incorporation would not be possible due to the attrition risks mentioned before. A secondary bed coupled to the vapour exit stream would, however, be viable.

2.8.2 Entrained and transported bed reactors

The reactor systems described in this Section are termed either 'transported bed' or 'entrained flow' reactor systems but all consist of the pyrolysing biomass particles moving continuously through tubular reactors. Processes involving the conveyance of biomass particles in a gas are termed 'entrained flow' reactors whereas those involving the conveyance of biomass particles, gas and particulate solids, for heat transfer purposes, are referred to as 'transported bed' reactors.

2.8.2.1 Entrained flow – Georgia Institute of Technology

At the Georgia Institute of Technology (G.I.T.) an entrained flow pyrolysis reactor was used. The wood particles were carried in a water saturated inert gas, generated via the stoichiometric combustion of propane and air, upstream through a tubular reactor. The energy generated by the combustion was used to heat the reactor. A heating value of 25 MJ kg^{-1} (114) was quoted for the oil produced at 400 °C (yield 33.7 wt%). Maximum yields of oil from oak wood of 51.3 wt% (dry ash free basis) were reported at a pyrolysis temperature of 475 °C.

A catalyst could be incorporated into the flow of pyrolysing biomass particles, depending on gas velocities and catalyst particle size and density, resulting in a transported catalytic bed.

2.8.2.2 'Entrained flow reactor' – University of Western Ontario

The University of Western Ontario used hot solids in a transported bed, despite referring to the reactor as 'entrained flow', to transfer heat to the biomass and cold solids to transfer heat away from the products (115). Biomass particles were contacted with hot solids in a cyclonic vessel which rapidly mixed the biomass particles with the hot solids due to the turbulence created by injecting opposing tangential streams of hot solids to initiate pyrolysis. The biomass and hot solids were then passed through the transported bed pyrolysis reactor, which consisted of a down flow tubular reactor, in a plug flow.

The transported bed pyrolysis reactor connected directly to a cyclonic quenching vessel containing cold solids with which the biomass products were rapidly mixed. Only preliminary results are available in the literature (115).

In-bed catalysis may be possible depending on gas velocities and the compatibility of catalyst particle size and density to the system but there may be a significant degree of catalyst attrition experienced when contacting the turbulent regions of solids.

2.8.2.3 Transported bed reactor – Ensyn Engineering Associates

At Ensyn Engineering Associates in Ontario, Canada, a fast pyrolysis process called Rapid Thermal Processing or RTP has been employed. The reactor system consisted of a rapid thermal mixer, in which preheated carrier gas and sand is mixed with the biomass, coupled to a tubular transport reactor, in which thermal reactions occurred. The maximum yield of liquid from biomass was reported to be 80 % (unspecified basis) at 500 °C and a residence time of 0.25 s (1). The optimum temperature range, for residence times of up to 1s, was between 500-525 °C.

In-bed catalysis has already been employed (117) but it would be expected that a large amount of catalyst attrition would have occurred although this was not commented upon.

2.8.3 Fluidised bed

Various organisations have made use of fluidised bed technology in coal hydropyrolysis (118, 119), solid waste pyrolysis/gasification (120), sugar cane bagasse gasification (121), catalytic pyrolysis of lignin (122) as well as fast pyrolysis of biomass (123).

2.8.3.1 Waterloo Fast Pyrolysis Process

The University of Waterloo have made extensive use of fluidised bed technology for biomass pyrolysis (124) and it is widely considered to be the most suitable method for fast pyrolysis to date (1). In the Waterloo Fast Pyrolysis Process (WFPP) sand was used as the fluidising medium with nitrogen as the fluidising gas. Liquid yields of up to 75 wt% (dry feed) were reported (125).

Good control of temperature, excellent mixing of biomass particles, quick removal of products from the bed, excellent heat transfer at very high heating rates and ease of operation were reported using this process (126, 127, 128).

In-bed catalysis would be possible depending on gas velocities.

2.8.4 Circulating fluidised bed reactor

At the Centre for Renewable Energy Sources (CRES) in Greece, a circulating fluidised bed was designed for biomass fast pyrolysis (129). Air was used to fluidise recirculated sand and to achieve combustion of recirculated char in the lower section of the reactor. The combustion gases, thus produced, subsequently fluidised the sand and biomass in the upper part of the reactor where heat transfer and pyrolysis took place. The hot vapour products, product char and sand exited at the top of the reactor where they were separated and the char and sand were recycled to the combustion zone in the lower section of the reactor.

2.8.5 Selection of fast pyrolysis method

The ablative methods for fast pyrolysis are unsuitable for the incorporation of solid catalysts within the pyrolysis zone due to the attrition that any such catalyst would suffer against the hot surfaces used for heat transfer to the biomass particles. The other methods of fast pyrolysis are based on entrainment or fluidisation of biomass particles in a stream of gas, and solids in transported beds, through a reactor. Heat transfer, in the reactor, can be achieved via the carrier gas alone, as in the case of GIT entrained bed reactor, or via the carrier gas and inert hot solids, such as sand, as in the cases of the Ensyn transported bed, Waterloo fluidised bed and CRES circulating fluidised bed. Addition of catalyst to any of these systems may require modification of the process.

The entrained bed which used hot gases alone for heat transfer would effectively become a transported bed if catalyst was added, perhaps comparable to a riser cracker, and the success of this transformation would depend on the careful calculation and control of gas velocities. The transported beds and fluidised beds which already incorporate a moving solid medium to effect heat transfer would effectively become multi-solid moving beds.

The effectiveness of pyrolysis vapour contact with a catalyst that can be achieved within these systems would be dependent on the ability to control solid particle sizes, densities and gas velocities.

From a design point of view, therefore, there is no obvious choice of system for pyrolysis zone solid catalysis from the selection of entrained, transported and fluidised beds available. If a catalyst is to be located after the pyrolysis zone but within the pyrolysis reactor, the suitability of a particular method for catalysis depends on the availability of sufficient space to place a catalyst bed. A fixed bed, or a shallow fluidised bed, would be required to avoid removal of the catalyst from the reactor. In such a system the dimensions and physical aspects of the catalyst must be such that the pyrolysis vapours can pass freely across it. In this case, the only suitable fast pyrolysis methods available are either the GIT entrained bed reactor or the Waterloo fluidised bed reactor. All of the other methods involve a constant through-put of solid material which would interfere with a fixed catalyst bed. These two fast pyrolysis methods demonstrate more flexibility, therefore, with respect to catalyst incorporation options although fixed catalyst beds have been found to be problematic due to catalyst coking (130) which is discussed more in Chapter 3.

Other important criteria for selection of a suitable fast pyrolysis method are the reliability, robustness and proven record of the process to be used. In this respect the Waterloo fast pyrolysis process is an excellent candidate due to the amount of experience gained and literature published. The circulating fluidised bed at CRES is a newer design and the degree of operating experience does not compare to the Waterloo fluidised bed. The Ensyn Rapid Thermal Process is an established technology for fast pyrolysis but detailed operating information is not available and it is a technically more complicated process than the Waterloo process.

The fast pyrolysis process will become more complex, in terms of process parameters, with the incorporation of a catalyst so it is advantageous to chose the most simple process to limit the overall complexity which in turn would simplify the possible design and reduce potential operational problems.

It is also advantageous to choose a relatively simple fast pyrolysis process so that more attention can be given to the effect of a catalyst rather than control and operation of a complicated process.

Table 2.8 shows the available fast pyrolysis methods and their suitability for use with catalysts.

Table 2.8 Comparison of fast pyrolysis reactors and their suitability to be used with solid catalysts in-bed pyrolysis zone, in-reactor post-pyrolysis zone and secondary close-coupled

Reaction Mode	In-Bed Catalysis in Pyrolysis Zone	In-Reactor Catalysis Post Pyrolysis zone	Secondary Close-Coupled Catalysis
Vortex	Impractical due to high attrition risk	No suitable zone due to recirculation of particles	Experiments in a secondary vapour cracker
Rotating Cone	Possible depending on gas velocities and catalyst attrition	No suitable zone due to recirculation of solids	Possible
Cyclone	Experimental data is unavailable at the conditions required for liquid product optimisation		
Ablative Plate	Impractical due to high attrition risk	Theoretically possible but technical problems would be encountered	Possible
GIT[a] – Entrained Flow	Possible - becomes a transported bed	Possible	Possible
UWO[b] – Entrained Flow	Possible - becomes a transported bed	Possible	Possible
Ensyn – Transported Bed	Possible depending on gas velocities	Not possible	Possible
Waterloo – Fluidised Bed	Possible depending on gas velocities	Possible	Possible
CRES[c] – Circulating Fluidised Bed	Possible depending on gas velocities	No suitable zone due to recirculation of particles	Possible

Where:

GIT[a]: Georgia Institute of Technology;

UWO[b]: University of Western Ontario; and

CRES[c]: Centre for Renewable Energy Sources.

From Table 2.8 it can be seen that there are six fast pyrolysis methods available for in-bed pyrolysis zone catalysis, four methods for in-reactor post pyrolysis zone catalysis and all methods achieving successful moderate temperature fast pyrolysis for close-coupled catalysis. The six methods suitable for in-bed pyrolysis zone catalysis are: Rotating cone, Ensyn transported bed, Waterloo fluidised bed, GIT entrained flow, UWO entrained flow and CRES circulating fluidised bed. The four methods suitable for in-reactor post pyrolysis zone catalysis are: Aston ablative, GIT entrained flow, UWO entrained flow and Waterloo fluidised bed. All methods are suitable for close-coupled fast pyrolysis and catalysis apart from the Cyclone reactor due to it's normal operating parameters producing low yields of liquid.

Taking all the criteria into account the Waterloo fluidised bed pyrolysis process is chosen for use in the current catalytic pyrolysis investigation because:

- either powdered or extrudate solid catalyst could be used inside the bed in the pyrolysis zone;
- a large amount of experimental yield data was available on many feedstocks at differing reactor parameters (123, 124);
- the reliability and robustness of the system for generating experimental data was second to none amongst the fast pyrolysis methods (126);
- the performance in terms of liquid yield was excellent (123);
- the system was easy to control (128); and
- the fluidised bed was well developed and known to produce satisfactory yields of organic liquids at about 75 wt% at 500 °C (123).

CHAPTER THREE

SELECTION OF CATALYST AND REVIEW OF CATALYTIC MODIFICATION OF BIOMASS DERIVED HOT VAPOUR PRODUCTS

3 SELECTION OF CATALYST AND REVIEW OF CATALYTIC MODIFICATION OF BIOMASS DERIVED HOT VAPOUR PRODUCTS

3.1 Introduction

Having chosen fluidised bed fast pyrolysis as the method with which to incorporate an in-bed heterogeneous catalyst for vapour phase modification of the biomass pyrolysis products, the next stage was to select a catalyst. The catalytic modification of biomass derived hot vapour products and the selection of a catalyst for experimentation are reviewed in this chapter. Firstly, the approach to selecting a catalyst is investigated by considering the basic chemical processes in fast pyrolysis, secondly the literature is reviewed and finally the catalyst chosen is described in as much detail as possible.

3.2 Chemistry of fast pyrolysis

3.2.1 Introduction

From a detailed review of the literature it was decided that the potential source of energy and chemicals present in biomass could be most advantageously recovered thermochemically as a liquid by fast pyrolysis. It was found that the quality of liquid produced by fast pyrolysis was insufficient for high grade fuel applications, such as gasoline or aviation fuel, or the economic extraction of valuable chemicals. It was concluded in Section 2.5, from a review of fast pyrolysis liquids, that catalytic modification of the hot vapour pyrolysis products is a suitable method in order to achieve a liquid for high grade fuel applications or the economic extraction of valuable chemicals. An analysis of fast pyrolysis methods in Section 2.8. resulted in the selection of a fluidised bed reaction system which holds several advantages over the alternative fast pyrolysis methods, as described in Section 2.8, and allows the inclusion of a heterogeneous catalyst into the process in several ways. It was necessary to select a catalyst for experimentation before designing the required modifications to the equipment and experimental procedure as the physical form of the catalyst will have a significant impact on how it can be introduced into the fluidised bed reactor system.

The ideal way of selecting a catalyst would be from fundamental investigation of:

- the composition of vapour products from biomass pyrolysed in the fluidised bed reactor;
- the exact thermal reactions occurring from the production of the vapour products until their condensation in the product collection system;
- the precise catalyst functions required during the secondary vapour reactions in order to manipulate the reactions to produce higher quality liquids than are produced without a catalyst function present; and
- the evaluation of all the available catalysts with the desired catalytic functions in order to chose the catalyst whose form and properties most suit the fluidised bed fast pyrolysis process.

This 'ideal' selection process is virtually impossible because:

- complete analysis of the hot vapour products is not possible as only up to 40 wt% of products have been characterised to date (10);
- the effect of a catalyst on the numerous reactions of hundreds of chemicals cannot be predicted;
- controlling the start point and rate of desired catalytic reactions is unlikely to be possible due to the rapid thermal reactions constantly taking place; and
- controlling other conditions such as reaction atmosphere for the desired catalytic reactions is not possible due to the complexity of the system.

The potential products from a given feedstock in the fluidised bed pyrolysis process, however, can be estimated to a certain extent from reaction knowledge of primary and secondary reactions typically occurring in fast pyrolysis (22) or from liquid analysis of the products from fluidised bed fast pyrolysis of pine wood (10).

3.2.2 Feedstock

In order to understand the complexity of the hot vapour products from fluidised bed pyrolysis it is necessary to first consider the type of feedstock. The feedstock chosen for use in this work was pine wood as described in Chapter 4. Pine consists of approximately 40 wt% cellulose, 30 wt% lignin and 25-30 wt% hemicellulose (131). The remaining 5 wt% consists of other polysaccharides, extractives and residual constituents. The structure of cellulose is uniform consisting of a linear sequence of anhydroglucose units (linked by 1,4-β-glucoside bonds) irrespective of wood type. Hemicellulose is a more complicated branched molecular structure consisting of varying sugar units depending on the wood type. For pine wood 65-80 % of hemicellulose is galactoglucomannans, which are partially substituted by acetyl groups, and 20-35 % of the hemicellulose is arabinoglucuronoxylans (131). Lignin is an extremely complex non-carbohydrate polymer consisting of several phenylpropane monomer groups connected by a variety of linkages, typically carbon-carbon or ether bonds (132), involving aromatic rings and functional groups (133).

3.2.3 Pyrolysis reactions

It is important to differentiate between primary, char layer and secondary pyrolysis reactions. Primary reactions are considered to be those occurring within the first few milliseconds of pyrolysis (22) inside the wood particle. As soon as the vapours diffuse out of the wood particle they undergo thermal and catalytic reactions in the char layer. Secondary thermal reactions continue outside the wood particle. According to this definition of pyrolysis reactions, all reactions occurring outside the wood and char layers are considered secondary pyrolysis reactions and as such can be affected by the presence of a catalyst. It should be noted, however, to avoid confusion that the secondary pyrolysis reactions are occasionally referred to as primary reactions in the literature whilst secondary reactions are considered to be thermal reactions taking part in a secondary reactor. Secondary reactions described in this chapter, and in the rest of this thesis, are defined as all reactions occurring outside the wood and char layers. Understanding secondary pyrolysis reaction pathways, and mechanisms where identified, in particular gaseous environments forms the basis of the selection of a catalytic function.

The main pyrolysis reactions are depolymerisation and fragmentation of cellulose and hemicellulose and depolymerisation of lignin (22). Hemicellulose decomposes first at 200-260 °C followed by cellulose at 240-350 °C and lignin at 280-500 °C (134). In the fast pyrolysis of biomass, at temperatures in excess of 450 °C, depolymerisation and fragmentation occur as competing pathways (22). The alkaline inorganic constituents present in biomass promote the fragmentation reaction and cause it to predominate in normal circumstances (22) as described below.

Cellulose depolymerisation is the splitting of the cellulose chain between the glucose units which results in levoglucosan as a major product from the glucose during scission as well as other compounds such as cellobiosan and hexoses. The mechanism through which depolymerisation is carried out is called transglycosylation and this intramolecular condensation of the cellulose chain is a linking reaction as opposed to cleavage. It has been hyopothesised that the reaction starts with an electron shift between the hydroxyl group on the number six carbon on the glucose monomer and the glycosidic bond between the monomers (135).

Cellulose fragmentation involves cleavage of the cellulose chain from within the glucose monomers producing hydroxyacetaldehyde as a major product and glyoxal, acetol, ethylene glycol, formic acid, methyl glyoxal (126), carbonyl compounds, double bond containing compounds and substituted furans (123) as minor products. This is called glycosidic cleavage and is thought to proceed via an attack on the glucose unit from an external hydroxyl group. The glucose unit then splits and goes through a series of electron shifts. The mechanism is catalysed by alkalis present as alkali metals in the inorganic component of the wood and can be enhanced by adding small amounts of alkali.

The mechanisms by which hemicellulose undergoes depolymerisation and fragmentation reactions may be different to the mechanisms experienced by cellulose (136). For example, xylan, a constituent derived from the pyrolysis of pine hemicellulose, was shown (136) to undergo transglycosylation without the presence of a hydroxyl group on the number six carbon which is necessary in the hypothesised transglycosylation mechanism for cellulose.

Evans and Milne (137) identified the two main pathways of fast pyrolysis reactions of lignin to be the rapid formation of alkenylmethoxyphenols, such as coniferyl alcohol, accompanied by the slower formation of low molecular weight aromatics, such as guaiacol. Masuku reported that lignin pyrolysis was initiated by cleavage of carbon-oxygen and carbon-carbon bonds to give guaiacol and pyrocatechol derivatives which react to produce phenols, substituted phenols and finally arenes and commented that free radical mechanisms can explain a large proportion of the pathways observed (138). The fast pyrolysis of lignin was reported by Britt et al. (139) to proceed predominantly via free radical mechanisms.

Pine wood also contains resin acids such as: abietic, neoabietic, palustric, levopimaric, dehydroabietic, aric, isopimaric and sandaracopimaric acid. Some of these acids are unstable and readily isomerise to other acids (131). These acids may effect the depolymerisation and fragmentation reactions of the major carbohydrates present but this has yet to be demonstrated.

Evans and Milne's molecular characterisation studies on biomass pyrolysis products showed that the pyrolysis of whole wood could be approximated to the summation of the separate pyrolyses of cellulose, hemicellulose and lignin (136). They found no species which appeared as a result of chemical interactions between the cellulose, hemicellulose and lignin components although they reported that relative proportions of products changed according to matrix effects and inorganic interactions from species' such as sodium and potassium compounds present in the wood. The three main wood polymers were found to break down into smaller monomer and oligomer fractions (136).

Fast pyrolysis minimises the secondary reactions by rapidly quenching the product vapours to liquids. The reactions occurring during this short time period of secondary vapour reactions, up to about 2 seconds before condensation to liquids, are of vital importance in determining the nature of the liquid products. An effective catalyst should alter these reactions in order to improve the resulting liquid product distribution with respect to fuel or chemical extraction potential. The greater the understanding, therefore, of these secondary vapour reactions immediately prior to vapour quenching, the easier it should be to select a catalyst.

Primary pyrolysis products are relatively unstable and undergo interaction by polymerisation, particularly due to the presence of chemically combined oxygen (this continues after quenching and condensation although at a slower rate). Once the major components of cellulose, hemicellulose and lignin have depolymerised and fragmented the resulting oligomer fractions will further degrade and cross-react with one another until the point of quenching. The reactions are complicated and rapid primarily due to the chemically combined oxygen in the compounds which is also responsible for the low heating value of the condensed liquid product. This is why the majority of catalytic modification studies so far have concentrated on deoxygenating the pyrolysis liquid.

A quantitative analysis of hot vapour fast pyrolysis products from pine was not available and, therefore, a bio-oil product distribution from pine fast pyrolysis is presented in Table 3.1. The bio-oil compounds were quantified by GC-FID analysis from the fast pyrolysis of pine wood in a 1 kg h^{-1} fluidised bed reactor (10). The compounds quantified are identified by chemical group and wood component that they are derived from.

There are no quantified compounds from the hemicellulose component of pine wood although 1,6-anhydro-β-D-mannopyranose was detected (10). Only 33 wt% of the liquids produced from the fluidised bed fast pyrolysis of pine wood could be quantified. This is typical of pyrolysis liquid analysis (11). The vast majority of compounds quantified were from the cellulose constituent of the pine wood and represented a range of oxygenated organic chemical groups. A number of lignin derived products were quantified but cumulatively constituted a very small fraction of the lignin in the initial wood. The majority of lignin derived products could not be quantified.

It is apparent that the reactions occurring within the fluidised bed fast pyrolysis process are complicated and selection of a catalyst to perform specific reactions on specific compounds under the conditions used is not feasible.

The biomass pyrolysis catalytic literature is reviewed to examine the type of catalysts and systems used to date and the change in product yield distributions achieved which should lead to a selection of a catalyst for the current work and suitable reaction conditions to use. The literature reviewed concentrates solely on atmospheric pressure 'bio-vapour' catalysis.

Bio-vapour catalysis is defined as catalytic action on pre-condensed freshly produced fast pyrolysis biomass vapours prior to their separation into permanent gases and liquids through the quenching process.

Table 3.1 Components of pine wood and resulting liquid compounds present in pine fast pyrolysis bio-oil

Pine Wood Component Derived From	Wt% Of Component In Wood	Type Of Compound	Identified Bio-oil Compound From Pine Fluidised Bed Pyrolysis	Amount Of Bio-oil Compound (wt% in water free liquid)
Cellulose	40	Carboxylic acid	Acetic acid	3.22
		Aldehyde	Hydroxyacetaldehyde	12.62
			5-Hydroxymethyl-2-furaldehyde	0.45
		Ketone	(5H)-Furan-2-one	0.77
			2-Hydroxy-1-methyl-1-cyclopentene-3-one	0.27
		Monossaccharide	Levoglucosan	5.42
		Alcohol	Acetol	7.02
		Ether	2,5-Dimethoxytetrahydrofuran (cis)	0.14
Lignin	30	Phenol	Phenol	0.06
			Guaiacol	0.53
			o-Cresol	0.05
			m-Cresol	0.31
			p-Cresol	0.02
			4-Methyl guaiacol	0.88
			2,4- and 2,5-Dimethyl phenol	0.05
			4-Ethyl guaiacol	0.14
			4-Vinyl guaiacol	0.06
			Eugenol	0.22
			Isoeugenol (cis)	0.25
			Isoeugenol (trans)	0.67
			Homovanillin	0.20
		Aldehyde	Vanillin	0.26
		Ketone	Acetoguaiacone	0.19
			Total quantified	33.46

3.3 Fundamentals of bio-vapour catalysis

Before the literature is reviewed, it is useful to highlight some of the fundamentals of bio-vapour catalysis. It is necessary to define certain terms and expressions used in catalytic modification:

- Weight hourly space velocity (WHSV), h^{-1}, is a term used in vapour phase processing of bio-oil. It is defined as g feed / g catalyst / hour and is the ratio of feed to catalyst each hour. WHSV is of particular significance to catalyst deactivation as it is a measure of bio-oil loading on the catalyst. Typical WHSVs are between 0.1-5.0 h^{-1};
- Coke is the term used to describe carbonaceous deposits on the catalyst which usually leads to deactivation; and
- Effective hydrogen index (EHI) expresses the hydrocarbon forming potential of a feedstock. It was defined by Chen et al. (130) as a calculated indicator of the 'net' hydrogen to carbon ratio of a pure or mixed heteroatom containing feed. The EHI is defined in Figure 3.1, where: H, C, O, N and S are atoms per unit weight of sample of hydrogen, carbon, oxygen, nitrogen and sulphur respectively.

$$\left(\frac{H}{C}\right)_{Effective} = \frac{(H - 2O - 3N - 2S)}{C}$$

Figure 3.1 Effective hydrogen index

The direction of the bio-vapour catalytic reaction depends on a number of variables which operate during the reaction time between contact of the bio-vapours with the catalyst and their subsequent quenching.

The variables that affect the extent of the catalytic reaction are:

- the contact time of the pyrolysis vapours with fresh catalyst;
- the temperature of the catalyst;
- the partial pressure of the pyrolysis vapours at the active catalyst site;
- the diffusivity and absorption of the pyrolysis vapours into the active sites of the catalyst;
- the strength and frequency of the active sites on the catalyst (usually determined by degree of protonation of the catalyst); and
- the concentration of the catalyst at the reaction zone.

Throughout the literature reviewed these variables are adjusted by catalytic reactor design, operation and parameters of the catalytic system, form of the catalyst and feeding methods employed. Chemical reaction is indirectly affected by reactor type and scale in a manner which is usually unpredictable on a quantitative basis; these changes may result in a change in the overall rate of reaction, different product distributions or both (140). In order to attempt to understand the chemistry of bio-vapour catalysis it is necessary to understand the relationships between these 'physical specifications' and reaction severity.

To take a general view, bio-vapour catalysis can be considered to consist of the following sequence:

$$\text{Biomass} \xrightarrow{a} \text{Bio} - \text{vapours} \xrightarrow{b} \text{Catalysed Vapours} + \text{Coke} + \text{Gas}$$
$$\text{Biomass} \xrightarrow{c} \text{Char} + \text{Gas}$$

Figure 3.2 Catalytic fast pyrolysis reaction paths

This model assumes that catalysis does not occur until the bio-vapours have diffused out of the biomass particle. Pyrolysis reactions a and c occur at the same time and are thermal reactions.

Factors that effect these reactions are:

- temperature at the reaction layer;
- residence time of the biomass particle in the reaction zone;
- heat transfer rate across the biomass particle;
- size of the biomass particle; and
- method of heat transfer.

The temperature and residence time increase the pyrolysis reaction severity. The heat transfer rate across the biomass particle determines the speed of the pyrolysis reaction. High heat transfer rates favour high yields of bio-vapours compared to yields of permanent gas and char and slow heat transfer rates increase intra-particle thermal reactions which result in lower yields of bio-vapours and higher yields of permanent gas and char. The greater the size of the biomass particle, the greater the extent of intra-particle thermal reactions, again resulting in an increase in the yield of char and permanent gas at the expense of bio-vapours. The method of heat transfer can reduce the effects resulting from larger particle sizes. In the case of ablative pyrolysis, for example, the liquid layer forming along the particle edge next to the hot surface is moved away quickly from the un-reacted biomass allowing it to directly contact the hot surface without requiring heat transfer across an already reacted layer, as is the case with fluid bed pyrolysis. This results in lower yields of char and gas from ablative pyrolysis compared to fluid bed pyrolysis with larger particle sizes.

Catalytic reactions, pathway b, may be preceded by further thermal reactions or polymerisation depending on the arrangement of the pyrolysis and catalytic zones. For example, when catalytic reaction is carried out in a secondary reactor close-coupled to the pyrolysis reactor, the thermal reaction time can be extended resulting in thermal cracking of the bio-vapours prior to catalysis. Alternately, if the temperature is lowered between the pyrolysis reactor and catalytic reactor, the bio-vapours will begin to polymerise prior to catalysis.

With in-bed catalysis, the catalytic reactions, pathway b, occur as soon as the bio-vapours diffuse out of the pyrolysing particle and contact the catalyst. The presence of the catalyst causes the bio-vapours to undergo specific reaction pathways, the severity of which is increased by the factors previously listed (at the start of Section 3.3). In some of the literature reviewed the catalytic reactions reach optimum reaction severities for the production of specific compounds. When reaction severities are increased above the optimum there is a deleterious effect on the yields of desirable compounds as they react to form other products.

Catalytic reaction severity can be controlled by limiting the factors contributing to catalytic reaction severity. The temperature of the catalyst can be altered to affect catalytic reaction severity. The active catalyst component can be reduced or diluted by mixing the catalyst with inert solids, supporting the pure catalyst on a binder or chemically preparing the catalyst at a lower activity. The ratio of bio-vapours to catalyst, or catalyst loading - WHSV, can be increased in order to lower catalytic reaction severity, for example: lowering the contact time of the bio-vapours with the catalyst by using a fluid bed catalytic reactor as opposed to a fixed bed. Throughout the literature the factors contributing to catalytic reaction severity are altered by the reactor set-up, catalysts and operating procedures employed.

3.4 Literature review

3.4.1 Background and scope

The use of catalysts to chemically modify biomass derived products has been investigated by several research organisations (91, 92, 93). The scope of biomass feedstocks, thermochemical conversion methods, age and phase of biomass-derived products, catalytic modification type and arrangement, presence of co-feeds, diluents and types of catalyst used is enormous. The breadth of work carried out is considered briefly here.

The current study considers the atmospheric pressure catalysis of bio-vapours (i.e. pyrolysis products in the vapour phase prior to condensation) from the fast pyrolysis of wood feedstocks only.

Atmospheric pressure vapour phase catalytic modification has been carried out on the biomass-derived products from a range of thermochemical processes, such as:

- freshly produced fast pyrolysis vapours modified at the University of Waterloo (141) and the National Renewable Energy Laboratory (93);
- revapourised conventional pyrolysis products modified at the Mobil Research and Development Corporation (130);
- revapourised high pressure liquefaction products modified at the University of Saskatchewan in Canada (142); and
- revapourised vacuum pyrolysis liquids modified at the University of Laval in Canada (143).

Atmospheric catalysis has been carried out on biomass pyrolysis products at different stages of production and storage. Researchers at the University of Leeds, the National Renewable Energy Laboratory and the University of Laval (147, 93, 143) carried out atmospheric pressure catalysis on freshly produced pyrolysis vapours whereas researchers at the University of Saskatchewan (142) and Mobil Research and Development Corporation (130) carried out atmospheric pressure catalysis on revapourised products (liquids at room temperature) which had been stored for unspecified amounts of time prior to catalysis. The most commonly used atmospheric pressure catalyst is ZSM-5, or it's protonated form HZSM-5, although other zeolites such as larger pore zeolites (144); clays such as silica alumina (141), alumina phosphates (145) and bentonite (146); and metal salts (147) have been used also.

In addition to catalysis of pyrolysis products, studies on the effect of catalysts on biomass model compounds have been conducted by various researchers (148, 149, 93, 139). Valuable insight has been gained into the catalytic reaction pathways, over zeolites in particular, of specific biomass pyrolysis liquid compounds (150). Only a small proportion of the total number of compounds present in biomass-derived pyrolysis products have been studied, however, which can only approximate the reactions occurring during pyrolysis of the total liquid as numerous uncontrolled interactions occur between components during the pyrolysis and catalysis stages.

The majority of investigations into the catalytic modification of biomass derived pyrolysis products have employed fixed bed catalytic reactor systems (136, 142, 143, 149). The review of the literature presented in this chapter will focus on studies carried out at the National Renewable Energy Laboratory in the U.S. since this is the only organisation to have employed catalytic modification of freshly produced fast pyrolysis biomass vapours. Catalytic modification of freshly produced pyrolysis vapours at the University of Leeds and the University of Laval are not discussed here as the pyrolysis process at Leeds does not conform to the strict definition of fast pyrolysis due to vapour residence times in excess of 2 s (151) and the process at Laval is according to the vacuum pyrolysis process.

3.4.2 Catalysts

ZSM-5 zeolite, in various forms, was used mainly during catalytic modification of biomass pyrolysis vapours at the National Renewable Energy Laboratory. Zeolites are porous aluminosilicates readily absorbing water which can be driven off on heating. The primary structure consists of four oxygen anions surrounding a silicon or aluminium cation. Their spatial arrangement is tetrahedral and each O^{2-} anion is shared by another silica or alumina tetrahedron forming a three dimensional crystal lattice. Each silicon ion possesses a +4 charge which is neutralised by 4 electrons, one from each of the O^{2-} ions, whereas each aluminium ion possesses a +3 charge and the 4 electrons surrounding it create a residual charge of –1 which is balanced by an additional cation in the zeolite structure, such as NH_4^+, H^+ or Na^+.

Silica and alumina tetrahedra are arranged into secondary building blocks, e.g. octahedral shapes, in which openings are formed by rings of linked oxygen atoms alternating with silicon and aluminium atoms. The shape of the secondary building block, or unit, defines the zeolite family that the structure belongs to. The units are linked together in different arrangements, which describe the specific zeolite, to form a porous network with a very large effective surface area. The secondary building block of ZSM-5, belonging to the pentasil family of zeolites, is formed by an arrangement of five-membered oxygen rings.

The units form a structure containing parallel pores, straight in one direction and sinusoidal in the other. The sinusoidal channels are 5.1 by 5.5 Å whereas the straight walled channels are 5.4 by 5.6 Å (152).

Zeolites are known as shape selective catalysts as they limit the entering and exiting of compounds from their pore structure depending on size and shape. There are three types of shape selectivity: reactant selectivity, product selectivity and reaction selectivity (153). Reactant selectivity relates to the shape and size of compounds which may enter the zeolite pore structure, preventing compounds which are too large or the wrong shape from entering and taking part in the catalytic reaction. Reaction selectivity originates in the effects of pore size on the transient molecular complexes inside the zeolite cavities which are necessary to produce certain products. Product selectivity is caused by isomeric products which have different diffusivities due to steric effects. An example of product selectivity is the alkylation of toluene with methanol over modified ZSM-5 which yields p-xylene in preference to o- or m-xylene due to a restriction in the effective diameter of the zeolite channels caused by the modification (153).

Throughout this review, the term 'catalytic modification' is used to describe any catalytic processing of biomass pyrolysis vapours or liquids or the incorporation of catalysts into a biomass pyrolysis process. The term 'bio-vapour catalysis' refers to catalytic action upon fresh pyrolysis vapours alone. The scope of this research is to investigate the modification of fresh biomass pyrolysis vapours via catalysis and to characterise the liquid products with a view to improving them with respect to either fuel application or chemical extraction.

3.4.3 Introduction to the National Renewable Energy Laboratory

As explained in Section 3.4.1 the National Renewable Energy Laboratory in the U.S. is the only organisation which carries out atmospheric pressure vapour phase catalytic modification of biomass derived products considered in detail in the literature review. A considerable amount of research into the catalytic modification of pyrolysis vapours in close coupled secondary reactors has been carried out by the National Renewable Energy Laboratory (NREL), a section of the U.S. Department of Energy, with a view to producing olefins and fuel products such as gasoline range hydrocarbons and fuel oil.

Fixed bed tubular catalytic reactors have been used at the micro, bench and plant scale containing 1-5 g, 100 g and 8.5 kg catalyst for biomass vapour feed rates of up to 10 g h^{-1}, 250 g $h^{-1}$and 260 kg h^{-1} respectively. The majority of work reported is from the micro tubular reactor which existed in many modified forms in order to allow variation of catalyst temperature, weight hourly space velocity (WHSV), the presence of co-feeds, carrier gas, pyrolysis vapour partial pressure, catalyst activation and catalyst dilution whilst screening the product vapours in real time using a molecular beam mass spectrometer (MBMS). Only experiments using fresh wood vapours for catalysis are considered here, i.e. those which involve pyrolysis of wood immediately prior to the catalytic reactor or zone.

3.4.4 Production of pyrolysis vapours

Fresh biomass pyrolysis vapours were used in all the catalytic experiments which were produced from solid biomass by either pyrolysis vapour generators - such as the contact pyrolysis vapour generator (154, 155) - for the micro catalytic studies or a vortex reactor for the 100 g and 8.5 kg studies. The 100 g catalytic reactor used pyrolysis vapours on a slipstream from the vortex (156) whereas the 8.5 kg catalytic reactor processed the whole vortex reactor stream (157). The pyrolysis vapour generators used were not always specified. Evans and Milne (158) found, however, that the mass spectra of the primary vapours from birch dowels pyrolysed in different pyrolysis vapour generators demonstrated only minor differences indicating that catalytic modification of vapours produced in different vapour generators can be compared directly. Oak, pine, birch and bass wood were all used as feedstocks.

3.4.5 Catalysts and preparation methods used

Zeolite catalysts were used in the majority of experiments. ZSM-5 was used in either the hydrogen or ammonium form. ZSM-5 was used in both the pure and an extrudate form and studies were carried out on fresh, deactivated and regenerated catalyst. Other zeolites were used but were not specified. Catalyst preparation procedures are detailed and given in Table 3.2 with other experimental details.

Table 3.2 Post fast pyrolysis catalytic reaction experiments carried out at the National Renewable Energy Laboratory

R.S.[a] No.	Feed	Pyrolysis Details	Co-feed (Biomass :Co-feed Ratio)	Reactor	Reactor Details	Catalyst	Catalytic Treatment	Temp.[b] (°C)	Vapour Residence Time[c] (s)	Carrier (Vol% pyr. vaps)	WHSV (h^{-1})	Results	Ref.[d]	Year
1	Pine bio-vapours	Pine splints (methanol pulsed)	None	Micro	Tubular reactor	Pure ZSM-5: 0.3 g loosely packed or 0.6 g on quartz wool [1]	None described	500	1-2	Helium (0.7)[e]	5-6 (wood), or 12 (methanol)	Verified activity of pure ZSM-5 and upper temperature limit of 600°C	(154)	1986
1	Pine bio-vapours	Pine splints (methanol pulsed)	None	Micro	Tubular reactor	Pure HZSM-5 on quartz wool [2]	550 °C nitrogen flow for 18 hours	400-500	1-3	Helium (1.0 wt%)[f]	6 (wood), or 16 (methanol)	Reaction pathway proposed: carbohydrates convert to furanic compounds which convert to aromatic compounds	(152, 159)	1987
1	Pine bio-vapours	Pine splints (methanol pulsed)	None	Micro	Tubular reactor	Partially deactivated pure HZSM-5 [3]	550 °C nitrogen flow for 18 hours	500	1-3	Helium (1.0 wt%)[f]	6 (wood), or 16 (methanol)	Furanic compounds are still produced from carbohydrates after partial deactivation but are not converted to aromatics	(159)	1987
1	Pine bio-vapours	pine splints (methanol pulsed)	Steam (1:2 nitrogen to steam)	Micro	Tubular reactor	Extruded HZSM-5 pellets in alumina binder [4]	None – used as received	500	1-3	Helium, nitrogen (1.0 wt%)[f]	0.9 (wood)[e], or 2.4 (methanol)[e]	Alkylated naphthalenes and high molecular weight lignin compounds more predominant than with fresh catalyst	(159)	1987
1	Birch and pine vapours	Birch splints, pine powder boats (pulsed with carrier)	Methanol (1:1 wt ratio methanol to wood)	Micro	Tubular reactor	Pure HZSM-5, HZSM-5 pellets in unspecified binder	Pellets ground to 250-350 mm	500	Not given	Helium (1.0)[h]	2.9 (wood), or 2.8 (methanol)	Synergistic effect of bio-vapour and methanol co-feeding observed producing more aromatic gasoline products	(160)	1988

Table 3.2 continued Post fast pyrolysis catalytic reaction experiments at the National Renewable Energy Laboratory

R.S.[a] No.	Feed	Pyrolysis Details	Co-feed (Biomass :Co-feed Rratio)	Reactor	Reactor Details	Catalyst	Catalytic Treatment	Temp.[b] (°C)	Vapour Residence Time (s)[c]	Carrier (Vol% Pyr. Vaps)	WHSV (h^{-1})	Results	Ref.[d]	Year
2	Basswood bio-vapours	Not specified apart from pulse flow	Steam (0.6 steam to biomass ratio)	Micro	Tubular reactor modified for dual flow	ZSM-5 extrudate [5] unspecified zeolites [6]	ZSM-5 ground to 350-700 µm	550	Not given	Helium (vol% pyr prods not given)	0.7, 7, 10	High yields of hydrocarbons at high WHSVs and low steam to biomass ratios	(161)	1991
2	Lumber yard pine splints	Pine splints (methanol pulsed)	None	Micro	Tubular reactor modified for dual flow	HZSM-5 extrudate	Ground to 350-700 µm [7] and dried at 500°C in helium	475-550	Not given	Helium (4-12 vol%)	1-6	Demonstrated combined effects of WHSV, catalyst temperature and pyrolysis vapour partial pressure on reaction severity	(162)	1988
3	Pine vortex vapours	1-3 % slipstream from vortex	Steam (100 % of carrier)	100 g	Tubular reactor	Extrudate HZSM-5 [8]	None specified	525 and above (not specified)	Not given	Steam	Not given	Showed agreement between 100 g and 1 g reactors and that bio-vapour reactions over ZSM-5 were mildly exothermic	(157)	1994
3	Softwood vortex vapours	1-3 % slipstream from vortex	Steam (steam to biomass wt ratio 2:1)	100 g	Tubular reactor	Extrudate HZSM-5 [8]	Unspecified regeneration from previous run	400-500	0.5 (transfer line prior to cat bed)	Steam, N_2 tracer (45 wt% pyr prods) [i]	2.44	Presence of catalyst increased production of alkenes and COx and reduced alkanes and hydrogen, 10 wt% yield of gasoline from dry wood	(156)	1988
4	Southern pine vortex vapours	Whole vortex stream	Steam (steam to biomass 1.33:1)	7.5-8.5 kg	Tubular reactor	Extrudate ZSM-5	1	520	Not given	Not specified	1.6-19	Confirmed bio-vapour reactions over ZSM-5 to be exothermic, decreasing over time	(157)	1994

Where catalyst sources and types in Table 3.2:

[1] pure ZSM-5 obtained from Mobil, no further details given;

[2] pure HZSM-5 catalyst obtained in the ammoniated form and converted to HZSM-5 by heating at 550 °C in a low flow of nitrogen for 18 hours;

[3] deactivated pure HZSM-5 prepared by deactivating fresh pure HZSM-5;

[4] HZSM-5 extrudate obtained from Mobil;

[5] ammonium form of ZSM-5 extrudate obtained from Mobil, packed between quartz wool in reactor;

[6] unspecified zeolites obtained from the University of Utah, packed between quartz wool in reactor;

[7] HZSM-5 in 1.6 mm pellet extrudate in an unspecified binder supplied by Mobil; and

[8] 1.4 mm extrudate ZSM-5 containing catalyst referred to as MCSG-2, thought to have a high silica to alumina ratio, supplied by Mobil Research and Development Corporation.

Notes indicated in Table 3.2:

[a]: Reactor system;

[b]: Temperature;

[c]: in the reactor;

[d]: Reference;

[e]: calculated from a 3.96 g h^{-1} flow of wood vapours in a 2 L h^{-1} stream of helium and assuming an average molecular mass of wood vapours of 100 Daltons;

[f]: quoted on a weight basis;

[g]: WHSV quoted are apparent as the ratio of active catalyst in the binder was not known;

[h]: approximation made in the literature based on 30 mg wood fed over 30 s with a weight of carrier gas to wood vapour of 4, assuming an average molecular mass of 100 Daltons for wood vapours; and

[i]: calculated from wood flow rate of 18.5 kg h^{-1}, steam to biomass ratio of 1.2 and nitrogen tracer flow rate of 0.224 kg h^{-1}.

3.4.6 Reactor system 1 – Micro catalytic reactor

The reactor system consisted of two quartz tubes in vertical series, each 2 to 2.5 cm diameter by 25 cm (163, 164). The helium carrier gas was preheated in the lower tube which acted as a pyrolysis zone (159). The upper reactor tube formed the catalytic reactor and was packed with 0.3 - 0.6 g of pure ZSM-5 catalyst (5-10 μm) suspended on quartz wool (approximately 3 g) or ZSM-5 containing extruded pellet catalyst (in an unspecified binder). The feedstock was placed in a sample holder at the top of the pyrolysis reactor tube. Typical feedstock weights were 0.03 g solid biomass. The pyrolysis reactor tube and the catalytic reactor tube were heated independently by two separate furnaces.

The micro catalytic reactor was coupled to a molecular beam mass spectrometer (MBMS) throughout the experiments to measure the product distribution in real time. Initial mass balances could not be obtained as the real time analysis allowed only qualitative relationships between reaction parameters and product distributions to be studied as the catalysed vapours entering the MBMS were not measured, although it should have been possible to make an approximation based on the average wood feed rate and the average carrier gas flow rate throughout the experiment. In a modification to the micro catalytic reactor an additional tube around the pyrolysis vapour generator was included to allow a flow of tracer gas to bypass the pyrolysis zone, in a 'dual' flow, before mixing with the pyrolysis vapours prior to the catalytic bed. The tracer gas flow rate was measured throughout and the tracer gas could be identified from the MBMS spectra which allowed quantification of the product vapours. A description of the dual reactor system and results obtained are presented in Section 3.4.7.

3.4.6.1 Description of preliminary quartz tube catalytic reactor experiments

Reed et al. (154) conducted preliminary experiments with a sample of pure ZSM-5 catalyst obtained from Mobil. Catalyst and experimental details can be found in Table 3.2. The objective of the work was to determine the optimum operating conditions for the conversion of biomass pyrolysis vapours to premium liquid fuel components (i.e. gasoline range hydrocarbons) over the catalyst. Pine wood vapours, produced in a preheater tube, were pulsed alternately with methanol over a catalyst bed.

The approach of pulsing reactants through a reactor is commonly used in screening purposes as, combined with a suitable product determination method, it provides a simple method with fast product identification for testing different reactants and reaction conditions (165, 166). The duration of the pulses was not specified in any reported NREL experiments but it would be expected that they would be in the region of 0.5-2 s in line with other researchers (167). It was reported that a pine vapour WHSV of 5-6 h^{-1} and a methanol WHSV of 12 h^{-1} resulted. Further experimental conditions are detailed in Table 3.2. Mass balances could not be determined for the preliminary experiments of Reed et al. (154), as there was no facility for product measurement with the system used, only the change in relative proportions of products from the MBMS spectra. They reported that the ZSM-5 catalyst was active for modification of pine fast pyrolysis vapours. Product details from these experiments can be found in Section 3.4.6.3.

3.4.6.2 The effect of catalyst activation on pure HZSM-5

Evans and Milne (159) studied the catalytic products derived from pyrolysis of pine vapours in the presence of HZSM-5 catalyst and compared them to products derived from methanol catalysis over pure HZSM-5. It was not possible to measure product yields in the system employed. They found from MBMS spectra of evolving products that methanol was converted to a mixture of C_2-C_6 olefins, toluene, xylene and trimethybenzene over HZSM-5 at 500 °C and a WHSV of 16 h^{-1}. Trimethylbenzene was the largest molecular weight product at 120 Daltons. All of the pine pyrolysis products were reported to appear to be converted to a mixture of aromatic hydrocarbons and some furanic species, irrespective of reactant molecular size, over fresh HZSM-5 at 500 °C and a WHSV of 6 h^{-1}.

The majority of catalytic products from pine pyrolysis vapours were reported to be below a molecular weight of 150 Daltons - i.e. methylnaphthalene and lower. It was suggested that the larger molecules were either converted to coke or cracked at acid sites on the outer surface of the catalyst, or binder, to smaller components since larger pyrolysis products would be prevented from entering the catalyst pores due to 'reactant' shape and size selectivity and all pyrolysis products were reported to be converted (170). It is also possible that some thermal cracking and cracking on the char occurred of larger molecules, allowing them to enter the catalyst pores.

At lower pine pyrolysis vapour WHSVs of 1-2 h^{-1} (achieved by reducing the flow rate of vapours over the catalyst corresponding to an increased reaction time from 1-3 s) larger products such as methylated naphthalenes became more prevalent (152). The increase in reaction time, from 1 s to 3 s, may have caused partial catalyst deactivation but this was not commented upon in the paper. Diebold et al. (152) suggested that the relative increase in the amount of larger products may have been due to macrosurface catalysis. The suggestion that the formation of larger compounds occurs outside the zeolite pore structure was supported by Dejaifve et al. (170) who studied the reaction pathways of methanol and olefins over HZSM-5 zeolite at a temperature of 370 °C and liquid hourly space velocities (LHSVs – defined as L feed / L catalyst / hour) from 0.7-11 h^{-1}. They reported (170) that there was an upper limit of C_{10} for compounds produced within the HZSM-5 pore structure which they observed by GC-FID (gas chromatography, flame ionisation detector) analysis which was due to size constraints within the HZSM-5 pore structure and hence the formation of polycyclic compounds and polyalkylnaphthalenes (> C_{10}) occurred outside the pore structure. They suggested that polycyclic and polynaphthalenes may act as coke precursors. Aromatics are known to form tar on metal surfaces which dehydrogenate to give coke (171). The high molecular weight of polycyclic and polynaphthalenic compounds prevents them entering the HZSM-5 pores which explains the high resistance of HZSM-5 to coking compared to larger pore zeolites.

If the catalyst in the Diebold et al. (152) experiments had undergone partial deactivation at the higher reaction time of 3 s, molecules may have been prevented from entering the catalyst pores due to coke deposition on the catalyst surface. In this case, macrosurface catalysis, possibly involving a catalytic effect of the coke, may have been responsible for the increased yield of larger molecular weight products since in the absence of catalysis, thermal reactions alone at 500 °C and just above (up to 600 °C) and at residence times of at least 1 s cause cracking of high molecular weight lignin-derived compounds to lighter aromatics and oxygenates (168). Water, carbon monoxide and carbon dioxide were reported to represent a substantial portion of the yield (159) although product yields could not be determined with the screening system used and their relative amounts compared to those resulting from pyrolysis alone were not commented upon.

Evans and Milne (159) continued the studies using deactivated HZSM-5 catalyst. Information was not given, however, on the degree of pyrolysis vapour processing required to deactivate the HZSM-5. Conversion of some pyrolysis vapours was found to occur after partial catalyst deactivation as a mixture of uncatalysed and catalysed products was observed from GC-MS spectra of the pine derived product stream. This was similar to the GC-MS product spectra from previous experiments when reaction time of pyrolysis vapours was increased from 1-3 s, corresponding to a change in WHSV from 6-2 h^{-1}, and the GC-MS spectra showed more prevalent lignin peaks and generally larger masses evolving over partially deactivated HZSM-5 than those evolving over fresh HZSM-5. This indicated that partial deactivation had occurred during 'fully activated' catalyst experiments at a WHSV of 2 h^{-1}, as opposed to a WHSV of 6 h^{-1}, where the reaction time was extended to 3 s.

3.4.6.3 Reaction pathway of wood pyrolysis vapours over ZSM-5 catalyst

Reed et al. (154) reported that the wood derived pyrolysis vapours appeared to be converted by the fresh pure ZSM-5 catalyst to volatile hydrocarbons. This would imply that no or few oxygenated species remained after catalysis but this was not supported by subsequent experimentation of ZSM-5 catalysed wood pyrolysis vapours. Reed et al. (154) proposed that furanic species may be intermediates in the ZSM-5 catalysis of pine wood pyrolysis vapours to hydrocarbons.

Other researchers have found acids to promote the production of furanic species during thermal reaction of biomass via acid pretreatment (172) and ZSM-5 catalysis, specifically, to promote the production of furanic species (177). Pavlath and Gregorski (172) observed the production of furfural and furfuryl alcohol during pyrolysis of $ZnCl_2$ acid pretreated carbohydrates, such as cellulose and cellobiose, in a thermogravimetric analyser (TGA) and suggested that the production of furfural was promoted by the acid. Chen et al. (177) reported that hydrolysis of cellulosic materials generated a large proportion of furfural and it's derivatives whose yields were observed to increase in the presence of HZSM-5.

Reed et al. (154) found that the relative yields of furan and methylfuran, thought to be intermediates in the conversion of pyrolysis vapours to hydrocarbons, in the catalysis products increased with decreasing catalytic activity. This was attributed to coking throughout the experiment which was believed to reduce catalyst activity, thus preventing the complete conversion of pyrolysis vapours to hydrocarbons.

Grandmaison et al. (91) carried out model compound studies on furfural over HZSM-5 and found that it decarbonylated over HZSM-5 to produce furan and formaldehyde. The formaldehyde was found to rapidly polymerise to paraformaldehyde whilst the furan further reacted to produce benzofuran, from condensation reactions and polymeric materials, via opening of the furan ring at temperatures between 400-450 °C and LHSVs of 0.56-1.36 h^{-1}.

Diebold et al. (152) reported that carbohydrates were converted over HZSM-5 to furanic compounds and then to aromatic hydrocarbons. Diebold et al. (152) reported that partially deactivated HZSM-5 catalyst possessed enough activity to convert carbohydrates to furan derivatives but not enough activity to convert them to aromatic hydrocarbons. It was suggested that the conversion of carbohydrates to furans occurred on weak acid sites although Diebold et al. did not attempt to postulate the nature of the 'weak' acid sites. There was no information provided by Mobil, who supplied the catalyst to Diebold et al., of the procedure used to prepare the HZSM-5 sample used for these experiments or details of acid site strength and frequency. This is usually the case with literature relating to commercial zeolites and ZSM-5 in particular.

It is possible that Diebold et al. were referring to Lewis acid sites as 'weak' acid sites as opposed to Bronsted acid sites and this would presume that the Bronsted sites were deactivated in preference to or before Lewis acid sites. It is probable that there were no Lewis acid sites on the initial HZSM-5 sample at all as the type, and strength, of acid sites on zeolites depends upon the method of preparation (173). The working conditions that a zeolite is subjected to may also alter the activity that it exhibits (174).

Fajula (174) indicated that H-form zeolites, HZSM-5 in this case, possess only Bronsted acid sites as all the 1- alumina tetrahedra are accompanied by a charge balancing proton. When the H-zeolite is heated above 600 °C (which was not the case in these experiments), the protons are driven off leaving the unbalanced aluminium tetrahedra which has electron-pair acceptor properties, i.e. it is a Lewis acid (175). It is also possible that zeolites can possess sites of Lewis and Bronsted acidity at the same time and in this case interactions between the sites may occur which enhance overall acidity (173).

It appears likely that the HZSM-5 catalyst used in the Diebold et al. (152) experiments contained Bronsted acid sites only. Without further information on the mechanism of catalyst deactivation it is not possible to know whether Lewis acid sites were created during the course of the reaction. Suggestions, therefore, about the nature and strength of HZSM-5 acid sites in the pyrolysis vapour environment can only be extremely tentative due to the lack of catalyst property information provided and the potentially complicated effects of the system.

In the catalyst experiments of Diebold et al. (152) reactions of biomass pyrolysis vapours over fresh active HZSM-5 produced practically no furan derivatives but a range of aromatics were found in the final products. Furans were identified as intermediate products in the conversion of carbohydrates to aromatics over active HZSM-5. The formation of furans in HZSM-5 modification of biomass vapours was considered by Diebold et al. (152) to be analogous to the formation of the intermediate dimethyl ether in the modification of methanol over HZSM-5 (176). The dimethyl ether intermediate produced during HZSM-5 processing of methanol is ultimately converted to aromatic compounds over active catalyst but not over partially deactivated catalyst (152). The production of the dimethyl ether intermediate continues after partial deactivation of the HZSM-5 catalyst although aromatic compounds are no longer produced.

As would be expected, Reed et al. (154) found that at ZSM-5 catalytic reactor temperatures above 600 °C a significant increase in the yield of permanent gases resulted with a corresponding decrease in the yield of liquid products due mainly to secondary thermal cracking reactions.

The reduction in the yield of liquid products from biomass due to thermal cracking reactions is a known phenomenon in pyrolysis at high temperatures (>600 °C) (14) and provided an upper temperature limit on the catalytic studies for Reed et al. (154).

Other researchers catalytically processing biomass derived vapours also studied catalyst temperatures below 600 °C (177, 178, 179, 180).

3.4.6.4 The effect of catalyst temperature on pure catalyst

Diebold et al. (159) also investigated the effect of catalyst temperature on the pure HZSM-5 catalyst in the range 400-500 °C but the relationship to product yields was not clear. It would be expected that an increase in temperature between 400-500 °C would increase the reaction severity of the catalysed reactions. The yield of oxygenated compounds in the product liquid from wood pyrolysis vapours converted over the pure HZSM-5 catalyst was lower and the yield of aromatic compounds was higher than wood pyrolysis vapours which did not undergo catalytic processing. The gaseous products from HZSM-5 catalysis of pyrolysis vapours contained a higher proportion of carbon oxides than those from pyrolysis alone. For hydrocarbon production it is desirable that the ratio of the yields of carbon oxides to water ($(CO+CO_2)/H_2O$) is as large as possible since it is preferable to remove oxygen as carbon oxides rather than water so that the hydrogen can be retained for hydrocarbon forming reactions.

Wood pyrolysis vapour processing over HZSM-5 by Diebold et al. (152) resulted in the following trends (between 400-500 °C):

- the $(CO+CO_2)/H_2O$ product ratio apparently increased with catalyst temperature which suggests a greater extent of decarbonylation and decarboxylation at 500 °C compared to 400 °C;
- the ratio of aromatics and aliphatic hydrocarbons (BTX+alkenes) to gaseous oxygenates ($CO+CO_2+H_2O$) also increased with catalyst temperature which indicated that catalytic reactions were predominant to thermal reactions;
- the ratios of aromatics to alkenes (BTX/alkenes) and aromatics to furans (BTX/furans) increased with catalyst temperature indicating a higher catalyst reaction severity at 500 °C compared to 400 °C;

- the ratio of benzene to alkyl benzene increased with catalyst temperature, demonstrating a tendency for dealkylation at higher temperatures; and
- the ratio of low molecular weight aromatics to high molecular weight aromatics (BTX/naphthalenes) increased with catalyst temperature.

The observed product ratio trends indicated that catalytic reaction severity increased with temperature between 400-500 °C resulting in a greater extent of decarbonylation and decarboxylation which led to preferential aromatics production.

3.4.6.5 The effect of catalyst dilution by using extrudate catalyst

Diebold et al. (159) also studied the performance of extrudate HZSM-5 obtained from Mobil in pelleted form. The catalyst was supported in an unspecified alumina binder which effectively diluted the active catalyst component. The experimental conditions employed are presented in Table 3.2. An apparent WHSV of 0.9 h^{-1} for wood pyrolysis products and 2.4 h^{-1} for methanol was used, the real WHSV of g reactant/g active catalyst component/ hour would be higher but could not be calculated as the percentage of pure HZSM-5 in the extrudate was not known. Typical zeolite catalysts for industrial scale cracking are composed of about 3 to 25 wt% of a zeolite embedded in a silica-alumina matrix (175).

The yield of alkylated naphthalenes from pine wood pyrolysis vapours over extruded HZSM-5 was greater than the yield over pure HZSM-5 catalyst over the 400-500 °C temperature range studied. This provides evidence for a decrease in catalytic reaction severity with catalyst dilution as strong catalytic effects cause the cracking of higher molecular weight compounds and contribute to dealkylation at higher temperatures (i.e. 500 °C rather than 400 °C). As the catalyst deactivated throughout the experiment, the proportion of primary products and intermediate (furan and methyl furan from wood) products were reported to increase as was the case with pure catalyst. High molecular weight lignin species were the predominant products from pyrolysis vapour processing over extruded HZSM-5 for both pine and aspen wood samples which is unexpected as generally the high molecular weight species would be cracked into smaller components. This is dissimilar to the case with pure HZSM-5 demonstrating a reduction in catalyst reaction severity with catalyst dilution.

GC-MS results from Diebold et al. (152) experiments processing pine pyrolysis vapours over an extrudate HZSM-5 containing catalyst showed that the precursor monomer peaks for coniferyl alcohol were not present alongside the other primary species. Diebold et al. suggested that the coniferyl alcohol precursor monomer peaks were coking on the catalyst but it is possible that they were reacting or cracking to produce different compounds. It is possible to remove the coniferyl alcohol precursor monomer from the pyrolysis vapour stream by pretreating the wood with acid (182). Alternatively the coniferyl alcohol precursor monomer can be removed by thermal cracking of the pyrolysis vapours at 500-600 °C prior to contact with the catalyst although an increased yield of permanent gases occurs at the expense of a significant reduction in the yield of oil (183). Renaud et al. (179) studied the effect of passing pyrolysis vapours through a precoker/preheater prior to catalysis over HZSM-5 and condensed heavier components out of the vapour stream before passing the lighter components over the catalyst bed. Renaud et al. (179) used vacuum pyrolysis oil for these studies which was vaporised prior to catalysis resulting in a tertiary catalytic mode. Significant decreases in the extent of coking were observed. Czernik et al. (86, 184) carried out preliminary thermal cracking between 450-700 °C at a residence time of 0.7 s and observed similar products from the pyrolysis vapours apart from an increase in gaseous compounds and smaller compounds. They did not, however, pass the resulting product stream over a catalyst.

3.4.6.6 The effect of regeneration on extrudate catalyst

Processing of wood pyrolysis vapours over 'quickly' regenerated catalyst, via coke burn off in the reactor, resulted in lower concentrations of primary products compared to those evolved in the presence of deactivated catalyst. The levels of furan and dimethyl furan from wood pyrolysis vapours, however, were higher in the presence of the quickly regenerated catalyst than those produced in the presence of the active catalyst. This demonstrates that 'quickly' regenerated catalyst via coke burn off in the reactor improves the activity of deactivated catalyst but not to the original level of fresh active catalyst.

This is analogous to fluid catalytic cracking catalyst whereby catalyst is continually recycled and regenerated during the process and a proportion of fresh catalyst is added continuously. The average catalyst activity in the reaction chamber is slightly lower than fully activated catalyst which is due mainly to very rapid initial catalyst deactivation followed by a more controlled deactivation, a process that has been observed with both methanol (191) and pyrolysis vapours (185).

3.4.6.7 The effect of carrier gas

Diebold et al. (152) studied the catalytic modification of wood vapours over HZSM-5 in helium, nitrogen and nitrogen/steam (1:2) to determine the effect of carrier gas on product distribution. Product distributions achieved with helium and nitrogen were similar except that with nitrogen, the ratio of benzene to furan and xylene was lower than with helium. The benzene level was even lower when using nitrogen/steam as a carrier.

Wood vapours were pulsed periodically over the HZSM-5 catalyst bed in order to study the effect of wood vapour conversion with catalyst time on stream. After sequential wood pulses, the changes in evolved product ratios were greater when using a steam (nitrogen to steam ratio 1:2) carrier than helium (100 % helium). After 10 sequential wood pulses, the ratio of intermediates to benzene, toluene and xylene (BTX) increased by 181 % in steam compared to an increase of only 13 % in helium. The increase in pyrolysis vapour products with sequential wood pulses was approximately the same for nitrogen/steam (1:2) and helium and the ratio of BTX/naphthalenes decreased in both cases demonstrating a reduction in catalyst activity with time on stream. The ratio of benzene to toluene was lower in the presence of both nitrogen/steam and helium than in the presence of nitrogen alone. The presence of steam during the reaction appeared to lower the rate of catalyst coking. This may be due to the steam occupying the catalyst pores and preventing entry of coke or coke precursors. This phenomenon would also be expected, however, to reduce overall activity. A second possibility is that the steam reacts with the coke precursors preventing them from producing coke. Sharma and Bakhshi (178) also found the presence of steam reduced the amount of coking on the catalyst during their studies involving catalytic modification of revapourised Ensyn bio-oil over HZSM-5 in a fixed bed catalytic reactor.

3.4.6.8 The effect of co-feeding methanol

Evans and Milne (186) studied the effect of passing birch and pine wood vapours, generated in a preheated pyrolysis reactor, over catalysts at 500 °C in a flow of hot carrier gas. Experimental conditions are given in Table 3.2. Catalysts used were HZSM-5 in it's pure form, for preliminary experiments, followed by an extrudate HZSM-5 containing catalyst in an unspecified alumina binder.

They reported that there was some absorption of water and light aromatics on to the catalyst when the vapour first contacted the catalyst but specific details were not given (186). Deactivation and coking details were not given either. Comparative catalyst studies on wood pyrolysis liquids using other acid type catalysts including wide-bore molecular sieves and silica/alumina were also carried out. These experiments demonstrated an increase in the production of high molecular weight compounds, such as methylated naphthalenes, compared to experiments with the HZSM-5. This was thought to be due to the larger pore sizes as opposed to the limited sizes of compounds produced over HZMS-5 (170). Further details were not given.

Evans and Milne (186) carried out experiments in which equal weights of wood pyrolysis vapours and methanol were co-fed. There were marked changes in certain product ratios from wood converted over HZSM-5 in the presence of methanol. For example, the ratio of light aromatics to inorganic (water, CO and CO_2) products increased by at least 3 times when wood pyrolysis vapours were processed in the presence of methanol. The ratio of trimethylbenzene to toluene also increased by a factor of 10 when methanol was co-fed. Finally, the ratio of carbon dioxide to water increased by about a third when co-feeding methanol indicating a greater extent of decarbonylation and decarboxylation and thus rejection of oxygen as CO_2 was possible in the presence of methanol whilst hydrogen was retained for hydrocarbon forming reactions instead of combining with oxygen in the form of water.

Contrary to the results of Evans and Milne (186), Chen et al. (130) found that the carbon dioxide production was eliminated when processing wood pyrolysis liquids and methanol together over HZSM-5 at 410 °C and 1 h^{-1} WHSV (in a 11:8 wood liquids to methanol ratio) as opposed to a yield of carbon dioxide of 7.6 wt% from wood liquids (wt% wood liquid fed) processed alone under the same conditions.

Chen et al. (130) also observed a corresponding increase in the yield of water when methanol was processed with wood liquids from 48 wt% (wt% wood liquid fed) for wood liquids processed alone to 62 wt% (wt% wood liquid fed) for wood liquids processed with methanol. These opposing findings by Chen maybe due to difference in catalyst temperature and the wood liquids used by Chen et al. (130) were which produced by a conventional pyrolysis method (wood sample heated at 20 °C min^{-1} up to 520 °C and held for 3 hours in 800 mL min^{-1} of helium) and as such were fundamentally different to the fresh pyrolysis vapours used by Evans and Milne (186).

It was hypothesised by Evans and Milne (186) that methanol, in the presence of wood pyrolysis vapours, does not undergo the dimethyl ether conversion step to alkenes as it does when pyrolysed alone, but rather reacts directly with the wood-derived products to form alkylated aromatics (186). The increase in methylated benzenes would be expected to occur at the expense of the normal distribution of products formed from pure methanol.

3.4.6.9 The effect of catalyst temperature and WHSV

Evans and Milne (186) also studied the effect of WHSV and temperature on the conversion of pine pyrolysis vapours over HZSM-5 at temperatures between 300-550 °C and WHSV's of 0.7-4.0 h^{-1}.

The proportions of organic products that form over HZSM-5 were reported to vary systematically with WHSV and temperature (186). This is due to the variation in reaction severity which depends on WHSV and temperature. Dealkylation reactions were found to increase with increasing temperature as indicated by the relative abundance's of trimethylbenzene, xylene, toluene and benzene.

Exact mass balance yields could not be determined from these catalyst screening studies as explained before in Section 3.4.6. Evans and Milne (186) estimated the product yields from 6 runs the average of which is presented in Table 3.3. 2 g of HZSM-5 were used in each run resulting in WHSV's of 4 h^{-1} and the temperature of the catalyst was 500 °C throughout. (Pyrolysis was carried out at 500 °C).

Table 3.3 Product yields (wt% moisture free) from calibrated MBMS runs with birch wood dowels

Compounds	Run Average
Char & coke	25.4
Water	24.9
CO	20.1
CO_2	17.5
Gaseous hydrocarbons	8.7
BTX	6.5
Naphthalenes, indenes and furanic species	3.3
Closure	106.4

There was no significant breakthrough of primary wood vapour organics until the weight of wood/weight of catalyst was about 1 which corresponded to a WHSV of 4-5 h^{-1}. Intermediate products in the conversion of wood vapours over HZSM-5 were furans from the carbohydrates – as discussed before in Section 3.4.6.3 – and phenols from the methoxyphenols derived from the lignin component during pyrolysis. Final products from these intermediates were alkenes, light aromatics and naphthalenes. Much of the oxygen content of the wood feed was rejected as CO and CO_2, their combined yield being 25 wt% of wood fed. The coke yield at 500 °C in helium was approximately 10 wt%. The hydrocarbon yield quoted was 18 ± 4 wt% but includes 8.7 wt% of gaseous hydrocarbons and 1.3 wt% of furanic compounds which are oxygenated organics and not hydrocarbons. The real yield of liquid phase hydrocarbons appears to be approximately 7.5 wt% from dry wood at 4 h^{-1} WHSV and 500 °C over HZSM-5 based on the preliminary calibrated experiments.

3.4.6.10 Model compound studies

Model compound studies investigating the HZSM-5 catalysis of hydroxyacetaldehyde, 5-hydroxymethylfurfural, α-angelicalactone and isoeugenol at between 2-4 h^{-1} WHSV and 500 °C indicated the following trends:

- light oxygenates, such as hydroxyacetaldehyde, give high yields of water, CO and CO_2 with relatively low yields of hydrocarbon products;
- carbohydrate-derived ring compounds, such as α-angelicalactone, gave the greatest yields of aromatics; and
- the methoxyphenols showed lower conversion rates at the relatively high space velocities used.

3.4.7 Reactor system 2 – Dual flow reactor

Milne et al. (162) used a modified version of the micro reactor tube described in Section 3.4.6. It was modified to allow a stream of carrier gas to be passed along an outer tube for tracing purposes. The effect of temperature, WHSV and steam to biomass ratio (S/B) with the different catalysts on the product yields of wood and refuse derived fuel (RDF) vapours was studied. The catalysts were packed between quartz wool, as before. Milne et al. (162) studied the conversion of pyrolysis vapours, from lumber yard pine splints generated in the pyrolysis vapour generator, in a pulsed mode over 1.6 mm HZSM-5 containing extrudate catalyst, from Mobil, in a dual flow fixed bed reactor. The catalyst reactor was coupled to an molecular beam mass spectrometer (MBMS) which allowed very quick identification of catalysed products. The pulsed mode minimised the amount of catalyst required and allowed the MBMS data to be related to the amount of pyrolysis vapour loading experienced by the catalyst. Continuous feeding was not attempted. The experimental conditions are given in Table 3.2.

Milne et al. (162) studied the effects of temperature in the range 475-500 °C, WHSV between 1-6 h^{-1} and pyrolysis vapour partial pressure between 4-12 vol% on the overall yield of hydrocarbons (C_2-C_5 and C_5^+), the ratio of the yields of aromatic species to olefinic species and the ratio of the yield of xylene to benzene.

3.4.7.1 The effects of pyrolysis vapour partial pressure

The main effect of increasing pyrolysis vapour partial pressure on the reaction system was to increase the product yields of both C_2-C_5 and C_5^+ hydrocarbons. This was most likely due to the increased number of pyrolysis vapour molecular collisions at the higher pyrolysis vapour partial pressure which lead to a higher degree of reaction at 12 vol% pyrolysis vapour partial pressure than at 4 vol%. Minor effects of pyrolysis vapour partial pressure were to increase the yield ratio of aromatics to olefins at a WHSV of 1 h^{-1} for all partial pressures studied, at a WHSV of 6 h^{-1} for only the higher partial pressures of 8-12 vol% studied and to decrease the aromatic to olefin product ratio at a WHSV of 6 h^{-1} at the lower partial pressures of 4-8 vol%. The combined effects of WHSV (or catalyst loading) and pyrolysis vapour partial pressure are complicated in this case. It appears that the higher the catalyst loading, the proportionally higher the pyrolysis vapour pressure needs to be for an equivalent amount of reaction severity. This is related to the contact time of the pyrolysis vapour molecules with the catalyst.

3.4.7.2 The effects of catalytic reaction temperature

Increasing the catalyst temperature between 400 to 500 °C increases the yields of C_2-C_5 and C_5^+ hydrocarbons. Increasing the temperature between 500 to 525 °C, however, decreases the yields of C_2-C_5 and C_5^+ hydrocarbons. Optimum temperatures for the production of hydrocarbons over HZSM-5 from biomass pyrolysis vapours or model compounds of biomass vapours by other researchers have typically been between 400-550 °C (187, 147, 188) with slightly lower temperatures for 'tertiary' catalysis of revapourised bio-oils between 290-400 °C (189). One unusual finding was that temperature didn't appear to have an effect on the ratio of yields of aromatic to olefin products. It would be expected that increasing temperature would increase the catalytic activity and therefore the ratio of yields of aromatics to olefins would also increase.

3.4.7.3 The effects of weight hourly space velocity

The effect of WHSV appeared to be dependent on the temperature. At the lower temperature of 475 °C, increasing the WHSV resulted in an increase in the amount of C_2-C_5 hydrocarbons with a slight decrease in the amount of C_5-C_{10} hydrocarbons. At the higher temperature of 550 °C, increasing the WHSV appeared to increase the amount of C_5-C_{10} hydrocarbons relative to the amount of C_2-C_5 hydrocarbons. This may be because at 475 °C the catalytic activity is lower and increasing the WHSV means that fewer vapours are converted completely to C_5-C_{10} hydrocarbons resulting in a higher proportion of uncatalysed pyrolysis vapours whereas at 550 °C the catalytic activity is higher and providing that the WHSV (or catalyst loading) is increased, even if the pyrolysis vapour pressure remains the same, there will still be a greater through put of pyrolysis vapours which may have a 'priming' effect on the catalyst active sites allowing more of the vapours to be converted to C_5-C_{10} hydrocarbons.

3.4.7.4 Summary of work carried out on dual reactor system

The major outcome of this series of experiments was the demonstration of how the reaction severity could be tuned by altering several parameters in conjunction with one another. With any chemical reaction system a certain amount of experimentation is required in order to optimise product yields. There were two optima in this study for C_5-C_{10} hydrocarbon production. These were at 480 °C, 1 WHSV h^{-1} and 12 vol% pyrolysis vapours pressure (in carrier gas) where the yield of C_5-C_{10} hydrocarbon was 8.2 wt% from dry wood and at 530 °C, 6 WHSV h^{-1} and 12 vol% where the yield of C_5-C_{10} hydrocarbon was 8.0 wt% from dry wood.

3.4.8 Reactor system 3 – Scale up to 100 g catalytic reactor

In addition to experiments carried out on a micro reactor scale up studies were carried out on a 100 g catalytic reactor on a slipstream from the vortex reactor. The limited number of operations carried out with the 100 g catalyst reactor showed general agreement with the 1 g catalyst reactor. The catalyst used in the first two experimental series reported, Table 3.2, reactor system 3, was a ZSM-5 containing catalyst called MCSG-2 obtained in 1.4 mm diameter extrudate form from Mobil (156) in a steam environment (steam to biomass 2:1). Further experimental conditions can be found in Table 3.2.

The catalyst used was thought to have a high silica to alumina ratio due to it's increased activity in an elevated temperature, steam environment compared to other zeolite catalysts. (The catalyst was repeatedly regenerated by controlled air oxidation, although the maximum amount of regenerations possible was not reported. It would not be expected that infinite regenerations would be possible without any deleterious affect on the catalyst).

Pine wood vapours were used as feedstock in the first series (157) in the second series they were described only as softwood sawdust pyrolysis vapours (156) and in the third series they were described as wood pyrolysis vapours (190). It is probable that the same pine wood feedstock was used throughout. Steam was co-processed in some of the experiments (see Table 3.2).

3.4.8.1 The effect of steam co-feeding

Diebold and Scahill (156) used steam as a carrier gas, in a 2:1 steam to biomass weight ratio, and found that it reduced the rate of catalyst deactivation at higher temperatures compared to processing in an inert carrier gas such as nitrogen or helium. At these temperatures, the steam reduced the rate of band-aging (the decline in catalyst activity demonstrated by the movement of an exothermic temperature profile down the bed as it deactivated). The exotherm created by the catalyst undergoing deactivation initially experienced a sharp high exotherm over fresh catalyst followed by a lower exotherm which gradually reduced until complete deactivation had occurred (156).

3.4.8.2 The effect of propene co-feeding

Diebold and Scahill (190) studied the co-feeding of wood with propene in order to simulate the effect of recycling olefins produced by biomass pyrolysis which remained after catalytic processing. Co-processing with propene (190) at a rate of 0.064 kg propene per kg wood resulted in 0.062 kg propene per kg wood leaving. The net consumption of propene being 0.002 kg propene per kg wood. In runs without propene co-feeding, 0.02-0.025 kg of propene per kg of wood was produced. This suggests that the net production of propene over the catalyst was suppressed in the presence of higher propene partial pressures which appears to shift the product equilibrium.

At higher partial pressures of propene, Evans and Milne (191) reported a definite synergistic effect in which gasoline yields are increased over the sum of those from propene or wood alone. This synergistic effect is different to the one of methanol co-processing as the propene appears to adjust the equilibrium of products whereas it is thought that the presence of methanol alters the basic reaction paths by providing hydrogen for hydrocarbon forming reactions from the pyrolysis vapours.

3.4.8.3 The effect of reactor design on reaction equilibrium

With a fixed bed reactor it is preferable for the reaction to stop before all the catalyst is deactivated as some deactivation will occur prior to taking the bed out of service for regeneration. It is difficult, however, to estimate how much active catalyst remains inside the reactor and how quickly it will deactivate between the end of the run and complete disassembly of the equipment. This can be overcome by using slightly more catalyst than necessary and is not a problem providing that products resulting at thermodynamic equilibrium are required. If, however, the desirable product is achieved before thermodynamic equilibrium, i.e. the production of intermediate olefin products are required rather than final aromatic products, it is necessary to have just enough catalyst to prevent breakthrough of unwanted products. This balance is difficult to achieve in a fixed bed system but can easily be controlled in a riser cracker, as the rate of catalyst recirculation to feeding rate can be readily adjusted. The non-steady state operation of a fixed bed reactor undergoing rapid catalyst deactivation was reported to interfere with downstream processing.

Diebold and Scahill (190) observed a shift in products corresponding to reaction equilibrium with temperature in the experiments. Runs carried out at higher (500 °C) catalyst temperatures resulted in the dealkylation of aromatics and an increase in the total liquid hydrocarbon yield compared to lower temperatures (400 °C). Alkylated aromatics are desirable for a good gasoline octane number (i.e. above a research octane number, RON, of 93.2 for typical gasoline (5)), therefore lower temperature catalytic processing is preferable if the intended application is gasoline.

In the Diebold and Scahill (190) experiments on the 100 g catalyst reactor, the amount of coke on the catalyst was calculated as the weight lost during the catalyst regeneration step. This weight loss, however, was not true coke as it included adsorbed water from steam stripping and any adsorbed hydrocarbons which were not removed by the steam stripping at the end of the run. A more useful expression of coke deposition was achieved by measurement of the temperature profile along the catalyst bed, after the initial high rate, to calculate the slow deactivation coking rate as g wood fed per g catalyst deactivated. There was a very high initial coking rate which resulted in rapid partial deactivation after which the catalyst retained sufficient activity to convert the pyrolysis vapours to intermediate products such as furanic compounds (157). Eventually, complete catalyst deactivation occurred and no more pyrolysis vapours were converted over the catalyst. In commercial zeolite cracking processes it is common practice to not completely regenerate the catalyst. This maintains the catalyst primarily in the slow deactivation regime in the reactor.

In the presence of steam the coking rate appeared to be very sensitive to the reactor temperature and was seen to undergo an apparent change of nearly an order of magnitude from about 2 to 19 as the temperature increased from about 475 °C to 525 °C.

3.4.9 Reactor system 3 – 100g reactor scalability

Diebold et al. (157), found that operation of the 100 g catalyst reactor demonstrated agreement with the 1 g reactor in the MBMS studies. It was observed that the overall reactions of the wood (and RDF) vapours over the catalyst were slightly exothermic at catalyst temperatures of 500 °C. The implications of this for scale-up to a riser cracker are that the rate of catalyst circulation will be dictated by chemistry alone unlike petroleum cracking, an endothermic process which requires heat produced by burning coke off the catalyst during regeneration. In petroleum cracking, therefore, there is a trade-off between energy requirement and chemistry.

Diebold and Scahill (156), reported that softwood pyrolysis vapours from the 100 g catalyst reactor were very reactive with ZSM-5 in a steam environment (2:1 weight ratio) forming a liquid hydrocarbon product similar to that formed from methanol.

At 400 °C, however, product yields presented from methanol conversion over ZSM-5 and biomass pyrolysis vapour conversion over ZSM-5 demonstrated the following differences: the yields of hydrogen, methane, propene and iso-butene from methanol were considerably higher than from biomass vapour; the yields of n-butene and C5+ hydrocarbons were significantly greater from methanol than from biomass vapour and the yields of carbon monoxide and carbon dioxide were considerably lower from methanol than biomass vapour processing over ZSM-5. They reported that the catalyst deactivated quickly compared to methanol and that, consequently, a reactor which could provide high catalyst activity in spite of coking such as an entrained bed (riser cracker) coupled to a fluidised bed for catalyst regeneration would be desirable. The gasoline product formed was almost entirely alkylated benzenes with only a small amount of benzene. This gasoline would be expected to have an octane rating in excess of 100 and a blending octane number between 115 and 135 which could fetch very high prices. (Iso-octane having an octane number of 100 and typical gasoline having an octane number of 93.2).

3.4.10 Reactor system 4 – Scale-up using whole vortex product stream - 8.5 kg catalytic reactor

A 8.5 kg catalytic reactor enabled processing of the whole product stream from the vortex reactor (93). Refuse derived fuel (RDF) was used and obtained from the MSW facility at Thief River Falls, MN, U.S.A. The recyclables and non-organic materials were removed from the RDF. Between 7.5 and 8.5 kg of ZSM-5 extrudate from Mobil was used to modify the RDF vapour product stream from the vortex fast pyrolysis reactor. Steam was co-fed with the RDF in a 2:1 weight ratio in order to minimise the rate of catalyst coking.

The experimental conditions employed are detailed in Table 3.2, reactor system 4. As with the 100 g scale reactor, results from limited operation of the 8.5 kg fixed bed reactor showed general agreement with the results from the 1 g reactor indicating scalability. Results were only available for RDF pyrolysis with subsequent modification in the 8.5 kg catalytic reactor and as such are out of the scope of the present work which is confined to the atmospheric catalytic modification of biomass pyrolysis products.

3.4.11 Summary of the catalytic modification carried out at the National Renewable Energy Laboratory

The National Renewable Energy Laboratory used various forms of ZSM-5 in the majority of their catalytic modification experiments with a limited amount of work on the use of silica alumina and unspecified larger pore zeolites. This work concentrated on fixed bed studies. The majority of experimental work was carried out on 1 g fixed catalyst bed screening reactors but good scalability was suggested by the limited operation of larger 100 g and 8.5 kg fixed catalyst beds. Experiments with larger pore zeolites yielded a higher amount of large molecular weight compounds compared to experiments with ZSM-5. There was evidence of the effects of temperature, WHSV, residence time and the concentration of pyrolysis vapours at the active catalyst site on the catalytic reaction severity and optimum conditions existed for the production of specific compounds. Yields of liquid hydrocarbons of 8 wt% from wood were experienced at 500 °C. Reaction pathways for the conversion of carbohydrates to aromatic hydrocarbons were suggested. Between 400-500 °C and WHSVs of 0.7 - 4 h^{-1} carbohydrates were observed to convert to furanic compounds and then to aromatic hydrocarbons over pure and extrudate HZSM-5. It was also observed that carbohydrates continued to convert to furanic compounds over partially deactivated HZSM-5 but that the reaction did not continue to produce aromatic hydrocarbons. It was reported that the reactions occurred via decarbonylation and decarboxylation pathways resulting in an increase in the proportion of carbon oxides in the yield of gas. Finally, there were problems with catalyst deactivation due to the coking experienced with the fixed beds used.

Specific parameter effects on catalytic reaction severity were:

- optimum reaction severities for the production of specific compounds (gasoline range hydrocarbons) were achieved by controlling the balance between WHSV and temperature;
- the yield of hydrocarbons were reported to increase in yield between 400-500 °C but decrease in yield between 500-525 °C;
- at high catalytic reaction severity using pure HZSM-5 the catalyst was deactivated by coking after 3 s residence time;
- the use of extrudate catalyst effectively reduced the reaction severity for the same WHSV of pure HZSM-5 catalyst due to the diluting effect of the binder;
- co-feeding of steam was thought to reduce reaction severity possibly by occupying catalyst pores and blocking active sites; and
- pyrolysis vapour pressure affected reaction severity in that the higher the catalyst loading (or WHSV), the proportionally higher the pyrolysis vapour pressure was required in order to create an equivalent reaction severity.

3.5 Catalyst selection and particle density estimation

3.5.1 Catalyst selection and catalytic reactor issues

The limited amount of work carried out on catalytic modification of freshly produced fast pyrolysis vapours from wood was carried out at the National Renewable Energy Laboratory (NREL) in the U.S. (as discussed in Section 3.4.1) . They used various forms of ZMS-5 in most of their experiments with a limited amount of work on the use of silica alumina and unspecified larger pore zeolites. The experiments carried out at NREL (186) with larger pore zeolites resulted in the production of high molecular weight lignin compounds which are undesirable from a fuel usage point of view, as described in Chapter 2, and do not hold any significant value for chemical extraction. ZSM-5 has been shown to have advantages over silica alumina with respect to it's acidity and shape selectivity (175) converting biomass pyrolysis vapours to a range of aromatic hydrocarbons which have potential application as fuel components (186).

The major disadvantage of fixed bed catalyst studies, like those at NREL, is the tendency towards coking on the catalyst which causes rapid catalyst deactivation and results in non-steady state reaction conditions (157). Coking is a problem associated with catalytic processing of all wood derived pyrolysis vapours as it is deposited on the acid sites reducing catalyst activity and increasing the rate of further vapour coking. Wood derived vapours produce more coke than feeds such as methanol due to their relatively low effective hydrogen index (defined Chapter 3, Section 3.3), typically 0.8 compared to 1.3 for methanol. Catalytic processing of wood pyrolysis vapours over ZSM-5, as opposed to other zeolites or cracking catalysts such as silica alumina, results in lower levels of coke formation. This has been shown to be due to the relatively small pore size of ZSM-5, pores are 5.1 Å by 5.5 Å and 5.4 Å by 5.6 Å (193) approximately 5.5, which limits the size of molecules entering the pore structure and thus provides a high resistance to coking (194).

Coking can also be minimised in wood vapour catalytic processing by modifying the catalytic reactor design and method of contacting catalyst with wood vapours. Chen et. al. (177) reported that low catalyst residence times (unspecified) and frequent catalyst regeneration (via burn off of organic deposits in a separate reactor) could minimise coke production and maximise the yield of hydrocarbons from carbohydrates, which have an EHI of 0.0. Grandmaison et. al. (91) found that coke production during the catalytic processing of furfural over HZSM-5 increased with reaction severity: either higher temperatures (i.e. 450 °C compared to 350 °C) or greater contact time of catalyst with furfural.

Sharma and Bakhshi (195) also reported that the production of coke was reduced during HZSM-5 processing of wood derived vapours, revapourised high pressure liquefaction oil in this case, by using a fluidised bed instead of a fixed bed. The lower coke production in the fluidised bed compared to the fixed bed was due mainly to the residence time of vapours over the catalyst being 0.5 s with the fluidised bed compared to 500 s with the fixed bed. Fluidised beds are preferable to fixed bed catalytic reactors for the exothermic bio-vapour reactions over ZSM-5 (157) as easier control of the reaction equilibrium is possible with fluidised bed reactors by adjustment of the catalyst to wood feed rates.

With a fixed bed reactor the catalytic deactivation period is non-steady state, going through periods of very rapid and slow deactivation, which interferes with downstream processing. This was why the petroleum refining business switched from fixed to fluid beds and then to the riser cracker – or fluid catalytic cracker, as it became known. The riser cracker, however, is a relatively complicated reactor to operate, particularly on the research scale. This is why a fluidised bed has been chosen with a commercial powdered catalyst for experimentation in this study.

3.5.2 Catalyst selection and physical properties

A commercial HZSM-5 containing catalyst has been chosen for the current work. The main advantage of choosing a commercial catalyst is it's proven suitability for fluidised bed operation which allows in-bed catalytic modification of vapours produced in the fluidised bed fast pyrolysis reactor chosen for biomass pyrolysis (as described in Chapter 2). The catalyst chosen has been used commercially in a fast fluidised bed to crack low boiling point material to liquid petroleum gas as part of the petroleum cracking process. It provides a high resistance to attrition and a capability for regeneration (196).

The catalyst chosen contains HZSM-5 supported on an alumina phosphate binder. Information about the percentage of active catalyst on the binder and it's degree of acidity was not available and investigation into it's properties was prohibited by the supplier. The experiments of Diebold et. al. (152) demonstrated the greater resistance to deactivation of HZSM-5 on a silica alumina binder compared to pure HZSM-5. This was due to the active catalyst sites being diluted over the binder reducing the occurrence of over-activity which leads to rapid coking.

The commercial catalyst chosen for use in this work was donated by Grace Davison and was obtained in a powdered form. Physical data of the catalyst is given in Table 3.4.

Table 3.4 Physical properties of the ZSM-5 containing Grace Davison catalyst (identification no. 10-5132.0101)

Property	Value	Unit
Particle size distribution		
0-20 μm	1	wt%
0-40 μm	9	wt%
0-80 μm	67	wt%
0-105 μm	88	wt%
0-149 μm	97	wt%
Average particle diameter	70	μm
Surface area (BET)	58	m^2g^{-1}
Pore volume (H_2O)	0.35	mLg^{-1}
Pore volume (N_2)	0.08	mLg^{-1}
Apparent bulk density	820	kgm^{-3}

3.5.3 Estimation of catalyst particle density

The specific catalyst particle density was not available but is essential in the calculation of minimum fluidising velocity and the determination of other important fluidising characteristics which are crucial to the incorporation of the catalyst into the fluidised bed fast pyrolysis reactor.

Particle density is defined as the mass of a single particle divided by the volume the particle would displace if its surface were non-porous. The apparent bulk density quoted in Table 3.4 is the volume that a mass of particles occupies and includes the voids between the particles (197). The particle density, therefore, is greater than the bulk density.

The particle density of powders can generally be measured in a specific gravity bottle or air pycnometer (197). This is not possible for the catalyst obtained from Grace Davison, however, as it is porous. The particle density of a coarse porous solid can be measured by a mercury 'porosimeter' but the Grace Davison catalyst is a fine powder and the mercury may not penetrate the voids between the particles (197). The particle density, therefore, has to be estimated indirectly by estimating the voidage. This is a typical procedure carried out in the petroleum industry.

Voidage depends on:

- particle shape: the lower the sphericity, ψ, of the particle, the higher the voidage;
- particle size: the larger the particle size, d_P, the lower the loosely packed voidage (densely packed particles are not so dependent);
- size distribution: the wider the size spread, σ, the lower the voidage; and
- particle and wall roughness: the rougher the surface, the higher the voidage.

Partridge and Lyall (198) give voidages of narrow size distribution loosely packed particles for spheres and irregular shaped sand particles. The loosely packed spheres, with a mean particle diameter of 72 μm, have a voidage, ε, of 0.441 whilst the loosely packed irregular sand particles have a voidage, ε, of 0.602. The sphericity, ψ, of the Grace Davison catalyst was not known but would be expected to be somewhere between the sphericity of the spheres and irregular packed sand quoted by Partridge and Lyall (i.e. voidage, ε, between 0.441-0.602). The voidage would also be expected to be smaller for the Grace Davison catalyst as it has a relatively wide particle size distribution spread, σ, quoted to be 149 μm (all of the particles fall into this spread). A sand having a mean particle size, d_P, of 195 μm and a size distribution spread, σ, of 75 μm has a voidage, ε, of 0.432 compared to a sand of mean particle size, d_P, 197 μm and a size distribution spread, σ, of 7 μm which has a voidage, ε, of 0.469 (199). The difference in voidages, in this case is 0.037, between narrow particle size spreads and larger particle size spreads. In summary, for d_P of 72 μm and a small σ, ε is between 0.441-0.602. For a difference in σ of 68 μm, there is a corresponding difference in ε of 0.037 for a sand with d_P of 195 μm, this difference will probably be even greater for a smaller average particle size such as the Grace Davison catalyst.

The voidage, ε, of the Grace Davison catalyst was estimated, by comparison with the data given above, to be no greater than between 0.602- 0.037 and 0.441- 0.037, i.e. between 0.565 and 0.404, the median of which is 0.485. In view of the fact that the Grace Davison particles appeared more spherical than irregular, with an estimated ψ of 0.85, had a high particle size spread at 149 μm and a smaller average particle size of 70 μm compared to the quoted example range, an assumed voidage, ε, of 0.30 was be taken for the calculations detailed in Chapter 4. For a bulk density of 820 kgm^{-3}, this corresponds to an individual particle density of approximately 1170 kgm^{-3}.

CHAPTER FOUR

EQUIPMENT DESCRIPTION, ADAPTATION AND COMMISSIONING

4 EQUIPMENT DESCRIPTION, ADAPTATION AND COMMISSIONING

4.1 Introduction

From the evaluation of thermal conversion processes detailed in Chapter 2 fluidised bed fast pyrolysis was selected as the method that would achieve optimum liquid production from biomass. Atmospheric pressure, vapour phase catalysis was chosen for modification of fresh fast pyrolysis vapours for thermal, economic and chemical reasons described in Chapter 2. The catalyst selected for catalytic modification of the pyrolysis vapours was a powdered ZSM-5 containing catalyst obtained from Grace Davison. Details of selection and description of the catalyst are presented in Chapter 3. The catalyst was used 'in-bed' as this was perceived to be the most thermally efficient and economical arrangement for modification of vapour phase biomass pyrolysis products.

The fast pyrolysis reactor set-up and adaptation of the operation of the process to allow incorporation of the catalyst are described in this chapter. Firstly the aims and objectives of the study undertaken in terms of the development needs for a viable process are discussed. The fluidised bed reactor and associated system equipment are described. Fluidisation characteristics of the catalyst are then examined for compatibility with fluidised bed operating parameters. Finally preliminary experiments, carried out to determine a suitable operating method, to achieve effective vapour phase catalysis of fast pyrolysis reactions are described. Subsequent experiments to determine the effect of catalyst concentration and reactor temperature on product yields are described in Chapter 6.

4.2 Aims and objectives of the study undertaken in terms of the development needs for a viable process

The ultimate objective of the equipment study, adaptation and commissioning was to identify a viable process by which pyrolysis vapours could be contacted with catalyst for an appropriate time period within the 150 g h^{-1} fluidised bed reactor. A number of steps were undertaken to develop this process.

Firstly the operating range of the current system must be defined or determined. It was necessary to calculate and study the fluidising behaviour of the sand and biomass in the

system over a range of gas velocities. It was also necessary to study the pyrolysis of biomass at different temperatures and particle sizes.

A full and complete understanding of the current system and it's limits were required to provide a basis upon which any modification should be considered. These are discussed in Section 4.3.

Secondly the behaviour of the catalyst must be understood within the system. It was necessary to investigate the fluidising behaviour of the catalyst over the gas velocities possible in the 150 g h^{-1} fluidised bed reactor. The minimum fluidising velocity, bubbling velocity and entrainment velocities of the catalyst were calculated according to theory. The calculated values were then checked by experimental determination in a test fluidised bed. The determination of the velocity at which significant entrainment of the catalyst occurred was crucial to the method of contact which could be used between the pyrolysis vapours and the catalyst. The catalyst fluidising behaviour is described in Section 4.4.

When the operating range of the system and the fluidisation characteristics of the catalyst were identified then methods for contacting the catalyst with the pyrolysis vapours were considered. Continuous feeding of the catalyst with the biomass feedstock was selected as the most suitable method of contacting the catalyst with the pyrolysis vapours and suitable operating conditions were investigated. Finally commissioning of the adapted system was carried out to investigate the range of reaction conditions possible and the product recovery and collection procedures required. This was necessary to test the practicality of conditions, procedures and additional equipment selected and to fine tune operation to facilitate subsequent experiments and improve reproducibility. This is discussed in Section 4.5.

4.3 Description of fluidised bed reactor and associated equipment

4.3.1 Nitrogen entrained biomass feeder

A nitrogen entrained biomass feeder (Figure 4.1) was used to introduce the feed via a polypropylene tube into the fast pyrolysis reactor stainless steel feed inlet tube. The feeder consisted of a cyclindrical perspex vessel with a flanged lid secured by three screws. A

metal impeller driven by a Citen Co. electric motor (speed 0-600 rpm) positioned through the lid was used to continuously stir the feed at the bottom of the vessel.

A stainless steel 'entrain tube' (2mm internal and 3mm external diameter) was asymmetrically located 10 mm from the centre and 25 mm above the base of the cylinder.

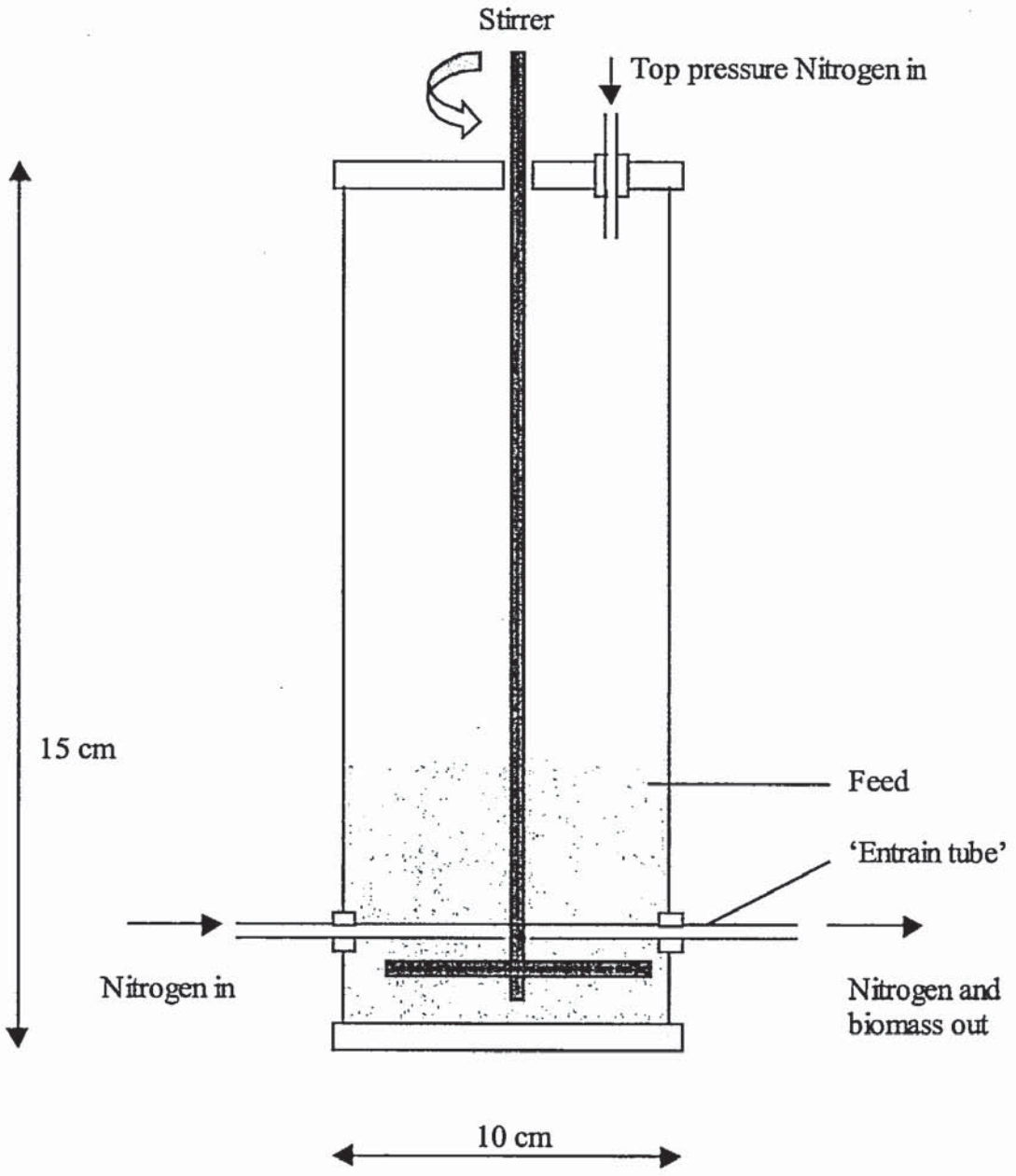

Figure 4.1 Biomass feeder (not to scale)

During operation nitrogen entrainment gas draws the feed into the entrainment tube through a small opening, located mid-way on the lower side of the tube, by controlled pneumatic transfer. The diameter of the opening was either 1.1, 1.3 or 1.7 mm depending on the particular 'entrain' tube required to feed specific sized particles.

A top pressure of nitrogen, exerted on the feeder bed through a nitrogen line entering the lid of the feeder, ensured successful entrainment of the particles into the entrainment tube. The pressure within the feeder was measured by a differential pressure meter between the nitrogen top line and the atmosphere. The nitrogen flows were controlled by Platon rotameters (operating range 0-2 L min^{-1}, nitrogen S.T.P.). Feed rate was controlled by a combination of entrain gas flow rate, stirrer speed and top pressure of nitrogen. Feed rate calibration is described in Chapter 5 together with reactor operation.

4.3.2 Fluid bed reactor

The fluid bed (Figure 4.2) was constructed of 316 stainless steel and consisted of a main reactor, cyclone, char pot and transfer line. The main reactor consisted of a fluidisation zone with a disengagement zone situated directly above it. The fluidising gas, nitrogen, was delivered to the bed via a vertical stainless steel tube which passed down outside the reactor body and entered the base of the reactor 50 mm below the perforated distribution plate. The nitrogen flow rate was controlled by a Platon rotameter (range of operation 0-25 L min^{-1} nitrogen at S.T.P.). The pressure across the fluidised bed was measured by a differential pressure meter between the fluidising gas entering the reactor and the atmosphere.

The feed was transferred from the feeder to the stainless steel inlet tube at the top of the reactor as described in Section 4.3.1. The inlet tube passed down through the reactor body to a height of 10 mm above the distribution plate where the feed was delivered to the fluidised bed. The feed tube, within the reactor, could be cooled along its length by a double walled air jacket. Air could be passed through the double walled jacket by means of an external compressor. The cool air passed down through the inner jacket along the whole length of feed tube before entering the second jacket, at the base of the feed tube, which it passed up through prior to exit. Cooling of the feed tube was not required during this work.

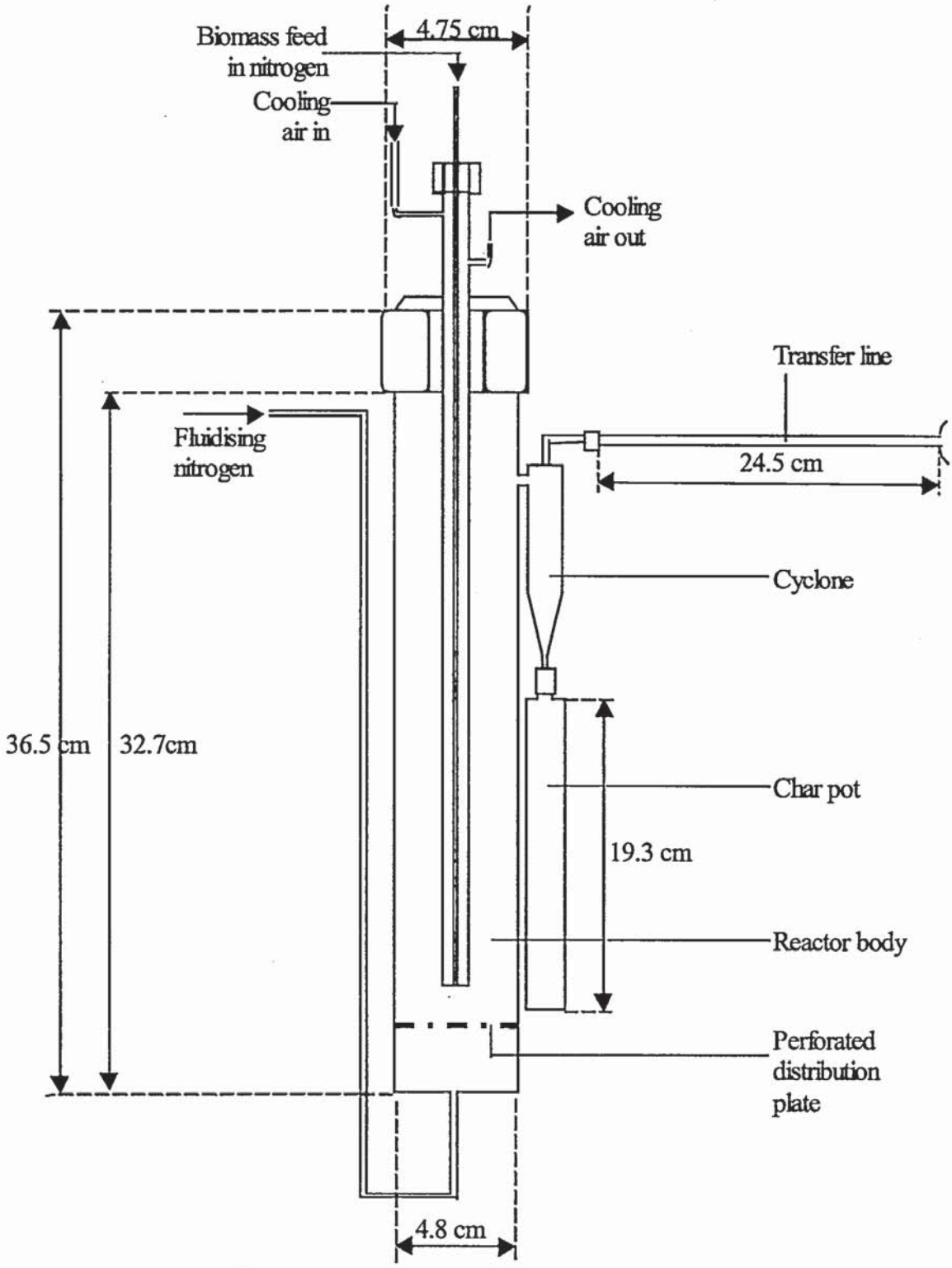

Figure 4.2 Fluidised bed reactor (not to scale)

The fluidised bed, cyclone, char pot and stainless steel nitrogen feed tube were heated by a purpose designed and fabricated electric furnace. Temperature was controlled by a proportional integral controller connected to a thermocouple located in the main body of the furnace. Reactor temperature, monitored on an LED display, was measured by an R.S. components type K thermocouple positioned at the base of the fluidised zone. The set point and actual furnace temperatures were displayed on the furnace control box.

The sand, i.e. the fluidised heat transfer medium, was supported at start-up by a perforated distribution plate positioned horizontally across the reactor 50 mm above the fluidising nitrogen inlet point. A sand particle size range of 350-500 μm was chosen. Sand particles in this size range exhibited fluidised behaviour at flow rates between 10 to 18 L min^{-1} nitrogen (S.T.P.). Upon fluidisation the sand bed expanded from a static height of approximately 4 cm to a height of 10 cm at the onset of fluidisation. The minimum fluidising velocity of the sand was calculated to be 0.083 m s^{-1} (Section 4.4.5.1).

Fluidising gas flow rates of 10 L min^{-1} were typically employed in the experiments described in Chapter 6. The gas velocity at this flow rate was approximately 0.146 m s^{-1} at S.T.P. or 0.38 m s^{-1} at 500 °C.

Above the fluidised zone, the disengagement zone acted as a region in which the gases and medium to fine sized char separated from the sand. Elutriation of the sand particles and relatively coarse char particles, which remained in the bed, did not occur at the gas velocities used within the fluidised bed. After the disengagement zone, the gas stream entered a reverse flow cyclone where the majority of the char was removed from the gas and collected in the char pot. The upper part of the reactor, which protruded from the furnace, and the stainless steel transfer line were lagged with a glass fibre insulating material to minimise heat loss during operation.

4.3.3 Liquid recovery system

The liquid product collection system (Figure 4.3) consisted of two cold-finger condensers (e.g. Aldrich Z16,403-8), an electrostatic precipitator and a cotton wool filter placed in series. The pyrolysis vapours and nitrogen carrier gas passed through each section in turn. The product vapours passed through a 0 °C condenser first (cooled by ice in water) followed by a –78 °C condenser (cooled by dry ice in acetone) which allowed partial fractionation of the pyrolysis liquid. The condensed liquid accumulated in two 100 mL round bottomed flasks designated as oil pot 1 and oil pot 2 respectively.

Non-condensible gases and the non-coalesced aerosols passed through the condenser arrangement into an electrostatic precipitator. The electrostatic precipitator was a relatively new addition to the product collection system and it's effectiveness, for the collection of aerosols previously collected by the cotton wool filter alone, was evaluated throughout the experimental series. Two condensers were used to ensure that all condensible vapours were collected prior to the electrostatic precipitator.

The electrostatic precipitator (Figure 4.3) consisted of a glass-walled container with a screw on lid. A large metal insert placed inside the precipitator body next to the glass was connected to the positive terminal of the power source through an opening in the glass and acted as the anode. A 0.1 mm diameter fine stainless steel wire, suspended from the lid of the electrostatic precipitator, was connected to the negative terminal and acted as the cathode. The cathode was held in a vertical position by magnetic attraction between a magnet at its lower end and another magnet on the outside of the glass precipitator wall (see Figure 4.3). A voltage of 15-20 kV, applied across the electrodes, was used to generate an electrostatic field between the two electrodes. In the field the aerosol particles became charged and were attracted to the outer, positively charged electrode where they condensed and ran down to collect at the base of the electrostatic precipitator.

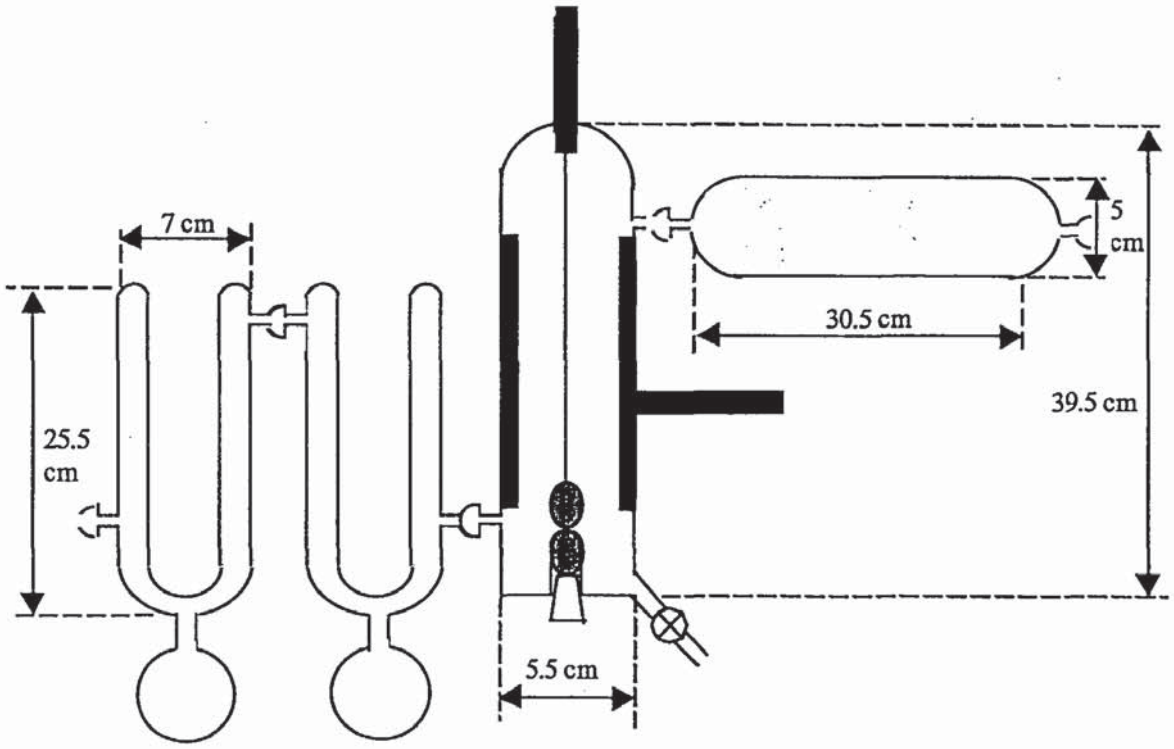

Figure 4.3 Product collection system (not to scale)

Finally the permanent gases passed through the cotton wool filter where any aerosols that escaped the electrostatic precipitator were collected. The cotton wool filter consisted of a horizontally mounted glass tube filled with cotton wool. The gas leaving the cotton wool filter was fed directly through a Gallus 2000 Schlumberger gas meter (range of operation 0.025-4 $m^3 h^{-1}$). Gas samples were collected periodically in pressurised 'bombs' using a manual gas sampling pump. The rest of the gas was vented to the atmosphere via an extraction hood.

Ball and socket type glassware was employed with the exception of the oil pot/condenser connections which were Quickfit joints. Three liquid fractions were obtained from oil pot one, oil pot two and the electrostatic precipitator (abbreviated to OP1, OP2 and EP) respectively.

4.4 Investigation of catalyst fluidising characteristics and theory

The fluidisation characteristics of the catalyst chosen for experimentation are calculated in this Section to determine if it is suitable for incorporation into the fluidised bed. The ZSM-5 catalyst used throughout this work was obtained from Grace Davison. The reasons for the selection of the catalyst and it's physical characteristics are described in Chapter 3. Fluidisation theory is explained in Sections 4.4.1 to 4.4.3 and the minimum fluidising velocity of the catalyst is calculated in 4.4.3.1.

There are many thorough texts available on fluidisation (197, 200, 201, 202, 203) but the general fluidisation theory discussed here is taken mainly from Howard (201) as it provides a concise text of the areas considered in this thesis. For specific fluidisation with small particles the more detailed texts of Geldart (197) and Basu et al. (200) were used. Entrainment theory is explained in Section 4.4.4 and typical entrainment velocities for the Grace Davison catalyst are calculated in 4.4.4.1. The minimum fluidising velocity of the sand is calculated in 4.4.5.1. The experimental determination of minimum fluidising velocity, bubbling velocity and minimum entrainment velocity of the catalyst are described in Section 4.4.6. A summary of calculated and experimentally determined catalyst fluidisation characteristics is given in Section 4.4.7.

4.4.1 General principles of fluidisation

When an evenly distributed flow of gas is passed upwards through a static bed of particles, unrestrained at the surface, a point is reached with increasing gas velocity where the drag on the particles becomes sufficient to support the weight of the particles (201). This is referred to as 'incipient fluidisation', at which point the bed resembles a liquid, and the gas velocity required for this is called the 'minimum fluidising velocity'. As the gas velocity through the bed of particles increases the bed expands whilst the pressure drop across the bed remains the same until the 'minimum bubbling velocity' is reached at which point the bed height drops due to gas passing through the bed in the form of bubbles (201).

After this, if the gas velocity is increased further, the pressure drop across the bed starts to fluctuate with the onset of a phenomenon called 'slugging', where very large bubbles pass

through occupying the entire width of the bed, and eventually 'entrainment' of the particles from the bed will occur (201).

4.4.2 Categorisation of particles

Particles of different sizes and densities behave differently during fluidisation. It is useful, therefore to categorise particle types according to size and density. A widely accepted system of categorising particle types in fluidised theory is Geldart's classification of particles (201). The Grace Davison catalyst chosen for this work, described in Chapter 3, falls into Geldart's Group A class of particles (201) which are often referred to as powders and are typically within the size range 20-100 μm with a particle density of less than 1400 kg m^{-3} (201). Fluidised catalytic cracking (FCC) catalyst is a good example of Geldart's class A particles, typical particle size being 56 μm and particle density 729 kg m^{-3} (204). The Grace Davison catalyst used in this work is also used by Mobil as an additive in fluidised catalytic cracking (FCC) units and has an average particle size of 70 μm and a bulk particle density of 820 kg m^{-3}. The individual particle density, d_P, has been calculated, in Chapter 3, to be 1170 kg m^{-3} using an estimated packed bed voidage, ε, of approximately 0.30.

4.4.3 Behaviour specific to class A particles (i.e. catalyst)

Beds of powders expand considerably as the velocity of the fluidising gas increases above the minimum fluidising velocity (U_{mf}). The minimum bubbling velocity of such powders is relatively high (as much as 2 or 3 times U_{mf}) compared to other particle classes due to the low cohesiveness of class A particles (197). During the quiescent period, i.e. before the bed begins to bubble, particle mixing is very limited. At U_{mb}, the bed collapses to a height comparable to that at minimum fluidisation (201).

Gross circulation of the powder (analogous to convection currents in liquids) commences at the onset of bubbling and this results in rapid mixing. At this point the surface of the bed resembles a boiling liquid (197). Bubbles split and coalesce frequently resulting in an equilibrium bubble size and considerable back mixing of gas. The bubble size is affected by the mean particle size, the mass fraction of particles less than 45 μm in diameter, pressure and temperature.

As the gas velocity is increased beyond the minimum bubbling velocity the bubble size increases until slug flow occurs during which very large bubbles travel upwards through the bed. Eventually bubble and slug flow breaks down as the fraction of particles being entrained approaches 1 and a transition from fluidisation to transport occurs. Further increase in velocity combined with the recirculation of elutriated solids results in fast fluidisation (197). The fluidisation properties improve as the mean particle size decreases, as the fraction of particles with diameters below 45 μm increases and as the pressure, temperature, viscosity and density of the gas increases.

4.4.3.1 Calculation of minimum fluidising velocity of Grace Davison catalyst

The minimum fluidising velocity of the catalyst is the lowest gas velocity at which the catalyst will fluidise and mix sufficiently with pyrolysis vapours. The minimum fluidising velocity for particles less than 100 μm can be calculated by Baeyens' equation, shown in Equation 4.1, which was reported to give the best agreement with experiments for particles less than 100 μm (197).

$$U_{mf} = \frac{\left(\rho_p - \rho_g\right)^{0.934} \; g^{0.934} \; d_p^{1.8}}{1111 \; \mu^{0.87} \; \rho_g^{0.066}}$$

Equation 4.1 Minimum fluidising velocity for Geldarts Group A particles (Baeyens' equation)

Where:

g = acceleration due to gravity;

d = average particle diameter;

μ = viscosity;

ρ_P = average particle density;

ρ_F = fluid density;

u = fluidising velocity;

u_{mf} = fluidising velocity at minimum fluidisation;

Re = Reynolds number $ud\rho_F / \mu$;

Ga = Galileo number $d^3\rho_F^2 g / \mu^2$; and

Mv = Density ratio $\rho_P - \rho_F / \rho_F$.

Table 4.1 shows the values used in the calculation of the minimum fluidising velocity of the catalyst

Table 4.1 Values used for calculation of the minimum fluidising velocity of catalyst

	Value	Unit	Symbol
Approximate particle density*	1170	$kg\ m^{-3}$	ρ_P
Nitrogen gas density at 500 °C	0.45	$kg\ m^{-3}$	ρ_F
Acceleration due to gravity	9.81	$m\ s^{-2}$	g
Average particle diameter	70×10^{-6}	m	d_P
Nitrogen fluid viscosity at 500°C	0.332×10^{-4}	$kg\ m\ s^{-1}$ (Pa.s)	μ

Where:

Approximate particle density* is estimated in Chapter 3.

Substituting the values into the equation, at 500 °C, gives:

$$U_{mf} = \frac{(1170 - 0.45)^{0.934} \; 9.81^{0.934} \; (70 \times 10^{-6})^{1.8}}{1111 \; (0.332 \times 10^{-4})^{0.87} \; 0.45^{0.066}}$$

$$= \frac{733.71864 \times 8.4375984 \times 3.3203 \times 10^{-8}}{1111 \times 1.2688 \times 10^{-4} \times 9.4866 \times 10^{-1}}$$

$$= \frac{2.0555 \times 10^{-4}}{1.3373 \times 10^{-1}}$$

$$= 1.5 \times 10^{-3} \; m \; s^{-1}$$

The minimum fluidising velocity of the Grace Davison catalyst was calculated to be 0.0015 m s^{-1} based on an average particle diameter of 70 μm and a particle density of 1170 kg m^{-3} in nitrogen at 500 °C. A nitrogen flow rate to the reactor at 20 °C of 0.06 L min^{-1} would be required to create the minimum fluidising velocity for the catalyst inside the reactor.

Based on a minimum fluidising velocity of 0.0015 m s^{-1}, a bubbling velocity for the Grace Davison catalyst would be expected between 0.003-0.0045 m s^{-1} corresponding to a nitrogen flow rate to the reactor of 0.012-0.018 L min^{-1} at 20 °C and the same pressure.

4.4.4 Entrainment theory

Entrainment of the catalyst is calculated in this section. The gas velocity at which catalyst particle entrainment occurs is an important value since gas velocities low enough to avoid catalyst entrainment may not fluidise the sand. Geldart (206) wrote a comprehensive overview of the nature and methods of calculating particle entrainment and the methods he described have been used for the calculation of catalyst entrainment at specific velocities. The terms 'elutriation' and 'entrainment' are used to describe the 'ejection of particles from the surface of a bubbling fluidised bed and their removal from the unit in the gas stream'.

Entrainment theory describes elutriation in terms of an elutriation rate constant, K^*_{ih}. It was stated that, the elutriation rate of solids, of size d_i, at one instant from the fluidised bed depends on the elutriation rate constant for those particles, the bed area and the fraction of the bed consisting of the particles of size d_i at time t. This is presented by Equation 4.2.

$$\frac{d}{dt}\left(x_{Bi}\ M_B\right) = K_{ih}\ A x_{Bi} = E_{ih}\ A$$

Equation 4.2 Equation for the elutriation rate of a specific size particle from a fluidised bed when the gas offtake is at height h above the bed surface

Where:

X_{Bi} = the fraction of the bed consisting of particle size d_i at time t;

M_B = the mass of the bed;

K_{ih} = the elutriation rate constant;

A = the bed cross-sectional area; and

E_{ih} = the net carryover flux for a component of size dpi when the gas offtake is at a height h above the surface of the bed.

It should be noted that the elutriation rate is not dependent on the total mass of particles in the bed. The rate of entrainment can not be calculated unless K^*_{ih} is known and K^*_{ih} cannot be calculated from first principles. The elutriation rate, E_{ih}, for a given component of size d_{pi}, has been described by Large et al. (205) as consisting of two partial fluxes: one continuous flux flowing upwards from the bed to outlet, $E_{i\infty}$, and another flux of agglomerates ejected by bursting bubbles which decreases exponentially as a function of freeboard height. This is expressed algebraically in Equation 4.3.

$$E_{ih} = E_{i\infty} + E_{io}\ e^{-a_i h}$$

Equation 4.3 Large et al. (205) expression for total elutriation rate

Where:

E_{io} = the component ejection flux - $E_o x_{bi}$;

ai = the component decay constant; and

h = distance above bed surface.

Providing that the bed height is large enough to make the flux of particles created by bursting bubbles negligible, E_{ih} can be approximated to $E_{i\infty}$. In this case, there are correlations available (206) for calculating the entrainment rate constant, K_i, for particles of size d_i elutriating from a fluidised bed.

One such correlation, the 1979 revised Geldart correlation (206), is suitable for the particle sizes and fluid velocities present in the fluidised bed pyrolysis reactor with catalyst and is expressed in Equation 4.4.

$$\frac{K_{i\infty}}{\rho_g \; U} = 23.7 \; e^{-5.4 v_t / U}$$

Equation 4.4 The revised Geldart correlation for elutriation rate constant (1979)

Where:

ρ_g = gas density;

U = superficial gas velocity; and

v_t = terminal (free fall) velocity of an isolated particle.

Terminal velocity of an isolated freely falling particle in an infinite fluid is the velocity the particle reaches when it is at a steady falling rate. Before terminal velocity is reached, the accelerating force is equal to the gravitational force minus the buoyancy force and the drag force. This is expressed algebraically in Equation 4.5.

$$\frac{\pi}{6} \left(\rho_p - \rho_f\right) g - F = \pi d_v^3 \; \rho_p \; \frac{dv}{dt}$$

Equation 4.5 Algebraic expression for forces acting upon a freely falling particle

Where:

ρ_p = particle density;

ρ_f = fluid density;

g = acceleration due to gravity;

F = drag force; and

d_v = volume diameter (i.e. particle size of a spherical particle of same volume).

The drag force can be expressed in terms of a drag coefficient, the projected area perpendicular to the flow, and the inertia of the fluid. Assuming the particle is spherical, the drag force can be expressed as shown in Equation 4.6.

$$F = C_D \frac{\pi d_v^2}{8} \rho_f v^2$$

Equation 4.6 Drag force acting upon a freely falling spherical particle in an infinite fluid

Where:

F = drag force;

C_D = drag coefficient;

d_v = volume diameter;

ρ_f = fluid density; and

v = particle velocity.

At terminal velocity the accelerating force is zero and $v = v_t$, therefore, the equation in Equation 4.5 becomes the equation in Equation 4.7.

$$F = \frac{\pi}{6} d_v^3 \left(\rho_p - \rho_f\right) g$$

Equation 4.7 Drag force on a spherical particle falling at terminal velocity

For the general case, combining the equations in Equation 4.4 and 4.5 gives the expression shown in Equation 4.8.

$$C_D = \frac{4}{3} \frac{(\rho_p - \rho_f)\ d_v\ g}{\rho_f\ v_t^2}$$

Equation 4.8 General case expression for drag force coefficient

From experimental data from spheres falling in a variety of fluids, log C_D can be plotted against log Re to give the standard drag curve (206) which has three regions: laminar, transitional and turbulent.

The Grace Davison catalyst falling in nitrogen at 500 °C falls within the laminar region, where Re < 0.2. For particles falling in the laminar region, Stokes found the drag on a smooth rigid spherical particle moving on a homogeneous viscous fluid at velocity v to be given by the expression in Equation 4.9.

$$F = 3\ \pi\ \mu\ v\ d_v$$

Equation 4.9 Stokes equation for drag force on a smooth rigid spherical particle falling in a homogeneous viscous fluid in the laminar region

Substituting this into Equation 4.7 with $v = v_{t,ST}$ we get the expression in Equation 4.10:

$$v_{t,ST} = \frac{(\rho_P - \rho_f)\ g\ d_v^2}{18\ \mu}$$

Equation 4.10 Substitution of Equation 4.9 into 4.7

4.4.4.1 Calculation of catalyst entrainment rate versus gas velocity

The revised Geldart correlation (1979) shown in Equation 4.4. can be used to calculate the elutriation rate constant for particle sizes d_i. Substituting values into equations 4.10, 4.4 and 4.2 the following values shown in Table 4.2. can be calculated for terminal velocity, elutriation rate constant and elutriation rate of the catalyst particle size ranges. A gas velocity of U = 0.1 m s^{-1} has been taken for this example.

Table 4.2 Instantaneous catalyst removal rates for the different size fractions in the fluidised bed reactor at a gas velocity of 0.1 m s^{-1}

Particle size	Percent weight	Ave. particle size	Terminal velocity	Elutriation rate constant	Elutriation flux	Elutriation rate	Elutriation rate
d_i	X_{bi}	$d_{i,ave.}$	V_t	K_i	E_i	$X_{bi}M_b$	$X_{bi}M_b$ (x1000)
μm		μm	m s^{-1}	kg m^{-2} s^{-1}	kg m^{-2} s^{-1}	kg s^{-1}	g s^{-1}
0-20	0.01	10	1.92×10^{-4}	1.06	1.06×10^{-2}	1.75×10^{-5}	0.0175
20-40	0.08	30	1.73×10^{-3}	9.71×10^{-1}	7.77×10^{-2}	1.29×10^{-4}	0.129
40-80	0.58	60	6.91×10^{-3}	7.34×10^{-1}	4.26×10^{-1}	7.07×10^{-4}	0.707
80-105	0.21	92.5	1.64×10^{-2}	4.39×10^{-1}	9.22×10^{-2}	1.53×10^{-4}	0.153
105-149	0.09	127	3.10×10^{-2}	2.00×10^{-1}	1.80×10^{-2}	2.99×10^{-5}	0.030
					Total elutriation rate =		1.037

The rate of total solids removed is equal to the sum of the rate of removal of the individual size fractions which equals 1.037 g s^{-1} for a gas velocity of 0.1 m s^{-1}. The elutriation rate is not dependent on the total mass of particles in the bed. The rate of total solids removal has been calculated for a range of gas velocities (Table 4.3).

Table 4.3 Instantaneous catalyst removal rates for various superficial gas velocities in the fluidised bed reactor

Nitrogen flow rate at 20 °C	Gas velocity (nitrogen at 500 °C)	Instantaneous removal of total catalyst size distribution
(L min^{-1})	(m s^{-1})	(g s^{-1})
0.4	0.01	0.01
2	0.05	0.35
3	0.083	0.79
4	0.1	1.04
10	0.26	3.70
12	0.32	4.59
18	0.48	7.28

4.4.5 Particle behaviour specific to class B particles (i.e. sand)

Suitable fluidisation behaviour of the sand has previously been demonstrated in the 150 g h^{-1} fluidised bed apparatus (207) and operating ranges for nitrogen fluidising gas were recommended on purchase of the system of between 10-18 L min^{-1} corresponding to gas velocities inside the bed of between 0.26–0.36 m s^{-1} nitrogen at 500 °C. It was not necessary, therefore, to investigate the fluidisation behaviour of the sand to the same degree as the catalyst. It should be noted, however, that the sand belongs to Geldart's group B particles and was of a higher particle size and density than the catalyst.

4.4.5.1 Calculation of minimum fluidising velocity of sand

The minimum fluidising velocity was calculated to find out the lowest possible fluidising gas flow rates that could be used in the system. The minimum fluidising velocity of the sand can be calculated by equation 4.11.

$$U_{mf} = \frac{\mu}{\rho_f \; d_v} \left\{ \left(1135.7 + 0.0408Ar\right)^{1/2} - 33.7 \right\}$$

Equation 4.11 Minimum fluidising velocity equation for sand

Where Ar is Archimedes number and is expressed in Equation 4.12

$$Ar = \frac{\rho_g \; d_v^3 \; \left(\rho_p - \rho_g\right) \; g}{\mu^2}$$

Equation 4.12 Archimedes number

A list of described symbols is given in Table 4.1 (page 119) in the calculation of catalyst minimum fluidising velocity. Values for sand properties can be found in Table 4.4.

Table 4.4 Values used for calculation of the minimum fluidising velocity of sand

	Value	Unit	Symbol
Approximate particle density	2600	$kg\ m^{-3}$	ρ_P
Nitrogen gas density at 500 °C	0.45	$kg\ m^{-3}$	ρ_F
Acceleration due to gravity	9.81	$m\ s^{-2}$	g
Average particle diameter	425×10^{-6}	m	d_P
Nitrogen fluid viscosity at 500 °C	0.332×10^{-4}	$kg\ s^{-1}m$ (Pa.s)	μ

Substituting values into Equation 4.12:

$$Ar = \frac{0.45 \times (425 \times 10^{-6})^3 (2600 - 0.45) \times 9.81}{(0.332 \times 10^{-4})^2}$$

$$= 7.9923 \times 10^2$$

The Archimedes number is 799.23.

Substituting the Archimedes number into Equation 4.11, we get:

$$U_{mf} = \frac{0.332 \times 10^{-4}}{0.45 \times 425 \times 10^{-6}} \left\{ \left(1135.7 + \left(0.0408 \times 7.9923 \times 10^2\right)\right)^{1/2} - 33.7 \right\}$$

$$= 8.3417 \times 10^{-2}$$

The minimum fluidising velocity of the sand has been calculated to be 0.083 $m\ s^{-1}$. This calculation assumes that the sand particles are spherical, although in reality the sand particles used were rough and not spherical. This value is approximately half the minimum gas velocity recommended for sand fluidisation in the 150 $g\ h^{-1}$ reactor used in this work. The equations used for these calculations are general and apply to a large range of particles sizes and densities. Exact values of fluidising velocities can only be determined experimentally because of the limitations of the correlations available. The calculated values were used as a guide.

4.4.6 Experimental determination of minimum fluidising velocity, bubbling velocity and entrainment velocity of Grace Davison catalyst

Experimental determination of minimum fluidising velocity, bubbling velocity and entrainment velocity was required to determine the validity of the calculations. It was important to know the fluidisation characteristics of the Grace Davison catalyst to use it in an in-bed catalytic mode in the fast pyrolysis fluidised bed. A fluidised bed 15 cm in diameter was used for the experimental determination. A quantity of catalyst particles were placed in the bed and fluidised vigorously to break down any packing of the particles, then the gas velocity was decreased to below the minimum fluidising velocity. The bed was gradually fluidised a second time and the flow rate was recorded against the bed height and pressure drop. The gas velocity was calculated from the volumetric flow rate and the pressure drop was plotted against gas velocity (Figure 4.4).

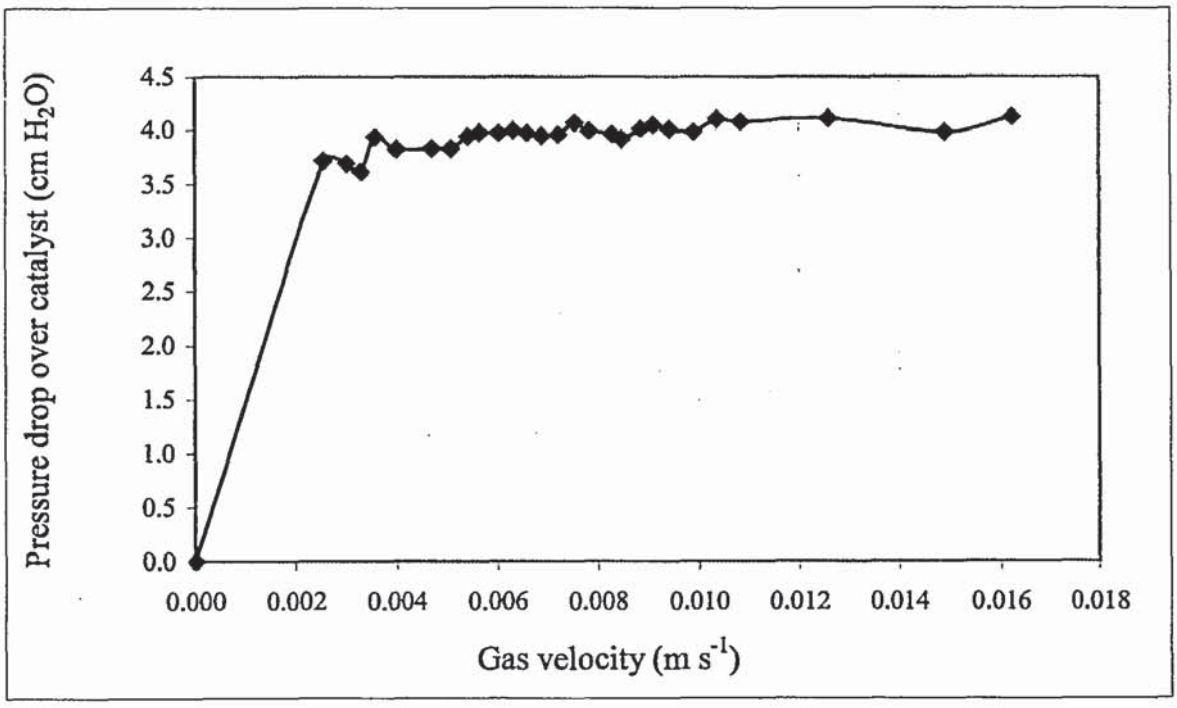

Figure 4.4 Experimental determination of catalyst minimum fluidising velocity: pressure drop over catalyst bed versus gas velocity

It is apparent from the graph that the point of minimum fluidisation, U_{mf}, occurred at a gas velocity of 0.004 m s^{-1}. This value is in reasonable agreement with the calculated value being just over twice the calculated size (Section 4.4.3.1.). The minimum bubbling velocity, U_{mb}, occurred at approximately 0.016 m s^{-1}. The fluidisation experiments experienced significant entrainment above a gas velocity of 0.018 m s^{-1}. There was a long fluidisation period, with respect to increasing gas velocity, but once bubbling occurred a relatively slight increase in gas velocity led to significant entrainment.

4.4.7 Summary of catalyst fluidising behaviour

The experimentally determined and calculated values of catalyst minimum fluidising velocity, bubbling velocities and velocities at which significant entrainment occurs were comparable. The results of the catalyst fluidisation investigations are presented in Table 4.5.

Table 4.5 Findings from catalyst fluidisation experimental determination and calculations

Gas Velocity (m s^{-1})	Fluidising Behaviour For Catalyst Particles
0.0015	Calculation of minimum fluidising velocity for catalyst with average particle size 70 μm
0.003-0.0045	Estimation of minimum bubbling velocity for catalyst based on minimum fluidising velocity
0.0042	Experimental determination of minimum fluidising velocity carried out at 20 °C in air
0.0162	Experimental determination of minimum bubbling velocity carried out at 20 °C in air
0.01	Catalyst entrains at a rate of 0.01 g s^{-1}
0.018	Point of significant entrainment, determined experimentally
0.05	Catalyst entrains at a rate of 0.35 g s^{-1}
0.083	Catalyst entrains at a rate of 0.79 g s^{-1}
0.1	Catalyst entrains at a rate of 1.04 g s^{-1}
0.26	Catalyst entrains at a rate of 3.70 g s^{-1}
0.32	Catalyst entrains at a rate of 4.59 g s^{-1}
0.48	Catalyst entrains at a rate of 7.28 g s^{-1}

The entrainment data presented in Table 4.3. indicates that at a gas velocity of 0.083 m s^{-1}, corresponding to the calculated minimum fluidising velocity of the sand (see Section 4.4.5.1), the catalyst will entrain at a rate of 0.79 g s^{-1} from the 150 g h^{-1} fluidised bed reactor which is equivalent to 2.8 kg in a 60 minute run. It should be noted that from previous studies on the 150 g h^{-1} fluidised bed reactor (208) a minimum nitrogen flow rate of 7 L min^{-1} was required to adequately fluidise the sand which corresponds to a gas velocity inside the bed of 0.19 m s^{-1}.

This data suggested that the sand and catalyst, in the form that it was obtained, could not be fluidised together in the 150 g h^{-1} reactor. The option of using the catalyst as the heat transfer medium, excluding sand completely, was considered. In this case, lower gas velocities could be used. There were, however, other factors to be taken into account when reducing gas velocity:

- biomass fluidisation – too low a gas velocity may fail to sufficiently fluidise the biomass particles resulting in inhomogeneous heat transfer;
- biomass pyrolysis – a reduction in gas velocity and replacement of fluidising medium will result in significant changes in heat transfer to the biomass particles, the amount of catalyst in the bed will also have an effect on heat transfer; and
- biomass feed rate – there will be a minimum biomass feed rate and nitrogen entrainment gas flow rate required for successful operation of the biomass feeder.

The complete redesign of the operating conditions of the 150 g h^{-1} fluidised bed reactor would be required in order to accommodate a sufficiently low gas velocity to avoid catalyst entrainment. Part of the reason for choosing the current system was that it's operation was established. Due to the complications presented it was decided to consider alternative methods of contacting the catalyst with the biomass vapours in the 150 g h^{-1} fluidised bed.

4.5 Adaptation of existing equipment to allow vapour phase catalysis of the biomass pyrolysis vapours

According to the combined results from theoretical calculations and experimental determination of minimum fluidising velocity, bubbling velocity and entrainment velocity the Grace Davison catalyst could not be fluidised in the fast pyrolysis fluidised bed operating at gas velocities necessary for biomass pyrolysis. It was necessary, therefore, to explore other options of adapting the fluidised bed equipment and corresponding peripheral equipment available in order to effect contact of the Grace Davison catalyst with the biomass pyrolysis vapours. Continuous feeding of the Grace Davison catalyst, allowing the catalyst to pass straight through the bed, was considered as an alternative to a fluidised bed of catalyst. Methods of feeding catalyst were explored and are described in the following Sections.

4.5.1 Catalyst feeding alone in entrained flow feeder – normal operation

The feeder was prepared as described in Section 5.3.1 but with catalyst as the feed instead of wood. The entrain tube with the 1.1 mm entrain hole was used. The plastic feed tube, which would normally connect to the reactor feed tube, was placed into a pre-weighed plastic bag, sealed at the top, in such a way as to prevent fine particles escaping but allow gas to pass out and thus prevent over inflation of the bag. The catalyst was used as received from Grace Davison, with a mean particle size of 70 μm and a particle size range from 0 to 149 μm.

It was not possible to achieve entrainment of the catalyst with the entrain hole facing downwards as the density of the catalyst was too large. Feeding was therefore attempted with the entrain hole facing upwards. This was partially successful but the catalyst flow rate:

- could not be controlled at a steady rate;
- was too high, between 360-870 g h^{-1}; and
- could only be sustained on an intermittent basis.

In order to overcome the excessive flow rate a feed tube with an entrain hole diameter of 0.45 mm was tested. The experiment was carried out as in the previous case with the feed tube facing upwards so that the catalyst could fall into the hole. A short burst of catalyst could be entrained by this method before blocking of the entrain tube occurred. The feed rate could not be calculated because of the low amount of catalyst fed before blocking. With an increase in the diameter of the entrain hole from 0.45 mm to 0.75 mm an intermittent flow rate of between 180-240 g h^{-1}, for up to 2 minutes, could be achieved before blocking occurred. The flow rate of the catalyst obtained with an entrain hole diameter of 0.75 mm was similar to the maximum feed rate for biomass into the reactor (150 g h^{-1}) Further catalyst feeding experiments, with modifications to the feeder top flow rate, entrain flow rate and use of stirrer, were carried out with the 0.75 mm feed tube entrain hole in an attempt to improve the feeding time prior to blocking. A summary of the nitrogen flow rate settings used and observations is given in Table 4.6.

From observations made during the experiments outlined in Table 4.6 it was concluded that as the volume of catalyst in the feeder decreased the occurrence of blockages was reduced and a more constant flow rate could be achieved. This indicated that the weight and compaction of the catalyst in the feeder could have contributed to the feeding problems. Also, the fact that blocking frequently occurred without a corresponding block across the entrain tube cross-section indicated that the catalyst was probably bridging across the entrain tube hole.

Table 4.6 Catalyst feeding experiments with an entrainment hole diameter of 0.75 mm

No.	Entrain Gas Flow Rate (cm)	Feeder Top Gas Flow Rate ($L\ min^{-1}$)	Result	Wood Feed Rate ($g\ h^{-1}$)	Stirrer Used	Observations	Action
1	6-7	0.2	8 g in 2 min	240	No	Intermittent due to blockages – found to be excess metal from drilling in tube	Metal removed with a fine metal rod
2	5-6	0.2 initially then turned off	9 g in 2 min 15 s	240	No	Intermittent due to blockages – no build up inside tube	Filed section of tube on hole to reduce metal thickness in order to encourage particle entrainment
3	5-6	0.2	3 g in 2 min 30 s	60	For part	Feeding blocks increased – tube X-section found to be clear on disassembly	Attempt again
4	5-6	0.2	6 g in 2 min	180	Yes	As before	Decrease depth of catalyst in feeder
5	7	0.2	5 g in 1 min 20 s	225	Yes	As before but – catalyst in X-section, on filed part near hole and freak large particle stuck in hole	Attempt again
6	7	0.2	9 g in 2 min 45 s	196	Yes	Intermittent still but not as bad as before – blockage in feed tube	Attempt again
At this point experiments were conducted where either the feeder top or entrain flow were altered but neither were found to have any effect on the flow rate or reliability.							
7	7	0.2	4 g in 1 min 8 s	211	Yes	Intermittent – no visible blockage	Attempt again
8	7	0.2	26 g in 6 min 48 s	132	Yes	Best so far – still some intermittence – the feeder top flow was maintained and unaffected by pressure build up this time – also the catalyst was quite low in the feeder by now	The combination of stirring and feeder top nitrogen flow moved the catalyst in a turbulent type, well aerated bed which helped

4.5.2 Catalyst feeding alone in entrained flow feeder - angled mode

Based on the results of the experiments described in Section 4.5.1, it was thought that if a constantly turbulent region of catalyst at the right dilution could be achieved at the entrain tube hole, feeding would be more reliable and controllable. In order to generate this turbulent region, feeding was attempted with the feeder positioned at differing angles to the horizontal so that the stirrer could aerate the catalyst. The results are presented in Table 4.7.

Table 4.7 Feeding studies with the feeder on an angle

No.	Angle To The Vertica l (°)	Entrain Flow Rate (cm)	Feeder Top Flow Rate (L min^{-1})	Result	Wood Feed Rate (g h^{-1})	Stirrer Used	Observations	Action
1	55	5	0.2	-	-	No	No catalyst fed	Turn off top and increase entrain
2	45	7	0.2	-	-	No	No catalyst fed	Try with stirrer (no. 3)
3	45	7	0.2	3 g in 2 min 30 s	72	Yes	Very difficult to achieve flow – either too dense or too dilute at entrain hole	New method needed

The results of the angled feeding experiments, presented in Table 4.7, indicated that a brief flow of catalyst could be achieved when the concentration of the catalyst particles in the vicinity of the entrain hole was appropriate. The upper surface of the static catalyst bed needed to be close to the stirrer rod and entrain tube so that the top layer of catalyst particles were moved turbulently around the hole in the entrain tube. The best position was when the entrain hole lay between 2-10 mm above the upper surface of the static catalyst bed, at which point the stirrer bar protruded from the surface of the static catalyst bed. The effective concentration of the catalyst particles depended on the stirrer speed and the total volume of catalyst. If the concentration of the catalyst particles was too high at the entrain hole bridging would occur across the entrain hole and if the concentration of the catalyst particles was too low at the entrain hole the flow rate would be insufficient. These factors made the angled arrangement unsuitable as a feeding method.

4.5.2.1 Catalyst feeding alone in entrained flow feeder - extra feed tube holes

Additional feed tube holes were drilled along the feed tube in order to increase the frequency at which the correct catalyst dilution surrounded an entrain hole and also to reduce the occurrence of total blockages which resulted from the bridging of the hole when only one hole was present. It was found, however, that bridging effects still caused the flow of feed to block completely and the correct dilution of catalyst next to an entrain hole was only improved slightly. Bridging effects could possibly be overcome by vibrating the entrain feed tube.

4.5.3 Catalyst feeding alone in inverted entrained flow feeder

In order to achieve a constantly turbulent region of catalyst particles around the entrain tube 'fluidisation' of the catalyst inside the feeder was attempted by inverting the bed and using the feeder top inlet to deliver 'fluidising' gas to the catalyst. The static height of the catalyst bed was between 25 % and 33 % of the feeder height The catalyst could not properly fluidise because of the absence of a distribution plate for the nitrogen but it was intended that the turbulence caused by the flow of nitrogen through the feeder top inlet would aerate the catalyst around the hole in the entrain tube. This was unsuccessful, however, and the concentration of catalyst particles at the feed entrain hole was too dilute.

4.5.4 Catalyst and wood mixed in the biomass feeder

As catalyst feeding alone in the entrained flow feeder was unsuccessful, co-feeding of the catalyst mixed with the biomass was investigated. It was thought that by mixing biomass and catalyst that catalyst compaction, apparent with catalyst alone, would be reduced as the voidage in a packed bed of biomass particles was greater than the voidage in the packed bed of catalyst. It was also thought that catalyst bridging effects would be reduced by the presence of biomass.

If feeding was successful, it was expected that the catalyst would pass through the reactor with the biomass vapours, as they were produced, to be collected in the char pot and glassware. The preliminary experiments are described in the following Sections.

4.5.4.1 Preliminary biomass and catalyst co-feeding experiments

The wood and catalyst were mixed together in varying proportions and placed into the entrained flow feeder. The feed tube with an entrain hole of 1.1 mm diameter was used unless otherwise stated. Feeding was initially carried out into a plastic bag as with previous experiments. Catalyst particles between 75-106 μm could be successfully co-fed with pine wood particles between 75-106 μm at concentrations up to 50 % for periods of up to 5 minutes. Two preliminary runs were then carried out to test whether a mixed biomass catalyst feed could be fed into the reactor with subsequent biomass pyrolysis.

In the first experiment, SFBC01, biomass was ground and sieved to a particle size between 75-106 μm. The catalyst was also sieved to this particle size range. SFBC01 achieved successful feeding of the biomass catalyst mixture. The average feed rate was 137 g h^{-1}, at a stirrer speed of 1, feeder top nitrogen flow rate of 0.5 L min^{-1} and nitrogen entrain flow rate of 1.0 L min^{-1}. Due to the small particle size most of the char and catalyst were not removed by the cyclone and collected in the condensers and the first oil pot. The char yield was very high with correspondingly low gas and liquid yields.

In the second experiment, SFBC02, a larger biomass particle size range of 250-355 μm was used to determine if extra grinding and sieving of the biomass could be avoided. Rapid blocking occurred with particles of this size at the 1.1 mm entrain hole. Improved feeding could be achieved using a feed tube with an entrain hole diameter of 1.7 mm, however there was still more blocking encountered than with the smaller particle size feed and the 1.1 mm entrain hole tube. The run conditions and product yields for the two preliminary runs are displayed in Table 4.8.

The reliability of product yields obtained during SFBC01 and SFBC02 were not of concern at this early stage and have not been included in the investigation of the effect of catalyst concentration and temperature on product yields and distribution presented in Chapter 6. The two preliminary experiments demonstrated the feasibility and identified some limitations (e.g.: biomass particle size, entrain tube size to be used) for co-feeding biomass and catalyst from the same feeder into the 150 g h^{-1} fluidised bed reactor for pyrolysis.

Due to the high feed rate in SFBC01 and the feeding problems encountered in SFBC02 the stirrer speed and feeder top nitrogen lines were reduced and both biomass and catalyst were screened to the smaller particle size range of 75-106 μm in subsequent experiments.

Table 4.8 Preliminary runs SFBC01 and SFBC02: reactor conditions and product yields

Run no.	**SFBC01**	**SFBC02**
Average reactor temperature (°C)	484	512
Average furnace temperature (°C)	517	535
% catalyst	20	10
Catalyst particle range (μm)	75-106	75-106
Wood particle range (μm)	75-106	250-355
Biomass feed rate (g min^{-1})	2.29	1.23
Entrain tube used (mm)	1.1	1.1, 1.3, 1.7
Run time (min)	17.2	31.9
Mass of products (g)		
Gas	3.3	7.2
Organics	17.9	26.3
Char	13.1	2.4
Water	2.6	2.1
Wood fed	39.3	39.3
Product yields from dry wood (wt%)		
Gas	8.4	18.3
Organics	45.6	66.8
Char	33.3	6.0
Water	6.7	5.3
Closure	94.0	96.4
Normalised product yields from dry wood (wt%)		
Gas	8.9	19.0
Organics	48.5	69.3
Char	35.5	6.2
Water	7.1	5.5
Closure	100.0	100.0
Reactor Residence time (s)	0.54	0.50
Total hot space residence time (s)	0.65	0.60
Nitrogen flow rate (L min^{-1})	10.75	10.75
% pyrolysis products in nitrogen (vol%)	1.8	5.8

4.5.4.2 Conclusions

It was concluded that biomass and catalyst co-feeding to the 150 g h^{-1} fluidised bed reactor from the nitrogen entrained feeder and successful pyrolysis was possible providing that:

- the biomass was ground and sieved to a particle size range of 75-106 μm;
- the catalyst was also sieved to a particle size range of 75-106 μm;
- the smallest entrain hole feed tube of 1.1 mm was used; and
- the feeder stirrer power setting was kept below 1 and the feeder top nitrogen flow rate was kept below 0.5 L min^{-1} so that the small particle sized feed can be fed at a rate below 120 g h^{-1}.

CHAPTER FIVE

DESCRIPTION OF REACTOR OPERATION AND ANALYTICAL PROCEDURES

5 DESCRIPTION OF REACTOR OPERATION AND ANALYTICAL PROCEDURES

5.1 Introduction

The operation of the equipment used and the specific procedures employed are described in this Chapter.

5.2 Feed preparation

5.2.1 Grinding of wood

Pine wood, obtained in the form of shavings from Union Fenosa in Spain, was used as the biomass feedstock. The shavings were ground to the correct particle size for pyrolysis in a 1500 W Fritsch grinder (model number 15.302/869) fitted with a 0.5 mm sieve ring. This ensured that the width and depth of each wood particle was no more than 0.5 mm. The length, however, could be considerably longer resulting in needle shape wood particles. For effective fast pyrolysis only one biomass particle dimension needs to be small to allow fast heat transfer across the particle. Needle shape wood particles cause feeding and blocking problems within the pyrolysis system if not removed. For this reason the feed was ground twice before sieving.

5.2.2 Sieving of wood and catalyst

The ground wood was sieved in order to obtain the 75-212 μm particle size range. This allowed trouble free feeding as explained in Chapter 4. The wood particles were sieved on an Endrock shaker (model number E20244K) obtained from Endecotts Filters Ltd. A 212 μm and 75 μm sieve were used in conjunction with a base collector and a top lid to prevent spillage. The top sieve was half filled with wood, the top lid and other components assembled and the sieve assembly secured in the sieve shaker. It was turned on and left for between one and three hours. Better size fractionation of the wood particles was achieved with longer sieving times with consequently fewer feeding problems during reactor operation.

Three batches of ground wood were sieved to produce approximately 75 g of wood with a particle size distribution of 75-212 μm. The desired particle range represented approximately 20 % of the total wood sieved. This fraction could be increased by using a smaller sieve ring in the grinder but this resulted in a larger proportion of fines, below 75 μm, which in turn took longer to sieve out. Removal of the fines was necessary to prevent bridging and blocking problems in the feeder. The catalyst was sieved using the same sieve assembly which was cleaned between changing from wood to catalyst. Facile separation (<5 s for 100 g) of the catalyst particle size fractions could be achieved by manual shaking of the sieve assembly. A dust mask was worn during these procedures.

5.3 Operation of equipment used in biomass-catalyst co-feeding experiments

5.3.1 Equipment set-up

The reactor (Figure 4.2) and product collection system (Figure 4.3) have been described in Chapter 4. The following procedure was used to set up the equipment for each run:

Prior to each run the reactor was cleaned with a brush and any loose sand or char from the previous run was removed. 135 g of sand was weighed and placed into the body of the reactor. The individual parts of the reactor were weighed: reactor body, reactor top, char pot and transfer line. These parts were then assembled and weighed altogether. A metal rod was placed in the biomass feed line inside the reactor at the beginning of the set-up. This was necessary to prevent sand passing into the biomass feed line and blocking it during assembly of the reactor parts and warm up of the reactor, where fluidising nitrogen was added to aid heat transfer.

The transfer line contact point with the first condenser was lubricated with high temperature lubricant (silver goop) prior to weighing as this remained on the contact point throughout the run. After weighing, the reactor threads were lubricated (Rocol anti-seize compound) as the excess lubricant burned off during the run at the temperatures experienced in the furnace. The fittings were tightened up with spanners and a monkey-wrench in the case of the reactor top. The reactor was then placed in the furnace and insulated.

The cotton wool filter assembly was filled with cotton wool that had been oven dried at 105 °C for 24 hours. The electrostatic precipitator was assembled and the glassware was greased at the contact points with petroleum jelly and individually weighed. The glassware was assembled according to the arrangement depicted in Figure 4.3 and secured by clamps. Pinch clamps were used at each point of contact between different pieces to ensure a good seal and Keck clamps were used to secure the oil pots to the bottom of the condensers. The electrostatic precipitator electrodes were connected to the power source but were not turned on at this point.

When the reactor and glassware set-up was complete the reactor temperature thermocouple connection was attached to the digital readout, the plastic fluidising nitrogen tube was attached to the stainless steel reactor fluidising line and the plastic product gas line leading to the gas meter was attached to the end of the cotton wool filter. The furnace could then be turned on to a set point of approximately 100 °C below the required temperature. The temperature was increased gradually to the set point over a period of about one hour.

During furnace heat up, the feeder was prepared. The feeder (Figure 4.1) has been previously described in Chapter 4. The following procedure was used: It was cleaned using a compressed air line to remove any biomass remaining from the previous run. The required entrain tube was selected, cleaned, and placed in position - in experiments with a small feed particle size (75-212 μm) the 1.1 mm hole tube was used. The prepared catalyst and biomass mixture was then placed into the feeder through a wide-necked funnel whilst the lid was partially on with the stirrer inside the feed vessel. It was necessary to place the stirrer inside the feed container before the feed as there was difficulty in inserting the stirrer after the feed. The feeder lid, hand tightened with wing nuts on the flanged lid, and the feeder were turned upside down one or two times, whilst placing a finger over the top nitrogen port, to evenly distribute the feed inside and prevent compaction occurring at the bottom. The stirrer was turned a few times manually to ensure that it moved freely. The feeder was then mounted onto a clamp and the stirrer rod connected to the electrical rotor above.

The feeder was calibrated to the required flow rate for a particular run as follows: The feeder top nitrogen line and entrain feed nitrogen lines were turned on to the desired settings to allow any feed present in the entrain tube to pass out. A preweighed plastic bag was then placed over the end of the entrain tube exiting the feeder and sealed along the top. The nitrogen entering the bag was at a very low flow rate and was let out of the bag periodically by unsealing part of the top. The stirrer, the nitrogen feeder top and entrain lines were turned on for 30 seconds. The plastic bag containing feed was removed and reweighed. The feed flow rate was calculated for the settings used on the nitrogen lines and stirrer speed. If the feed rate was satisfactory, the required settings were noted for operation. If the feed rate was not satisfactory, the settings were altered accordingly and the calibration process was repeated until the correct feed rate was achieved. When the calibration procedure was complete the feeder was weighed, prior to the start of the experiment.

After approximately 45 minutes to an hour, the reactor temperature approached the set point. The fluidising gas into the reactor was turned on to aid heat transfer across the bed, ensuring that the metal rod was still positioned in the feed inlet tube. It was necessary to set the furnace temperature to approximately 7-8 degrees above the desired reaction temperature to compensate for the decrease in reactor temperature when the feed entered the reactor.

As the reactor temperature approached the set point, the plastic feed tube from the feeder was connected to the feed inlet tube to the reactor according to the following procedure: Firstly any biomass particles present in the entrain tube were removed and weighed by turning the entrain tube nitrogen on. Secondly, fluidising gas to the reactor was turned off so that the metal rod could be removed without the feed inlet tube inside the reactor becoming blocked with sand. When the metal rod had been removed the plastic feed tube was connected to the reactor inlet tube. Once the feed tube was connected and both the top nitrogen and entrain nitrogen flows to the feeder were on the fluidising gas could be turned back on without risk of blockage formation.

It was important that this procedure was followed to prevent blockage formation in the reactor feed inlet tube which would delay the experiment by at least 2 hours whilst the reactor was cooled, the blockage removed and the reactor heated up again.

When the desired reactor temperature was reached the two condensers were filled with ice and water and dry ice and acetone, respectively, and the electrostatic precipitator turned on. The reactor was then ready to run.

5.3.2 Start-up of pyrolysis run

At start-up the fluidising gas was increased to the required flow rate and the feeder stirrer and stop clock were started simultaneously. The initial reading from the meter monitoring the reactor exit gas was noted.

5.3.3 Operation

Readings of the reactor temperature, furnace temperature, set point, fluidised bed pressure, feeder pressure and gas meter volume were taken manually every minute. Careful attention was shown to the reactor temperature to ensure that it stayed within ± 3 °C. If the temperature shifted beyond this range the furnace set point was adjusted accordingly. The first gas sample was taken at 15 minutes by a manual gas sampling pump into pressurised 'bombs'. The 'bomb' was purged twice with exit gases prior to sample collection. Second and third gas samples were taken at 30 and 45 minutes respectively. The run time was approximately one hour.

5.3.4 Shut-down

At the end of the experiment, the stirrer was switched off, the time noted and a reading taken from the gas meter. The fluidising gas was then turned off followed by the feeder nitrogen flows. The furnace was turned off and the insulation removed. The nitrogen supply to the reactor was turned off at the cylinder. The power to the electrostatic precipitator was switched off five minutes after feeding ceased in order to collect residual vapours and aerosols and the system was left to cool.

5.3.5 Disassembly

When the reactor had cooled, all the parts were disconnected and isolated starting with the cotton wool filter assembly working back towards the reactor. Rubber bungs were placed in the ends of each piece of glassware to prevent losses of liquids and release of potentially hazardous vapours. An organic vapour mask was worn throughout this procedure. Although some mass may have been lost on the bungs before weighing, the corresponding reduction in the risk of spillage and the reduction of air borne products provided justification. The melted ice and acetone were emptied and the condensers dried prior to weighing. All the glassware and reactor parts were weighed before recovery of the products. The sand from the reactor was placed in a container in a muffle furnace at 800 °C to burn the char off.

5.3.6 Product recovery

The contents of the oil pots and the electrostatic precipitator were drained into sample jars. When these were completely drained the glassware was washed with ethanol to remove residual liquids, char, catalyst and associated coke - a carbonaceous deposit on the catalyst - which were on the glass walls. The ethanol dissolved products were then passed through a pre-weighed oven dried filter paper, to collect char and blown-through catalyst and coke, into a pre-weighed dry volumetric flask where the liquids were collected. A no. 20 Whatman filter paper used with a pore size of 10 μm to avoid passage of the smallest 75 μm catalyst and char particles through into the filtrate. At the end of this process the volumetric flask was weighed, the filter paper was dried in the oven overnight and then reweighed so that the fraction of char, catalyst and coke in the liquids could be calculated. A small sample of the ethanol washings were taken and stored with the two oil pot samples and electrostatic precipitator sample in a fridge for subsequent analysis. A sample of the char from the char pot was collected and kept for future analysis.

5.4 Analysis of fractions collected

5.4.1 Gas analysis

Three gas samples were collected, in sample bombs, during each run and analysed by Gas Chromatography on a molecular sieve, a Porapak Q and a picric acid column. The three columns were selected to allow detection of the following range of gaseous compounds: methane, ethane, ethene, propane, propene, n-butane, n-butene, carbon monoxide, carbon dioxide, oxygen and hydrogen. A series of gas standards in nitrogen, containing the gases of interest at known concentrations, was put through each column, prior to the gas sample in the bomb, to enable quantitative analysis of the gaseous pyrolysis products.

A total of five gas standards were used to calibrate the chromatography columns. Standards 1 and 2 were used to calibrate the molecular sieve column, standards 2 and 3 the Poropak Q column and standards 4 and 5 the picric acid column. The first standard contained 5.10 % carbon monoxide, the second 1.67 % carbon dioxide, 1.30 % oxygen, 1.54 % hydrogen and 1.57 % carbon monoxide, the third 3.09 % carbon dioxide, the fourth 1.08 % methane, 1.1 % ethane, 0.93 % propane, 0.99 % n-butane and the fifth 1.27 % methane, 1.27 % ethene, 1.00 % propene and 1.04 % n-butene. The conditions used and compounds detected by each column are presented in Table 5.1.

5.4.2 Karl Fischer - water determination of liquid products

Water determination of the pyrolysis liquid samples was conducted by Karl Fischer titrimetry on a CA-20 Moisturemeter made by the Mitsubishi Kasei Corporation. Water determination was carried out within a week of sample production. The samples were diluted by a factor of 20 in HPLC grade methanol prior to water determination since the relatively large amount of water present in the samples would have increased determination time if the sample had been injected directly. A stoppered 100 mL round bottomed flask was dried overnight in an oven at 105 °C. The flask was cooled in a desiccator and weighed to four decimal places.

Table 5.1 GC columns and relevant information

Column	Molecular Sieve 5A, Mesh Range 80/100	Poropak Q, Mesh Range 80/100	Picric Acid on Graphpac-GC, Mesh Range 80/100
Gases detected	H_2, O_2, N_2, CO	CO_2	Methane, ethane, ethene, propane, propene, n-butane, n-butene
Machine	Pye Unicam Series 204	Pye Unicam Series 204	Perkin-Elmer Sigma 2B
Detector	Thermal conductivity	Thermal conductivity	Flame ionisation
Column	5' stainless steel, 1/4" OD, 3/16" ID	5' stainless steel, 1/4" OD, 3/16" ID	6' stainless steel, 1/8" OD, 0.085" ID
Manufacturer	Phase Separations	Phase Separations	Alltech
Carrier gas	Helium	Helium	Helium
Carrier flow rate	30 mL min^{-1}	30 mL min^{-1}	15 mL min^{-1}
Detector temperature	150 °C	150 °C	150 °C
Injector temperature	150 °C	150 °C	150 °C
Column temperature	70 °C	70 °C	30 °C
Sampling valve temp	70 °C	70 °C	30 °C
Sample volume	1mL	1mL	1mL
Detector range & attenuation	-	-	32 x 10
Integrator	-	-	Spectra-Physics SP4100 computing integrator

Approximately 0.5 mL of pyrolysis liquid sample was injected into the round bottomed flask, from a 10 mL syringe, the stopper replaced and the flask reweighed. 10 mL of HPLC grade methanol was added to the pyrolysis liquid sample using the 10 mL syringe, the stopper replaced and the flask reweighed. The syringe was thoroughly rinsed with methanol prior to dilution of the pyrolysis liquid sample. The flask was swirled to ensure complete mixing of the methanol and pyrolysis liquid sample.

A 1 mL glass syringe was rinsed with HPLC grade methanol, air dried and weighed to four decimal places. 1 mL of the diluted sample was taken up into the pre-weighed syringe. The needle was sealed with a small pre-weighed rubber bung to prevent evaporation and the syringe reweighed. The mass of the sample could then be accurately determined. The contents of the syringe were injected into the sample chamber of the Karl Fischer titrator and the water content determined automatically.

5.4.3 Liquids analysis

5.4.3.1 Gas Chromatography-Mass Spectroscopy (GC-MS)

GC-MS analysis was carried out at the Institute of Wood Chemistry in Hamburg, Germany. A GC/MSD from Hewlet Packard was used with a 60 m x 0.25 mm Chromopak column, CP Si119 CB (equivalent to DB 1701). Helium, at a flow rate of 1 mL min^{-1}, was used as the carrier gas. The injector temperature was set at 250 °C, the oven at 45 °C for 4 minutes followed by an increase of 3 °C min^{-1} up to 280 °C. The interface temperature between the GC and the MS was set at 280 °C.

5.4.3.2 Gas Chromatography-Flame Ionisation Detector (GC FID)

GC-FID was also carried out by the Institute of Wood Chemistry, Hamburg, Germany on a Chrompack (NL) CP9000 gas chromatograph. The detector temperature was set at 280 °C, the injector at 250 °C and the carrier gas was helium at a pressure of 2 bar. The oven program used was as follows: 4 minutes isothermal at 45 °C followed by an increasing temperature of 3 °C min^{-1} up to 280 °C followed by 15 minutes at 280 °C. A DB1701 (J&W) column was used (60 m long by 0.25 mm wide with a film thickness of 0.25 μm). The split ratio was 1:35. 30 mg of the bio-oil sample for analysis was prepared by dilution in 1 mL of methanol which contained the internal standard, fluoranthene. Approximately 1 mL of the prepared sample was placed in a vial, labelled and put into the GC-FID system for automated injection and analysis.

5.4.3.3 High Performance Liquid Chromatography (HPLC)

HPLC was used to analyse the aqueous soluble components of the pyrolysis liquid samples. Samples were prepared for analysis by HPLC as follows. Approximately 0.3 g of oil sample was weighed accurately into a standard micro centrifuge tube, distilled water was then added in a 2:1 ratio, the lid on the vial was closed and the vial shaken vigorously for 30 seconds. The sample was then centrifuged for 5 minutes at 5000 rpm. The clarified aqueous liquid was decanted from the heavier oil phase into a 2 mL glass syringe barrel and then transferred through a 0.5 μm syringe filter (e.g. Gelman Acrodisc, PTFE; Millipore Millex-LCR_{13}) into another vial. The aqueous insoluble oil phase contained the pyrolytic lignin and fine particulate char. Methanol was added and left to evaporate before re-weighing to determine the lignin content.

A standard mix of chemicals was used to calibrate the column prior to analysis of the aqueous fractions of the three oil samples of the run. 5 mL of the sample was injected into the Rheodyne injection valve port in the load position. The Rheodyne valve was rotated to the inject position and the start button on the Data Capture Unit (DCU) simultaneously pressed to start the analysis.

5.4.4 Char and catalyst analysis

In many runs, it was unclear exactly what proportion of collected solids consisted of char and what proportion consisted of catalyst and associated coke. The following procedures were designed and carried out to separate the catalyst from the char collected in the char pot samples. The ash or coke content of the char or catalyst was then carried out according to the American Standard Test Method Determination (ASTM) 1762.

5.4.4.1 Water floatation method

The char/catalyst sample (approximately 10 g) was weighed and dried in an oven at 105 °C for two hours, placed in a dessicator for one hour and re-weighed (ASTM D1762, 7.2). This procedure was repeated until consecutive weights agreed in order to make sure the catalyst/char mixture was dry. The moisture content was then calculated by difference.

The sample was then placed in a 1 L beaker with 500 mL distilled water whilst swirling to ensure good mixing of sample and water. It was sometimes necessary to stir the mixture with a glass rod. Two filter papers for each sample were labelled and placed in an oven for at least two hours to dry. The suspended mixture was allowed to settle out with the catalyst sinking to the bottom whilst the majority of the char floated on the top. Some heavy char sank as well. When the catalyst had reached the bottom, the top part was carefully decanted off into one of the pre-dried and pre-weighed filter papers. It was sometimes necessary to repeat this floatation stage in order to lift the heavier char from the bottom. In this case the liquid was filtered as soon as the catalyst had sunk whilst the char was still suspended. When as much of the char as possible was removed from the beaker, the remaining catalyst was poured into the second pre-dried and pre-weighed filter paper. The water was allowed to drain off and the filter papers were placed in the oven for at least two hours to dry. When dry, the filter papers were re-weighed and the catalyst to char ratio in the sample calculated.

5.4.4.2 Ash and coke content

Before this procedure is explained, it should be noted that the carbon deposition on the catalyst is termed coke. ASTM D1762 was used as a guide and modified slightly due to the catalyst.

Uncovered crucibles and lids were first prepared by placing them in a furnace at 750 °C for at least two hours to allow any deposits to be burned off. The crucibles were then placed in a desiccator to cool for one hour. The crucibles were weighed and the catalyst or char (approximately 1 g each time) from the dried filter papers placed into separate crucibles and re-weighed. The crucibles were then placed in the furnace with their lids part on for six hours, to burn off all the volatile char and coke.

When this was complete, the crucibles were taken out of the furnace and placed in a desiccator to cool for one hour and then reweighed. This process was repeated until a succeeding one hour period of heating results in a loss of less than 0.0005 g (D1762, 7.4). The ash and coke contents were calculated by difference.

CHAPTER SIX

RESULTS AND DISCUSSION

6 RESULTS AND DISCUSSION

6.1 Introduction

The experiments carried out with a 150 g h^{-1} fluidised bed reactor are discussed and compared to those results achieved with a 1 kg h^{-1} fluidised bed reactor in this chapter. Terms used to describe the experiments carried out are defined. A run is defined as one complete operation of the fluidised bed reactor and associated equipment which includes set up, feed preparation, fast pyrolysis inside the reactor, shut down, collection and weighing of product fractions, as described in Chapter 5 Section 5.3. A series of runs is defined as a number of runs which were carried out to investigate the effect of a specific parameter or operating arrangement. A catalytic run is defined as a run which involves the incorporation of catalyst whereas a non-catalytic run is defined as a run which does not involve the incorporation of catalyst.

Four series of runs were carried out using pine wood as feedstock. Temperature was varied within each series whilst keeping catalyst concentration and reactor size constant. The first series, called LAC/CMD, was non-catalytic and carried out on a 1 kg h^{-1} fluidised bed reactor. The second, third and fourth series, designated LAC1, LAC2 and LAC3 respectively, were carried out on a 150 g h^{-1} fluidised bed reactor. Runs constituting LAC series 1, 2 and 3 were numbered in chronological order from SFBC03-SFBC34. LAC1 refers to all non-catalytic runs, LAC2 to all runs which contained 25 % (by weight) catalyst in the feed and LAC3 to all runs which contained 50 % (by weight) catalyst in the feed (where feed refers to the sum of catalyst and wood fed to the reactor). All LAC series runs (SFBC03-SFBC34) were carried out in a totally random order with respect to reaction temperature, catalyst concentration in the feed and specific operational objectives. Product yields from a fifth series of non-catalytic runs, called RAH, carried out by Hague (208) have been included for comparison with LAC1 and LAC/CMD. A summary of the five series is given in Table 6.1.

Table 6.1 Summary of fluidised bed fast pyrolysis series presented

Series	Reactor	Feedstock	Feed Particle Size	Catalyst Content Of Feed (%)
LAC1	150 g h^{-1}	pine	75-212 μm	0
LAC2	150 g h^{-1}	pine	75-212 μm	25
LAC3	150 g h^{-1}	pine	75-212 μm	50
RAH	150 g h^{-1}	pine	350-500 μm	0
LAC/CMD	1 kg h^{-1}	pine	0.6-1.7 mm	0

The data obtained from runs in series LAC1, LAC2 and LAC3 is analysed in detail in the first part of the chapter. The mass balance methodology is defined and an assessment of the run stability is made. The reliability of the product yield results is also assessed in terms of deviation from their apparent product yield trends. Errors are calculated for specific run conditions carried out in triplicate and the sources of experimental error are discussed. In the second part of the chapter the non-catalytic series LAC1 is compared to series RAH and LAC/CMD. The product yields from series LAC1, RAH and LAC/CMD are discussed with respect to differing variable levels such as particle size and temperature. In the third part of the chapter the series LAC1, LAC2 and LAC3 are compared and discussed in order to assess the effect of catalyst in the feedstock on the yields and composition of products. Finally the reactor system is discussed in terms of a model.

6.2 Mass balance methodology for LAC series on 150 g h^{-1} reactor

6.2.1 Introduction

A mass balance accounts for all of the mass entering a system in terms of the mass exiting a system and the mass accumulated within the system. The mass balance is necessary in order to calculate the yields of desirable products which can be taken to be a measure of the efficiency of the process. The mass balances calculated for the LAC series are on a dry wood feed basis. The expression used to calculate the mass balances for series LAC1, LAC2 and LAC3 is given in Equation 6.1.

$$\text{Dry wood in} = \text{Char (pyrolysis product \& catalytic coke)} + \text{Liquid pyrolysis product} + \text{Gaseous pyrolysis product}$$

Equation 6.1 Basic mass balance expression for series LAC1, LAC2 and LAC3

Note: Char refers to all loose carbonaceous deposits and those on the sand whereas coke refers to all carbonaceous deposits on the catalyst. The coke and char yields are presented together. Catalyst is not included in this expression as it is neither consumed or produced during the reaction. Catalyst is included, however, in the mass balance breakdown in Tables 6.2-6.4 to demonstrate it's association with pyrolysis products.

6.2.2 Definitions of mass balance constituents

A brief description of reactor inlets and the product collection and measurement procedures is provided as a reminder of the equipment operating procedure described in Chapter 5. Wood and catalyst fed to the reactor throughout the run were measured by calculating the difference in weight of the feeder vessel before and after the run. The ratio of catalyst to wood was achieved during feed preparation by mixing the two materials thoroughly before filling the feeder vessel. The ratio of catalyst to wood remaining in the feeder at the end of each run was checked according to the procedure in Section 5.4.4.1 to ensure that separation or unequal feeding of catalyst and wood had not occurred during the run. The moisture contents of the catalyst/wood feed were measured, from the average of three samples taken from the feed at the start of each run, by the oven method described in Chapter 5.

Nitrogen was metered to the reactor vessel throughout the run via two nitrogen lines: a fluidising nitrogen line and a feed entrain nitrogen line via the feeder. In addition a nitrogen top pressure was exerted on the feeder via a feeder top pressure nitrogen line which ensured entrainment of wood and catalyst to the entrain tube. Nitrogen flow rates were controlled by rotameters and readings were taken throughout the run so that the total nitrogen entering the system could be calculated.

The reactor parts were weighed before and after each run to allow the measurement of weight increases in:

- the stainless steel reactor, including reactor top, transfer line, char pot and reactor body separately;
- condenser 1 and oil pot 1;
- condenser 2 and oil pot 2;
- the electrostatic precipitator; and
- the cotton wool filter.

The reactor and stainless steel accessories contained deposited char, catalyst and associated coke after the run. Solids collected in the char pot and transfer line were analysed for char: catalyst ratio and their respective ash and coke contents as described in Chapter 5. Solids collected in the reactor body were too small an amount for further analysis to be feasible (1.5 wt% or less). The glassware contained liquid products, some fine char, catalyst and coke. Most of the solids were deposited on the glassware walls but a small amount of very fine material passed into the oil pots. After collection of the samples from the condenser oil pots and the electrostatic precipitator, the remainder of the products collected in the glassware were recovered in ethanol. Removal of fine char and catalyst from the glassware walls proved to be problematic in the initial runs but improved with experimental experience (Section 6.3.9). The ethanol washings were filtered to separate the char and catalyst for quantification. The amount recovered, however, was too small to calculate char: catalyst ratios, coke or ash contents. In the mass balance calculation, the combined yield of char and coke products was determined by subtracting the amount of catalyst fed from the total solids collected (i.e. solids accumulated in reactor, cyclone, char pot and fraction accumulated in the glassware with the liquids).

Tables 6.2 and 6.3 describe the mass balance with respect to: the total mass entering, exiting and accumulated within the system - highlighted in bold text; and the mass of dry wood entering the system and the mass of pyrolysis products from dry wood exiting and accumulated within the system - highlighted in bold and underlined text. Example masses from run no. SFBC08 are given.

Table 6.2 Description of constituents entering system with mass balance example (SFBC08)

Constituent	Description	SFBC08 (g)
Dry Wood	**Wet wood (feeder weight loss x wood fraction) – moisture content (oven determination)**	**33.69**
Dry Catalyst	Wet catalyst (feeder weight loss x catalyst fraction) – moisture content (oven determination)	33.69
Feed water	Water in wood and water in catalyst (oven determination)	4.32
Total in	**Dry wood + dry catalyst + feed water**	**71.70**

Table 6.3 Description of constituents exiting and collected within system with mass balance example (SFBC08)

Constituent	Description	SFBC08 (g)
Solids recovered	**Solids in reactor + char pot/transfer line + glassware**	**42.04**
Reactor solids	Reactor weight increase	0.52
Char pot/transfer line solids	Char pot/ transfer line weight increase	41.10
Glassware solids	Glassware weight increase x fraction of recovered solids from ethanol wash and filtration	0.42
Pyrolysis char and coke	**Solids recovered – catalyst fed**	**8.33**
Total liquids	**Glassware weight increase – solids**	**21.94**
Organic liquids	Total liquids – water (Karl Fischer determination)	13.92
Pyrolysis water	Total water – water in feed	3.79
Pyrolysis liquid	**Total liquid – water in feed**	**17.62**
Pyrolysis gases	**Gases vented (gas metered) x percentage of G.C. detectable pyrolysis products in gas samples**	**9.30**
Total out	**Solids recovered + Total liquid + Pyrolysis gases**	**73.28**
Total from dry wood	**Pyrolysis char & coke + Pyrolysis liquid + Pyrolysis gases**	**35.25**

Table 6.4 describes the analysis of solids collected in the char pot and transfer line. Example masses from run no. SFBC08 are given and it can be seen that 32.48 g of catalyst from 33.69 g fed are recovered in the char pot and transfer line – corresponding to 96 wt%. The balance of catalyst of 1.21 g being located in the reactor body, glassware and possibly the liquid products.

Table 6.4 Description of char pot and transfer line solid analysis with mass balance example SFBC08

Constituent	Description	SFBC08 (g)
Solids	Char pot/ transfer line weight increase	41.10
Char	Calculated from char: catalyst & coke ratio from water flotation separation	5.60
Catalyst & coke	As for char	8.62
Coke	Calculated from burning coke off catalyst in furnace	3.02
Catalyst	As for coke	32.48
Catalyst balance	Dry catalyst in – catalyst in char pot and transfer line	1.21

6.3 Run stability of LAC series on 150 g h^{-1} reactor

Run stability is defined as the degree of trouble-free operation during the run. The three series of runs carried out on the 150 g h^{-1} reactor were conducted according to the mode of operation described in Chapters 4 and 5 and mass balances were calculated according to the method described in Section 6.2. In order to assess the operation of the 150 g h^{-1} reactor throughout this mode it was necessary to examine the degree of stability achieved using the data collected throughout the runs. It should be noted that the data collected is preliminary and prone to scatter due to the limited amount of experience. Only one run was carried out at many of the experimental conditions presented although selected conditions were carried out in triplicate and are discussed in Section 6.4. Repeatability of the data presented needs to be investigated by further experimentation. The objective of the majority of the runs, SFBC03-SFBC34, was to study the effect of temperature and catalyst feed concentration on the mass balance product yields and the chemical composition of the liquids and gaseous fractions produced.

A smaller proportion of runs had specific operational objectives to study the effects of process parameters, other than temperature or catalyst concentration, on the yields of the main product fractions and the effects of collection procedure on the accuracy of product yield determination. These were as follows:

- SFBC10 was carried out to investigate the effect of condenser arrangement;
- SFBC14 and SFBC16 were carried out to investigate pyrolysis at low temperature, 450 °C, operation at 0 % and 50 % catalyst feed concentration, respectively;
- SFBC18 was carried out to determine the lowest temperature at which pyrolysis could be carried out successfully in the operating system used; and
- SFBC33 and SFBC34 were carried out to measure the yield of char produced at 0 % and 50 % catalyst concentration in the feed, respectively.

All of the runs, SFBC03-SFBC34 constituting LAC series 1-3, were carried out in a random order, with respect to reactor temperature and catalyst concentration. This was particularly important for the investigation of the effect of catalyst concentration and temperature so that any effects arising due to other variables could not contribute to the product yields achieved. These variables were:

- learning effects associated with reactor operation including experimental technique and procedure;
- developments in analytical techniques; and
- uncontrollable variables such as ambient temperature and humidity which could affect feed storage and preparation.

The runs carried out to study the effect of catalyst concentration and temperature alone are considered in Sections 6.3.2 to 6.3.5 followed by runs with specific operational objectives in Sections 6.3.6 to 6.3.8. Finally improvements to operating procedures are outlined in Section 6.3.9.

6.3.1 Run stability and the assignment of instability values

The stability of each run was prone to variation in terms of:

- reactor temperature fluctuations throughout the run caused by furnace temperature control;
- feeding problems such as blockages caused by bridging biomass particles;
- pressure fluctuations across the reactor and feeder throughout the run caused by partial and total feed blockages; and
- nitrogen flow rate fluctuations into the reactor throughout the run also caused by feeder blockages creating back pressures in the nitrogen lines.

Profiles of the reactor temperature, furnace temperature, furnace temperature set-point and the gas flow rate out of the system throughout a run were plotted against the total time for each run. Example profiles can be found in Appendix A. Biomass feed rates and nitrogen flow rates into the system were also examined for consistency although they were not monitored continuously throughout the run as was the case with reactor temperature and gas flow rate out.

These fluctuations, monitored throughout the runs, have been analysed to assess the degree of instability in each run. Values have been assigned to the degree of deviation of each variable from the desired point to the following 'instability factors':

- reactor temperature standard deviation;
- degree of feed blockages;
- feeder pressure standard deviation; and
- reactor pressure standard deviation.

Values have also been assigned to the following 'instability indicators':

- degree of rotameter adjustments – reflecting the nitrogen flow rate fluctuations to the reactor; and
- mass balance closure – reflecting errors in product collection and measurement.

Real values are assigned where applicable and arbitrary values are assigned to instability factors and indicators which cannot be precisely quantified. Instability values assigned for each fluctuating variable and the 'instability index' are presented in Tables 6.5 (for runs carried out without specific operational objectives) and 6.6 (for runs carried out with specific operational objectives). The values are converted to positive integers and summed to give the 'instability index'.

A complete description of the arbitrary numbers assigned to instability factors is given after Table 6.5, for example, the degree of total blockages throughout run is assigned a value of 0 for runs where there were no blockages during operation and a value of 6 for runs which were extremely problematic due to either the severity or frequency of blockages.

6.3.2 'Product yield deviation' from apparent product yield trends

The objective of this section is to identify anomalous results and to analyse the general scatter. The product yield data for most of the experimental conditions presented is derived from individual runs and shows a degree of scatter. Trends were therefore fitted based on established product yield trends from fast pyrolysis with temperature (78, 207, 208 above).

Over the 450 to 550 °C temperature range the yield of total liquids follow a positive polynomial trend peaking at around 500 °C, the yield of char follows an opposing negative polynomial curve dipping at around 500 °C, the yield of gas follows a negative polynomial trend increasing with temperature and the yield of water follows a linear trend remaining constant throughout.

Figures 6.1, 6.2 and 6.3 show graphs of product yield of the major mass balance fractions against temperature for non-catalytic, 25 % feed catalyst concentration and 50 % feed catalyst concentration respectively. Product yield trends are plotted for the yield of total liquids, water, char and gas based on established fast pyrolysis product trends with temperature (78, 207, 208).

Best fit trends were identified for each run series against temperature, after discounting anomalies, using the Microsoft Excel chart facilities. The yields of total liquids from each run are identified by their corresponding run number. The apparent product yield trends in Figures 6.1, 6.2 and 6.3, and throughout Chapter 6, are either polynomial, and denoted as 'Poly.', or linear, and denoted as such. In order to assess the degree of scatter from the fitted trendlines each product yield was categorised as to whether deviations of ± 2.5 %, ± 5 %, ± 7.5 % or ± 10 % overlapped the fitted trend. The deviation in the individual product yields and sum of deviation in product yields for each run is presented in Tables 6.5 and 6.6.

Real, as opposed to normalised, product yields have been used as the low mass balance closures calculated for certain runs are due to one of the product yields being disproportionally low compared to the other product yields from a specific run due to experimental error. In such a case normalisation of the data would result in the rest of the product yields being over represented in a normalised mass balance.

The variation of the yield of each product (total liquids, gas and char) from their apparent product yield trend is quantified in terms of a percent deviation from that yield trend and presented in Tables 6.5 and 6.6. For each run, the percent deviation of each product yield (total liquids, gas and char) are summed giving a 'sum of product yield deviations', from apparent product yield trends, in each run. The product yield deviation obtained for the yield of water is also presented in Tables 6.5. and 6.6 but is omitted from the 'sum of product yield deviations' as it is directly dependant on Karl Fischer water analysis.

This 'sum of product yield deviations', from apparent product yield trends, for each run is compared to the instability index for that run in Section 6.3.3.

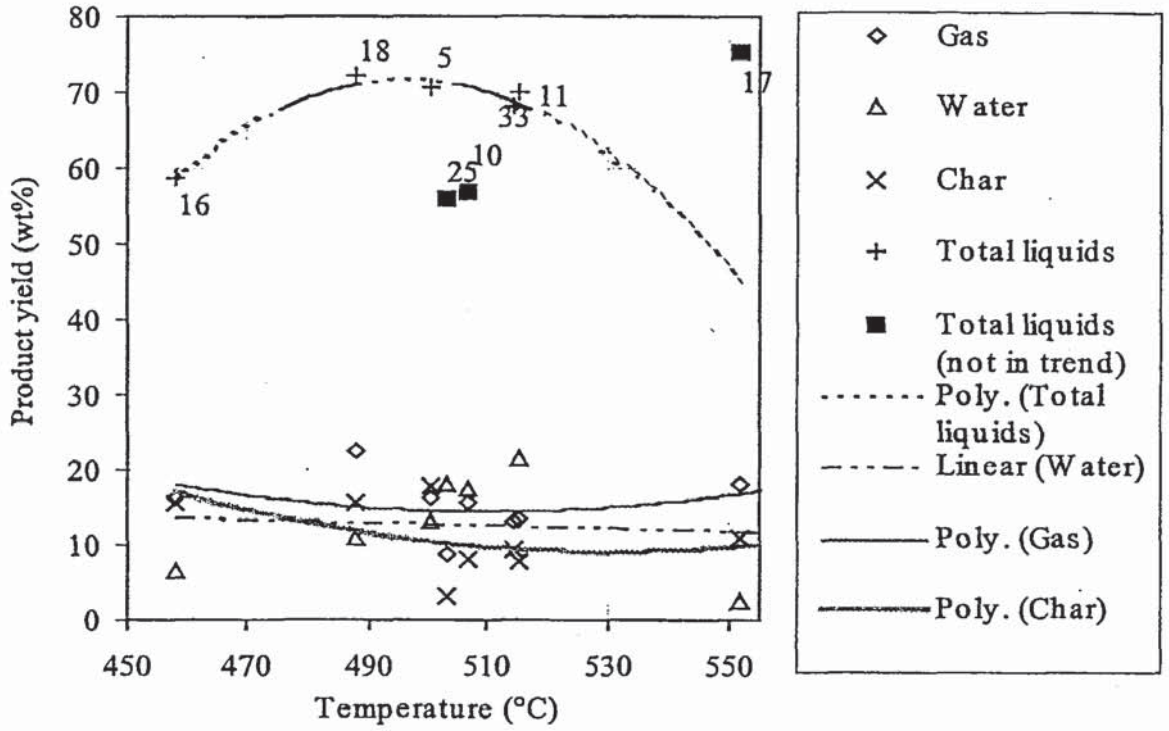

Figure 6.1 Real product yields versus temperature for non-catalytic runs

Yields of total liquids for SFBC25, SFBC10 and SFBC17 are shown in Figure 6.1. but were not included in the data used to plot the trend of total liquids. SFBC25 was omitted due to the anomalous yields of total liquids which does not agree with past work for pine pyrolysis on either this system (208), the larger 1 kg h^{-1} fluidised bed (207) or softwood pyrolysis work carried out on a similar fluidised bed (78). (SFBC25 was a repeat of SFBC05 and suffered severe blocking throughout and achieved a very low closure and yield of total organics). SFBC10 was omitted from product yield trends in Figure 6.1 as it was carried out with the specific objective of studying the effect of condenser temperature which affected the product yield distribution as quenching was less rapid than with other runs allowing a greater degree of gas phase reactions to occur. This is discussed in more detail in Section 6.3.6. The yield of total liquids for run SFBC17 is anomalous. It is much higher than would be expected.

Other runs which were carried out with specific operational objectives, i.e. SFBC14, 16, 18, 33, 34, were included, in the relevant graphs shown in Figure 6.2 and 6.3, as their objectives were either low temperature operation or collection of products to ensure all the char was filtered out of the liquids for a complete char balance. Neither of these operational objectives interfered in the overall product yield results versus temperature and catalyst concentration.

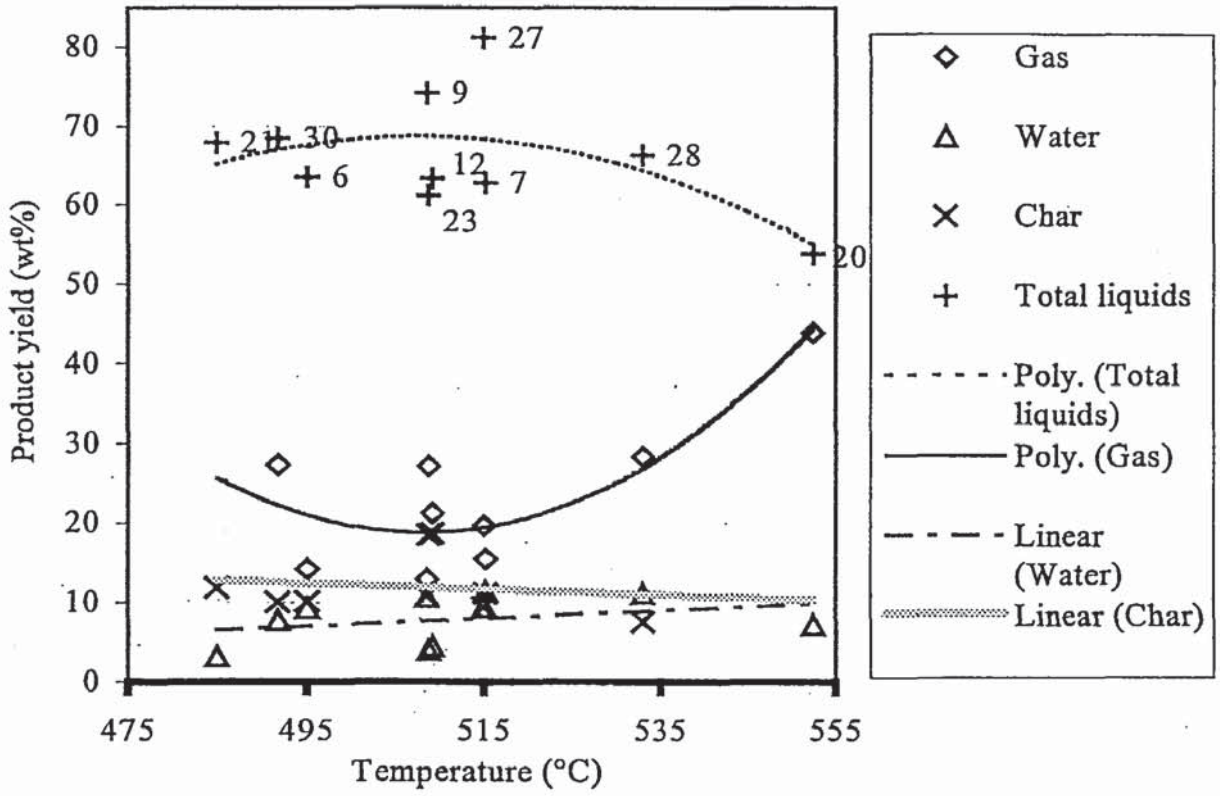

Figure 6.2 Real product yields versus temperature for 25 % catalyst runs

From Figures 6.1 to 6.3 it appears that the degree of scatter of the product yields increases with increasing catalyst concentration. This may be a reflection of the increased difficulty in separating and quantifying products in catalytic runs due to the presence of catalyst with the liquid products in the glassware. The efficiency of collection, and thus the accuracy of product quantification, from the glassware was particularly prone to learning effects as experimental technique and collection procedure improved with experience.

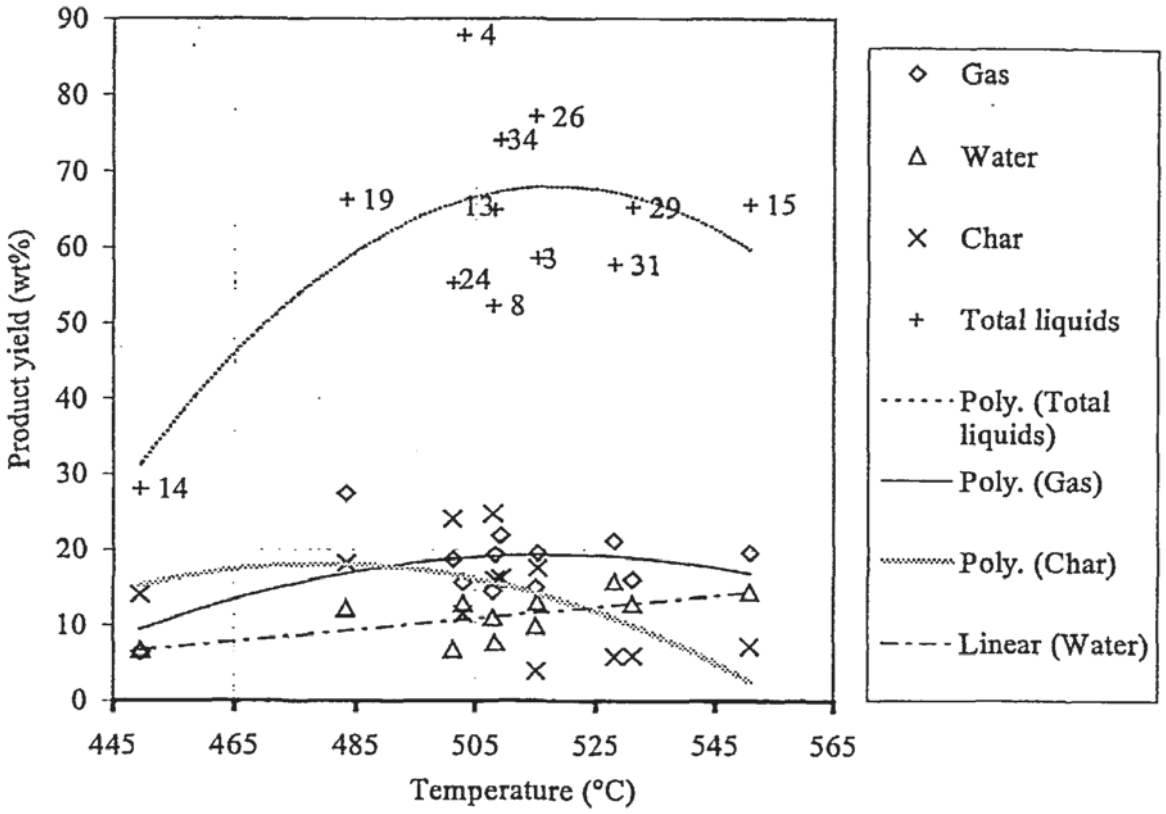

Figure 6.3 Real product yields versus temperature for 50 % catalyst runs

6.3.3 Comparison of instability index and product yield deviation from apparent trends

A summary of the 'sum of product yield deviations', from apparent product yield trends, (Fig. 6.1, 6.2 and 6.3) and 'instability indexes' from LAC1, 2 and 3 (SFBC03-SFBC34) is presented in Table 6.5 for runs which were carried out to investigate reactor temperature and catalyst feed concentration and Table 6.6 for runs which were carried out to investigate specific operating conditions. Nitrogen flow rate into the reactor remained between 11.28 and 12.30 L min^{-1} apart from run numbers SFBC14, 16, 18, 19, 21, 31, 33 and 34 all of which had lower flow rates in the range 8.10 to 10.02 L min^{-1}. A complete description of arbitrarily assigned values is given after Table 6.5.

Table 6.5 Instability and 'product yield deviation' from runs investigating the effects of reactor temperature and catalyst feed concentration

Run No.	Average Vapour Residence Time[a]	Average Pyrolysis Products In N_2	Feed Moisture Content	Reactor Temp. Standard Deviation	Feeder Pressure Standard Deviation	Reactor Pressure Standard Deviation	Mass Balance Closure Deviation	Degree Of Total Blockages[b]	Degree Of Rotameter Adjustments	'Product Yield Deviations' From Apparent trends (Fig 6.1-6.3) Within Stated Error Bars (± wt%)				Instability Index	'Sum Of Product Yield Deviations'
	(s)	(%)	(wt%)							Gas	Liquids[c]	Water	Char		
SFBC03	0.44	6.05	4.55	3	1.2	1.2	0	0	0	2.5	7.5	2.5	5	5.4	15
SFBC04	0.44	7.56	4.87	5	0.7	1.2	+2	0	0	5	25	2.5	5	8.9	35
SFBC05	0.45	6.01	8.77	3	0	0.8	0	0	0	2.5	2.5	2.5	5	3.8	10
SFBC06	0.48	1.00	6.24	3	0.7	0.8	-2	0	0	7.5	5	2.5	2.5	6.5	15
SFBC07	0.44	6.42	7.47	3	0.6	0.4	-2	0	0	5	10	5	2.5	6	17.5
SFBC08	0.45	6.87	6.41	5	0.1	0	-1	0	0	5	12.5	2.5	10	6.1	27.5
SFBC09	0.45	5.13	8.04	4	0	0.3	0	0	0	10	7.5	2.5	2.5	4.3	20
SFBC11	0.44	6.73	8.65	1	0	0	-1	0	0	5	2.5	12.5	5	2	12.5
SFBC12	0.45	5.09	7.57	2	0.4	0	0	0	0	2.5	7.5	5	7.5	2.4	17.5
SFBC13	0.47	2.33	6.7	2	0.8	3.1	0	0	0	2.5	2.5	5	2.5	5.9	7.5
SFBC15	0.43	5.46	5.83	1	0	0	-1	0	0	5	7.5	2.5	5	2	17.5
SFBC17	0.42	5.13	8.39	2	0.5	0.5	0	1	-1	2.5	2.5	7.5	2.5	5	7.5
SFBC19	0.69	6.13	6.36	6	1.1	2.2	+2	0	+1		10	5	2.5	12.3	12.5
SFBC20	0.43	2.77	7.15	3	1.2	0	0	0	0	2.5	2.5	5		4.2	5
SFBC21	0.64	6.35	7.54	1	2.0	1.5	-2	1	0		2.5	5	2.5	7.5	5
SFBC23	0.45	4.91	6.4	2	1.3	1.1	+1	5	-1	7.5	7.5	5	7.5	11.4	22.5
SFBC24	0.45	9.44	7.46	3	0.6	0.5	0	0	0	2.5	10	5	7.5	4.1	20
SFBC25	0.48	4.15	4.08	3			-4	6	-1	7.5	15	7.5	10	14	32.5
SFBC26	0.45	5.12	0.6	3	0	0	0	6	0	5	12.5	2.5	10	9	27.5
SFBC27	0.44	6.33	2.63	2	0	0	+1	3	0	2.5	15	2.5	2.5	6	20
SFBC28	0.45	7.90	1.71	7	0.4	0.4	0	1	-1	2.5	2.5	2.5	5	9.8	10
SFBC29	0.44	5.95	1.71	10			+1	6	1	5	2.5	2.5		18	7.5
SFBC30	0.36	6.90	0.42	4	0		+1	4	0	5	2.5	2.5	2.5	9	10
SFBC31	0.44	2.83	0.31	10	4		-1	4	0	2.5	10	5	5	19	17.5

Where:

- mass balance closures of 100 ±5 wt% = 0, 100 ± 10 wt% = +1 or -1 respectively and 100 ± 20 wt% = +2 or -2 respectively;
- degree of rotameter adjustments required range from: continually increasing at +2 to continually decreasing at -2; and
- degree of blockages throughout the run takes both severity and frequency into account ranging from 1 for a minor block to 2 for continuous minor blocking, 2 for a severe block up to 6 for continuous severe blocking;
- [a]: Average vapour residence time in the reactor;
- [b]: Degree of total blockages in reactor and feeder;
- [c]: Total liquids

Table 6.6 Instability and 'Product yield deviation' from runs with specific operational objectives

Run No.	Average Vapour Residence Time[a]	Average Pyrolysis Products In N_2	Feed Moisture Content	Reactor Temp. Standard Deviation	Feeder Pressure Standard Deviation	Reactor Pressure Standard Deviation	Mass Balance Closure Deviation	Degree Of Total Blockages[b]	Degree Of Rotameter Adjustments	'Product Yield Deviations' From Apparent trends (Fig 6.-6.3) Within Stated Error Bars (± wt%)				Instability Index	'Sum Of Product Yield Deviations'
	(s)	(%)	(wt%)							Gas	Liquids[c]	Water	Char		
SFBC10	0.45	5.87	7.9	7	1.0	23.5	0	0	0	2.5	15	7.5	5	31.5	22.5
SFBC14	0.58	6.29	6.5	3	0.6	18.5	-6	0	-3	5	5	2.5	2.5	31.1	12.5
SFBC16	0.77	11.27	8.4	4	2.0	15	-1	0	-2	2.5	2.5	7.5	2.5	24	7.5
SFBC18	0.76	13.29	8.2	4	2.6	21	0	0	0	7.5	5	2.5	2.5	27.6	15
SFBC33	0.68	2.12	8.3	1		16	-1	0	0	5	5	10	5	18	15
SFBC34	0.69	2.65	6.6	8	0	20	-2	0	-1	2.5	5	12.5	2.5	31	10

The 'instability index' is plotted in Figure 6.4 against the 'Sum of product yield deviation', from apparent product yield trends, for each run.

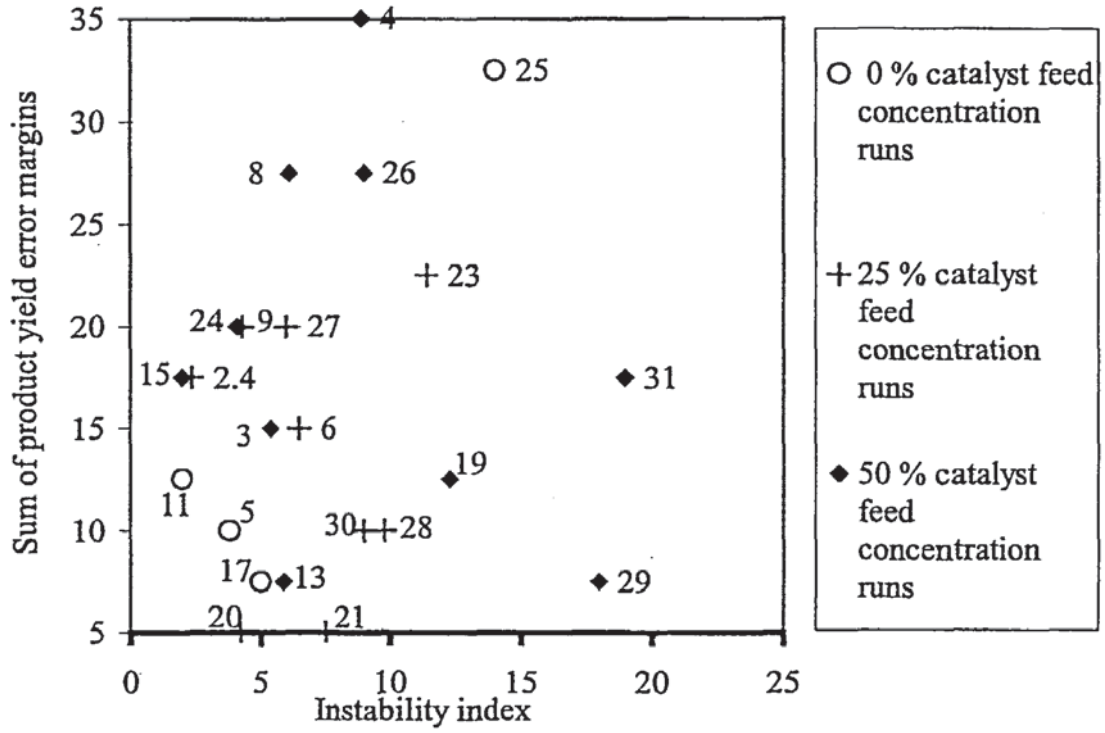

Figure 6.4. 'Sum of product yield deviation', from apparent product yield trends, versus the 'instability index' for each run

There is no clear correlation between the 'sum of product yield deviation', from the apparent product yield trends, for each run and the 'instability index' in Figure 6.4. There is more scatter of the 'sum of product yield deviation' versus 'instability index' for runs carried out at catalyst feed concentrations of 50 % . These runs experienced either very high instabilities or resulted in product yields which varied more than most from the apparent product yield trends. With the exception of non-catalytic run SFBC25, which was unusually problematic, the non-catalytic runs appear to have the lowest values of both 'sum of product yield deviation' and 'instability index'. Variables other than those accounted for in the 'instability index' may have an effect on the 'product yield deviation'. The highest 'sum of product yield deviation' values obtained for 50 % catalyst concentration feed runs, SFBC04, 08 and 26 show a high degree of 'product yield deviation' without a comparable 'instability index'.

Figure 6.5 shows the 'instability index' and 'sum of product yield deviation', from apparent product yield trends, versus the run number (in chronological order).

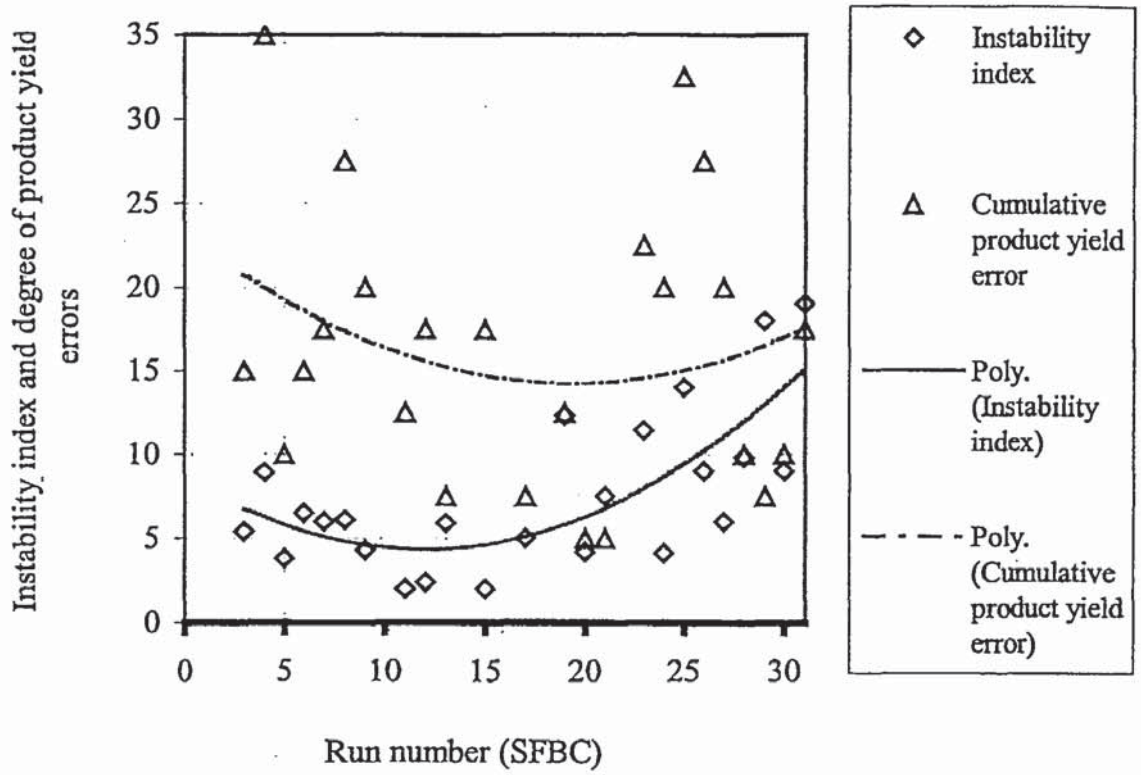

Figure 6.5 'Sum of product yield deviation', from apparent product yield trends, and 'instability indexes' versus run numbers (SFBC03-SFBC34)

There is no clear correlation between 'sum of product yield deviation' and run chronology although there are very high values of 'sum of product yield deviation' found both intially and in the latter stages of the experimental work. The 'instability index' decreases slightly with run chronology to a minimum, at around run no. SFBC15, and then increases again, towards the end. The decrease in 'instability index' is due to initial learnings at the start of reactor operation. This increase in 'instability index' is due to blockage problems which became problematic from run no. SFBC25 onwards. The blockage problems encountered are most likely due to insufficient sieving time which left a large proportion of fines in the feedstock.

6.3.4 The effect of reactor temperature standard deviation on product yields

It was thought that reactor temperature standard deviation would affect the stability of the pyrolysis reaction. Reaction rates of pyrolysing biomass and interactions of freshly formed vapours depend on temperature. The reactor temperature standard deviation and the yield of total liquids were compared throughout the run data but no apparent relationship was identified. This indicates that the yields achieved depend on the average temperature throughout the run and are not significantly affected by temperature fluctuation during the run.

6.3.5 The effect of feeder blockages

Occasional severe feed blockages were a problem and were found to contribute to the sum of product yield deviations but they could not be linked directly. The major source of feed blockages was discovered to be due to inadequate sieving which could be resolved by altering preparation procedure. Modifications to the preparation procedure are described in Section 6.3.9 under improvements to operating procedure. Throughout the runs, experimental technique in managing feed blockages was improved. For example, run no. SFBC25 was one of the first runs to encounter severe blockages and resulted in a relatively low mass balance closure of 67.5 wt% and the pressures across the feeder and reactor could not be monitored manually due to the constant blockages. Severe blocking was encountered in run numbers SFBC26 and SFBC29, however, but achieved mass balance closures of 96 wt% and 109 wt% respectively.

This was directly due to improvements in experimental technique which enabled more effective management of blockages as they occurred.

6.3.6 The effect of condenser temperature

Run SFBC10 was carried out in order to investigate the effect of condenser temperature. Ice/water was used in both condensers instead of ice/water in condenser 1 followed by dry ice/acetone in condenser 2. An unusually high yield of water resulted. The yield of organics, calculated by difference from the total measured yield of liquids and the yield of water determined by Karl Fischer titrometry, was consequently low. The higher yield of water may have been due to the extended cooling time of the pyrolysis vapours at 0 °C. When the remaining pyrolysis vapours reached the second condenser the volatile compounds with boiling points below 0 °C did not condense on the glassware, as they would in a dry ice/acetone condenser at –78 °C, and allowed a higher surface area for water to condense. The additional water which condensed in the second condenser during run SFBC10 would normally continue reacting until the pyrolysis vapours reached the electrostatic precipitator, by which time they would have taken part in chemical reactions resulting in alternative products.

SFBC10 demonstrates the importance of the pyrolysis vapour quenching method in determining the composition of the liquid product.

6.3.7 The effect of operation at low reactor temperature

In runs carried out at low reactor temperatures, i.e. 450 °C rather than 500 °C, pyrolysis of the relatively fine biomass particles (75-212 μm) was not achieved. This was due to an insufficient heat transfer rate to the biomass particles to effect pyrolysis before elutriation from the bed.

Run SFBC14 (at 450 °C and 50 % feed catalyst concentration) was unstable due to unsuccessful pyrolysis at the lower temperature and the particles were blown out of the bed before pyrolysis could occur. All the yields of products were very low with the exception of the apparent yield of char which visibly contained unconverted wood. Fluidising gas, feed entrain gas, feeder top gas flow rates and stirrer speed were all dropped continuously throughout the run to reduce the elutriation rate of particles in an attempt to achieve pyrolysis.

Run SFBC16 (at 455 °C and 0 % feed catalyst concentration) was comparable to run SFBC14 from an operational point of view, i.e. the wood did not pyrolyse due to blow through of biomass particles through the reactor before pyrolysis could occur. Product yields calculated are particularly prone to errors in collection since unpyrolysed wood (approximated to be 64 wt%) was collected in the first condenser with the liquid products. As a result, the apparent yield of char was very high and the yield of organics fairly low although the yield of water was at a reasonable level. Again, the biomass feed rate was lowered throughout (to encourage pyrolysis), the fluidising gas flow rate was lowered throughout to reduce blow through and the reactor temperature was increased initially from 450 °C to 465 °C over the first 35 minutes in an attempt to achieve pyrolysis.

After the failure of run SFBC14 and SFBC16 to achieve pyrolysis of wood at an approximate temperature of 450 °C, run no. SFBC18 was carried out to determine the lowest temperature at which pyrolysis could be successfully carried out with this system and operating mode. It was found, by altering the furnace temperature throughout the run, that 485 °C was the lowest reactor temperature at which successful pyrolysis could be achieved with this system. The average reactor temperature for run SFBC18 was 488 °C. The yields had acceptable 'product yield deviations' apart from the yield of char which was slightly high. Temperature control was difficult at the start of the run and the temperature had to be raised initially to ensure complete pyrolysis. The feed rate and the nitrogen flow rates in to the reactor were kept static throughout.

6.3.8 Total char balance

Run SFBC33 was carried out in order to conduct a complete char balance on the system during a non-catalytic run. This prevented the collection of oil pot samples as it was necessary to collect all of the liquids in ethanol for filtering so that the overall char content could be calculated more accurately. The char content obtained in this experiment was taken as a standard for comparison to other non-catalytic runs. The yield of water was low, which was most likely due to all the liquids being collected in ethanol and stored prior to analysis - which could possibly prevent water forming reactions that may occur between collection by normal methods, i.e. without ethanol, and analysis. The mass balance closure for run no. SFBC33 was low although it was a very stable run overall and feed rate and nitrogen flow rates in to the system were static.

Run no. SFBC34 was carried out in order to conduct a complete char balance on the system during a 50 % feed catalyst concentration run. It was carried out using the same procedure of product collection as was used in run SFBC33. The yields of organics and char had acceptable 'product yield deviations', the yield of gas was slightly high and the yield of water was slightly low, as with SFBC33, compared to other runs conducted at this feed catalyst concentration and temperature. The feeder top and entrain tube nitrogen flow rates into the reactor were reduced marginally during the course of the run.

6.3.9 Operating procedure improvements

Throughout the runs, fine char was carried over from the cyclone and deposited onto the wall of condenser one opposite the inlet. In catalytic runs the catalyst was also deposited in the same place. The simultaneous condensation of pyrolysis vapours resulted in a combination of char, catalyst and liquid on the condenser wall opposite it's inlet. The removal of this localised char, catalyst and liquid was not possible with ethanol washing alone as the mixture of the solids and the liquid was stuck firmly to the glass. In early runs in particular, the amount of char and catalyst in the liquid products was underestimated resulting in slightly higher yields of liquids and slightly lower yields of char.

The collection technique was improved by the use of a spatula to scrape hardened catalyst/char/liquid product off the inside of the condenser walls which enabled increased accuracy in product yield determination. From SFBC23 onwards there was a slight change in collection procedure which allowed more accurate estimates of products collected from the glassware. Condenser one was reweighed after ethanol washing in order to measure the char, catalyst and hardened liquid product remaining and the balance accounted for in the char yields.

From the beginning of the SFBC experimental series, the wood feed was ground twice for each run, using the Fritsch grinder and a 0.5 mm screen as described in Chapter 5, so that needle shaped particles, which can cause blockages, were eliminated. The wood was then sieved to obtain the 75-212 μm fraction. The main cause of blockages was due to the presence of fines less than 75 μm. During feeding, the fines bridged across the small entrain tube hole blocking the entrainment of further particles. Fines were present in prepared wood feed which had not been sieved for a sufficient length of time. The sieving procedure was altered so that wood was sieved on the sieve shaker for a minimum of 2 hours in order to thoroughly shake out fines.

Operation at low temperature, i.e. 450 °C, was a problem with small particle sized wood (75-212 μm) as demonstrated in runs SFBC14 and SFBC16 because of elutriation of particles from the bed. This led to a minimum temperature of 485 °C for the 75-212 μm fine particle sized biomass pyrolysis.

The effects of catalyst concentration in the feed and pyrolysis reaction temperature on product yields and liquid composition are discussed in Sections 6.5.2-6.6.6.

6.4 Treatment of data including sources and assessment of experimental error

This section discusses the treatment of experimental data and the sources of error. It also assesses errors for the experimental conditions which were repeated.

The data collected is preliminary and prone to scatter due to the limited amount of experience with the system. Only one run was carried out at many of the experimental conditions presented. Repeatability of the data presented needs to be investigated by further experimentation. Trends were fitted based on established product yield trends from fast pyrolysis with temperature (78, 207, 208).

The deviation of the product yields from the trends fitted for yields of total liquids, gas and char (including coke) were summed for each run to assess the general scatter. The 'instability indexes' for each run were developed by summing values for factors and indicators of instability during the run (Section 6.3). There was no clear correlation found between the sum of product yield deviations from trends and the 'instability indexes' for the runs carried out. The sum of product yield deviations from trends appeared to increase with catalyst concentration. Both the sum of product yield deviations from trends and the 'instability indexes' appeared to decrease with run chronology until around SFBC15 and then increase until SFBC31 towards the end.

Experimental error can originate during the preparation or operation of a run or the recovery of products from a run. Possible sources of error are from:

- calculation of the fraction of solids present in the glassware;
- water determination of the wood and catalyst feed;
- water determination of the liquids collected by Karl Fischer titrometry;
- determination of the yield of pyrolysis gases by gas chromatography of gas samples.

The most consistent source of error is from the calculation of the fraction of solids in the glassware. This is because the solids (catalyst, coke and char) which were carried over to the glassware were combined with liquid products. Recovery was extremely difficult as the solids and liquids formed congealed masses at the inlets to the condensers.

They were removed by a combination of scraping using a spatula and dissolution in ethanol. Assessment of the run data suggested that product yield deviations from the fitted trends appeared to increase with feed catalyst concentration indicating that the presence of catalyst made the mass balance more prone to errors.

The water content of liquids determined by Karl Fischer titrometry demonstrated a degree of variation. Comparison between the yield of total liquids (organic and aqueous fractions) from the experimental series was therefore used to avoid such errors.

The determination of the yields of pyrolysis gas by gas chromatography may also have been erroneous in certain runs as the thermostat on one of the gas chromatographs used failed during analysis of gas from SFBC21. This is discussed in detail in Section 6.5.4.

Gas analysis and water analysis are carried out a few days after each run and therefore are susceptible to more variability. It was not possible to analyse them immediately after each run.

It is unlikely that the water determination of the wood and catalyst feed contributed significant error to the mass balance calculation due to the simplicity of the oven moisture determination method.

In order to ascertain typical experimental error three repeat runs were carried out at two specific levels of catalyst feed concentration and temperature. This enabled the reproducibility of the operating procedure to be gauged.

SFBC09, SFBC12 and SFBC23 were carried out using 25 % catalyst concentration in the feed, a reactor temperature of 508.8 ± 0.3 °C and vapour residence time of 0.45 s. Table 6.7 shows the product yields achieved from run numbers SFBC09, SFBC12 and SFBC23 with the corresponding standard deviation and mean absolute deviation for each of the product yields.

SFBC08, SFBC13 and SFBC34 were carried out using 50 % catalyst concentration in the feed, a reactor temperature of 508.3 ± 0.8 °C and vapour residence time of 0.54 ± 0.09 s. Table 6.8 shows the product yields from run numbers SFBC08, SFBC13 and SFBC34 with corresponding standard deviation and mean absolute deviation for each product yield.

Table 6.7 Standard deviation and mean absolute deviation of product yields from 25 % catalyst feed concentration fast pyrolysis at 509 °C and 0.45 s vapour residence time

Run no. (SFBC)	Yield Of Total Liquids (wt%)	Yield Of Gas (wt%)	Yield Of Organic Liquids (wt%)	Yield Of Water (wt%)	Yield Of Char (wt%)	Mass Balance Closure (wt%)
09	74.20	19.80	63.50	10.70	10.80	104.80
12	63.30	28.30	58.90	4.40	18.70	110.40
23	61.30	27.20	57.20	4.10	18.50	106.80
Average (Mean)	66.27	25.10	59.90	6.40	16.00	107.30
Standard Deviation	6.94	4.62	3.26	3.73	4.50	2.84
Standard Deviation (% Of Yield)	10.48	18.42	5.44	58.23	28.15	2.64
Mean Absolute Deviation	5.29	3.53	2.42	2.87	3.47	2.04
Mean Absolute Deviation (% Of Yield)	**7.98**	**14.08**	**4.04**	**44.79**	**21.67**	**1.91**

Table 6.8 Standard deviation and mean absolute deviation of product yields from 50 % catalyst feed concentration fast pyrolysis at 508 °C and 0.54 s vapour residence time

Run no. (SFBC)	Yield Of Total Liquids (wt%)	Yield Of Gas (wt%)	Yield Of Organic Liquids (wt%)	Yield Of Water (wt%)	Yield Of Char (wt%)	Mass Balance Closure (wt%)
08	52.29	14.50	41.30	10.98	24.70	91.50
13	65.00	10.59	57.30	7.70	15.90	91.50
34	61.35	7.90	57.20	4.14	16.22	85.48
Average (Mean)	59.55	11.00	51.93	7.61	18.94	89.49
Standard Deviation	6.54	3.32	9.21	3.42	4.99	3.48
Standard Deviation (% Of Yield)	10.99	30.18	17.73	44.97	26.35	3.88
Mean Absolute Deviation	4.84	2.34	7.09	2.31	3.84	2.68
Mean Absolute Deviation (% Of Yield)	**8.12**	**21.24**	**13.65**	**30.38**	**20.27**	**2.99**

The repeated runs for 25 % and 50 % catalyst feed concentration error analyses demonstrated a good replication of conditions. The error demonstrated by product yields increased in the following order: mass balance closures, yield of total liquids, yield of organic liquids, yield of gas, yield of char (and coke), yield of water. The mean absolute deviation of each product yield, e.g. yield of gas, is expressed as a percentage of the average product yield obtained from the three repeated runs (see Tables 6.7 and 6.8). These percent errors are applied to the relevant yields for single runs..

Due to the error experienced when calculating yields of organic liquids and water from Karl Fischer determination, yields of total liquids are used throughout the subsequent discussions when comparing product yields from:

- large (1 kg h^{-1}) and small (150 g h^{-1}) fluid bed reactors;
- the large (1 kg h^{-1}) fluidised bed reactor with temperature; and
- the small (150 g h^{-1}) fluidised bed reactor whilst varying catalyst feed concentrations and temperatures.

6.5 Comparison of product yields for non-catalytic series

6.5.1 Non-catalytic 1 kg h^{-1} fluidised bed series LAC/CMD

A series of non-catalytic runs was carried out on a 1 kg h^{-1} reactor (207) with pine wood as feedstock. Temperature was varied over the series whilst the residence time (approximately 1s) and feed particle size (0.6-1.7 mm) were kept constant. Feed rates were typically 0.5 kg h^{-1}. Table 6.9 shows product yields from pine wood pyrolysis carried out on the 1 kg h^{-1} fluid bed reactor. The results of catalytic runs are discussed later in Section 6.6.

Table 6.9 Mass balance product yields for non-catalytic runs on the 1 kg h^{-1} reactor

Run No.	Average Reactor Temp.* (°C)	Pyrolysis Products In Nitrogen (%)	Yield Of Gas (wt%)	Yield Of Total Liquids (wt%)	Yield Of Organics (wt%)	Yield Of Water (wt%)	Yield Of Char (wt%)	Mass Balance Closure (wt%)	Vapour Residence Time In Reactor (s)
FB22	449	7.41	12.7	58.1	46.2	11.9	24.8	95.6	1.06
FB24	476	6.70	12.7	67.5	55.9	11.6	15.8	96.1	1.29
FB26	514	6.31	15.4	71.8	59.4	12.4	10.1	97.3	1.19
FB23	525	6.86	16.4	68.9	54.1	14.8	14.4	99.7	1.05
FB25	562	6.90	23.8	53.3	39.6	13.7	19.9	97.0	1.13

Where:

Temp.*: Temperature

Figure 6.6 shows the product yields versus temperature for non-catalytic runs on the 1 kg h^{-1} reactor. Polynomial product yield trends (denoted as Poly. on the chart legend) are fitted to each product yield with the exception of the yield of water, to which a linear trend is fitted. Error bars have not been included as there were insufficient data points to calculate them.

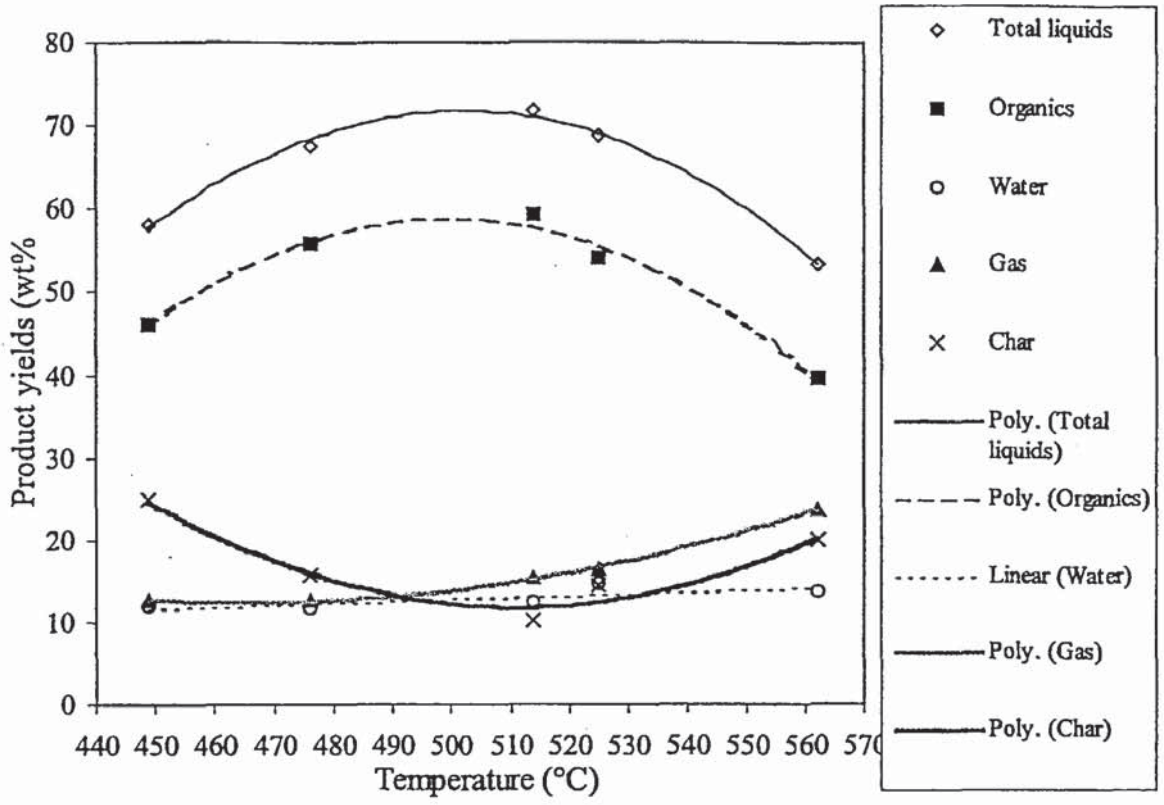

Figure 6.6 Product yield versus temperature for non-catalytic 1kg h^{-1} reactor runs

The maximum yield of total liquids of 71.8 wt% and the corresponding maximum yield of organics of 59.4 wt% were achieved at 514 °C for run no. FB26. The maximum yield of total liquids and organics for this 1 kg h^{-1} pyrolysis reactor system were calculated from the equations of the trends in Figure 6.5 to be 72 wt% and 59 wt% respectively at a temperature of 502 °C. The yield of total liquids and organics show typical trends achieved with increasing temperature during the fast pyrolysis of wood (209). The yield of water increased gradually and linearly with temperature over the range investigated. The yield of gas also increased with temperature following a polynomial trend, no minima or maxima were experienced within the temperature range studied. The yield of gas is typically maximised from the fast pyrolysis of biomass at temperatures in excess of 700 °C (21). The yield of char decreased to a minimum of 10.1 wt% at a temperature of 514 °C before increasing up to 19.9 wt% at a temperature of 562 °C following a polynomial trend. These product yield trends achieved showed good comparison to other fast pyrolysis work with softwoods at the reaction conditions studied (78).

6.5.2 Non-catalytic 150 g h^{-1} fluidised bed series LAC1

A series of non-catalytic runs was carried out on a 150 g h^{-1} fluid bed reactor with pine wood as feedstock (particle size 75-212 μm). Product yield errors, the fitting of product yield trends and the reproducibility of the series have been discussed in Sections 6.3 and 6.4. Each run lasted approximately 1 hour although occasional runs that encountered problems were shorter. The average feed rate for the run series was 50 g h^{-1} of wood. Typical residence times were around 0.5 s which had been found to be optimal for producing liquid yields from woody biomass (78). On the lower temperature runs, these residence times were increased in order to allow sufficient time in the reactor for the biomass to pyrolyse completely.

The mass balance results are presented in Table 6.10 and correspond to run numbers SFBC 16, 18, 05, 25, 10, 33, 11, 17. The last two rows contain product yields obtained from the pyrolysis of poplar by the University of Waterloo (31) which was carried out under similar residence times and is included for comparison purposes.

Table 6.10 Mass balance product yields from non-catalytic runs on the 150 g h^{-1} reactor (series LAC1) and two poplar fast pyrolysis runs from the University of Waterloo (31)

Run No.	Average Reactor Temp.[a] (°C)	Pyrolysis Products In Nitrogen (vol%)	Yield Of Gas (wt%)	Yield Of Total Liquids (wt%)	Yield Of Orgs [b] (wt%)	Yield Of Water (wt%)	Yield Of Char (wt%)	Mass Balance Closure (wt%)	Reactor Res.[c] Time (s)
SFBC16	458.3	11.27	27.4	58.6	51.9	6.7	15.7	101.6	0.77
SFBC18	488.0	13.29	22.5	72.1	61.1	11.0	15.5	110.1	0.76
SFBC05	500.5	6.01	16.1	70.6	57.5	13.1	17.9	104.6	0.45
SFBC25	503.1	4.15	30.3	61.1	48.7	12.4	5.8	89.2	0.48
SFBC10	506.7	5.87	15.7	56.9	39.4	17.5	8.2	80.7	0.45
SFBC33	514.3	2.12	32.8	68.3	65.7	2.6	9.5	110.5	0.68
SFBC11	515.2	6.73	13.3	70	48.5	21.5	7.7	91.0	0.44
SFBC17	551.9	5.13	18.2	75.3	72.9	2.4	10.8	104.3	0.42
poplar	504.0	-[d]	11.0	77.0	62.2	14.8	11.8	99.8	0.48
poplar	500.0	-[d]	12.4	75.0	60.0	15.0	12.1	99.5	0.55

Where:

Temp.[a]: Temperature;

Orgs[b]: Organics;

Res.[c]: Residence; and

[d]: pyrolysis products in recirculation gases: CO and CO_2.

The product yields from the non-catalytic 150 g h^{-1} reactor series, LAC1, are plotted against temperature in Figure 6.7. Error bars have not been included as there were insufficient data points produced to calculate them. The yields of total liquids from fluidised bed fast pyrolysis at the University of Waterloo on poplar wood (particle size 1 mm and 0.59 mm for 504 °C and 500 °C, respectively) are included for comparison with the 150 g h^{-1} non-catalytic runs. The maximum yield of total liquids of 72 wt% was achieved at a temperature of 550 °C, run no. SFBC17. This maximum is not in agreement, however, with the 1 kg h^{-1} experimental data or by co-researchers in similar fluidised bed systems (78). Other researchers have found total liquid yields to decrease at temperatures above 520 °C (78, 207, 208) although larger particle sized feed stocks were used in most of these investigations. SFBC17 was not included, therefore, when fitting the polynomial trend line for the yield of total liquids. The polynomial trend fitted has an R^2 value of 0.99 demonstrating a very good fit to the product yield data. Other runs producing unusual yields of liquids in the non-catalytic series were identified as SFBC10 and 25. This was due to run instability described in Section 6.3.1 - 6.3.3 and the runs were consequently omitted from the trend for yield of total liquids. A maximum yield of 72 wt% at 497 °C was calculated for this system.

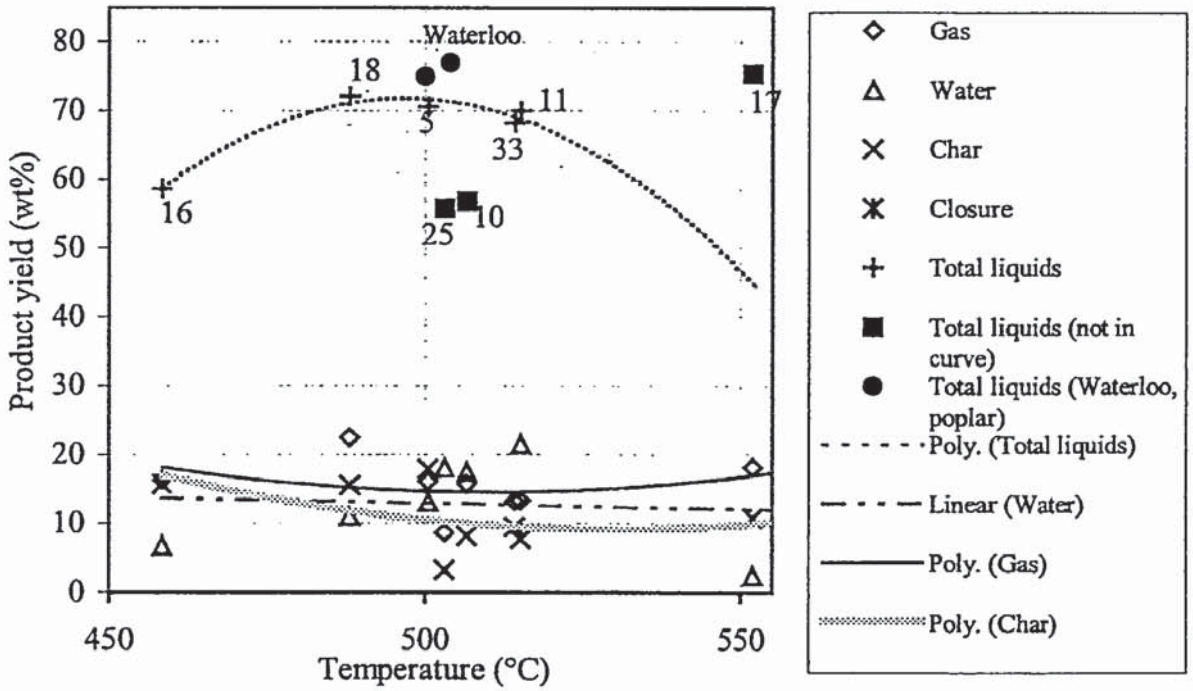

Figure 6.7 Product yields versus temperature for non-catalytic pine runs (LAC1) on 150 g h^{-1} fast pyrolysis reactor with a wood feed particle size of 75-212 μm

Due to the limited number of runs in series LAC1 the data points from these runs have been combined with those obtained by Hague (208), on the same 150 g h^{-1} fluidised bed reactor with pine wood, and with those from the University of Waterloo (31), from poplar wood, and are presented versus temperature in Figure 6.8. The increased number of data points provides a more reliable set of trends for comparison with catalytic runs in Section 6.5, despite the difference in particle size which was believed to have only a minor effect on product yields (210).

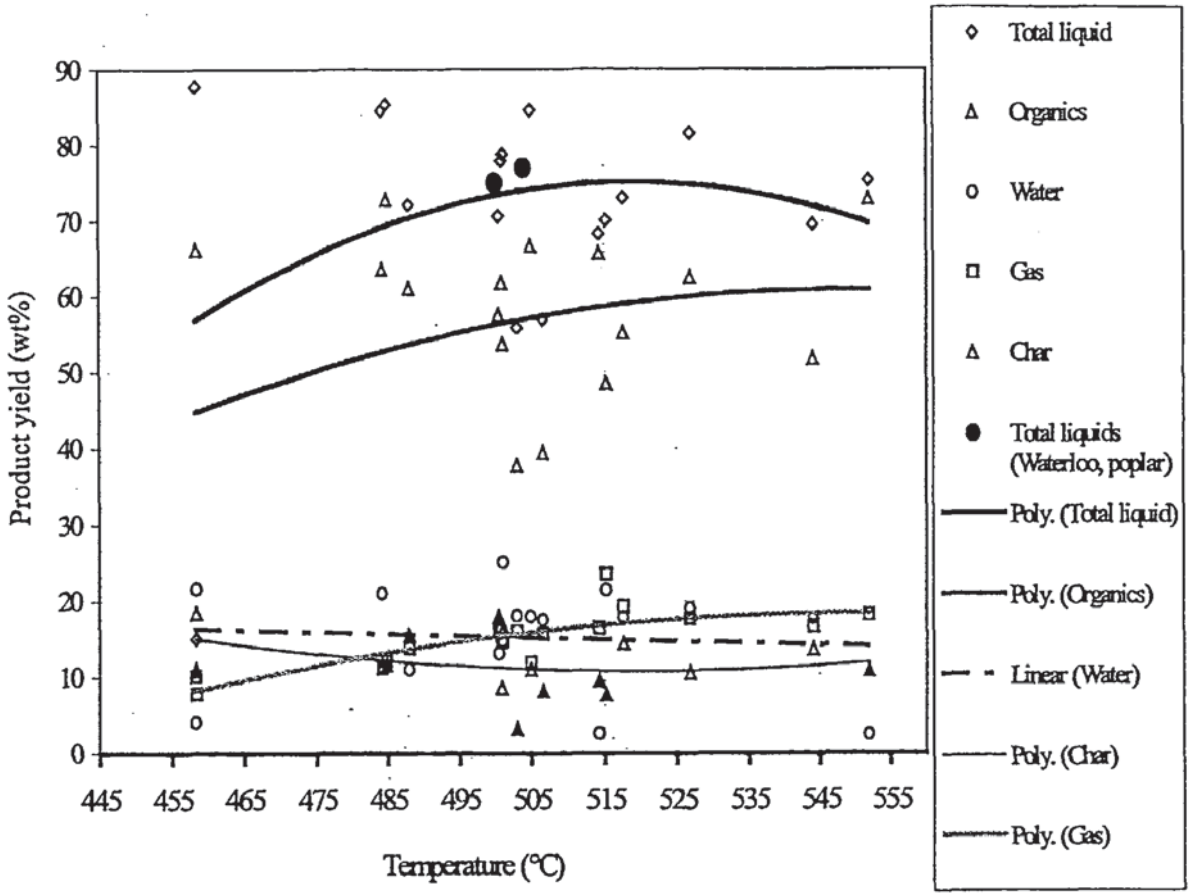

Figure 6.8 Product yields versus temperature for non-catalytic fast pyrolysis of pine wood at particle sizes of 75-212 μm – solid shapes – and 350-500 μm (208) – open shapes – and poplar (31) – larger solid circles

The maximum yield of total liquids from the yield trend was 75 wt% at a temperature of 519 °C. The yield of organics increased over the temperature range, although it is usual for the organics to experience a maximum within the 450 to 550 °C temperature range (78, 207). The yield of water was relatively stable at approximately 15 wt% over the temperature range. The yield of gas increased throughout the temperature range to approximately 19 wt% at 550 °C and the yield of char passed through a minimum at 11 wt% corresponding to a temperature of approximately 517 °C.

6.5.3 Comparison of product yield trends from non-catalytic pine runs on 150 g h^{-1} and 1 kg h^{-1} reactors.

The product yields achieved from non-catalytic operation of the 150 g h^{-1} reactor using pine wood differed from those achieved from non-catalytic operation of the 1 kg h^{-1} reactor using pine in several ways. All yields presented were on a real yield basis (from dry wood), as described in Section 6.3.2, and as such were affected by any loss of mass that occurred during the run. The average closure experienced by the 150 g h^{-1} reactor runs and the 1 kg h^{-1} reactor runs were 97.6 wt% and 97.1 wt% respectively. The 150 g h^{-1} reactor run closures ranged from 80.7-114.2 wt% (Table 6.10) and the 1 kg h^{-1} reactor run closures ranged from 95.6-99.7 wt% (Table 6.9). This was due to 'best only' mass balance product yields being presented for the 1 kg h^{-1} reactor runs as experience had already been gained on the larger system (207).

The yield of total liquids and the yield of organics from the 1 kg h^{-1} reactor displayed more pronounced trends across the temperature range studied than the 150 g h^{-1}. The 150 g h^{-1} reactor appeared to be less affected by temperature. This may be due to the variation in vapour residence times at lower temperatures in the 150 g h^{-1} reactor runs compared to the constant vapour residence times across the temperature range with the 1 kg h^{-1} reactor runs. An objective of both series of runs (150 g h^{-1} and 1 kg h^{-1}) was to keep the residence time constant throughout but this was not possible for the 150 g h^{-1} reactor runs. At low temperatures (i.e. 495 °C and below) the small particle sized wood (75-212 μm) blew straight through the 150 g h^{-1} reactor and the fluidising gas flow rate had to be lowered in order to pyrolyse the particles. This resulted in a higher residence time of 0.75 s as opposed to the desired residence time of 0.5 s which was used in the higher temperature runs.

The 1 kg h^{-1} reactor runs were carried out at a residence time of 1.1 s ± 0.2 which resulted in higher reaction severities compared to the 150 g h^{-1} reactor series with residence times of 0.6 s ± 0.2 over the same temperature ranges contributing to the more pronounced product yield trends experienced on the 1 kg h^{-1} reactor. Residence times from the RAH series on the 150 g h^{-1} reactor were 0.7 s ± 0.1. The increase in vapour residence time effectively increased the thermal reaction severity which was defined by Czernik et. al. (86) to be the product of residence time and an exponential function of temperature.

The maximum yields of total liquids and organics occurred at the slightly lower temperature of 502 °C with the 1 kg h^{-1} reactor compared to 519 °C with the 150 g h^{-1} reactor (combined data from series LAC1 and RAH). This may be due to the higher residence time which increased the pyrolysis reaction severity resulting in the optimum yield of liquid being produced at a lower temperature. Yields of char were higher from the 1 kg h^{-1} runs due to the larger particle size (see Fig 6.6). The trend of the yields of char against temperature achieved from the 1 kg h^{-1} reactor were similar to the 150 g h^{-1} reactor (see Fig 6.7) but, as was the case with the yields of total liquids and organics, were more pronounced at the temperature extremes. At the higher residence times, experienced during the 1 kg h^{-1} compared to 150 g h^{-1} series, greater thermal reaction severities were achieved at similar temperatures. This produced maximum yields of total liquids and organics at lower temperatures of approximately 500 °C before the production of gas and char from secondary thermal reactions increased between 500-550 °C reducing the yields of liquids. The lower residence times used in the 150 g h^{-1} reactor runs resulted in a peak in yields of total liquids and organics at 519 °C. This demonstrates the change in pyrolysis reaction severity with particle size, residence time and temperature and the effect of scale on a chemical reaction.

The maximum yields of total liquids and organics was lower from the 1 kg h^{-1} reactor than the 150 g h^{-1} reactor by approximately 3 wt%. This is significant as the approximate difference is based on many runs on the 1 kg h^{-1} and 150 g h^{-1} reactors and is consistent across the temperature range. This was due to greater particle sizes and residence times in the 1 kg h^{-1} reactor. Larger particles pyrolyse more slowly than smaller particles since the rate of heat transfer through the particles is lower than the rate of heat transfer to the surface of the particles.

In order to completely pyrolyse the whole particle, longer residence times are required for larger particles. Whilst heat is still transferring to the centre of a large particle, the vapours diffusing from the outer layers are undergoing secondary thermal reactions producing a greater yield of permanent gases and char at the expense of the yield of liquid. Also, as the pyrolysis vapours from the centre of the wood particle diffuse out through the outside char layer, they undergo char catalysed reactions which increase the yields of gas and char at the expense of the yield of liquids.

The trend from the yields of water against temperature achieved from the two reactor systems were comparable within the temperature range studied although there was a large amount of deviation in the 150 g h^{-1} (LAC1 only) data. The yields of gas were also comparable between the two systems, although yield trends demonstrate oppositely curving polynomials, this is probably due to experimental deviation in the 150 g h^{-1} runs.

In conclusion the 1 kg h^{-1} reactor product yields displayed less scatter; produced steeper yield trends versus temperature for liquid, char and gas; produced a lower maximum yield of total liquids at a slightly lower pyrolysis temperature than the 150 g h^{-1} and greater yields of char due to the larger particle size. The differences between the 150 g h^{-1} product yield trends and the 1 kg h^{-1} product yield trends were due to differences in vapour residence times and particle sizes between the systems. The higher degree of product yield deviation from the 150 g h^{-1} compared to the 1 kg h^{-1} reactor was possibly due to either the lack of run experience in the 150 g h^{-1} runs, 'best only' yields being presented for 1 kg h^{-1} runs or, more probably, the larger amount of feedstock processed with the 1 kg h^{-1} runs which reduces the effects of small changes in product recovery.

6.5.4 Gas analysis of 150 g h^{-1} and 1 kg h^{-1} non-catalytic run series

Yields and composition of the pyrolysis gases are important indications to the severity of the pyrolysis reaction. Carbon monoxide and carbon dioxide typically represent the largest fraction of the pyrolysis gas, 94-99 vol% for pyrolysis of fir (211). The yields of carbon monoxide and carbon dioxide increase with temperature and have been characterised as decomposition products resulting from dehydration and decarbonylation reactions, in the first seconds of fast pyrolysis, by Antal (212).

Low molecular weight hydrocarbons are also present in pyrolysis gases. It has been reported that these hydrocarbons are not produced at pyrolysis reaction temperatures below 500 °C as they result from secondary thermal reactions which occur at higher temperatures (213). Gas analyses for the 150 g h^{-1} LAC1 series and the 1 kg h^{-1} LAC/CMD series are presented in Tables 6.11 and 6.12 respectively. Errors could not be calculated as there were insufficient data points produced.

Table 6.11 Yield of gas (wt% dry basis) from non-catalytic 1 kg h^{-1} reactor series (LAC/CMD)

Run no.	FB22	FB24	FB26	FB23	FB25
Average reactor temperature (°C)	449	476	514	525	562
Feed moisture content (wt%)	9.25	9.25	9.25	9.25	9.25
Pyrolysis products in nitrogen (%)	7.41	6.70	6.31	6.86	6.90
Yield of carbon monoxide (wt%)	4.8	6.4	7.2	8.1	11.9
Yield of carbon dioxide (wt%)	7.5	5.6	7.1	7.1	9.6
Yield of methane (wt%)	0.2	0.4	0.6	0.8	1.5
Yield of ethane (wt%)	0.1	0	0	0	0
Yield of ethene (wt%)	0	0.1	0.3	0.3	0.6
Yield of propane (wt%)	0.1	0.1	0.1	0.2	0.3
Yield of propene (wt%)	0	0	0	0	0
Yield of total gas (wt%)	12.7	12.7	15.4	16.4	23.8
Vapour residence time in the reactor (s)	1.06	1.29	1.19	1.05	1.13

Table 6.12 Yield of gas (wt% dry basis) from non-catalytic 150 g h^{-1} reactor series (LAC1)

Run no. (SFBC)	16	18	05	25	10	33	11	17
Average reactor temperature (°C)	458	488	501	503	507	514	515	552
Feed moisture content (wt%)	8.4	8.2	8.8	4.1	7.9	8.3	8.7	8.4
Pyrolysis products in nitrogen (%)	11.3	13.3	6.0	4.2	5.9	2.1	6.7	5.1
Yield of carbon monoxide (wt%)	10.1	6.3	9.1	2.4	5.1	7.4	5.7	10.2
Yield of carbon dioxide (wt%)	0	4.9	6.5	5.9	6.0	5.1	7.1	0.37
Yield of methane (wt%)	0.06	0.32	0.34	0.27	0.49	0.45	0.48	0.61
Yield of ethane (wt%)	0	0	0	0	0	0	0	0
Yield of ethene (wt%)	0	0.04	0	0	0.22	0.21	0.07	0.58
Yield of propane (wt%)	0	0	0	0	0	0	0	0
Yield of propene (wt%)	0	0	0	0	0	0	0	0.26
Yield of total gas (wt%)	10.2	11.5	16.0	8.6	11.8	13.2	13.3	12.0
Vapour residence time in the reactor (s)	0.77	0.76	0.45	0.48	0.45	0.68	0.44	0.42

Table 6.12 shows some interesting gas compositions from runs which either suffered instability during the run or produced anomalous yields of other products. The wood in run no. SFBC16 did not pyrolyse completely. There was a low yield of total liquids, providing evidence of partial pyrolysis but the majority of the wood fed was unconverted. The yield of carbon monoxide dominates the gas composition at 99 % (by weight) of the gas detected (10.1 wt% from wood, dry basis) as a result of the partial pyrolysis. Run no. SFBC25 suffered from severe blocking throughout. In this case, the yield of carbon dioxide dominates the gas composition at 69 % (by weight) of the gas detected (5.9 wt% from wood, dry basis). During the blockages, the biomass feed rate is inconsistent experiencing periods of no feed to sudden bursts of high feed rate when blockages are removed (by 'pinching' the plastic feed tube and creating pressure build up in the feeder). The variable partial pressure of pyrolysis vapours in the reactor may have led to the relatively high proportion of carbon dioxide in the yield of gas. Finally, an anomalously high yield of total liquids was produced in run no. SFBC17. The yield of carbon monoxide dominates the gas composition at 85 % (by weight) of the gas detected (10.2 wt% from wood, dry basis) which may have been a combined effect of the high temperature (551 °C) and the small particle size of the wood which allowed very high heat transfer rates to the whole of the biomass particle minimising the extent of reactions occurring inside the particle. If this was the case, it would suggest that carbon monoxide is the first gaseous product to be produced during the first milliseconds of pyrolysis and that carbon dioxide results from extended reaction time both inside and outside of the biomass particle. Alternatively, the yields of carbon monoxide may have been over-represented in the yields of gas during runs SFBC16 and SFBC17 due to the problems experienced with carbon dioxide detection which may have been due to a fault with the gas chromatogram.

Yields of carbon monoxide and carbon dioxide versus temperature are shown in Figure 6.9 and yields of the major hydrocarbons, methane and ethene, produced versus temperature are shown in Figure 6.10 for the 150 g h^{-1} LAC1 series and the 1 kg h^{-1} LAC/CMD series. Error bars have not been included for the yields of the gases as there were insufficient data points produced to calculate them.

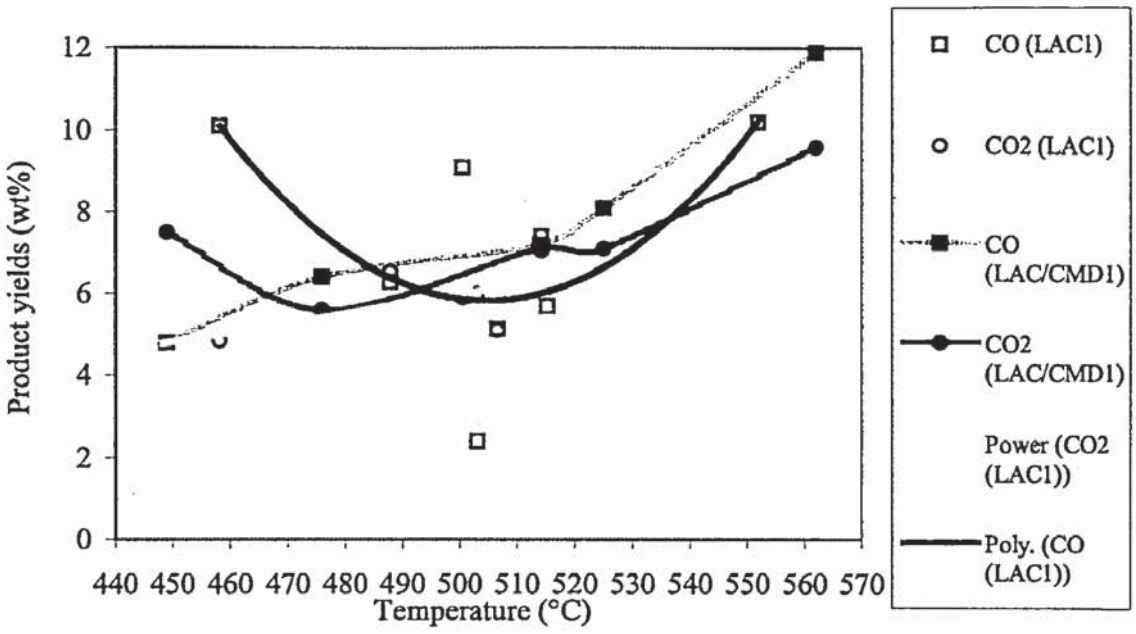

Figure 6.9 Yields of carbon monoxide and carbon dioxide versus temperature for non-catalytic series on 150 g h^{-1} (LAC1) and 1 kg h^{-1} (LAC/CMD) reactors

The yields of carbon dioxide from both the 150 g h^{-1} (LAC1) and 1 kg h^{-1} (LAC/CMD) reactor runs increase with temperature. The yields of carbon monoxide from the 1 kg h^{-1} reactor runs also increase with temperature. The yield of carbon monoxide from the 150 g h^{-1} (LAC1) reactor run follows a polynomial trend with a minimum yield at approximately 500 °C but is tentative due to a high yield of carbon monoxide during run SFBC16 in which the wood did not pyrolyse properly and consequently the products were difficult to separate causing possible mass balance error. The yields of carbon monoxide and carbon dioxide from the 150 g h^{-1} LAC1 reactor series, however, differed from both the 1 kg h^{-1} product yield trends and from one another. The yield of carbon monoxide from the 150 g h^{-1} reactor series was greater across the temperature range studied than the yield of carbon dioxide.

Closer inspection of G.C. results found a problem in the identification of carbon dioxide for run numbers SFBC16 and 17 (omitted from Figure 6.9) which gave either very low yields or yields of 0 %. G.C. analysis of SFBC16 and 17 was carried out on the same day and other analyses carried out on this day (SFBC14 and 15) also resulted in no carbon dioxide detection. It is very likely that G.C. results from run nos.

SFBC14-SFBC17, analysed on the same day, were carried out at different conditions of catalyst feed concentration and temperature including 0 %, 25 % and 50 % catalyst concentrations and it is highly probable that the G.C. results were erroneous. Carbon dioxide was detected in gas samples from all other pyrolysis experiments, catalytic or non-catalytic, described in this thesis. Some small peaks from run SFBC14-17 gas samples were detected by the porapak Q column, used for carbon dioxide detection, but these did not correspond with the retention times of the carbon dioxide in the gas standard. A number of runs later, during gas analysis of run SFBC21, the G.C. machine used for carbon dioxide detection suffered technical failure due to a faulty column thermostat. It is possible that the thermostat had been gradually failing for an unknown period of time and could have caused the anomalous results.

The product yield trends for carbon monoxide on the 150 g h^{-1} reactor are tentative as they experience a significant degree of scatter. Carbon dioxide and carbon monoxide yields were found to increase with increasing pyrolysis temperature as found by other workers (211) but incomplete or partial pyrolysis, as experienced in run no. SFBC16, led to relatively high yields of carbon monoxide.

The yields of methane and ethene from 1 kg h^{-1} reactor runs were higher than from 150 g h^{-1} LAC1 series reactor runs. Yields of both methane and ethene increased with temperature for both reactor systems. The yields of methane were greater than the yields of ethene for both the 1 kg h^{-1} and the 150 g h^{-1} reactor systems. The combined yields of methane and ethene, on average, represented 5.3 wt% of the total yield of gas for the 1 kg h^{-1} reactor runs compared to 4.1 wt% of the total yield of gas for the 150 g h^{-1} LAC1 series reactor runs. This shows that increased residence time and particle size can result in an increase in the production of lower hydrocarbons (other lower hydrocarbons were present in trace amounts) from either extended primary pyrolysis reaction time inside the particle, secondary pyrolysis reaction time outside the particle or a combination of both. These increases in lower hydrocarbons were accompanied by a corresponding decrease in the proportion of carbon oxides in the gas composition.

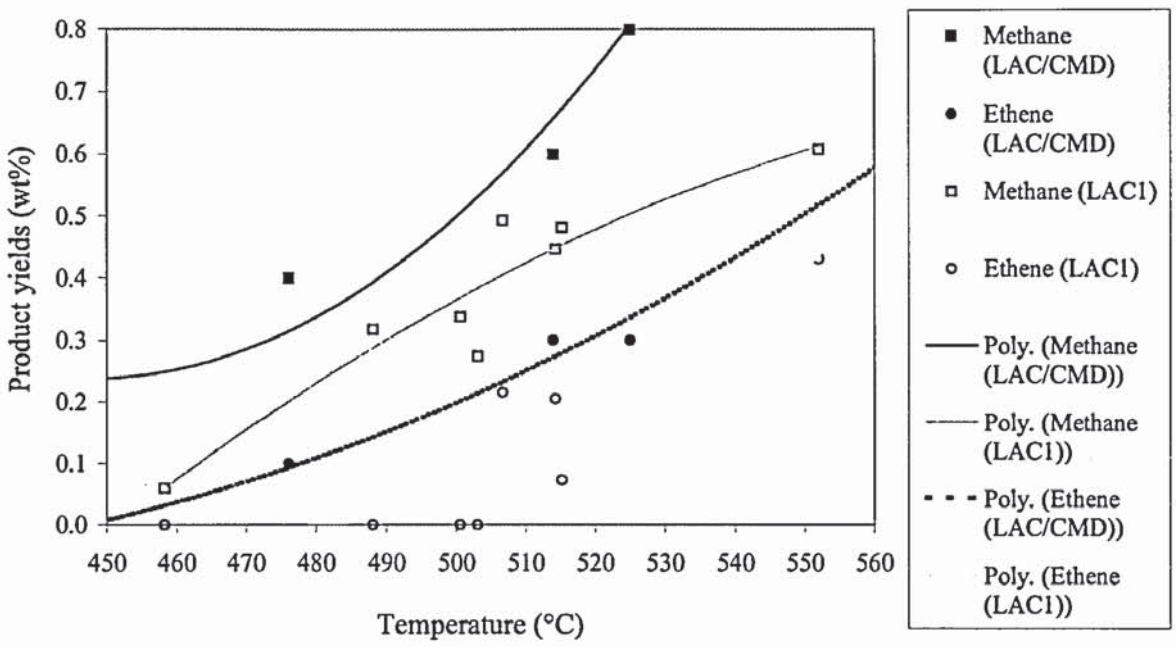

Figure 6.10 Yields of methane and ethene versus temperature for non-catalytic pine runs on 150 g h^{-1} and 1 kg h^{-1} reactors (LAC1 and LAC/CMD)

The effect of experimental conditions on the composition of gaseous and liquid products from biomass fluid bed pyrolysis was studied by Samolada and Vasalos (213). They reported that temperature was the only reaction condition that significantly affected the yields of pyrolysis products, the recommended bed temperature being around 500 °C. They also reported, however, that the particle size of the biomass had an effect on the composition of the gases. They reported that large particles favoured the production of pyrolysis gases rich in methane and ethene because the retention time of the pyrolysis products inside the pyrolysing particle was increased and secondary decomposition reactions became more dominant.

6.6 Comparison of catalytic product yields to non-catalytic product yields on the 150 g h^{-1} fluidised bed reactor

6.6.1 25 % catalyst 150 g h^{-1} fluidised bed series

10 runs were carried out at a catalyst concentration of 25 % (by weight) in the feed. These were: SFBC 21, 30, 06, 09, 23, 12, 27, 07, 28 and 20. Table 6.13 shows the mass balance product yields achieved from the 25 % catalyst feed concentration runs, series LAC2. Wood feed rate was kept at a constant 50 g h^{-1} as with the non-catalytic run series (LAC1). Product yield errors, the fitting of product yield trends and the reproducibility of the series have been discussed in Sections 6.3 and 6.4.

Table 6.13 25 % catalytic mass balance product yields from 150 g h^{-1} reactor

Run No.	Average Reactor Temperature (°C)	Pyrolysis Products In Nitrogen (vol%)	Yield Of Gas (wt%)	Yield Of Organics (wt%)	Yield Of Water (wt%)	Yield Of Char (wt%)	Mass Balance Closure (wt%)	Reactor Residence Time (s)
SFBC21	485	6.35	-	65	3	12	80	0.64
SFBC30	492	6.9	27	61	8	10	106	0.36
SFBC06	495	1.0	14	54	9	10	88	0.48
SFBC09	509	5.13	13	63	11	11	98	0.53
SFBC23	509	32.19	27	57	4	19	107	0.45
SFBC12	509	5.09	21	59	4	19	103	0.45
SFBC27	515	6.33	20	72	10	9	110	0.44
SFBC07	515	6.42	16	51	11	11	89	0.44
SFBC28	533	27.73	28	55	11	8	102	0.35
SFBC20	552	2.77	44	47	7	0	98	0.43

Figure 6.11 shows the product yields from series LAC2 (25 % catalyst) against temperature. Error bars derived from the mean absolute deviation of product yields obtained at 508.8 ± 0.3 °C, during run numbers SFBC09, 12 and 23, are included for all of the data points.

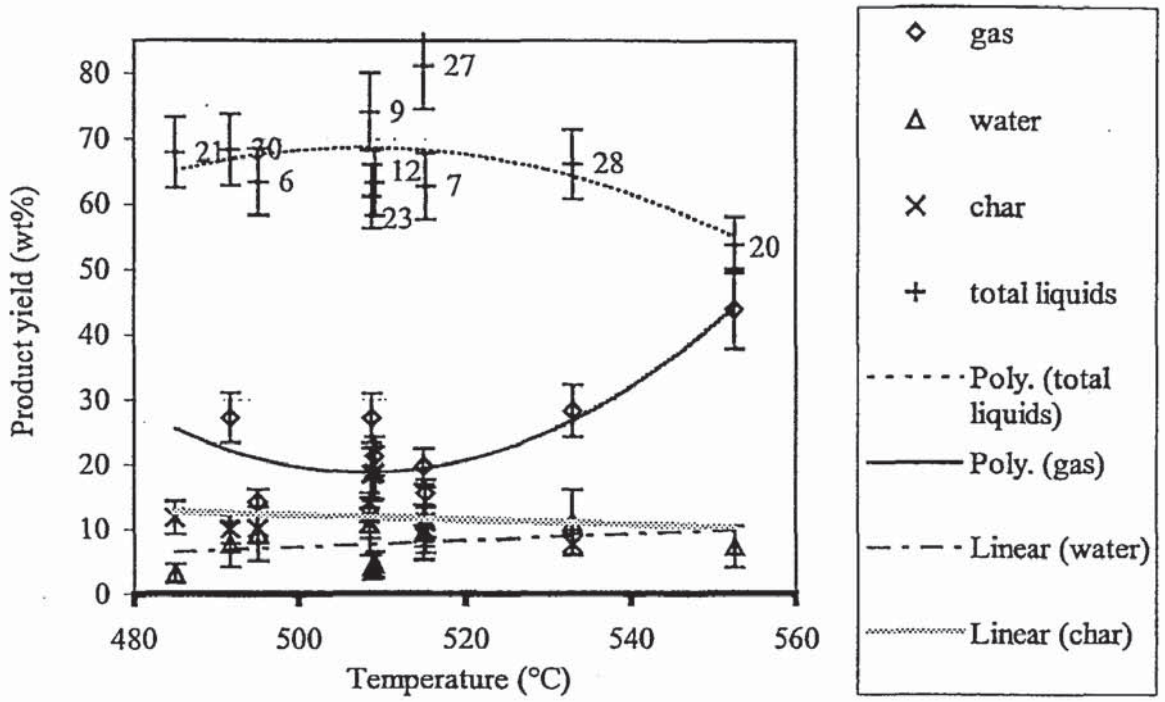

Figure 6.11 Product yields versus temperature from 25 % catalyst feed concentration run series (LAC2)

6.6.2 50 % catalyst 150 g h^{-1} fluidised bed series

10 runs were carried out at a catalyst concentration of 50 % (by weight) in the feed, these are: SFBC 14, 19, 24, 04, 08, 13, 26, 03, 31 and 15. Catalyst was mixed with wood feed as described in chapter 5 and wood feed rate was 50 g h^{-1}. Table 6.14 shows the mass balances achieved from 50 % catalyst runs. Product yield errors, the fitting of product yield trends and the reproducibility of the series have been discussed in Sections 6.3 and 6.4.

Figure 6.12 shows the product yields versus temperature for 50 % catalyst runs. Error bars derived from the mean absolute deviation of product yields obtained at 508.3 ± 0.8 °C, during runs SFBC08, 13 and 34, are included for all of the data points.

Table 6.14 50 % catalytic mass balance product yields from 150 g h^{-1} reactor

Run No.	Average Reactor Temperature (°C)	Pyrolysis Products In Nitrogen (vol%)	Yield Of Gas (wt%)	Yield Of Organics (wt%)	Yield Of Water (wt%)	Yield Of Char (wt%)	Mass Balance Closure (wt%)	Reactor Residence Time (s)
SFBC14	450	6.29	4	12	0	78	93	0.67
SFBC19	483	6.13	27	54	12	18	112	0.69
SFBC24	501	9.44	19	49	7	24	98	0.45
SFBC04	503	7.56	16	75	13	12	115	0.44
SFBC08	508	6.87	15	41	11	25	92	0.45
SFBC13	508	2.33	19	57	8	16	100	0.47
SFBC26	515	5.12	15	67	10	4	96	0.45
SFBC03	515	6.05	20	46	13	18	96	0.44
SFBC31	528	2.83	29	42	16	6	93	0.68
SFBC15	551	5.46	20	51	14	7	92	0.46

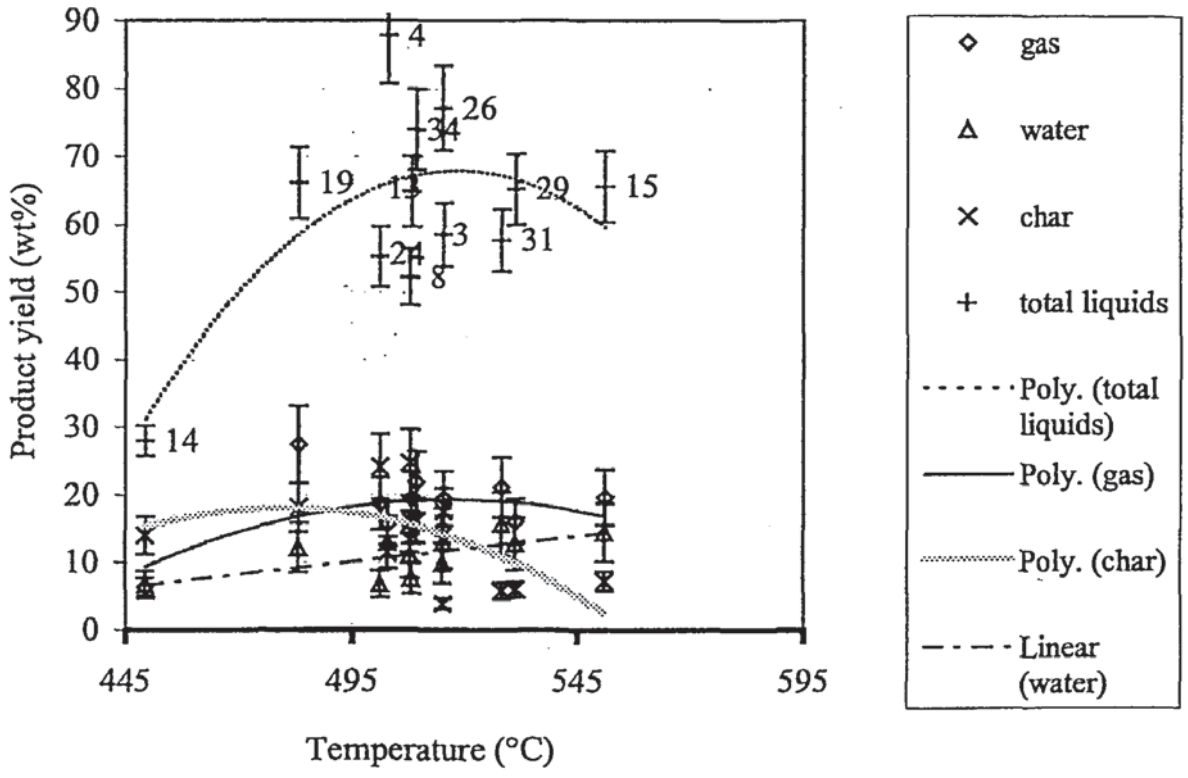

Figure 6.12 Product yields versus temperature from 50 % catalyst feed concentration run series (LAC3)

6.6.3 Comparison of product yield trends

Figure 6.13 shows the product yield trends of total liquids from the 0 %, 25 % and 50 % catalyst feed concentration runs carried out on the 150 g h^{-1} reactor, series LAC1 and RAH combined, LAC2 and LAC3 respectively.

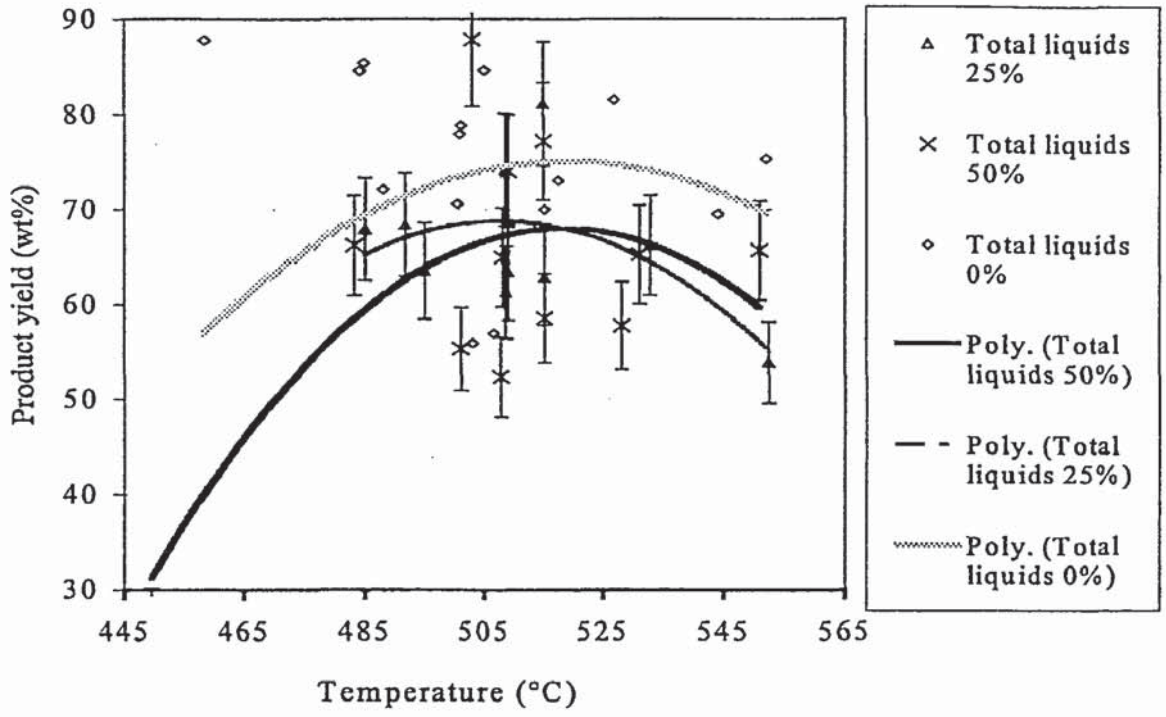

Figure 6.13 Total liquid yields versus temperature for 0 %, 25 % and 50 % catalyst runs on 150 g h^{-1} reactor

The yield of total liquids from the 50 % catalyst feed concentration series demonstrates the same trend with temperature as the combined LAC1/RAH non-catalytic series but with approximately 10 wt% lower yields of total liquids. The yield of total liquids from the 25 % catalyst feed concentration series reaches a maximum at a lower temperature than the 0 % and 50 % catalyst feed concentration series.

The mean absolute deviation of yield of total liquids was calculated for triplicated runs carried out at 508.5 ± 1.0 °C and 25 % and 50 % catalyst feed concentrations described in Section 6.4. The percentage of the mean absolute deviation of the triplicate average was calculated to be 8 % for both 25 % and 50 % catalyst feed concentrations. An error of ± 8 % is assigned to data points from runs carried out at 25 % and 50 % catalyst feed concentration in Figure 6.13.

The yield of total liquids displayed the lowest error of all the product yields achieved during series LAC1-3 on the 150 g h^{-1} fluidised bed reactor.

Shafizadeh (216) reported that the presence of acidic catalysts in trace amounts (i.e. less than 1 %) lowered the temperature of pyrolysis and catalysed the rate of depolymerisation (transglycosylation) reactions whereas the presence of acids in higher amounts (i.e. 1-5 %) led to the dehydration of sugars depending on the amount of water present. Although the catalyst was present in the feed in concentrations of 25 % and 50 % the active ZSM-5 component may have been present in the feed at concentrations between 2.5-3.75 % and 5-7.5 % respectively (based on an assumed percentage of 10-15 % of active ZSM-5 component on the alumina phosphate binder – the real percentage not being available). It is possible that a similar effect occurred with the 150 g h^{-1} catalyst series to that reported by Shafizadeh.

Figure 6.14 shows the yields of organic liquids for combined non-catalytic series LAC1 and RAH catalytic series LAC2 and catalytic series LAC3.

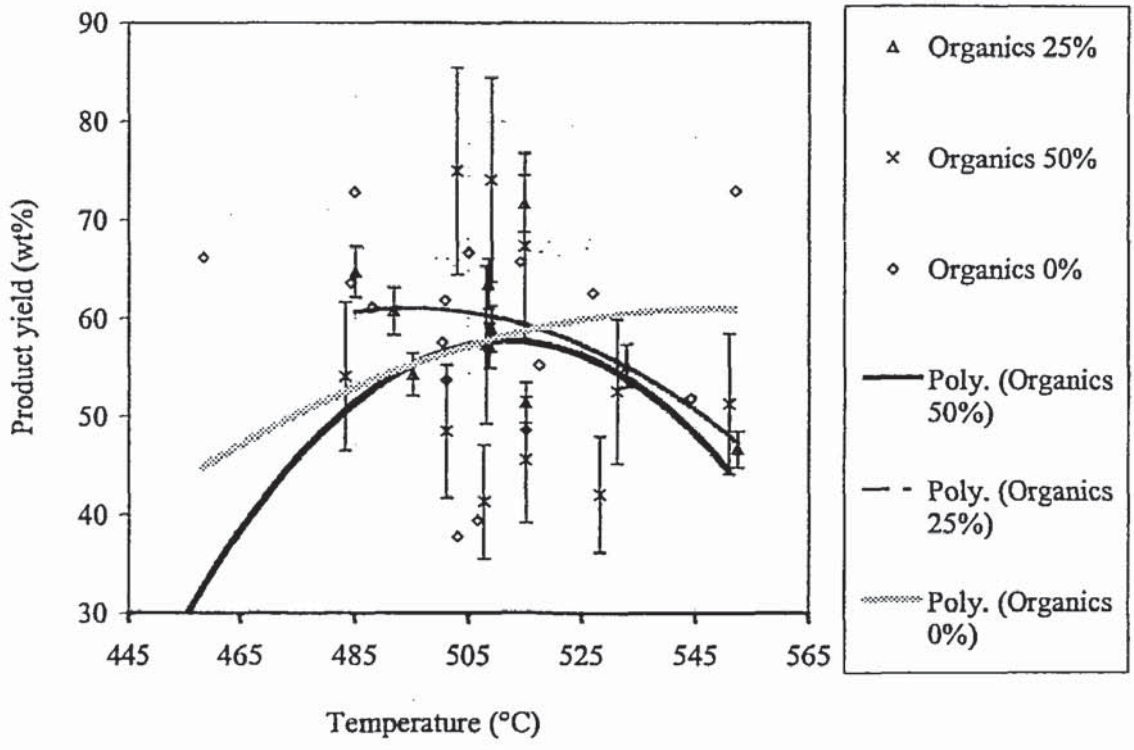

Figure 6.14 Yield of organic liquids for combined non-catalytic series LAC1 and RAH, catalytic series LAC2 and catalytic series LAC3

The mean absolute deviation of yield of organic liquids was calculated for triplicated runs carried out at 508.5 ± 1.0 °C and 25 % and 50 % catalyst feed concentrations. The percentage of the mean absolute deviation of the triplicate average was calculated to be 4 % and 14 % for 25 % and 50 % catalyst feed concentrations respectively. These are assigned to data points produced from 25 % and 50 % catalyst feed concentration runs, respectively, in Figure 6.14. Errors are not assigned to data points from 0 % catalyst feed concentration runs as there was insufficient data produced to calculate them. The yield of organic liquids displays the next lowest error, after the yield of total liquids, of all the product yields achieved during series LAC1-3 on the 150 g h^{-1} fluidised bed reactor.

The trend in the yield of organic liquids for the three feed catalyst concentration series (LAC1-LAC3) are similar to the trend in the yield of total liquids where the trend in the yield of organic liquids for 0 % and 50 % catalyst concentrations peak at similar temperatures and the trend in the yield of organics for 25 % catalyst concentration series peaks at a lower temperature. The trend in the yield of organic liquids from the series with a catalyst concentration of 50 % (LAC3) appears to be more comparable to that from the non-catalytic series (LAC1) below 500 °C whereas the trend in the yield of organics from the series with a catalyst concentration of 25 % (LAC2) appears to be more comparable to that from the non-catalytic series (LAC1) above 500 °C. It would be expected that the yield of total liquids trend and the yield of organic liquids trend from the non-catalytic series would be the same shape curves but with the yield of organic liquids trend being slightly lower as the yield of water (i.e. the difference between the two) does not typically vary with temperature over the 450-500 °C range for non-catalytic fluidised bed fast pyrolysis of wood (78, 207).

Figure 6.15 shows the trends for the yields of water for the three series with temperature. The yield of water from the non-catalytic series decreases slightly with temperature in contrast with the 1 kg h^{-1} reactor where the yield of water increases marginally with temperature. The trends in the yield of water from the catalytic series 25 % and 50 % catalyst feed concentration both increase over the temperature range. The yields of water for the catalytic runs are also lower on average than the non-catalytic series indicating a possible catalytic effect.

The mean absolute deviation of yield of water was calculated for triplicate runs carried out at 508.5 ± 1.0 °C and 25 % and 50 % catalyst feed concentrations (Section 6.4). The percentage of the mean absolute deviation of the triplicate average was calculated to be 45 % and 30 % for 25 % and 50 % catalyst feed concentrations respectively. These percentages are assigned to the respective data points in Figure 6.15. The yield of water displays the highest error of all the product yields achieved during series LAC1-3 on the 150 g h^{-1} fluidised bed reactor.

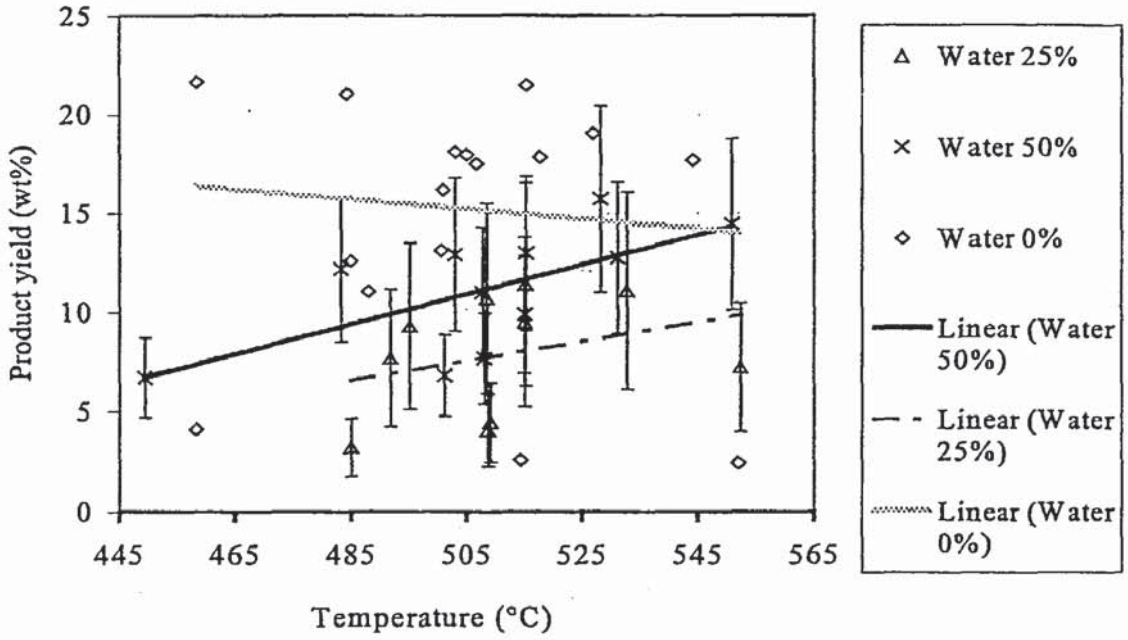

Figure 6.15 Yield of water versus temperature for non-catalytic, 25 % and 50 % catalyst feed concentration series on the 150 g h^{-1} reactor

It is not possible to draw significant conclusions for the trend in yield of water with temperature and catalyst concentration due to the scatter and degree of calculated error but it is suggested that the presence of catalyst either reduces the amount of water produced or absorbs it. It appears unlikely that the reduction in the yield of water experienced in the presence of catalyst is due to absorption as there is a greater yield of water at 50 % catalyst concentration than at 25 % catalyst concentration. These different effects for 25 % and 50 % catalyst concentration could be due to there being different catalytic effects at different levels of catalyst in the feed or it could be that some catalytic reactions continue to a greater extent at the higher catalyst level producing a different product distribution.

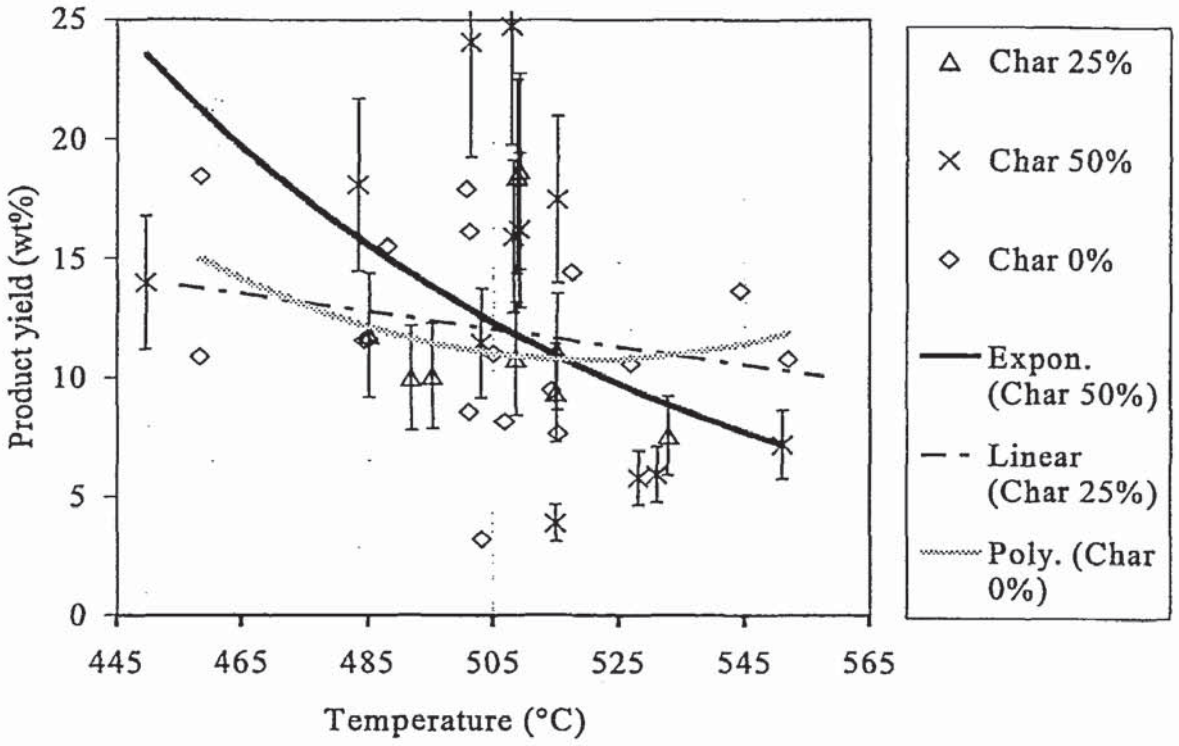

Figure 6.16 Yield of char for non-catalytic, 25 % and 50 % catalyst feed concentration runs against temperature

Finally, Figure 6.16 shows the yield of char (including coke) with increasing temperature for non-catalytic, 25 % and 50 % catalyst concentration runs. These trends are not significant due to the degree of error experienced in the data. In the catalytic runs there appears to be a decrease in the yield of char as the temperature increases. There were difficulties experienced quantifying the amount of char and coke in catalytic runs and it was necessary to make estimations. Quantification improved throughout the LAC series and was discussed in Sections 6.3.8 and 6.3.9.

The mean absolute deviation of yield of char (including coke) was calculated for triplicated runs carried out at 508.5 ± 1.0 °C and 25 % and 50 % catalyst feed concentrations (Section 6.4). The percentage of the mean absolute deviation of the triplicate average was calculated to be 22 % and 20 % for 25 % and 50 % catalyst feed concentrations respectively. These are assigned to the relevant data points in Figure 6.15. The yield of char (including coke) experiences the highest error, of all the product yields, after the yield of water achieved during series LAC1-3 on the 150 g h^{-1} fluidised bed reactor.

6.6.4 Gas composition from 0, 25 and 50 % feed catalyst concentration series

Yields of carbon monoxide and carbon dioxide from 25 % and 50 % catalytic runs are shown versus temperature in Figure 6.17. The mean absolute deviation of the yields of carbon monoxide and carbon dioxide were calculated for triplicated runs carried out at 508.5 ± 1.0 °C and 25 % and 50 % catalyst feed concentrations. The percentages of the mean absolute deviations of the triplicate averages were calculated and are represented as errors bars in Figure 6.17.

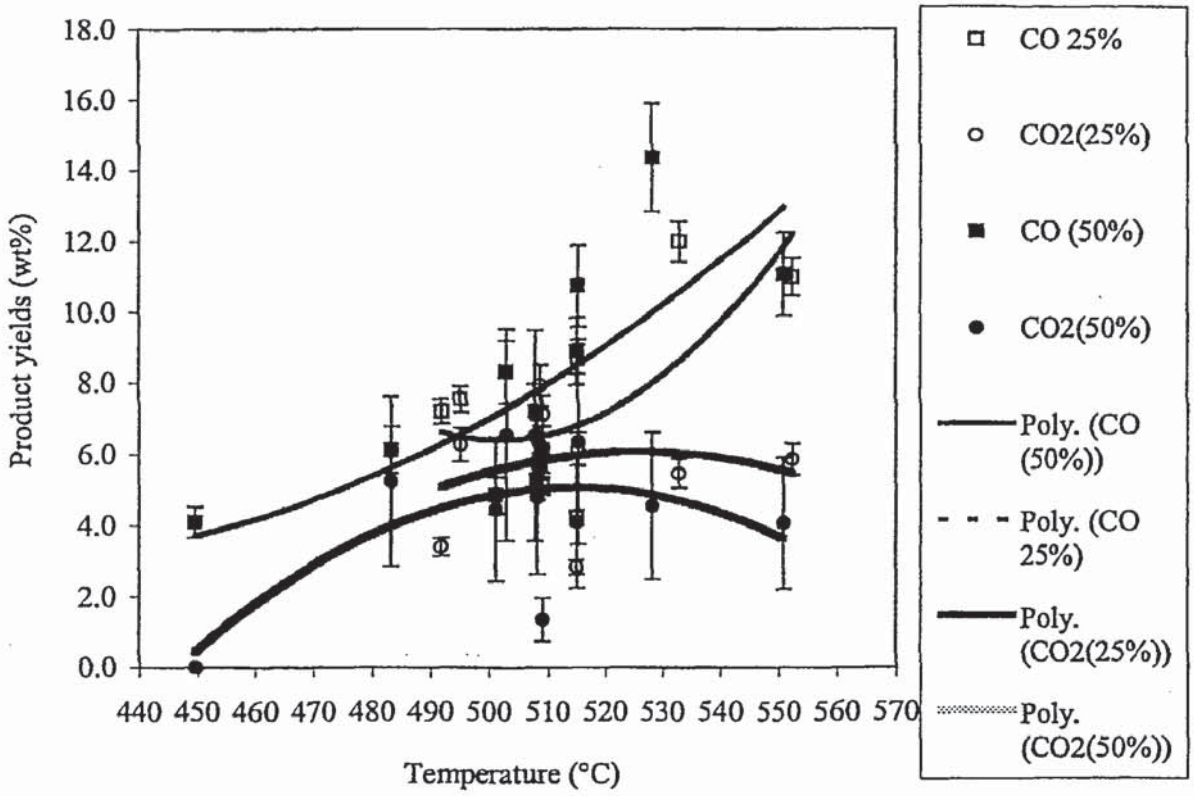

Figure 6.17 Carbon monoxide and carbon dioxide composition for 25 % and 50 % catalyst feed concentration runs

In the catalytic runs the yields of carbon monoxide and carbon dioxide increase with temperature as was the case with non-catalytic runs, on the 1 kg h^{-1} and 150 g h^{-1} reactors. Product yields achieved at the National Renewable Energy Laboratory (152) indicated that catalytic reaction severity increased with temperature (between 400-500 °C) resulting in higher yields of carbon oxides due to the greater extent of decarbonylation and decarboxylation.

The 50 % catalytic runs result in stronger effects than the 25 % catalytic runs with respect to the increase in carbon monoxide with temperature and the decrease in carbon dioxide with temperature.

The presence of catalyst in the pyrolysis reaction results in an increase in the formation of carbon monoxide at the expense of carbon dioxide. ZSM-5 has been reported to deoxygenate oxygenated compounds such as aldehydes and ketones in bio-oil via decarbonylation producing carbon monoxide and carbon dioxide. It would be expected for the catalytic reaction severity to increase with increasing catalyst concentration in the feed. Since more oxygen can be rejected as carbon dioxide than as carbon monoxide, it would be expected for the yield of carbon dioxide to be increased with increasing presence of ZSM-5 catalyst but this was not the case.

Figure 6.18 shows the yields of methane and ethene versus temperature for 25 % and 50 % catalyst feed concentration runs.

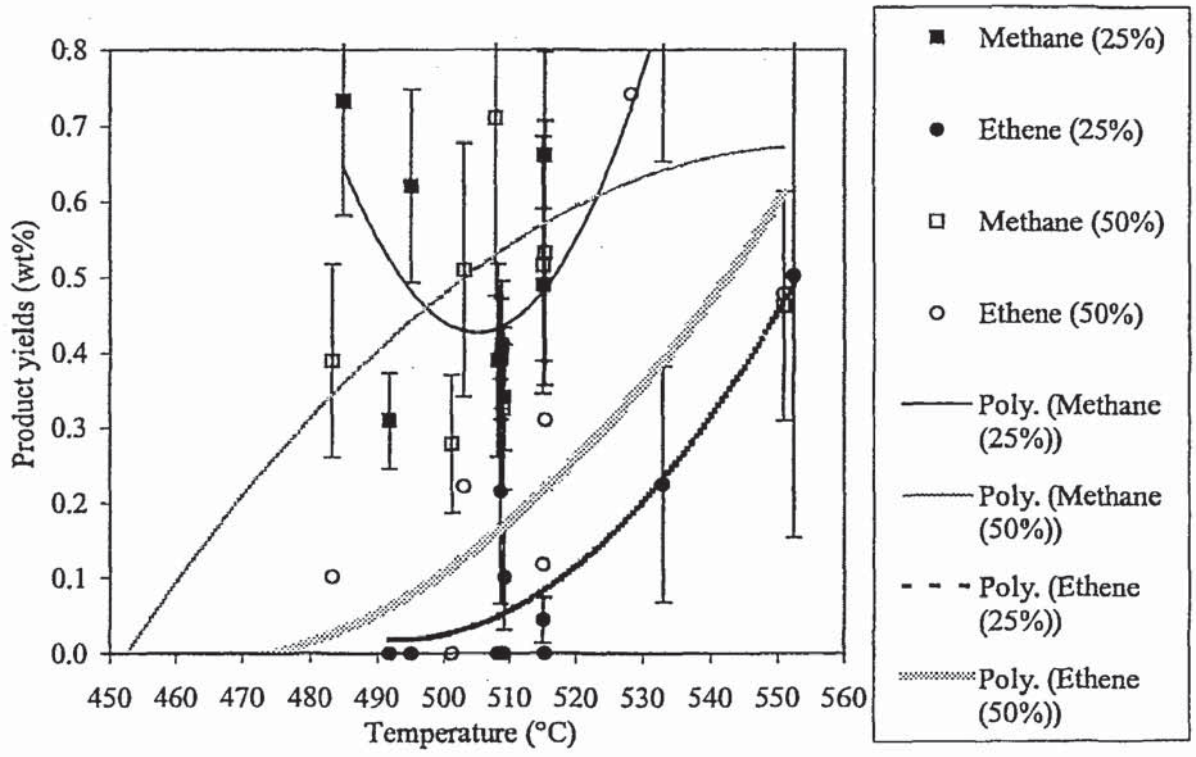

Figure 6.18 Methane and ethene composition for 25 and 50 % catalyst feed concentration runs

The mean absolute deviation of the yields of methane and ethene were calculated for triplicated runs carried out at 508.5 ± 1.0 °C and 25 % and 50 % catalyst feed concentrations.

The percentages of the mean absolute deviations of the triplicate averages were calculated, with the exception of the yield of ethene at 50 % catalyst feed concentration, and are represented as errors bars in Figure 6.18.

The yield of ethene increases with temperature for both catalyst concentrations as was the case with the non-catalytic runs. The yield of methane also increases with temperature for runs carried out at 50 % catalyst concentration in the feed.

The yield of methane from runs carried out at 25 % catalyst concentration follows a polynomial trend which decreases initially and then increases quite rapidly within the 450-600 °C temperature range studied.

This is a tentative trend, due to the degree of scatter present in the product yields, and more experimentation would be needed to confirm it. The presence of catalyst increases the yield of ethene. It is unclear whether the presence of catalyst has an effect on the yield of methane.

6.6.5 GC-FID liquid analysis of LAC series

Figure 6.19 shows the distribution of compound types identified by GC-FID on specific LAC series runs. Errors could not been calculated as there were insufficient data points produced. A typical example of a GC-FID trace can be found in Appendix B.

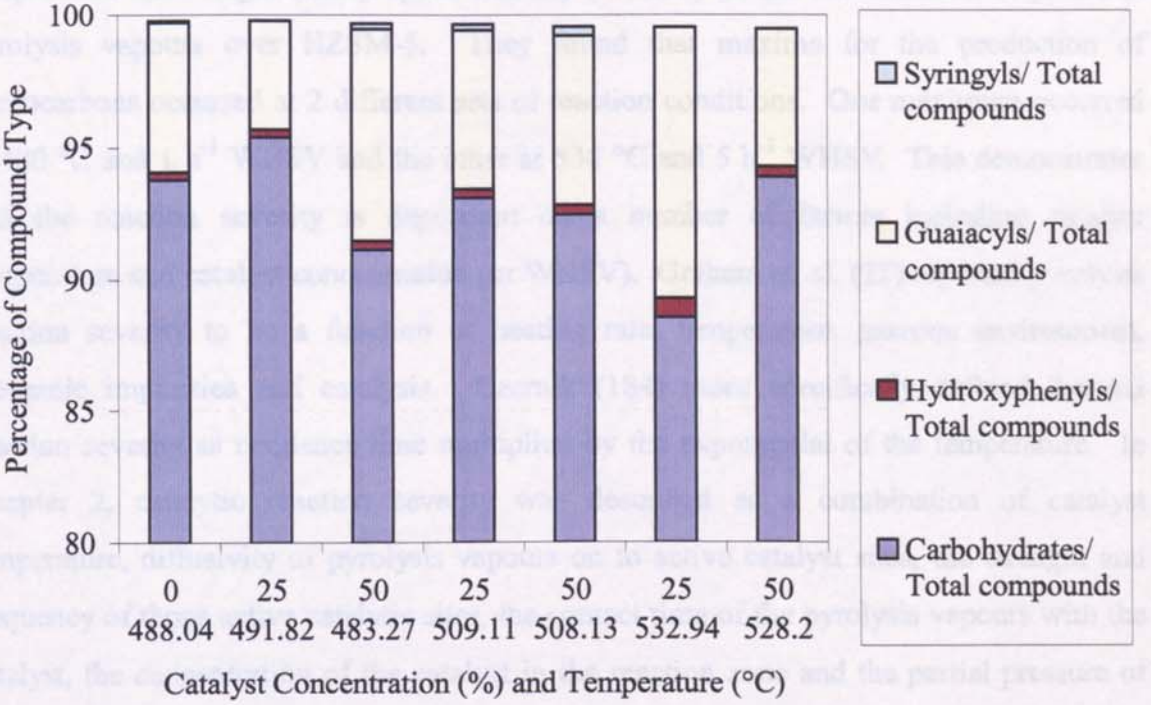

Figure 6.19 Distribution of GC-FID identified liquid products

At a catalyst concentration of 25 % in the feed, the proportion of carbohydrates present in the liquid product decreases with temperature. At 50 % catalyst concentration in the feed, the proportion of carbohydrates increases with temperature. Over the 483-492 °C temperature range, the proportion of carbohydrates increases from 0 % to 25 % catalyst concentration in the feed and decreases from 25 % to 50 % catalyst concentration in the feed. It appears that increasing the catalyst concentration in the feed from 25 % to 50 % does not result in the same effects on product yields as increasing the catalyst concentration from 0 % to 25 % in the feed. There appears to be an optimum concentration of catalyst in the feed for the production of certain liquid products and above this concentration different product distributions result.

Temperature appears to have an effect on the catalytic reactions occurring, thus the proportion of syringyl compounds in the liquid product at 25 % increase with increasing temperature but the reverse effect on the proportion of syringyl compounds in the liquid product at 50 % catalyst concentration is seen.

This is analogous to work reported by Milne et. al. (162) who studied the effect of temperature and weight hourly space velocity (WHSV) on the modification of pine fast pyrolysis vapours over HZSM-5. They found that maxima for the production of hydrocarbons occurred at 2 different sets of reaction conditions. One maximum occurred at 480 °C and 1 h^{-1} WHSV and the other at 530 °C and 5 h^{-1} WHSV. This demonstrates that the reaction severity is dependant on a number of factors including catalyst temperature and catalyst concentration (or WHSV). Graham et. al. (22) reported pyrolysis reaction severity to be a function of heating rate, temperature, gaseous environment, inorganic impurities and catalysis. Czernik (184) more specifically defined thermal reaction severity as residence time multiplied by the exponential of the temperature. In Chapter 2, catalytic reaction severity was described as a combination of catalyst temperature, diffusivity of pyrolysis vapours on to active catalyst sites, the strength and frequency of those active catalytic sites, the contact time of the pyrolysis vapours with the catalyst, the concentration of the catalyst in the reaction zone and the partial pressure of pyrolysis vapours at the active catalyst sites. Catalyst temperature and catalyst concentration, however, appear to be the predominant factors, at constant residence time.

6.6.6 HPLC liquid analysis of LAC series

Figures 6.20, 6.21 and 6.22 show the yields of liquid products identified by HPLC from non-catalytic, 25 % and 50 % catalyst feed concentration 150 g h^{-1} reactor series respectively. The yields of specific liquid products are discussed with respect to their trend with increasing temperature and the differences resulting from increasing concentrations of catalyst. Errors could not been calculated as there were insufficient data points produced. A typical example of an HPLC trace can be found in Appendix C.

The HPLC procedure allowed detection of water soluble components of the bio-oil. Yields for glucose and fructose were the lowest out of the compounds detected. They appear to decrease in concentration with increasing concentration of catalyst.

At all the catalyst concentrations formic and acetic acids decrease in yield from 480 °C to a minimum, at approximately 510 °C for non-catalytic and 25 % catalyst concentration runs and 530 °C for 50 % catalyst concentration runs, and then increase with temperature up to 550 °C, the highest temperature in the range studied.

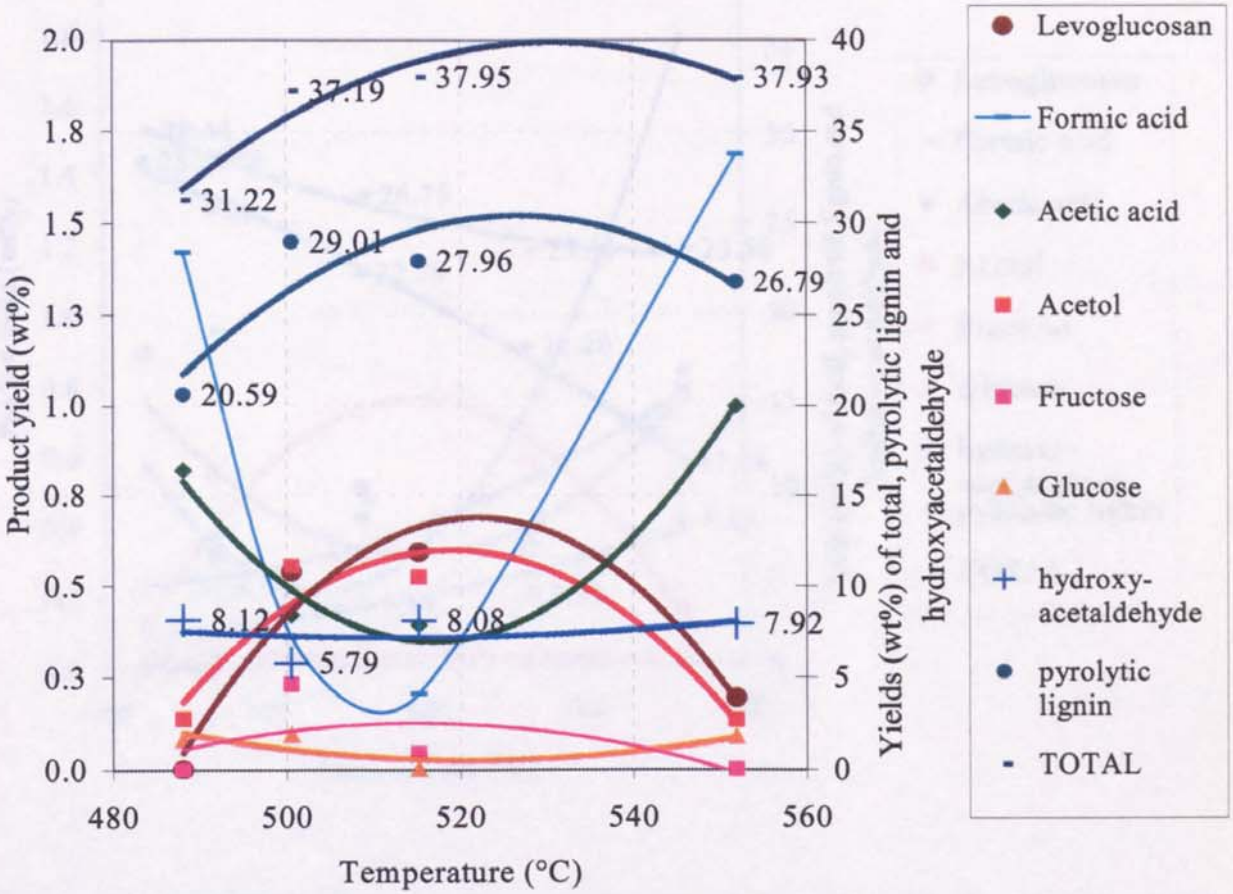

Figure 6.20 Liquid product yields identified by HPLC from 0 % catalyst feed concentration runs

The yield of acetol follows an opposing trend with temperature to formic and acetic acids. At 0 % and 25 % catalyst concentrations the yield of acetol increases from 480 °C to a maximum at approximately 520 °C before decreasing again towards 550 °C. At 50 % catalyst concentration the yield of acetol increases steadily throughout the 480-550 °C temperature range studied.

The yields of levoglucosan appear less clear as the trend for 0 % and 50 % catalyst concentrations are similar, increasing to a maximum around 525 °C but the trend for 25 % catalyst concentration runs is the opposite, displaying a minimum at around 525 °C.

The trend in the yield of levoglucosan with temperature at a catalyst concentration of 25 % is tentative, however, as the data has a higher degree of scatter than that from the 0 % or 50 % catalyst concentration runs.

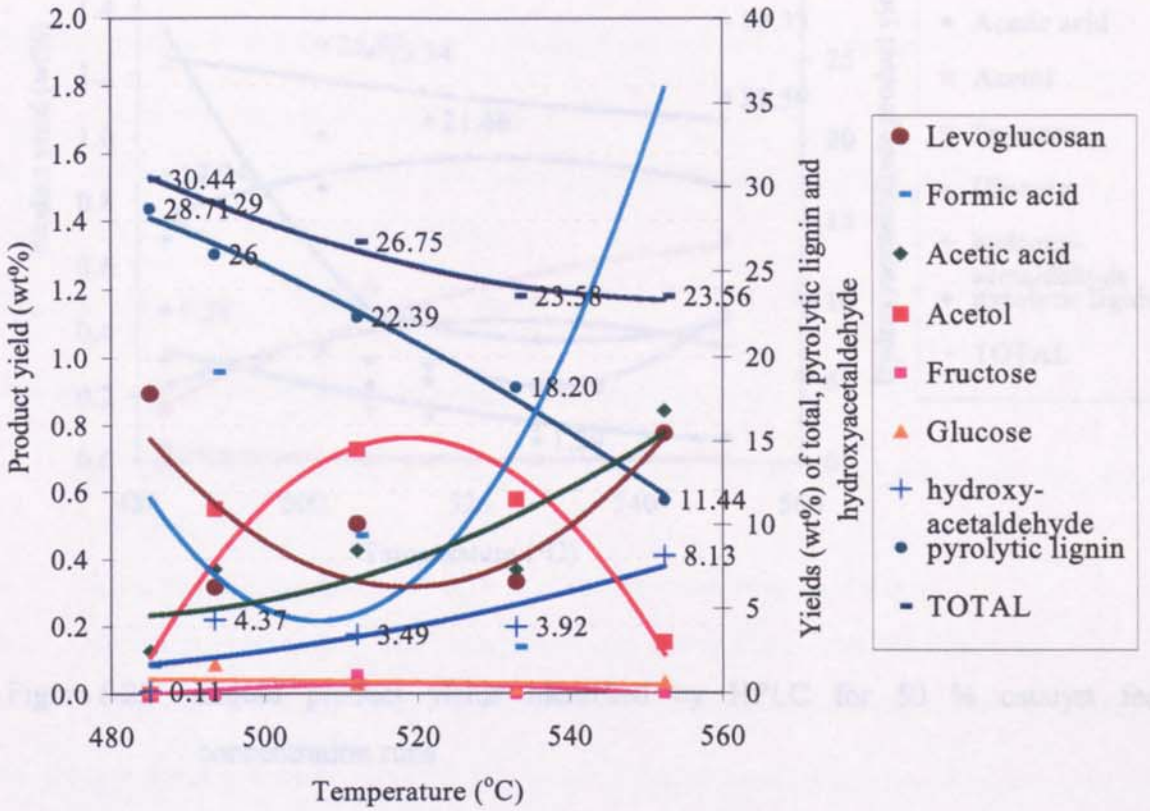

Figure 6.21 Liquid product yields identified by HPLC for 25 % catalyst feed concentration runs

The yield of hydroxyacetaldehyde dominates the water soluble fraction of the bio-oil. The scale for the yield of hydroxyacetaldehyde and the yield of pyrolytic lignin is shown on the right hand side y axis so that the trends can be compared to the trends of lower yielding components. At a catalyst concentration of 0 % the yield of hydroxyacetaldehyde remains relatively constant across the temperature range. At a catalyst concentration of 25 % the yield of hydroxyacetaldehyde increases linearly over the temperature range and at a catalyst concentration of 50 % the yield of hydroxyacetaldehyde decreases linearly over the temperature range.

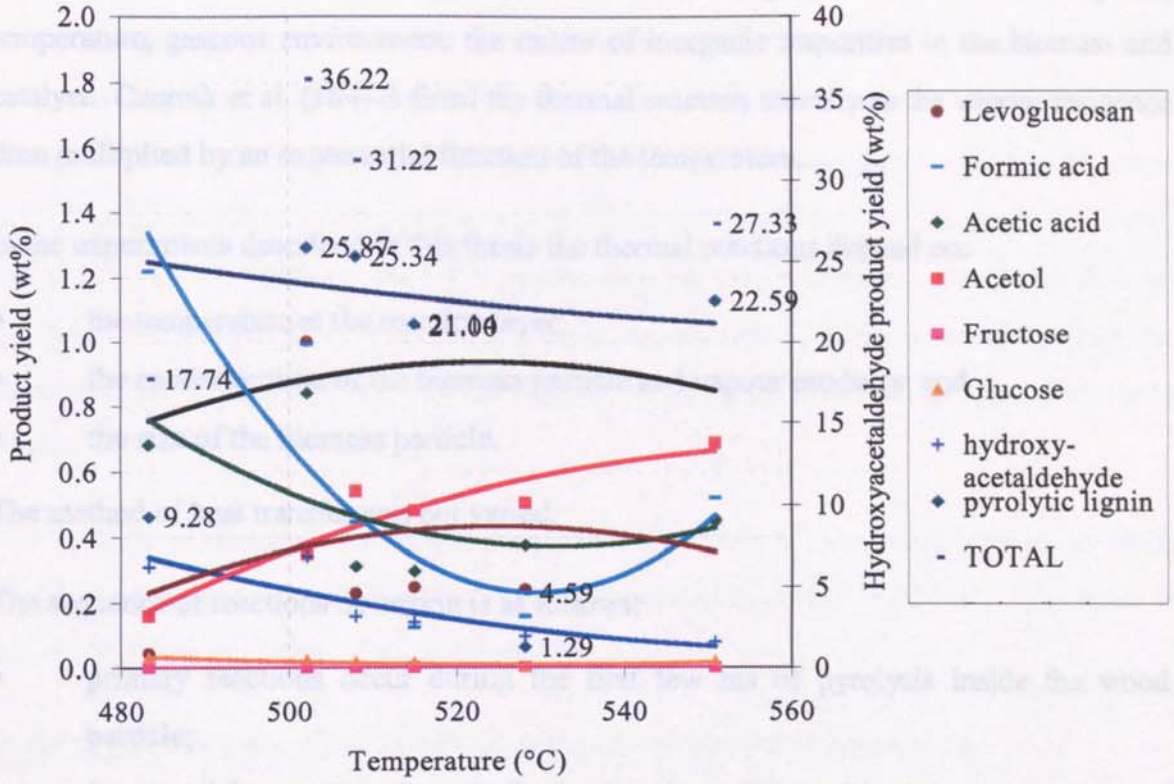

Figure 6.22 Liquid product yields identified by HPLC for 50 % catalyst feed concentration runs

The yield of levoglucosan was lower at a catalyst concentration of 50 % in the feed than at catalyst concentration of 0 % or 25 % which supports Shafizadeh's findings that acidic catalysts in quantities over a trace amount (1-5 %) dehydrate levoglucosan and other sugar units with a corresponding increase in the yield of char, 15.3 wt% on average from catalyst runs at a catalyst concentration of 50 % compared to averages of 10.8 wt% and 11.1 wt% from catalyst runs at catalyst concentrations of 25 % and 0 %, respectively.

6.7 Model of the reactor system

The fast pyrolysis reaction, described in Section 3.3, is a function of:

- temperature at the reaction layer;
- residence time of the biomass particle in the reaction zone;
- heat transfer across the biomass particle;
- size of the biomass particle; and
- method of heat transfer.

Graham et al. (22) described the pyrolysis reaction severity as a function of heating rate, temperature, gaseous environment, the extent of inorganic impurities in the biomass and catalyst. Czernik et al. (184) defined the thermal reaction severity as the vapour residence time multiplied by an exponential function of the temperature.

In the experiments described in this thesis the thermal reactions depend on:

- the temperature at the reaction layer;
- the residence time of the biomass particle and vapour products; and
- the size of the biomass particle.

The method of heat transfer was not varied.

The sequence of reactions occurring is as follows:

- primary reactions occur during the first few ms of pyrolysis inside the wood particle;
- intra-particle reactions occur in the particle depending on it's size;
- secondary reactions occur in the char layer which has a catalytic effect; and
- secondary reactions occur outside the particle depending on vapour residence time.

As the pyrolysis reactions increase the yield of liquid products increase to a maximum after which they decrease and the yields of char and gas increase. This can be seen from the product yields obtained from the 150 g h^{-1} and 1 kg h^{-1} reactor series against temperature. The increased vapour residence times employed in the 1 kg h^{-1} compared to the 150 g h^{-1} reactor series, discussed in Section 6.5.3., results in an increase in the yield of gas and char, at the expense of the liquid product, as the extent of secondary reactions outside the particle are increased. The larger particle size used in the 1 kg h^{-1} reactor compared to the 150 g h^{-1} reactor demonstrates the effect of increased reactions within the particle which result in higher yields of gases and particularly hydrocarbons.

During the 150 g h^{-1} reactor experiments a lower limit for pyrolysis was experienced at a vapour residence time of 0.76 s, temperature of 488 °C and wood particle size of 75-212 μm. At a vapour residence time of 0.77 s, temperature of 458 °C, average gas velocity of 7 L min^{-1}, and the same particle sized wood, pyrolysis in the 150 g h^{-1} reactor was not possible as the wood blew through the reactor before pyrolysis could occur.

Experiments carried out by Hague (208) on the 150 g h^{-1} reactor using the same pine wood feedstock and a particle size of 350-600 μm demonstrated that pyrolysis could be achieved at a vapour residence time of 0.63 s, temperature of 458 °C and gas velocity of 9 L min^{-1}. The particle size determines the temperature at which fast pyrolysis can be carried out in the 150 g h^{-1} reactor. At low particle sizes of 75-212 μm and low temperatures the rate of wood entrainment from the reactor is greater than the rate of heat transfer to the biomass particle. With larger particle sizes of 350-600 μm the rate of wood entrainment from the reactor is lower than the rate of heat transfer to the particle allowing fast pyrolysis to occur.

The higher temperature limit for fast pyrolysis in the 150 g h^{-1} reactor system occurs when the yield of gas is markedly increased at the expense of the yield of liquids. This starts to occur above temperatures of approximately 520-525 °C.

In the experiments described in this thesis the catalytic reaction depends on:

- the temperature of the catalyst; and
- the concentration of the catalyst in the reaction zone.

Contact time between the catalyst and pyrolysis vapours was kept as constant as possible throughout the 150 g h^{-1} experimental series and catalyst from the same sample was used in all experiments eliminating any variation due to diffusion through the catalyst and strength and frequency of active catalyst sites.

The presence of catalyst in the 150 g h^{-1} reactor system:

- reduces the yield of liquids from pine fast pyrolysis over the temperature range studied;
- reduces the temperature of pyrolysis at 25 % catalyst feed concentration;
- reduces the yield of water; and
- alters the composition of the liquid products depending on the catalyst feed concentration.

The effects of catalyst feed concentration with temperature within the system on the products yields are complicated and cannot be fully characterised without further experimentation. It is apparent, however, that the rates of specific reactions are changed by the presence and concentration of catalyst and variation of temperature.

CHAPTER SEVEN

CONCLUSIONS

7 CONCLUSIONS

7.1 Adaptation and commissioning of the 150 g h^{-1} reactor for catalytic pyrolysis

Investigation of the fluidising characteristics of the powdered ZSM-5 containing catalyst from Grace Davison was carried out to determine if it could be incorporated into the 150 g h^{-1} fluidised bed fast pyrolysis reactor. The catalyst entrainment rate was calculated to be between 3.70 – 7.28 g s^{-1} at nitrogen fluidising gas flow rates necessary for biomass pyrolysis within the 150 g h^{-1} fluidised bed reactor. This correlates to complete blow through of a 135 g (mass of fluidising medium used during normal operation) catalyst bed in 18 to 36 seconds. A run period of at least 20 minutes was required on the 150 g h^{-1} reactor to allow pyrolysis of a sufficient quantity of biomass to allow a mass balance to be carried out. Operation of the 150 g h^{-1} reactor with a catalyst fluidising medium, therefore, was not possible.

In order to contact biomass vapours and catalyst successfully in the 150g h^{-1} reactor the biomass and catalyst were co-fed via an entrained flow feeder into the reactor. It was necessary to grind and sieve the biomass to the particle size fraction 75-212 ? m and to sieve the catalyst to the same range in order to achieve co-feeding. At larger biomass and smaller catalyst particle sizes bridging occurred in the feeder and the catalyst was too dense to be fed alone in the entrained flow feeder. In order to avoid incomplete pyrolysis of a large flow rate of wood to the reactor it was necessary to limit the combined flow rate of biomass and catalyst to below 120 g h^{-1}. This was accomplished by:

- using an entrain tube with a feed hole of 1.1 mm rather than 1.7 mm as was used for non-catalytic pyrolysis with larger particle sized wood;
- maintaining the feeder stirrer power setting below 1 (an arbitrary setting corresponding to an RPM of 60); and
- maintaining the feeder top nitrogen flow rate below 0.5 L min^{-1}.

7.2 Operation of the 150 g h^{-1} fluidised bed reactor with 75-212 μm particle sized biomass for catalytic pyrolysis experiments

The following conclusions can be drawn from the discussion of runs carried out on the 150 g h^{-1} fluidised bed reactor with 75-212 μm particle sized pine wood alone (series LAC1 – 0 % catalyst feed concentration) and co-fed with catalyst (series LAC2 and LAC3 - 25 % and 50 % catalyst concentrations in the feed, respectively).

Run instability was caused by a combination of: reactor temperature deviation, feeder pressure deviation, reactor pressure deviation, the degree of feed blockages and was exacerbated by the number of adjustments made to rotameters in response to instability factors.

For each series of runs (at constant catalyst feed concentration) trends in product distribution were identified with reactor temperature. Deviations from these general trends were noted in specific runs but there was no significant correlation between the deviation of a run from the general trend identified and the degree of instability calculated for that run.

The magnitude of deviation of the product yields of a specific run from the trends identified for a particular series, over the temperature range studied, decreased over the SFBC series with experience demonstrating a learning effect. The reduction in deviations was most likely due to improvements made in collection procedure.

A temperature of 485 °C was identified as the lower limit at which pyrolysis could be successfully achieved in the 150 g h^{-1} fluidised bed reactor with wood particles in the size fraction 75-212 μm. At temperatures below 485 °C the heat transfer rate was not high enough to achieve pyrolysis of the wood particles before they elutriated from the bed.

The major cause of feeder blocking was the presence of catalyst 'fines', defined as particles less than 75 μm in size, which bridged across the hole in the entrain tube. This could be avoided by sieving catalyst prior to the run for a minimum of two hours.

The major source of experimental error is thought to be the calculation of the fraction of solids in the glassware due to difficulties in recovery and separation.

7.3 Product yields and reaction pathways

7.3.1 Product yields achieved from the 1 kg h^{-1} reactor series

The trends identified in product yield with temperature were comparable to those reported by other workers (78) on softwood fast pyrolysis under the conditions studied.

The maximum yield of total liquids of 72 wt%, indicated by the trendline, occurred at a temperature of approximately 500 °C. The maximum yield of organic liquids of 55 wt%, indicated by the trendline, occurred at a temperature of approximately 500 °C.

The closures achieved in the runs on the 1 kg h^{-1} reactor ranged between 95.6-99.7 wt% with an average of 97.1 wt%.

The yield of total liquids and the yield of organic liquids from the 1 kg h^{-1} reactor displayed more pronounced trends across the temperature range studied than the trends obtained from the 150 g h^{-1} reactor. This was possibly due to the increase in vapour residence times at lower temperatures in the 150 g h^{-1} reactor compared to the constant vapour residence times across the temperature range with the 1 kg h^{-1} reactor runs. Vapour residences times were increased from 0.5 s to 0.75 s in low temperature (485 °C) 150 g h^{-1} reactor runs to increase the heat transfer rate in order to effect pyrolysis before biomass elutriation occurred.

The maximum yield of total liquids and organic liquids achieved from the 1 kg h^{-1} reactor series occurred at lower temperatures than maximum yields of total liquids and organic liquids from the 150 g h^{-1} reactor series. This was ascribed to increased thermal reaction severity due to a higher average residence time of 1.1 s in the 1 kg h^{-1} reactor series compared to 0.6 s in the 150 g h^{-1} reactor series.

Higher residence times were required in the 1 kg h^{-1} reactor in order to completely pyrolyse the larger particle sized biomass used (0.6-1.7 mm) compared to the 150 g h^{-1} reactor (75-212 μm). Yields of char were higher from runs carried out on the 1 kg h^{-1} compared to runs carried out on the 150 g h^{-1} reactor as a direct result of the larger particle sized biomass used in the 1 kg h^{-1} reactor and higher residence times used in 1 kg h^{-1} reactor.

Larger particles are pyrolysed more slowly than smaller particles, since the rate of heat transfer through the particle is lower than the rate of heat transfer to the surface of the particle. Vapours diffusing from the centres of large particles have further to travel to the outer particle surface than those diffusing from the centres of smaller particles. During this extended diffusion time the vapours from large particle pyrolysis undergo secondary char catalysed thermal reactions to a greater extent than with smaller particle pyrolysis resulting in a higher yield of char.

7.3.2 Gas composition from 1 kg h^{-1} and 150 g h^{-1} non-catalytic reactor series

The yields of methane and ethene from the 1 kg h^{-1} reactor runs were higher than those from the 150 g h^{-1} reactor runs indicating either a higher degree of pyrolysis reactions (inside the particle), pyrolysis reactions in the gas phase or a combination of both due to the larger particle size and the higher degree of reaction severity experienced by the biomass particles in the 1 kg h^{-1} reactor series.

The yield of gas from both reactor systems increased with temperature over the range studied. Yields of methane and ethene increased more sharply with temperature than the increase in the yields of carbon monoxide and carbon dioxide indicating a preference for low hydrocarbon production at higher reaction severities.

7.3.3 Product yields achieved in the catalytic 150 g h^{-1} reactor series

The trend in yield of total liquids with temperature at catalyst concentrations of 50 % is similar to that at a catalyst concentration of 0 % but the yield of liquids from runs carried out at 50 % catalyst concentration is approximately 10 wt% lower across the temperature range investigated than the yield of total liquids from runs carried out at 0 % catalyst concentration.

The yields of total liquids at a catalyst feed concentration of 25 % in the feed with temperature reaches a maximum at a lower temperature than in the series of runs at catalyst concentrations of 0 % and 50 %. This may be due to there being a different catalytic effect at lower catalyst concentrations, as noted by Shafizadeh (216), but further experimentation is required to confirm it.

7.3.4 Analysis of liquid products from the non-catalytic and catalytic 150 g h^{-1} reactor series

Differences in the product distribution of pyrolysis liquids produced in the presence of 0 %, 25 % and 50 % catalyst in the feed were identified by GC-FID and HPLC analyses. There were apparently different effects in liquid product distribution resulting from pyrolysis with 0 %, 25 % and 50 % catalyst in the feed. It was observed that increasing the concentration of catalyst in the feed from 25 % to 50 % did not simply result in an increase in the differences in product distribution seen between the runs conducted with 0 % and 25 % catalyst concentration in the feed. This is similar to the effect reported by Shafizadeh (216) who found that acidic catalysts in trace amounts catalysed certain reactions but that acidic catalysts in greater amounts catalysed different reactions. Further experimentation is required to ascertain whether the differences observed in liquid composition are due to the HZSM-5 component, the acidic nature of the catalyst, the alumina phosphate binder alone or the presence of a small particle sized, unheated, solid co-fed with biomass.

It was observed, from HPLC analysis of the liquid products, that:

- the yields of glucose and fructose were the lowest of the compounds detected and appeared to decrease in concentration with increasing concentration of catalyst, possibly due to a dehydrating effect of the acidic catalyst;
- the trends in yields of formic acid, acetic acid, acetol and levoglucosan with temperature were similar for 0 % and 50 % catalyst concentrations but were the inverse for 25 % catalyst concentrations indicating an effect of catalyst concentration in the feed;
- the yield of hydroxyacetaldehyde dominated the yield of components in the water soluble fraction of the bio-oil; and
- the yield of levoglucosan was lower at a catalyst concentration 50 % in the feed than at a catalyst concentration of 0 % or 25 % in the feed.

It was observed, from GC-FID analysis of liquid products, that:

- the proportion of carbohydrates decreased and the proportion of guaiacyl compounds increased with temperature at a catalyst concentration of 25 % in the feed; and
- the reverse occurred at a catalyst concentration of 50 % in the feed.

The trends in product yield and the liquid analyses for series with concentrations of catalyst of 0 %, 25 % and 50 % in the feed on the 150 g h^{-1} reactor suggest that the presence of 25 % of catalyst in the feed increases the rate of certain reactions with temperature whereas the presence of 50 % catalyst concentration in the feed possibly promotes further conversion of initial products or promotes different reaction pathways.

7.4 Summary of conclusions

Operation of the 150 g h^{-1} fluidised bed reactor in co-fed biomass and catalyst mode provided an efficient method of contacting a powdered catalyst with freshly produced bio-vapours. Run stability could be improved by sieving of the wood for a minimum of two hours prior to the run. The reliability of product yields was increased by improvements in product collection procedure.

The effects of 0 %, 25 % and 50 % catalyst concentration in the feed resulted in different product yield distributions in each case.

CHAPTER EIGHT

RECOMMENDATIONS

8 RECOMMENDATIONS

8.1 Operational and equipment recommendations

The efficiency of the separation of solids from the pyrolysis vapour products could be improved to allow separation and recovery of the catalyst without mixing with the liquid product. Either the current cyclone could be redesigned to separate the small particle sized catalyst, as well as char, from the vapour stream; or an additional cyclone or series of cyclones could be added to collect all solid particles. Care should be taken in modifying cyclone capacity to avoid increasing the hot space vapour residence time to an extent that significant thermal cracking may occur prior to product collection. Larger catalyst particle sizes could possibly overcome the need for improved solid separation but modification of physical or chemical catalyst properties was out of the scope of this work.

A catalyst feeder has been designed and manufactured for solo feeding of fine particle catalysts to the 150 g h^{-1} reactor over a range of flow rates. This will allow a larger particle size of wood to be fed, as the small size would not be required for catalyst co-feed mixing, and allow greater flexibility in the preparation of catalyst prior to feeding, e.g. preheating. This should be commissioned in conjunction with modification to the fluidised bed reactor inlets to allow separate catalyst feeding to the reactor. The addition of an entry point for a catalyst feeding line into the lid of the fluidised bed reactor may prove problematic due to the limited space available on the lid for another weld union. A previous attempt had been made to introduce the catalyst via an inlet entering a point on the side of the main reactor body, 10 mm above the distribution plate. However, the 3 mm stainless steel feed tube contained a 90 degree bend to allow vertical placement, through the open top of the furnace, alongside the reactor body and problems due to blocking at the 90 degree bend in the line were encountered. An alternative solution would be to feed the catalyst through a horizontal line passing through the side of the furnace. This may not be possible due to the placement of the furnace internal heating elements.

Direct measurement of the nitrogen flow rate into the reactor using a gas meter would allow more precise calculation of the yield of gas produced during the run.

Inclusion of an online gas chromatography system would allow immediate compositional analysis of the pyrolysis product gas thus avoiding the necessity for manual gas sampling and storage of sample bombs prior to analysis. This would enable faster quantification of the yield and composition of gas allowing modification of reactor parameters for the next run based on the information. It would also avoid any possible leakage of gases during storage.

Determination of the biomass feed rate throughout the run could be achieved by mounting the feeder on digital scales for continuous monitoring producing a delivery profile of feed over the run period.

Automatic monitoring (with the potential for automated closed loop control) of pressures, temperatures and flow rates via a data logger would ensure consistent monitoring of these process parameters. When operational problems were experienced continuous monitoring of variable levels was not possible due to trouble shooting of specific problems at that time. These readings would be particularly important from a diagnostic point of view when reviewing and rationalising run stability. Operational problems such as feeder blockages were seen to build up gradually throughout the run. Bridging of small particles across the hole in the feed entrain tube would be easily cleared initially, at the start of the run. They would become more frequent throughout the run, being more difficult to solve and causing pressure build up in the rotameters, until a severe blockage across the hole in the feed entrain hole could not be removed and it was necessary to shutdown the reactor immediately. Automatic monitoring of process parameters would have been particularly useful in run numbers SFBC25-32 where blocking occurred.

8.2 Analytical requirements

The HPLC analytical method for identifying and quantifying liquids in the water soluble fraction of the bio-oil could be expanded to the non-aqueous fraction of the bio-oil which contains many interesting chemical components, with respect to catalytic reaction chemistry, prone to change in the presence of a catalyst.

8.3 Recommendations for further experiments

Further runs should be carried out over the 485-530 °C temperature range using a range of catalyst concentrations in the feed between 15 % to 35 % in order to identify the optimum catalyst concentration and catalytic pyrolysis reaction temperature for the production of specific liquid components. Experiments should also be conducted with the alumina phosphate binder alone, if possible, to ascertain which effects in resulting product yield distribution are due to the HZSM-5 component, the alumina phosphate alone or a combination of both.

A great deal of experimentation and analysis is required in order to attempt to define catalytic reaction pathways in the system due to the chemical complexity of biomass pyrolysis and the added effects of catalysts.

Other catalysts should also be studied in this mode of operation with the effects of concentration in the feed and temperature.

Other areas for potential future work lie in the commissioning of the catalyst feeder and feeding of catalyst alone to the reactor and the use of different catalysts including modified ZSM-5 and pillared clays in order to investigate the chemistry of catalytic pyrolysis.

8.4 Reactor system further development

The optimum system in which to carry out vapour phase catalysis using a powdered catalyst, such as the Grace Davison ZSM-5 containing catalyst used in this thesis is a circulating fluidised bed where catalyst is removed from the vapour product stream exiting the reactor and recycled to the bed. Successful catalyst separation from the char should be ensured using a multi-cylcone system or else a catalyst regeneration zone to burn off char and any catalyst coke. Regeneration of catalyst to burn off coke would be required depending on coking rates within the pyrolysis zone and the number of recycles required in a typical run, which would also depend on the run time.

If a larger wood particle size was used than catalyst particle size, achieved by separate catalyst and wood feeding, then cyclone separation of catalyst and char would be facilitated due to the differences in particle size and density between the catalyst and char.

Since the catalyst is likely to require coke burn off through regeneration at some point, the char could be burnt off at the same time avoiding the need for two cyclones.

A commercial process could include:

- separate catalyst and wood feeding;
- a cyclone to separate char from vapour product stream;
- a cyclone to separate catalyst from vapour product stream;
- a catalyst regeneration zone to burn off coke - temperature controllable; and
- a catalyst recycle to the reactor pyrolysis zone.

Catalyst and biomass flow rates should be controllable over a range. There should be a fresh catalyst entry point to the recycle stream. Product collection should be designed to collect specific product or products and a quench column may be required depending on the physical properties of the product.

This system would be similar to those currently used in FCC in the petroleum cracking and refinery business.

REFERENCES

9 REFERENCES

1 Bridgwater, A. V. and Bridge, S. A., 'A review of biomass pyrolysis and pyrolysis technologies', in Biomass Pyrolysis Liquids Upgrading and Utilisation, pp. 11-92, Ed: Bridgwater, A. V. and Grassi, G., Elsevier Applied Science, 1991.

2 Maggi, R. and Delmon, B., 'Comparison between 'slow' and 'flash' pyrolysis oils from biomass', in Fuel, vol. 73, no. 5, pp.671-677, 1994.

3 Maggi, R. E. and Elliott, D. C., 'Upgrading Overview', in Proceedings of Conference: Developments in Thermochemical Biomass Conversion, vol. 1, pp. 575-588, Ed: Bridgwater, A. V. and Boocock, D. G. B., Blackie, 1997.

4 Radlein, D. and Piskorz, J., 'Production of chemicals from bio-oil', in Biomass Gasification and Pyrolysis: Proceedings of Conference: State of the Art and Future Prospects, Stuttgart, 9-12 Apr. 1997, pp. 495-497, Ed: Kaltschmitt, M. and Bridgwater, A. V., CPL, 1997.

5 Stoikos, T., 'Upgrading of biomass derived liquids to high value chemicals and fuel additives', in Biomass Pyrolysis Liquids Upgrading and Utilisation, pp. 227-241, Ed. Bridgwater, A. V. and Grassi G, Elsevier, 1991.

6 Bridgwater, A. V., 'Production of high-grade fuels and chemicals from catalytic pyrolysis of biomass', in Catalysis Today, vol. 29, no. 1-4, pp. 285-295, 1996.

7 Diebold, J. P. and Bridgwater, A. V., 'Overview of fast pyrolysis of biomass for the production of liquid fuels', in Proceedings of Conference: Developments in Thermochemical Biomass Conversion, pp. 5-23, Ed: Bridgwater, A. V. and Boocock, D. G. B., Blackie, 1997.

8 Graham, R. G., Freel, B. A. and Overend, R. P., 'Thermal and catalytic fast pyrolysis of lignin by rapid thermal processing (RTP)', in Proceedings of: 7th Canadian Bioenergy R&D Seminar, Ontario, pp. 669-673, 1989.

9 Bridgwater, A. V., 'Catalysis in thermal biomass conversion', in Applied Catalysis A: General, vol. 116, pp. 5-47, 1994.

10 Meier, D., Oasmaa, A. and Peacocke, G. V. C., 'Properties of fast pyrolysis liquids: status of test methods', in Proceedings of Conference: Developments in Thermochemical Biomass Conversion, pp. 391-408, Ed: Bridgwater, A. V. and Boocock, D. G. B., Blackie, 1997.

11 Milne, T. A., Agblevor, F., Davis, M., Deutch, S. and Johnson, D., 'A review of the chemical composition of fast pyrolysis oils from biomass', in Proceedings of Conference: Developments in Thermochemical Biomass Conversion, pp. 409-424, Ed: Bridgwater, A. V. and Boocock, D. G. B., Blackie, 1997.

12 Bridgwater, A. V., 'A survey of thermochemical biomass processing activities', in Biomass, vol. 22, pp. 279-292, 1990.

13 Soltes, E. J., 'Hydrocarbons from lignocellulosic residues', in Journal of Applied Polymer Science: Applied Polymer Symposium, no. 37, pp. 775-786, John Wiley, 1983.

14 Bridgwater, A. V., 'Pyrolysis technologies', Presented at 2nd E.C. Biomass Contractors Meeting, Paestrum, Italy, 25-27 May, 1988.

15 Bitowft, B., Andersson, L. A. and Bjerle, I., 'Fast pyrolysis of sawdust in an entrained flow reactor', in Fuel, vol. 68, pp. 561-566, 1989.

16 Bridgwater, A. V., Czernik, S., Meier, D. and Piskorz, J., 'Fast Pyrolysis Technology', Proceedings of Conference: 4th Biomass Conference of the Americas, National Renewable Energy Laboratory, 1999.

17 Vitolo, S. and Ghetti, P., 'Physical and combustion characterization of pyrolytic oils derived from biomass material upgraded by catalytic hydrogenation', in Fuel, vol. 73, no. 11, 1994.

18 Baldauf, W., Balfanz, U. and Rupp, M., 'Upgrading of flash pyrolysis oil and utilization in refineries', in Biomass and Bioenergy, vol. 7, no. 1-6, pp. 327-244, 1994.

19 Elliott, D. C., 'Upgrading liquid products – Notes from the workshop at the International Conference Research in Thermochemical Biomass Conversion', Proceedings of Conference: Research in Thermochemical Conversion, pp. 1170, Blackie, 1988.

20 Elliott, D. C., Ostman, A., Bevert, S. B., Beckman, D., Solantausta, Y. and Hornell, C., 'A technical and economic analysis of direct biomass liquefaction'.

21 Lede, J., Verzaro, F., Antoine, B. and Villermaux, J., 'Flash pyrolysis of wood in a cyclone reactor', in Chemical Engineering and Processing, vol. 20, no. 6, pp. 309-317, 1986.

22 Graham, R. G., Bergougnou, M. A. and Overend, R. P., 'Fast pyrolysis of biomass', in Journal of Analytical and Applied Pyrolysis, vol. 6, pp. 95-135, 1984.

23 Bouvier, J. M., Gelus, M. and Maugendre, S., 'Direct liquefaction of wood by solvolysis', in Pyrolysis Oils from Biomass: Producing, Analyzing and Upgrading, ACS Symposium Series 376, pp. 129-138, 1988.

24 Oasmaa, A., Leppamaki, E., Koponen, P., Levander, J. and Tapola, E., 'Physical characterisation of biomass-based pyrolysis liquids: Application of standard fuel oil analyses', in VTT Publication no. 306, Technical Research Centre of Finland, 1997.

25 Roy, C., Yang, J., Blanchette, D., Korving, L. and de Caumia, B., 'Development of a novel vacuum pyrolysis reactor with improved heat transfer potential', in Proceedings of Conference: Developments in Thermochemical Biomass Conversion, pp. 351-367, Ed: Bridgwater, A.V. and Boocock, D.G.B., Blackie, 1997.

26 Bridgwater, A. V., 'Biomass pyrolysis products characterisation, upgrading and utilisation', Contract report, contract no. JOUB-0100, March, 1995.

27 Roy, C., Labrecque, B. and de Caumia, B., 'Recycling of scrap tires to oil and carbon black by vacuum pyrolysis', in Resour. Conserv. Recycl., vol. 4, pp. 203-213, 1990.

28 Roy, C., Lemieux, R., de Caumia, B. and Blanchette, D., 'Processing of wood chips in a semicontinuous multiple-hearth vacuum-pyrolysis reactor', in Pyrolysis Oils from Biomass: Producing, Analyzing and Upgrading, Ed: Soltes and Milne, pp. 16-30, A. C. S. Symposium Series 375, 1988.

29 Pakdel, H., Zhang, H. G. and Roy, C., 'Detailed chemical characterization of biomass pyrolysis oils, polar fractions', in Proceedings of Conference: Advances in Thermochemical Biomass Conversion, pp. 1068-1085, Ed: Bridgwater, A. V., Blackie, 1993.

30 Roy, C., de Caumia, B. and Plante, P., 'Performance study of a 30 kg/h vacuum pyrolysis process development unit'.

31 McKinley, 'Biomass Liquefaction: Centralised Analysis', Final report, Project no. 4-03-837, Prepared by B.C. Research for Science Branch, Science Procurement Department of Supply and Services, DSS file no. 23216-4-6192, Quebec, Canada, 1989.

32 Churin, E., 'Catalytic treatment of pyrolysis oils', EU Contact report, publication no. GP-EUR/12480, 1990.

33 Bridgwater A. V., Meier, D. and Radlein, D., 'An overview of fast pyrolysis of biomass', in Organic Geochemistry, vol. 30, no. 12, pp. 1479-1493, 1999.

34 Van de Kamp, W. L. and Smart, J. P., 'Atomisation and combustion of slow pyrolysis biomass oils', in Proceedings of Conference: Advances in Thermochemical Biomass Conversion, pp. 1265-1274, 1994.

35 White, D. H., Wolf, D., and Zhao, Y., 'Biomass liquefaction utilizing extruder-feeder reactor system, in Abstracts of the papers of the American Chemical Society, vol. 193, pp. 36-46, 1987.

36 White, D. and Wolf, D., Thermochemical Conversion Program Annual Meeting, Solar Energy Research Institute, Golden, Colorado, pp. 57-66, 1988.

37 Yokoyama, S.-Y., Ogi, T., Koguchi, K., and Nakamura, E., 'Efficient catalytic gasification of cellulose for production of hydrogen and carbon monoxide', in Liq. Fuels Technol. vol. 2, no. 2, pp. 155-163, 1984.

38 Ogi, T., Yokoyama, S.-Y. and Koguchi, K., in J. Jpn. Pet. Inst., vol. 28, no. 3, pp. 239-245, 1985.

39 Yokoyama, S.-Y. Ogi, T., Koguchi, K., Minowa, T., Murakami, M. and Suzuki, A., in Proceedings of Conference: Research in Thermochemical Biomass Conversion, pp. 792-803, Ed: Bridgwater, A. V., Kuester, J. L., Elsevier, 1988.

40 Beckman, D. And Elliott, D. C., 'Comparisons of the yields and properties of the oil products from direct thermochemical biomass liquefaction processes', in Canadian Journal of Chemical Engineering, vol. 63, pp. 99-104, 1985.

41 Nelte, A., Meier Zu Kokcker, H., in Euroforum New Energies, Proc. Int. Congr., Saarbrucken, FRG, Oct. 24-28, pp. 673-675, 1988.

42 Gharieb, H. K., Faramawy, S. and El-Amrousi, F. A., 'Liquefaction of cellulosic wastes: 3. Production, characterization and evaluation of pyrolytic oils', in J. Chem. Tech. Biotechnol., vol. 58, pp. 395-402, 1993.

43 Elliott, D. C., Sealock Jr., L. J. and Butner, R. S., 'Product analysis from direct liquefaction of several high-moisture biomass feedstocks', in Pyrolysis Oils from Biomass: Producing, Analyzing and Upgrading, ACS Symp. 376, Ed: Soltes, J. and Milne, T. A., pp. 179-188, 1988.

44 Heitz, M., Carrasco, F., Rubio, M., Chauvette, G., Chornet, E., Jaulin, L. and Overend, R. P., 'Generalized correlations for the aqueous liquefaction of lignocellulosics', in the Canadian Journal of Chemical Engineering, vol. 64, pp. 647-650, 1986.

45 Vanasse, C., Chornet, E. and Overend, R. P., 'Liquefaction of lignocellulosics in model solvents: Creosote oil and ethylene glycol', in the Canadian Journal of Chemical Engineering, vol. 66, pp. 112-120, 1988.

46 Boocock, D. G. B., Chowdhury, A. and Kosiak, L., in Proceedings of Conference: Research in Thermochemical Biomass Conversion, pp. 843-853, Ed: Bridgwater, A. V. and Kuester, J. L., Elsevier, 1988.

47 Meier, D. and Faix, O., 'Effect of hydrogen pressure on yields and quality of oils obtained from direct liquefaction of pine wood', in Energy from Biomass 2: proceedings of 2nd E.C. Biomass Contractors Meeting, Paestum, Italy, 25-27 May, 1988.

48 Davis, H., Figueroa, C. and Schaleger, 'Research and development activities on direct liquefaction technology, in Proceedings of 14th Biomass Thermochemical Conversion Contractor's Meeting, NTIS no. CONF-820685, 1982.

49 Rust International, 'Final report, An investigation of liquefaction of wood at the Biomass Liquefaction Facility, Albany, Oregon', Report for U.S. Dept. of Energy, Contract no. DE-AC01-78ET-23032, 1982.

50 Eager, R. L., Mathews, J. F. and Pepper, 'A small-scale semi-continuous reactor for the conversion of wood to fuel oil', in Can. J. Chem. Eng., vol. 61, pp. 189-193, 1983.

51 Boocock, D. G. B., Mackay, D., Franco, H. and Lee, P., 'The production of synthetic organic liquids from wood using a modified nickel catalyst', in Can. J. Chem. Eng., vol. 58, pp. 466-469, 1980.

52 Thigpen, P. L. and Berry, W. L., Jr., 'Liquid fuels from wood by continuous operation of the Albany, Oregon Biomass Liquefaction Facility', in Proceedings of Conference: Energy from Biomass and Waste 6, pp. 1057-1093, Chicago, I.G.T., 1982.

53 Bean, F. R. and McAuliffe, C. A., 'Conversion of municipal waste to fuel', Canadian Patent no. 1 164 378, issued March 27j, 1984.

54 Benn, F. R. and McAuliffe, 'Conversion of municipal waste to fuel', U.K. patent application no. 2 166 154A, filed Sept. 1984.

55 Bult, J. M. E., 'The MANOIL project', Presented at the 89th Annual Conference of the Institute of Wastes Management, Torbay, U.K., June 16-19, 1987.

56 Abreu, C. A. M., Lima, N. M. and Zoulalian, A., 'Catalytic hydrogenolysis of starch: Kinetic evaluation of selectivity in polyol and monoalcohol formation', in Biomass and Bioenergy, vol. 9, no. 6, pp. 487-492, 1995.

57 Elliott, D. C. and Schiefelbein, 'Liquid hydrocarbon fuels from biomass', in Fuel Chemistry, American Chemical Society.

58 Chornet, E. and Overend, R. P., 'Biomass liquefaction: An overview', in Proceedings of Conference: Fundamentals of Thermochemical Biomass Conversion, pp. 967-1002, Elsevier Applied Science, 1985.

59 Elliott, D. C., Beckman, D., Bridgwater, A. V., Diebold, J. P., Gevert, S. B. and Solantausta, Y., 'Developments in direct thermochemical liquefaction of biomass: 1983-1990', in Energy and Fuels, vol. 5, pp. 399-410, 1991.

60 Elliott, D. C., 'Description and utilization of product from direct liquefaction of biomass', in Biotechnology and Bioengineering Symp. no. 11, pp. 187-198, 1981.

61 Ergun, S., 'Biomass liquefaction efforts in the United States', from Lawrence Berkeley Laboratory, publication no. LBL-10456, pp. 20, 1980.

62 Vanasse, C., Lemonnier, J. P., Eugene, D. and Chornet, E., 'Pretreatment of wood flour slurries prior to liquefaction', in the Canadian Journal of Chemical Engineering, vol. 66, 1988.

63 Yu, S.-M. G., 'Solvolytic liquefaction of wood under mild conditions', Ph.D. thesis, LBL-14096, Prof. T.Vermeulen, Dept. Chem. Eng., U.C., Berkeley.

64 Chornet, E., Eugene, D. and Overend, R. P., 'Fluidodynamic effects in the fractional solubilization of biomass leading to liquefaction', in Proceedings of Conference: Fundamentals of Thermochemical Biomass Conversion, Ed. Overend, R. P., Milne, T. A. and Mude, L. K., Elsevier Applied Science Publishers, pp. 839-848, 1984.

65 Davis, H. G. and Watt, D. W., 'Preliminary experiments on direct liquefaction of biomass by solvolysis and catalytic hydrogenation', in Proceedings of 15th U.S. Dept. of Energy Contractors Meeting, March, 1983.

66 Mok, S.-L., W., and Antal, Jr., M. J., 'Uncatalyzed solvolysis of whole biomass hemicellulose by hot compressed liquid water', in I & EC Research, vol. 31, 1992.

67 Abatzoglou, N. Bouchard, J. Chornet, E. and Overend, R., 'Dilute acid depolymerization of cellulose in aqueous phase: Experimental evidence of the significant presence of soluble oligomeric intermediates', in the Canadian Journal of Chemical Engineering, vol. 64, pp. 781-786, 1986.

68 Wan, E.I. and Fraser, M.D., 'Economic assessment of producing liquid transportation fuels from biomass', in Proceedings of Conference: Research in Thermochemical Biomass Conversion, pp. 61-76, Ed: Bridgwater, A. V. and Kuester, J. L., Elsevier, 1988.

69 Roy, C., de Caumia, B. and Pakdel, 'Preliminary feasibility study of the biomass vacuum pyrolysis process', in Proceedings of Conference: Research in Thermochemical Biomass Conversion, pp. 585-591, Ed: Bridgwater, A. V. and Kuester, J. L., Elsevier, 1988.

70 Solantausta, Y., Diebold, J., Elliott, D. C., Bridgwater, A. V. and Beckman, D., 'Assessment of liquefaction and pyrolysis systems', in Research notes, PB-95-129797/XAB, VTT/RN-1573, 1994.

71 Toft, A. J., 'A Comparison of Integrated Biomass To Electricity Systems', Ph.D Thesis, University of Aston in Birmingham, U. K., October 1996.

72 Roy, C., Pakdel, H. and Zhang, H. G., 'Characterization and catalytic gasification of the aqueous by-product from vacuum pyrolysis of biomass', in Canadian Journal of Chemical Engineering, vol. 72, pp. 98-105, 1994.

73 Elliott, D. C., Beckman, D., Bridgwater, A. V., Diebold, J. P., Gevert, S. B. and Solantausta, Y., 'Developments in direct thermochemical liquefaction of biomass: 1983-1990', in Energy and Fuels, vol. 5, pp. 399-410, 1991.

74 Elamin, A., Rezzoug, S., Capart, R. and Gelus, M., 'Solvolysis and catalytic hydrotreatment of wood', in Proceedings of Conference: Advances in Thermochemical Biomass Conversion, Ed: Bridgwater, A. V., Blackie, pp. 1415-1423, 1993.

75 Diebold, J. and Power, A., 'Engineering aspects of the vortex pyrolysis reactor to produce primary pyrolysis oil vapours for use in resins and adhesives', in Proceedings of Conference: Research in Thermochemical Biomass Conversion, pp. 609-628, Ed: Bridgwater, A. V., Kuester, J. L., Elsevier, 1994.

76 'Catalogue handbook of fine chemicals, 1996-1997', Aldrich, 1996.

77 Sinskey, A. J., 'Organic chemicals from biomass: An overview', in Organic Chemicals from Biomass, Ed: Wise, D. L., pp. 11, chap. 1, Benjamin Cummings, 1983.

78 Scott, D. S., Piskorz, J., Radlein, D. and Czernik, S., 'Sugars from cellulosics by the Waterloo fast pyrolysis process', in Pyrolysis and Gasification, Ed: Ferrero, G. L., Maniatis, K., Buckens, A. and Bridgwater, A. V., pp. 201-208, Elsevier Applied Science, London, 1989.

79 Radlein, D., Piskorz, J. and Majerski, P., 'Method of producing slow-release nitrogenous organic fertilizer from biomass', U.S. Patent 5,676,727, 1997 and European Patent application 0716056.

80 Pakdel, H., Roy, C. and Lu, X., 'Effect of various pyrolysis parameters on the production of phenols from biomass', in Proceedings of Conference: Developments in Thermochemical Biomass Conversion, pp. 509-522, Ed: Bridgwater, A. V. and Boocock, D. G. B., Blackie, 1997.

81 McKinley, J. W., Overend, R. P. and Elliott, D. C., 'The ultimate analysis of biomass liquefaction products: the results of the IEA Round Robin #1', in Specialist Workshop on Biomass Oil Properties and Combustion, Estes Park, Colorado, Sept. 26-28, 1994.

82 Rezzoug, S.-A. and Capart, R., 'Solvolysis and hydrotreatment of wood to provide fuel', in Biomass and Bioenergy, vol. 11, no. 4, pp. 343-352, 1996.

83 Solantausta, Y. and Oasmaa, A., 'Utilisation of biomass pyrolysis oil in power production', in Proceedings of EC Contractor's Meeting: Energy from Biomass: Progress in Thermochemical Conversion, 7 Oct 92, Florence, Italy, pp. 137-141, ECSC-EEC-EAEC, 1994.

84 Diebold, J. P., Milne, T. A., Czernik, S., Oasmaa, A., Bridgwater, A. V., Cuevas, A., Gust, S., Huffman, D. and Piskorz, J., 'Proposed specifications for various grades of pyrolysis oils', in Proceedings of Conference: Developments in

Thermochemical Biomass Conversion, pp. 433-447, Ed: Bridgwater, A. V. and Boocock, D. G. B., Blackie, 1997.

85 Solantausta, Y., Nylund, N.-O., Westerholm, M., Koljonen, T. and Oasmaa, A., 'Wood pyrolysis oil as fuel in a diesel power plant', in Bioresource Technology, vol. 46, no. 1-2, pp. 177-188, 1993.

86 Czernik, S., Scahill, J. and Diebold, J., 'The production of liquid fuel by fast pyrolysis of biomass', in Proceedings of 28th Intersociety Energy Conversion Engineering Conference, vol. 2, pp. 429-436, ACS, 1993.

87 Soltes, E.J. and Lin, S.C.K., 'Vehicular fuels and oxychemicals from biomass thermochemical tars', in Biotechnology and Bioengineering Symposium no. 13, pp, 53-64, 1983.

88 Leech, J., 'Running a dual fuel engine on pyrolysis oil', in Proceedings of Conference: Biomass Gasification and Pyrolysis: State of the Art and Future Prospects, Stuttgart, 9-12 Apr. 1997, Ed: Kaltschmitt, M. and Bridgwater, A. V., CPL, pp. 495-497, 1997.

89 Agblevor, F. A. and Besler, S., 'Inorganic compounds in biomass feedstocks. 1. Effect on the quality of fast pyrolysis oils', in Energy and Fuels, vol. 10, pp. 293-298, 1996.

90 Elliott, D. C. and Baker, E. G., 'Hydrotreating biomass liquids to produce hydrocarbon fuels', in Proceedings of Conference: Energy from Biomass and Wastes X, Washington D.C., April 7-10, 1986, Ed: Klass, K., pp. 765-784, 1987.

91 Grandmaison, J.- L., Chantal, P. D. and Kaliaguine, S. C., 'Conversion of furanic compounds over HZSM-5 zeolite', in Fuel, vol. 69, pp. 1058-1061, 1990.

92 Horne, P. A. and Williams, P. T., 'Premium quality fuels and chemicals from the fluidised bed pyrolysis of biomass with zeolite catalyst upgrading', in Renewable Energy, vol. 5, pt. 2, pp. 810-812, 1994.

93 Evans R J, Milne T A, 'Molecular-Beam, Mass-Spectrometric Studies of wood Vapour and Model compounds over an HZSM-5 catalyst', in Pyrolysis oils from biomass - Producing, Analyzing and Upgrading, Ed. Soltes, J. and Milne, T. A., ACS symposium series 376, pp. 311-327, 1988.

94 Scott, D. S. and Legge, R. L., 'Fast pyrolysis of biomass for recovery of speciality chemicals', in Proceedings of Conference: Developments in Thermochemical Biomass Conversion, pp. 523-535, Blackie, 1997.

95 Longley, C J., Howard, J. and Fung, D. P. C., 'Levoglucosan recovery from cellulose and wood pyrolysis liquids', in Proceedings of Conference: Advances in Thermochemical Biomass Conversion, Ed: Bridgwater, A. V., pp. 1441-1451, Blackie, 1994.

96 Samolada, M. C., Grigoriadou, E., Patiakaand, D. and Vasalos, I. A., 'Use of biomass pyrolysis liquids for producing components for gasoline blending', in Proceedings of 7th E. C. Conference of Biomass for Energy and Industry, Ed: Hall, Grassi, Scheer, pp. 954-958, Ponte Press, 1994.

97 Renaud, M., Grandmaison, J. L., Roy, C. and Kaliaguine, S., 'Low-Pressure Upgrading of Vacuum-Pyrolysis Oils from Wood', in ACS Symposium Series, no. 376, pp. 290-310, 1988.

98 Churin, E., 'Upgrading of pyrolysis oils by hydrotreatment', in Biomass Pyrolysis Liquids Upgrading and Utilisation, Ed: Bridgwater, A. V. and Grassi, G., pp. 103-117, 1986.

99 Elliott, D. C., and Neuenschwander, G. G., 'Liquid fuels by low-severity hydrotreating of biocrude', in Proceedings of Conference: Developments in Thermochemical Biomass Conversion, Ed: Bridgwater, A. V. and Boocock, D. G. B., pp. 611-621, Blackie, 1997.

100 Elliott, D. C., 'Upgrading liquid products: Notes from the workshop at the

international conference Research in thermochemical biomass conversion', in Proceedings of Conference: Research in Thermochemical Biomass Conversion, pp. 1170-1176, Ed: Bridgwater, A. V. and Kuester, J. L., Elsevier, 1988.

101 Adjaye, J. D. and Bakhshi, N. N., 'Production of hydrocarbons by catalytic upgrading of a fast pyrolysis bio-oil. Part 1: Conversion over various catalysts', in Fuel Processing Technology, vol. 45, pp. 161-183, 1995.

102 Marshall, A. J., 'Catalytic conversion of pyrolysis oil in the vapour phase', Masters of Applied Science thesis, Presented to the University of Waterloo, 1984.

103 Dao, L. H., Haniff, M., Houle, A. and Lamothe, D., 'Reactions of model compounds of biomass-pyrolysis oils over ZSM-5 zeolite catalysts', in Pyrolysis Oils from Biomass: Producing, Analyzing and Upgrading, Ed: Soltes, J. and Milne, T. A., pp. 328-341, ACS Symposium Series 376, 1988.

104 Evans, R. J. and Milne, T., 'Molecular-Beam, Mass-Spectrometric Studies of Wood Vapour and Model Compounds over an HZSM-5 Catalyst', in Pyrolysis Oils from Biomass - Producing, Analyzing and Upgrading. Ed: Soltes and Milne, p.311-327, 1988.

105 Baker, E. G and Elliott, C. E., 'Catalytic hydrotreating of biomass-derived oils', in Pyrolysis Oils from Biomass: Producing, Analyzing and Upgrading', Ed: Soltes and Milne, ACS Symposium Series, 1988.

106 Peacocke, G. V. C. and Bridgwater, A. V., 'Ablative plate pyrolysis of biomass for liquids', in Proceedings of. ACS Symposium, no. 310, Denver, 1993.

107 Lède, J., Verzaro, F., Antoine, B. and Villermaux, J., 'Flash pyrolysis of wood in a cyclone reactor', in Chemical Engineering and Processing, vol. 20, no. 6, pp. 309-317, 1986.

108 Diebold, J. P. and Scahill, J. W., 'Production of primary pyrolysis oils in a vortex reactor', in Pyrolysis Oils from Biomass: Prducing, Analyzing and Upgrading, Ed: Soltes, J. and Milne, T. A., pp. 31-40, 1988.

109 Diebold, J. and Scahill, J., 'Progress in the entrained flow, fast ablative pyrolysis of biomass', in Proceedings of 13th Biomass Thermochemical Conversion Contractors Meeting, pp. 332-365, 27-29 Oct, Virginia, 1981.

110 Wagenaar, B. M., Kuipers, J. A. M., Prins, W. and van Swaaij, W. P. M., 'The rotating cone flash pyrolysis reactor', in Proceedings of Conference: Advances in Thermochemical Biomass Conversion, Ed: Bridgwater, A. V., pp. 1122-1133, Blackie, 1993.

111 Janse, A. M. C., Prins, W. and van Swaaij, W. P. M., 'Development of a small integrated pilot plant for flash pyrolysis of biomass', in Proceedings of Conference: Developments in Thermochemical Biomass Converison, Ed: Bridgwater, A. V. and Boocock, D. G V., pp. 368-377, Blackie, 1997.

112 Lède, J., Verzaro, F., Antoine, B. and Villermaux, J., 'Flash pyrolysis of wood in a cyclone reactor', in Chemical Engineering and Processing, vol. 20, no. 6, pp. 309-317, 1986.

113 Peacocke, G. V. C., 'Ablative Pyrolysis of Biomass', PhD Thesis, University of Aston in Birmingham, U. K., October 1994.

114 Knight, J., Gordon, C. W. and Kovac, R. J., 'Entrained flow pyrolysis of biomass', in Proceedings of 16th Biomass Thermochemical Contractors' Meeting, Portland, Oregon, May 8-9, 1984.

115 Graham, R., Bergougnou, M. A., Mok, L. K. and de Lasa, H. L., 'Flash pyrolysis (ultrapyrolysis) of biomass using solid heat carriers', in Proceedings of Conference: Fundamentals of Thermochemical Biomass Conversion, pp. 397-410, Colorado, October, 1982.

116 Maniatis, K., Baeyens, J.,. Peeters, H. and Roggeman, G., 'Flash pyrolysis of biomass in an entrained bed pilot plant reactor', in Biomass Thermal Processing,

Proceedings of 1st Canada-European Community R&D Contractors Meeting, Ottawa, Canada, Oct 90, pp. 39-43, CPL, 1992.

117 Graham, R. G, Freel, B. A., Huffman, D. R. and Bergougnou, M. A., 'Applications of rapid thermal processing of biomass', in Proceedings of Conference: Advances in Thermochemical Biomass Conversion, Ed: Bridgwater, A. V., vol. 2, pp. 1275-1288, Blackie, 1993.

118 Takarada, T., Tonichi, T., Takezawa, H. and Kato, K., 'Pyrolysis of Yallourn coal in a powder-particle fluidized bed', in Fuel, vol. 71, pp. 1087-1092, 1992.

119 Takarada, T., Tonishi, T., Fusegawa, Y., Morishita, K., Nakagawa, N. and Kato, K., 'Hydropyrolysis of coal in a powder-particle fluidized bed', in Fuel, vol. 72, no. 7, pp. 921-926, 1993.

120 Burton, R. S. and Bailie, R., 'Fluid bed pyrolysis of solid waste materials', in Combustion, pp. 13-18, Feb 1974.

121 Sanchez, C. G, Silva, E. and Santos, F. J., 'Experimental research of the fluidized bed devolatilization of sugar cane bagasse and paddy husk', Presented at the 13th Brazilian Congress of Mechanical Engineering.

122 Kuznetsov, B. N. and Shchipko, M. L., 'The conversion of wood lignin to char materials in a fluidized bed of Al-Cu-Cr oxide catalysts', in Bioresource Technology, vol. 52, pp. 13-19, 1995.

123 Scott, D. S. and Piskorz, J., 'Production of liquids from biomass by continuous flash pyrolysis', in BioEnergy 84, vol. 3, pp. 15-23, 1985.

124 Scott, D. S. and Piskorz, J., 'Continuous flash pyrolysis of wood for production of liquid fuels', in Can. J. Chem. Eng., vol. 62, pp. 404-412, 1984.

125 Piskorz, J., Radlein, D. and Scott, D. S., 'Thermal conversion of cellulose and hemicellulose in wood to sugars', in Proceedings of Conference: Advances in Thermochemical Biomass Conversion, Ed: Bridgwater, A. V., pp. 1432-1440, Blackie, 1993.

126 Scott, D. S. and Piskorz, J., 'Flash pyrolysis of wood in a fluidized bed', in Proceedings of American Chemical Society Symposium 'Fuels from Biomass', chap. 23, Ed: Klass, D., pp. 421-434, Ann Arbor Science Publishers, 1981.

127 Scott, D. S., Piskorz, J., Westerberg, I. B. and McKeough, P., 'Flash pyrolysis of peat in a fluidized bed', in Fuel Proc. Tech., vol. 18, pp. 81-95, 1988.

128 Scott, D. S., Piskorz, J. and Radlein, D., 'Liquid products from the continuous flash pyrolysis of biomass', in Ind. Eng. Chem. Proc. Des. Devel., vol. 24, pp. 581-588, 1985.

129 Boukis, I., Maniatis, K., Bridgwater, A. V., Vassilatos, V. and Kyritsis, S., 'Design concept and hydrodynamics of an air-blown circulating fluidized bed reactor for biomass flash pyrolysis', in Proceedings of Conference: Advances in Thermochemical Biomass Conversion, vol. 2, pp. 1151-1164, Ed: Bridgwater, A. V., Blackie, 1993.

130 Chen, N. Y., Walsh, D. E. and Koenig, L. R., 'Fluidized-bed upgrading of wood pyrolysis liquids and related compounds', in Pyrolysis Oils from Biomass - Producing, Analyzing and Upgrading, Ed: Soltes and Milne, ACS Symposium Series 376, 1988.

131 Theander, O. 'Cellulose, hemicellulose and extractives', in Proceedings of Conference: Fundamentals of Thermochemical Biomass Conversion, Ed: Overend, R. P., Milne, T. A. and Mudge, L. K., pp. 35-60, Elsevier, 1985.

132 Phillips, J. A. and Humphrey, A. E., 'An overview of process technology for the production of liquid fuels and chemical feedstocks via fermentation', in Organic Chemicals from Biomass, Ed: Wise, D. L., chap. 8, pp. 249-304, Elsevier, 1983.

133 Glassier, W. G., 'Lignin', in Proceedings of Conference: Fundamentals of Thermochemical Biomass Conversion, Ed: Overend, R.P., Milne, T. A. and Mudge, L. K., pp. 61-76, Elsevier, 1985.

134 Soltes, E. J., Wiley, A. T. and Kenny Lin, S.-C., 'Biomass pyrolysis – Towards an understanding of its versatility and potentials', in Biotechnology and Bioengineering Symposium, no. 11, pp. 125-136, 1981.

135 Richards, G. N., 'Chemistry of polysaccharides and lignocellulosics', in Proceedings of Conference: Advances in Thermochemical Biomass Conversion, Ed: Bridgwater, A. V., pp. 727-745, Blackie, 1994.

136 Evans, R. J. and Milne, T. A., 'Molecular characterization of the pyrolysis of biomass. 1. Fundamentals', in Energy and Fuels, vol. 1, no. 2, pp. 123-137, 1987.

137 Evans, R. J. and Milne, T. A., 'Molecular characterization of the pyrolysis of biomass. 2. Applications', in Energy and Fuels, vol. 1, no. 4, pp. 311-319, 1987.

138 Masuku, C., 'Thermal reactions of the C-O and alkyl C-C bonds in lignin model compounds', in Acta Polytechnica Scandinavica, Chemical Technology and Metallurgy Series no. 196, pp. 2, Finnish Academy of Technology, 1991.

139 Britt, P. F., Buchanan III, A. C., Thomas, K. B. and Lee, S- K., 'Pyrolysis mechanisms of lignin: surface-immobilized model compound investigation of acid-catalyzed and free-radical reaction pathways', in Journal of Analytical and Applied Pyrolysis, vol. 33, no. 1-9, pp. 1-19, 1995.

140 Perry, R. H. and Chilton, C. H., 'Chemical Engineers' Handbook', 5th Edition, pp. 4-16, New York, London, McGraw-Hill, 1973.

141 Marshall, A. J., 'Catalytic conversion of pyrolysis oil in the vapour phase', Masters of Applied Science thesis, presented to the University of Waterloo, 1984.

142 Adjaye, J. D., Sharma, R. K. and Bakhshi, N. N., 'Catalytic upgrading of wood derived bio-oil over HZSM-5 catalyst: effect of co-feeding steam', in Proceedings of Conference: Advances in Thermochemical Biomass Conversion, Ed: Bridgwater, A. V., pp. 1032-1045, 1994.

143 Renaud, M., Grandmaison, J.L., Roy, C. and Kaliaguine, S., 'Low Pressure Upgrading of Vacuum Pyrolysis Oils from Wood', in Pyrolysis Oils from Biomass: Producing, Analyzing, and Upgrading, Ed. Soltes, E. J., Milne, T. A., vol. ACS Symposium Series, no. 376, pp. 290-310, 1988.

144 Adjaye, J. D. and Bakhshi, N. N., 'Production of hydrocarbons by catalytic upgrading of a fast pyrolysis bio-oil. Part 1: Conversion over various catalysts', in Fuel Processing Technology, vol. 45, pp. 161-183, 1995.

145 Bakhshi, N. N., Sai, P. K., and Adjaye, J. D., 'Potential production of hydrocarbons from the conversion of a wood-derived oil over some aluminophosphate catalysts', in Proceedings of Conference: 2nd Biomass Conf. of the Americas: Energy, Environment, Agriculture and Industry, pp. 1089-1098, National Renewable Energy Laboratory, 1995.

146 Dao, L. H., Haniff, M., Houle, A. and Lamothe, D., 'Reactions of model compounds of biomass-pyrolysis oils over ZSM-5 zeolite catalysts', in Pyrolysis Oils from Biomass: Producing, Analyzing and Upgrading, Ed: Soltes, J. and Milne, T. A., pp. 328-341, ACS Symposium Series 376, 1988.

147 Williams, P. T. and Horne, P. A., 'The role of metal salts in the pyrolysis of biomass', in Renewable Energy, vol. 4, no. 1, pp. 1-13, 1993.

148 Horne, P. A. and Williams, P. T., 'Catalysis of model biomass compounds over zeolite ZSM-5 catalyst', in Proceedings of 7th E.C. Conference: Biomass for Energy and Industry, Ed: Hall, D.O., Grassi, G. and Scheer, H., Ponte Press, pp. 901-907, 1992.

149 Horne, P. A. and Williams, P. T., 'Reaction of oxygenated biomass pyrolysis model compounds over a ZSM-5 catalyst', in Renewable Energy, vol. 7, no. 2, pp. 131-144, 1996.

150 Fuhse, J. and Bandermann, F., 'Conversion of organic oxygen compounds and their mixtures on H-ZSM-5', in Chem. Eng. Tech., vol. 10, pp. 323-329, 1987.

151 Williams, P. T. and Horne, P. A., 'Analysis of aromatic hydrocarbons in pyrolytic oil derived from biomass', in Journal of Analytical and Applied Pyrolysis, vol. 31, pp. 15-37, 1995.

152 Diebold, J. P., Evans, R. J., Levie, B. E., Milne, T. A. and Scahill, J. W., 'Low pressure upgrading of primary oils from biomass', Solar Energy Research Institute report, contract no. B-L5950-A-Q for U.S. Dept. of Energy, 1986.

153 van Bekkum, H., and Kouwenhoven, H. W., 'The use of zeolites in organic reactions', in Recueil des Travaux Chimiques des Pay-Bas, vol. 108, pp. 283-294, 1989.

154 Reed, T. B., Diebold, J. P., Chum, H. L., Evans, R. J., Milne, T. A. and Scahill, J. W., 'Overview of biomass fast pyrolysis and catalytic upgrading to liquid fuels', in Proceedings of the American Solar Energy Society, Inc., Boulder, Colorado, pp. 92-105, June, 1986.

155 Evans, R. J., Filley, J. and Milne, T. A., 'Molecular beam mass spectrometric studies of HZSM-5 activity during wood pyrolysis product conversion', in Thermochemical Conversion Program Annual Meeting, June 21-22, Solar Energy Research Institute, pp. 33-43, 1988.

156 Diebold, J. P. and Scahill, J. W., 'Biomass to gasoline: Upgrading pyrolysis vapours to aromatic gasoline with zeolite catalysts at atmospheric pressure', in Pyrolysis oils from Biomass: Producing, Analyzing and Upgrading, Ed: Soltes, J. and Milne, T. A., pp. 264-276, ACS Symposium Series, 1988.

157 Diebold, J., Phillips, Tyndall, D., Scahill, J., Feik, C. and Czernik, S., 'Catalytic upgrading of biocrude oil vapours to produce hydrocarbons for oil refinery applications', Proceedings of 208th National Meeting of ACS: Div. Fuel Chem., vol. 39, no.4, pp. 1043-1047, 1994.

158 Evans, R. J. and Milne, T. A., 'Molecular characterization of the pyrolysis of biomass. 2. Applications', in Energy and Fuels, vol. 1, no. 4, pp. 123-137, 1987.

159 Evans, R. J. and Milne, T. A., 'Molecular-beam, mass spectrometric studies of wood vapor and model compounds over an HZSM-5 catalyst', in Pyrolysis Oils from Biomass: Producing, Analyzing and Upgrading, Ed: Soltes, J. and Milne, T.A., ACS Symposium Series 376, pp. 311-327, 1988.

160 Diebold, J. P., Overend, R., Rejai, B. and Power, A. J., 'Reformulated gasoline components production from renewable feeds'.

161 Rejai, B., Evans, R. J., Milne, T. A., Diebold, J. P. and Scahill, J. W., 'The Conversion of Biobased Feedstocks to Liquid Fuels through Pyrolysis', in Proceedings of Conference: Energy from Biomass and Wastes XV, Ed: Klass, D.L., pp. 855-876, 1991.

162 Milne, T. A., Evans, R. J. and Filley, J., 'MBMS studies of HZSM-5 activity during wood pyrolysis product conversion', in Proceedings of Conference: Research in Thermochemical Biomass Conversion, pp. 910-926, Ed: Bridgwater, A. V. and Kuester, J. L., Elsevier, 1988.

163 Milne, T. A. and Soltys, M. N., 'Direct mass-spectrometric studies of the pyrolysis of carbonaceous fuels. 1', in Journal of Analytical and Applied Pyrolysis, vol. 5, no. 2, pp. 93-110, 1983.

164 Milne, T. A. and Soltys, M. N., 'Direct mass-spectrometric studies of the pyrolysis of carbonaceous fuels. 2' in Journal of Analytical and Applied Pyrolysis, vol. 5, no. 2, pp. 111, 1983.

165 Spencer, M. S. and Whittam, T. V., 'Catalysis by highly siliceous zeolites', in Properties and Applications of Zeolites, Ed: Townsend, R. P., The Chemical Society, pp. 342-352, 1980.

166 Côme, G.-M., 'Laboratory reactors for pyrolysis reactions', in Pyrolysis Theory and Industrial Practice, chap. 11, pp. 256-275, Ed: Albright, L. F., Crynes, B. L. and Corcoran, W. H., Academic Press, 1983.

167 Côme, G.-M., 'Laboratory reactors for pyrolysis reactions', in Pyrolysis Theory and Industrial Practice, chap. 11, pp. 256-275, Ed: Albright, L. F., Crynes, B. L. and Corcoran, W. H., Academic Press, 1983.

168 Evans, R. J. and Milne, T. A., 'Molecular Characterisation of the Pyrolysis of Biomass.1. Fundamentals,' in Energy and Fuels, vol. 1, no. 2, pp. 123-137, 1987.

169 Evans, R. J. and Milne, T. A., 'Molecular Characterisation of the Pyrolysis of Biomass. 2. Applications', in Energy and Fuels, vol. 1, no. 4, pp. 311-319, 1987.

170 Dejaifve, P., Vedrine, J. C., Bolis, V. and Derouane, E. G., 'Reaction pathways for the conversion of methanol and olefins on H-ZSM-5 zeolite', in Journal of Catalysis, vol. 63, pp. 331-345, 1980.

171 Albright, L. F. and Chung-Hu Tsai, T., 'Importance of surface reactions in pyrolysis units', in Pyrolysis Theory and Industrial Practice, chap. 10, pp. 242-245, Ed: Albright, L. F., Crynes, B. L. and Corcoran, W. H., Academic Press, 1983.

172 Pavlath, A. E. and Gregorski, K. S., 'Carbohydrate pyrolysis 2. Formation of furfural and furfuryl alcohol during the pyrolysis of selected carbohydrates with acidic and basic catalysts', in Proceedings of Conference: Research in Thermochemical Biomass Conversion, pp. 155-163, Ed: Bridgwater, A. V. and Kuester, J. L., Elsevier, 1988.

173 Makarova, M. A., Bates, S. P. and Dwyer, J., 'Bronsted sites of enhanced acidity in zeolites: experimental modelling', in Zeolites: A refined tool for designing catalytic sites, Ed: Bonneviot, L. and Kaliaguine, S., pp. 79-86, Elsevier, 1995.

174 Fajula, F., 'Geometry of the active sites in zeolites under working conditions', in Zeolites: A refined tool for designing catalytic sites, Ed: Bonneviot, L. and Kaliaguine, S., pp. 133-141, Elsevier, 1995.

175 Gates, B. C., Katzer, J. R. and Schuit, G. C. A., 'Chemistry of Catalytic Processes', New York, McGraw-Hill, 1979.

176 Chang, C. D., 'Methanol-to-Gasoline Process', in Perspectives in Molecular Sieve Science, chap. 39, pp. 596-615, ACS, 1988.

177 Chen, N. Y., Degan, Jr, T. F. and Koenig, L. R., 'Liquid Fuel from Carbohydrates', in Chemical Technology, vol. 506, pp. 506-511, 1986.

178 Sharma, R. K. and Bakhshi, N. N., 'Catalytic upgrading of pyrolysis oil', in Energy and Fuels, vol. 7, pp. 306-314, 1993.

179 Renaud, M., Grandmaison, J. L., Roy, C. and Kaliaguine, S., 'Low Pressure Upgrading of Vacuum Pyrolysis Oils from Wood', in Pyrolysis Oils from Biomass: Producing, Analyzing, and Upgrading, Ed. Soltes, E. J., Milne, T. A., vol. ACS Symposium Series, no. 376, pp. 290-310, 1988.

180 Horne, P. A. and Williams, P. T., 'Premium quality fuels and chemicals from the fluidised bed pyrolysis of biomass with zeolite catalyst upgrading', in Renewable Energy, vol. 5, pt. 2, pp. 810-812, 1994.

181 Miller, B. J. and Drummond, J., 'The mobil methanol to gasoline process', in Petroleum Review, pp. 32-37, April, 1981.

182 Evans, R. J., Milne, T. A. and Soltys, M. N., 'Direct mass-spectrometric studies of the pyrolysis of carbonaceous fuels 3, Primary pyrolysis of lignin', in Journal of Analytical and Applied Pyrolysis, vol. 9, pp. 207-236, 1986.

183 Evans, R. J. and Milne, T. A., 'Applied mechanistic studies of biomass pyrolysis', in Proceedings of the 1985 Biomass Thermochemical Conversion Contractors' Meeting, October 14-18, Minneapolis, pp. 57-77, 1986.

184 Czernik, S., Scahill, J. and Diebold, J., 'The production of liquid fuel by fast pyrolysis of biomass', in Journal of Solar Energy Engineering, vol. 117, pp. 2-6, 1995.

185 Scahill, J., Diebold, J. and Power, A., 'Engineering aspects of upgrading pyrolysis oil using zeolites', in Research in Thermochemical Biomass Conversion, pp. 927-940, Ed: Bridgwater, A. V. and Kuester, J. L., Elsevier, 1988.

186 Evans R J, Milne T A, 'Molecular-Beam, Mass-Spectrometric Studies of wood Vapour and Model compounds over an HZSM-5 catalyst', in Pyrolysis oils from biomass - Producing, Analyzing and Upgrading, Ed. Soltes, J. and Milne, T.A., ACS Symposium series 376, pp. 311-327, 1988.

187 Chantal, P. D., Kaliaguine, S., Grandmaison, J. L. and Mahay, A., 'Production of hydrocarbons from aspen poplar pyrolytic oils over HZSM-5', in Applied Catalysis, vol. 10, pp. 317-332, 1984.

188 Williams, P. T. and Horne, P. A., 'Characterisation of oils from the fluidised bed pyrolysis of biomass with zeolite catalyst upgrading', in Biomass and Bioenergy, vol. 7, no. 1-6, pp. 223-236, 1994.

189 Adjaye, J. D. and Bakhshi, N. N., 'Production of hydrocarbons by catalytic upgrading of a fast pyrolysis bio-oil. Part 2: Comparative catalyst performance and reaction pathways', in Fuel Processing Technology, vol. 45, pp. 185-202, 1995.

190 Diebold, J. P. and Scahill, J. W., 'Zeolite catalysts for producing hydrocarbon fuels from biomass', in Thermochemical Conversion Program Annual Meeting, pp. 21-31, 1988.

191 Evans, R. J. and Milne, T. A., in Thermochemical Conversion Program Annual Meeting, 1988.

192 Diebold, J. P. and Scahill, J. W., 'Conversion of wood to aromatic gasoline with zeolite catalysts', in Energy Progress, vol. 8, no. 1, 1988.

193 Diebold, J. P., Evans, R. J., Levie, B. E., Milne, T. A. and Scahill, J. W., 'Low pressure upgrading of primary oils from biomass', annual report for U.S. D.o.E., 1987.

194 Rollmann, L. D. and Walsh, D. E., 'Shape selectivity and carbon formation in zeolites', in Journal of Catalysis, 56, pp. 139-140, Academic Press, 1979.

195 Sharma, R. K. and Bakhshi, N. N., 'Catalytic upgrading of pyrolytic oils over HZSM-5'.in Canadian Journal of Chemical Engineering, vol. 71, no. 3, pp. 383-391, 1993.

196 Plank, C. J., Woodbury and Rosinski, E. J., 'Catalytic hydrocarbon conversion with a crystalline zeolite composite catalyst', U.S. Patent no. 3 140 253, May 1, 1964.

197 'Gas Fluidization Technology', Ed: Geldart, D., Wiley Interscience, 1986.

198 Partridge, B. A. and Lyall, E., AERE Rep. M2152, 1969.

199 Geldart, D., 'Single particles, fixed and quiescent beds', in Gas Fluidization Technology, chap. 2., pp. 11-32, Ed: Geldart, D., Wiley Interscience, 1986.

200 'Circulating fluidized bed technology III', Ed: Basu, P., Horio, M. and Hasatani, M., Pergamon, 1991.

201 Howard, J. R., 'Fluidized bed technology: Principles and Applications', chap. 2, pp. 26, Adam Hilger, 1989.

202 'Fluization', Ed: Davidson, J. F. and Harrison, D., London Academic Press, 1971.

203 Fluidization bed boilers, design and application', Ed: Prabir, Basu, Toronto, Oxford Pergammon C, 1984.
204 Mori, S., Yan, Y., Kato, K., Matubara, K. and Liu, D., 'Hydrodynamics of a circulating fluidized bed', in Circulating fluidized bed technology III, pp.113-118, Pergamon, 1991.
205 Large, J. F., Martini, Y. and Bergougnou, M. A., Proceedings of Conference: Int. Powder and Bulk Handling, Chicago, 1976.
206 Geldart, D. 'Gas Fluidization Technology', chap. 6, pp. 131, Ed: Geldart, D., Wiley Interscience, 1986.
207 Peacocke, G. V. C., Dick, C. M., Hague, R. A., Cooke, L. A. and Bridgwater, A. V., 'Comparison of ablative and fluid bed fast pyrolysis products: Yields and analyses', in Proceedings of Conference: Developments in Thermochemical Biomass Conversion, pp. 191-205, Ed: Bridgwater, A. V. and Boocock, D. G. B., Blackie, 1997.
208 Hague, R. A., 'The Pre-Treatment and Pyrolysis of Biomass for the production of Liquids for Fuel and Speciality Chemicals', PhD Thesis, University of Aston in Birmingham, U.K., September 1998.
209 Piskorz, J., Scott, D. S. and Radlein, D., 'Composition of oils obtained by fast pyrolysis of different woods', in Pyrolysis Oils from Biomass: Producing, Analyzing and Upgrading, pp. 167-178, Ed: Soltes, J. and Milne, T. A., ACS Symposium Series 376, Washington D.C., 1988.
210 Samolada, M. C. and Vasalos, I. A., 'A kinetic approach to the flash pyrolysis of biomass in a fluidized bed reactor', in Fuel, vol. 70, no. 7, pp. 883-889, 1991.
211 Antal, M. J. Jr., in Advances in Solar Energy, chap. 4, pp. 175, American Solar Energy Society, New York, 1982.
212 Samolada, M. C., Stoikos, T. and Vasalos, I. A., in Journal of Analytical and Applied Pyrolysis, vol. 18, pp. 127, 1990.
213 Samolada, M. C. and Vasalos, I. A., 'Effect of experimental conditions on the composition of gases and liquids from biomass pyrolysis', in Proceedings of Conference: Advances in Thermochemical Biomass Conversion, Ed: Bridgwater, A.V., Blackie, pp. 859-873, 1993.
214 Connor, M. A., 'Heat and mass transfer considerations in fuel production from wood wastes by pyrolysis', Journal Energy Heat Mass Transfer, vol. 5, pp. 179-194, 1983.
215 Simmons, G. M. and Gentry, M., 'Kinetic formation of CO, CO2, H2 and light hydrocarbon gases from cellulose pyrolysis', in Journal Analytical and Applied Pyrolysis, vol. 10, pp. 129-138, 1986.
216 Shafizadeh, F., 'Pyrolytic reactions and products of biomass', in Proceedings of Conference: Fundamentals of Thermochemical Biomass Conversion, chap. 11, Elsevier, pp. 183-217, 1985.

APPENDIX A
150 G H^{-1} REACTOR RUN PROFILES

Reactor, furnace and furnace set point temperatures and gas flow exiting reactor versus run time for SFBC13 (508 °C, 50 % catalyst feed concentration)

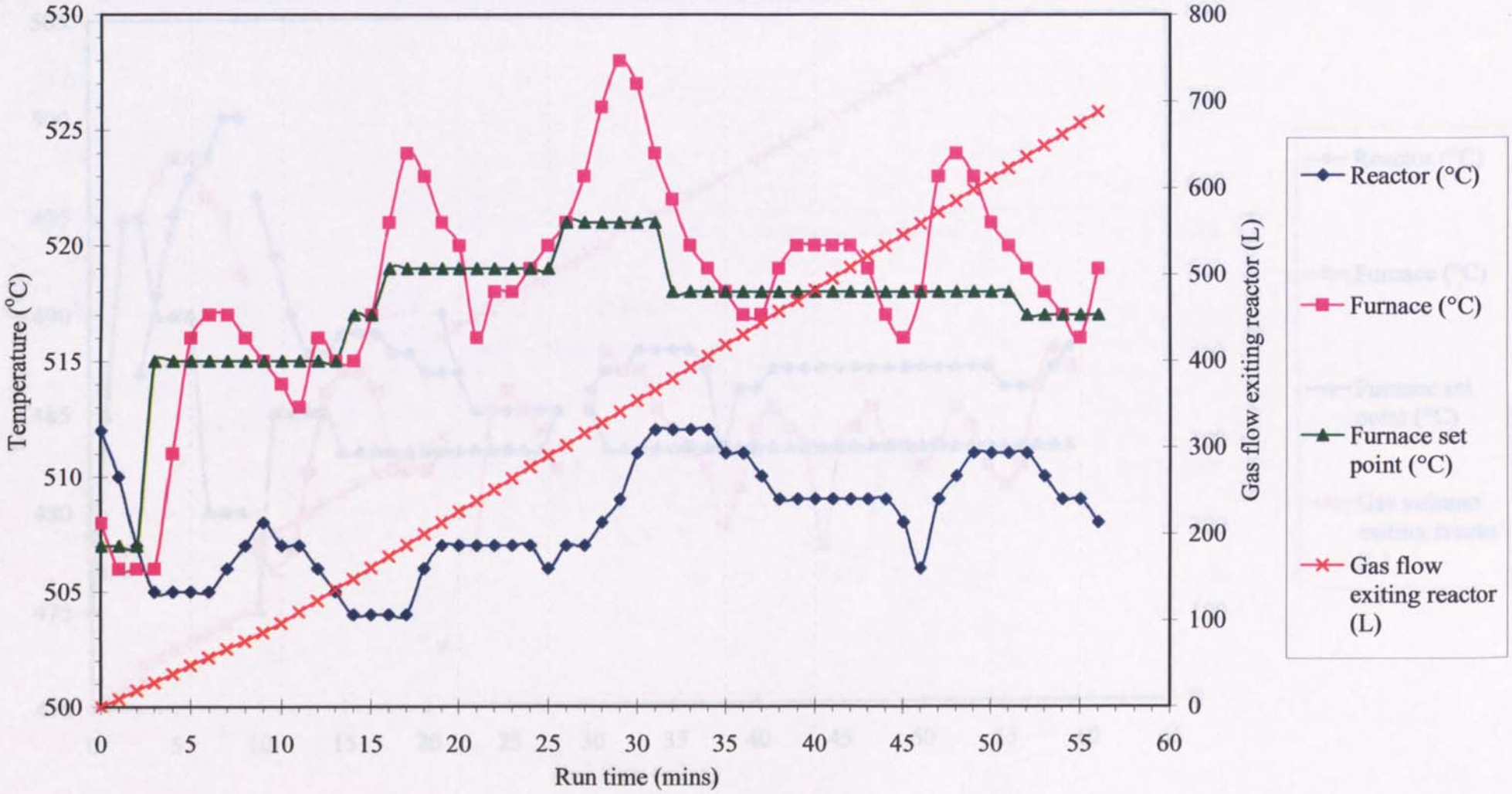

Reactor, furnace and furnace set point temperatures and gas volume exiting reactor versus run time for SFBC18 (488 °C, 0 % catalyst feed concentration)

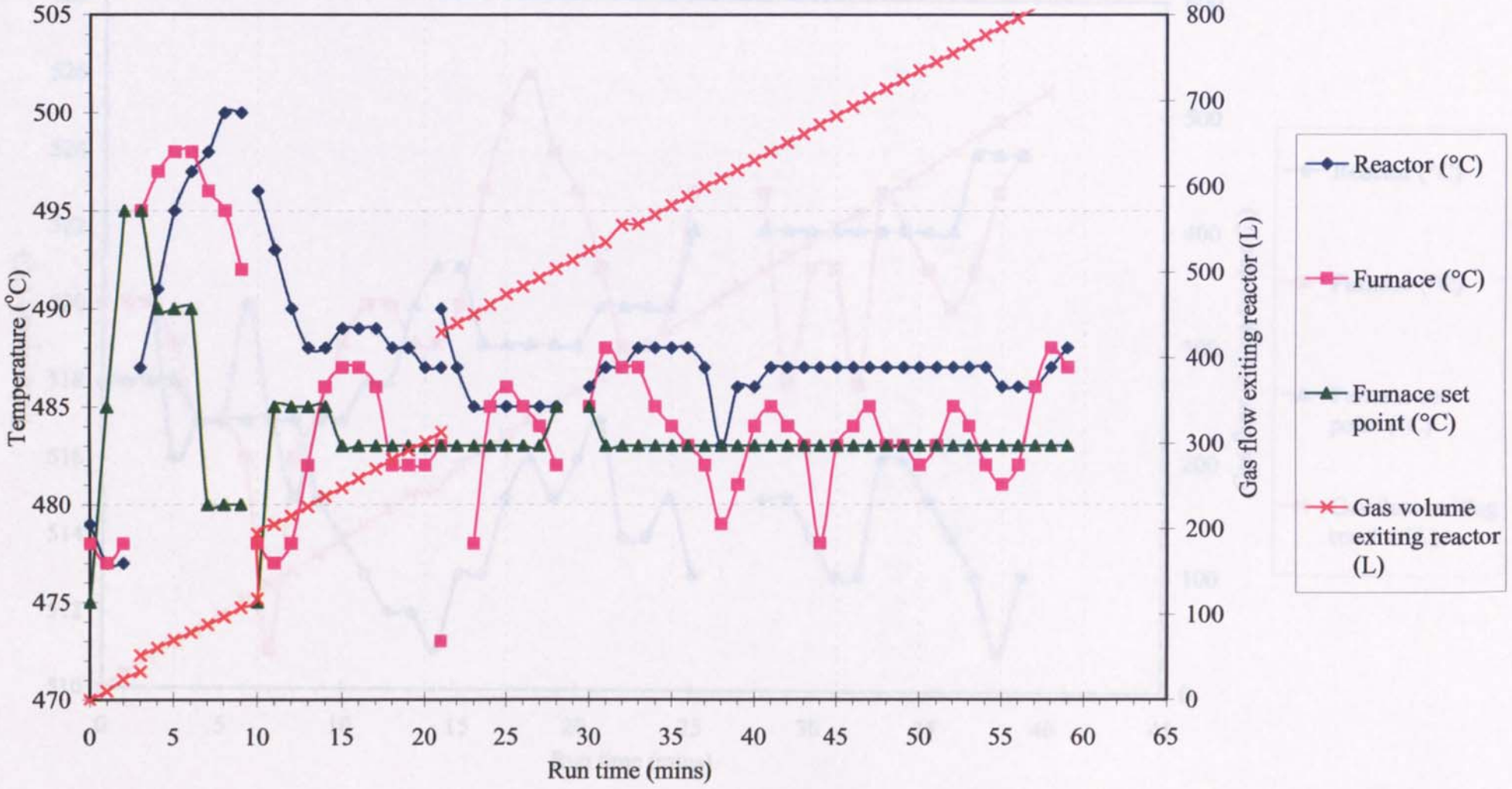

Reactor, furnace and furnace set point temperatures and gas volume exiting reactor versus run time for SFBC27 (520 °C, 25 % catalyst feed concentration)

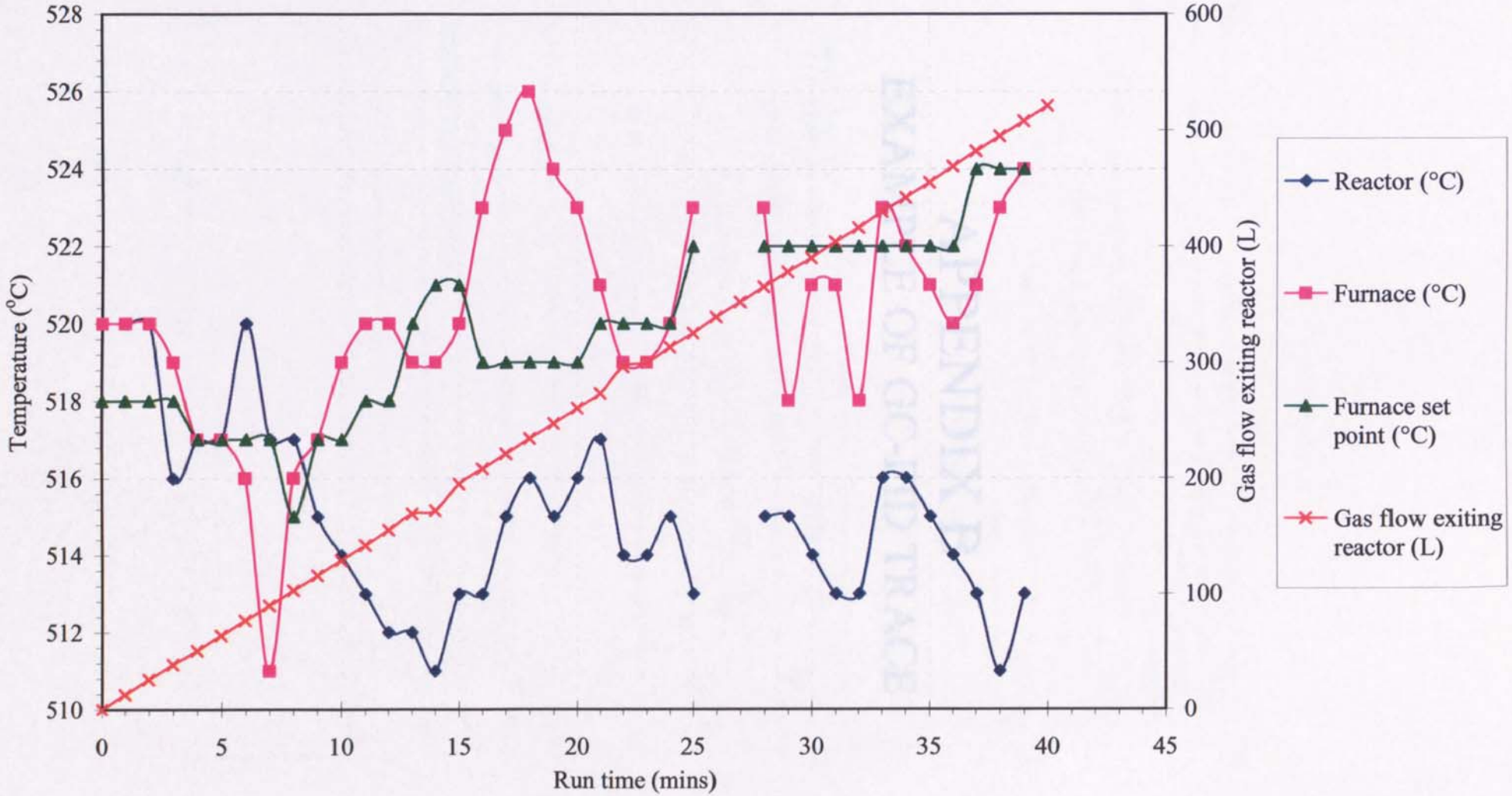

APPENDIX B
EXAMPLE OF GC-FID TRACE

GC-FID trace of pyrolysis liquid collected in Oil Pot 1 during run SFBC13 (508 °C, 50 % catalyst feed concentration)

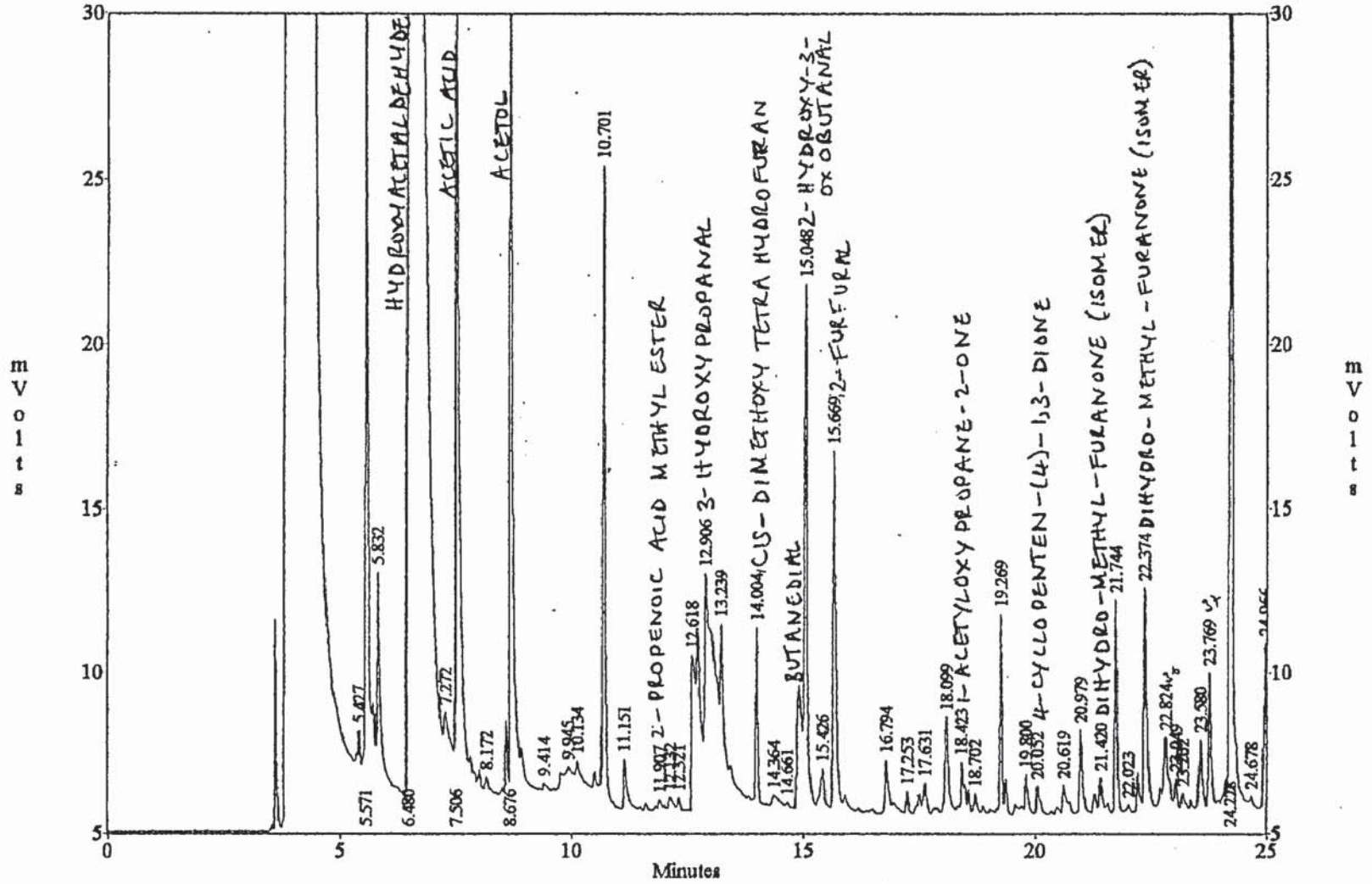

GC-FID trace of pyrolysis liquid collected in Oil Pot 1 during run SFBC13 (508 °C, 50 % catalyst feed concentration)

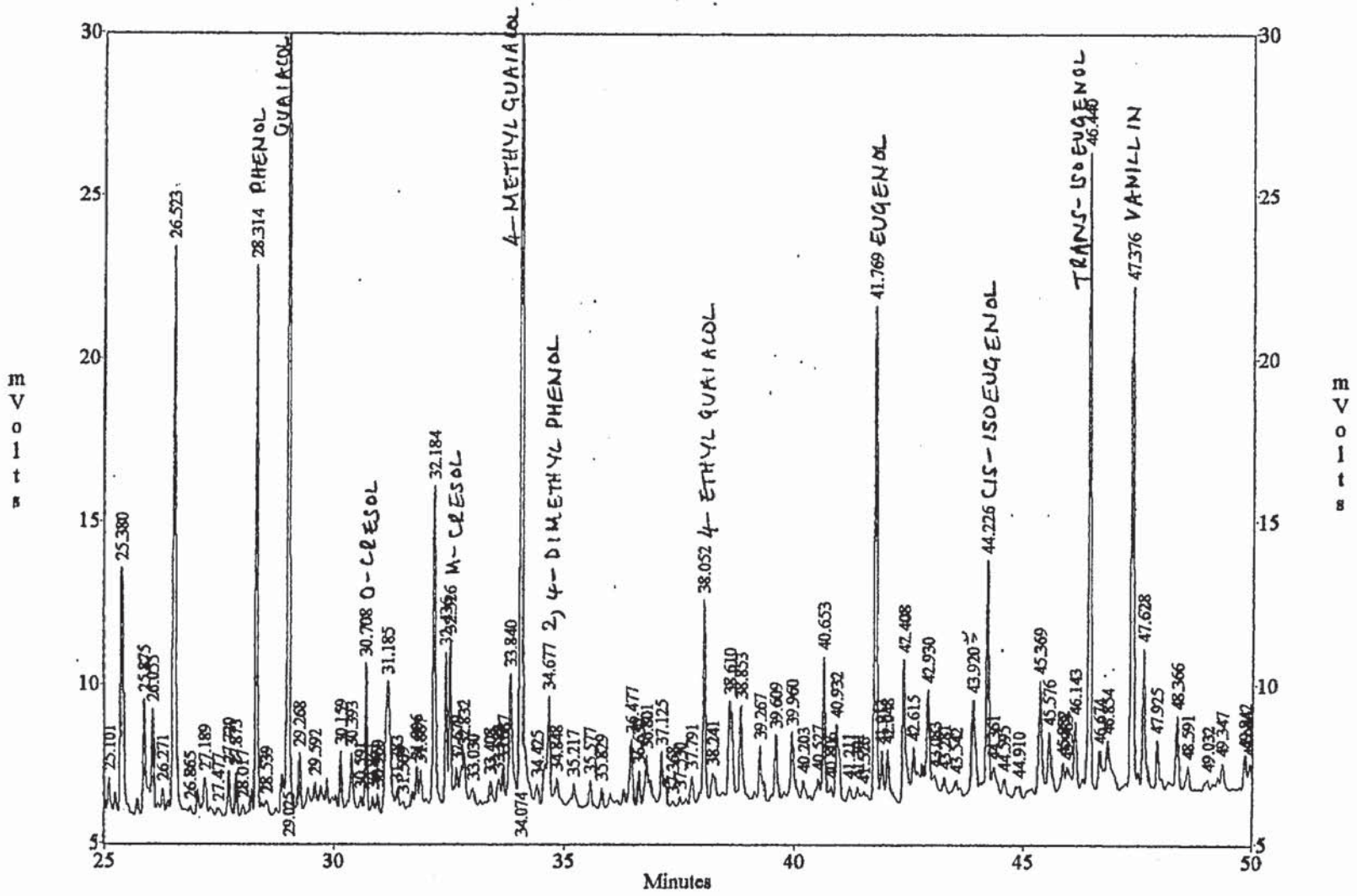

GC-FID trace of pyrolysis liquid collected in Oil Pot 1 during run SFBC13 (508 °C, 50 % catalyst feed concentration)

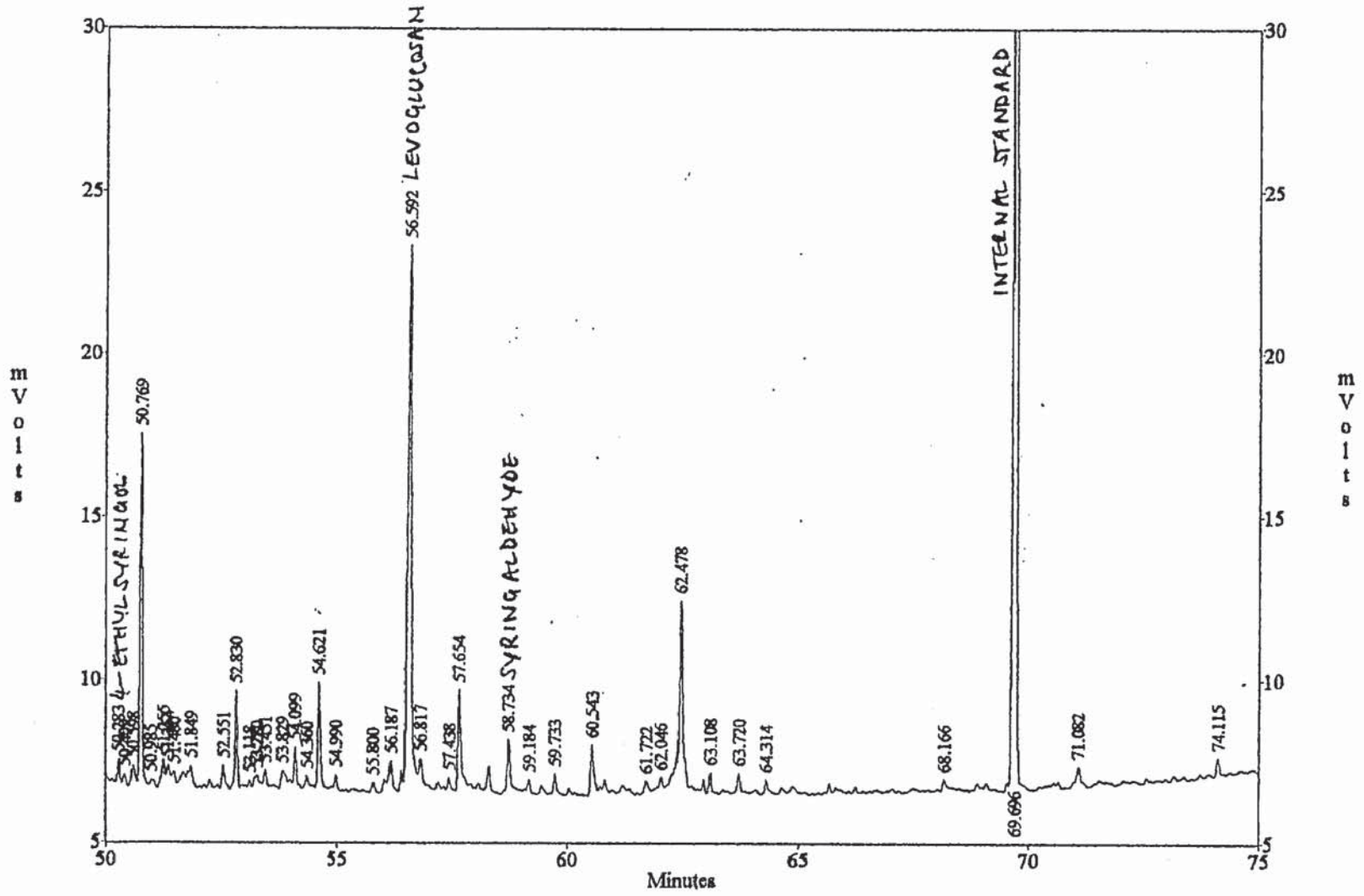

APPENDIX C
EXAMPLE OF HPLC TRACE

HPLC trace of pyrolysis liquid collected in Oil Pot 1 during run SFBC13 (508 °C, 50 % catalyst feed concentration)